frontiers | Research Topics

Brain arteriovenous malformations: Cerebrovasculature behaving badly

Edited by
Lorelei Shoemaker, Marcus Stoodley and Richard Daneman

Published in
Frontiers in Human Neuroscience
Frontiers in Neurology
Frontiers in Surgery

ISSN 1664-8714
ISBN 978-2-8325-2774-0
DOI 10.3389/978-2-8325-2774-0

About Frontiers

Frontiers is more than just an open access publisher of scholarly articles: it is a pioneering approach to the world of academia, radically improving the way scholarly research is managed. The grand vision of Frontiers is a world where all people have an equal opportunity to seek, share and generate knowledge. Frontiers provides immediate and permanent online open access to all its publications, but this alone is not enough to realize our grand goals.

Frontiers journal series

The Frontiers journal series is a multi-tier and interdisciplinary set of open-access, online journals, promising a paradigm shift from the current review, selection and dissemination processes in academic publishing. All Frontiers journals are driven by researchers for researchers; therefore, they constitute a service to the scholarly community. At the same time, the *Frontiers journal series* operates on a revolutionary invention, the tiered publishing system, initially addressing specific communities of scholars, and gradually climbing up to broader public understanding, thus serving the interests of the lay society, too.

Dedication to quality

Each Frontiers article is a landmark of the highest quality, thanks to genuinely collaborative interactions between authors and review editors, who include some of the world's best academicians. Research must be certified by peers before entering a stream of knowledge that may eventually reach the public - and shape society; therefore, Frontiers only applies the most rigorous and unbiased reviews. Frontiers revolutionizes research publishing by freely delivering the most outstanding research, evaluated with no bias from both the academic and social point of view. By applying the most advanced information technologies, Frontiers is catapulting scholarly publishing into a new generation.

What are Frontiers Research Topics?

Frontiers Research Topics are very popular trademarks of the *Frontiers journals series*: they are collections of at least ten articles, all centered on a particular subject. With their unique mix of varied contributions from Original Research to Review Articles, Frontiers Research Topics unify the most influential researchers, the latest key findings and historical advances in a hot research area.

Find out more on how to host your own Frontiers Research Topic or contribute to one as an author by contacting the Frontiers editorial office: frontiersin.org/about/contact

Brain arteriovenous malformations: Cerebrovasculature behaving badly

Topic editors

Lorelei Shoemaker — Stanford University, United States

Marcus Stoodley — Macquarie University, Australia

Richard Daneman — University of California, San Diego, United States

Citation

Shoemaker, L., Stoodley, M., Daneman, R., eds. (2023). *Brain arteriovenous malformations: Cerebrovasculature behaving badly*. Lausanne: Frontiers Media SA. doi: 10.3389/978-2-8325-2774-0

Table of contents

frontiers | Frontiers in Human Neuroscience

TYPE Editorial
PUBLISHED 07 June 2023
DOI 10.3389/fnhum.2023.1212184

OPEN ACCESS

EDITED AND REVIEWED BY
Leonhard Schilbach,
Ludwig Maximilian University of Munich, Germany

*CORRESPONDENCE
Lorelei D. Shoemaker
lshoemaker@stanford.edu

RECEIVED 25 April 2023
ACCEPTED 19 May 2023
PUBLISHED 07 June 2023

CITATION
Shoemaker LD, Daneman R and Stoodley MA (2023) Editorial: Brain arteriovenous malformations: cerebrovasculature behaving badly. *Front. Hum. Neurosci.* 17:1212184. doi: 10.3389/fnhum.2023.1212184

Editorial: Brain arteriovenous malformations: cerebrovasculature behaving badly

Lorelei D. Shoemaker[1]*, Richard Daneman[2] and Marcus A. Stoodley[3]

[1]Department of Neurosurgery, Stanford School of Medicine, Stanford, CA, United States, [2]Department of Neurosciences, Department of Pharmacology, School of Medicine, University of California, San Diego, San Diego, CA, United States, [3]Faculty of Medicine, Health and Human Sciences, Macquarie University, Sydney, NSW, United States

KEYWORDS

cerebrovascular disease, hemorrhage, endothelial cells, neurovascular unit (NVU), Hereditary Hemorrhagic Telangiectasia (HHT), arteriovenous malformations (AVMS), neuroinflammation, Sturge-Weber syndrome

Editorial on the Research Topic
Brain arteriovenous malformations: cerebrovasculature behaving badly

Brain arteriovenous malformations (bAVMs) are a rare disease, consisting of a nest of abnormal arteries and veins, and lacking a capillary bed. Diagnosis is often made when patients present with seizures, migraines or, more seriously, hemorrhage, although identification of asymptomatic AVMs is occurring more frequently, owing to increased imaging. AVMs are heterogeneous and vary in terms of blood flow, age of onset/treatment, size, venous drainage, and brain location. With no clear standard of care, treatment is on a case-by-case basis, with limited ability to predict hemorrhage risk. Guided by the specific features of the AVM, treatment proceeds with increasing invasiveness, consisting of any combination of monitoring, embolization, radiosurgery, to surgical removal. Complete AVM resolution often requires years, with risk of hemorrhage – and increasing patient stress - throughout. Understanding hemorrhage risk for symptomatic and asymptomatic AVMs would present a breakthrough in treatment decisions. However, AVM disease biology remains unclear, hindering improvements in diagnosis and treatment. Our goal for this Research Topic is to highlight advances in the field of AVMs, and to suggest where gaps remain.

The blood vessels and myriad cell types in the brain share an intimate relationship during development, in the adult, and in disease. Within the neurovascular unit (NVU), endothelial cells (ECs), pericytes, vascular smooth muscle cells (SMCs), astrocytes, microglia, and neurons, together with a complex basement membrane, interact to establish the blood-brain barrier (BBB) and normal brain function. The AVM microenvironment is complex and involves interplay between the cells present in the NVU (Shabani et al.). There are likely transitional or immature cell types present, involved in pathogenic processes such as endothelial-to-mesenchymal transition (EndMT). Mural cells - the SMCs and pericytes that normally stabilize the vasculature - are also affected. In a rodent model of Hereditary Hemorrhagic Telangiectasia (HHT), EC-specific deletion of Rbpj, a mediator of Notch signaling, results in altered pericyte coverage, highlighting EC and pericyte communication in neurovascular disease (Selhorst et al.). A compromised BBB and/or shear stress drives an

inflammatory response, with the presence of macrophages, neutrophils, and T lymphocytes (Shabani et al.). Understanding how these cells interact in a pathological environment may hold clues to disease mechanisms, initiating event(s), and probability of hemorrhage.

Mechanistic insight into the pathogenesis of AVMs has focused on Notch, SMADs, VEGF, TGFβ, BMPs, KRAS, microRNAs and somatic mutations, among others. Interestingly, many of the signaling pathways implicated in AVMs are shared in cancer, including PI3K/AKT/mTOR, RAS/MAF/MEK, and KRAS. Re-purposing FDA-approved cancer drugs targeting angiogenesis and inflammation has promise in AVM research (Mansur and Radovanovic). Ultimately, there is likely no singular driver of the pathology, but rather a complex interplay amongst these mechanisms, underlining the challenges in designing treatments.

Approximately 95% of bAVMs are sporadic but can also occur as a part of genetic syndromes. HHT is characterized by various mutations in the transforming growth factor β (TGFβ) signaling pathway, with ENG and ACVRL1 genes accounting for ∼90% of the cases (Drapé et al.). Importantly, genotype does not equate to phenotype, as each HHT patient has unique clinical features. Vascular malformations are also a component of Sturge-Weber syndrome, associated with somatic mutations in the GNAQ gene (Van Trigt et al.). Is there overlap with other vascular anomalies and AVMs? Given the heterogeneity of malformations, accurate molecular classification is crucial to understanding the pathophysiology, developing therapeutic targets, and guiding treatment (Mansur and Radovanovic; Drapé et al.).

Is this achievable? Biopsies are clearly not an option for bAVMs, but there has been some success in defining the molecular landscape in biofluids such as blood (Mansur and Radovanovic) and cerebrospinal fluid (Wichmann et al.). This goal remains distant, given the technical challenges of developing a "biomarker matrix" to identify and characterize relatively small AVMs amidst the ∼100,000 km of vasculature in the body.

Animal models of AVMs have provided valuable insight into vascular malformations (Selhorst et al.). Rodent and zebrafish models not only highlight therapeutic targets but also provide systems amenable to hypothesis testing and molecular manipulation (Drapé et al.). An important consideration is how these largely genetic models compare with human AVMs. The clear advantage to human tissue and models is the more direct translation to human AVMs. In practice however, working with human tissue/models is challenging and there remains space to expand research tools to multidimensional cell models, vascularized brain organoids, and iPSC technologies (Van Trigt et al.).

Treatment goals are clear: low complication and mortality rates, and efficacy. Hemorrhage risk is the most potent driver of the treatment plan but clinicians cannot evaluate this to choose between conservative and aggressive management. This creates tremendous uncertainty in what the future holds for AVM patients. Improved diagnostic imaging has the potential to evaluate AVM flow and BBB leakage and to assist in estimating hemorrhage risk but is still in its early stages.

Conventional treatments are inadequate and often have detrimental effects. For instance, radiosurgery may result in damage to otherwise healthy tissue (Ung et al.). Embolization (endovascular therapy or EVT) is successful as a first line treatment in another rare vascular anomaly (Zhou et al.) but is an adjunct treatment prior to radiosurgery or surgery for AVMs. EVT may be suitable as a curative treatment for specific AVMs but this is controversial. In addition, the presence of other vascular anomalies complicates the treatment of AVMs (Wang et al.).

AVMs and cancer share many signaling pathways, opening the door to a tremendous arsenal of FDA-approved cancer drugs (Mansur and Radovanovic). With accurate molecular definitions of AVMs, therapeutics may be the least invasive and most precise, although the question remains of the impact these therapeutics will have on existing AVMs. Finally, development of treatments for the complications of AVMs, such as hemorrhagic stroke, is necessary (Dou et al.).

This Research Topic highlights the progress in understanding AVM microenvironment and mechanisms, molecular classification, development of models, and diagnosis and treatment. There remains a real need for hemorrhage-risk evaluation and for novel anti-angiogenesis and vascular targeting therapies. This effort will require a multidisciplinary approach, from basic research to patient care.

Author contributions

LS, RD, and MS wrote and edited the manuscript. All authors contributed to the article and approved the submitted version.

Acknowledgments

We are grateful to all of the authors and reviewers for their time and contributions to this Research Topic.

Conflict of interest

The authors declare that the research was conducted in the absence of any commercial or financial relationships that could be construed as a potential conflict of interest.

Publisher's note

frontiers in Human Neuroscience

MINI REVIEW
published: 21 January 2022
doi: 10.3389/fnhum.2021.737217

A Brief Overview of the Cerebrospinal Fluid System and Its Implications for Brain and Spinal Cord Diseases

Thea Overgaard Wichmann[1]*, *Helle Hasager Damkier*[2] and *Michael Pedersen*[3]

[1]Department of Neurosurgery, Aarhus University Hospital, Aarhus, Denmark, [2]Department of Biomedicine, Faculty of Health, Aarhus University, Aarhus, Denmark, [3]Comparative Medicine Lab, Department of Clinical Medicine, Faculty of Health, Aarhus University, Aarhus, Denmark

A comprehensive understanding of the cerebrospinal fluid (CSF) system is essential for our understanding of health and disease within the central nervous system (CNS). The system of CSF refers to all components involved in CSF production, movement, and absorption. In recent years, extensive research has resulted in vastly improved understanding of the CSF system in health and disease. Yet, several aspects remain to be fully clarified, notably along the spinal cord as the preponderance of research has focused on the brain. This review briefly summarizes the CSF system and its implications for CNS diseases and highlights the knowledge gaps that require further research.

Keywords: cerebrospinal fluid, brain, spinal cord, lymphatic network, glymphatic system, aquaporin

OPEN ACCESS

Edited by:
Nico Melzer,
Universitätsklinikum Düsseldorf, Germany

Reviewed by:
Jan Lewerenz,
University of Ulm, Germany

***Correspondence:**
Thea Overgaard Wichmann
thewic@rm.dk

Specialty section:
This article was submitted to Brain Health and Clinical Neuroscience, a section of the journal Frontiers in Human Neuroscience

Received: *06 July 2021*
Accepted: *29 December 2021*
Published: *21 January 2022*

Citation:
Wichmann TO, Damkier HH and Pedersen M (2022) A Brief Overview of the Cerebrospinal Fluid System and Its Implications for Brain and Spinal Cord Diseases. Front. Hum. Neurosci. 15:737217. doi: 10.3389/fnhum.2021.737217

INTRODUCTION

Renewed attention has come to the cerebrospinal fluid (CSF) system due to its importance for central nervous system (CNS) homeostasis. The CSF system constitutes a crucial role in the CNS as it provides mechanical protection, ensures homeostasis, and facilitates communication between the CNS and peripheral nervous system, lymphatic system, vascular system, and immune system (Damkier et al., 2013; Aspelund et al., 2015; Louveau et al., 2015; Adigun and Al-Dhahir, 2021). Yet, some aspects of the CSF system remain to be fully clarified, notably along the spinal cord. Of utmost importance is bridging the knowledge gap between the brain and the spinal cord regarding the controversies of a glymphatic system and a lymphatic network, and further to understanding how these complex relationships in the CSF system contribute to health and disease. This review aims to describe the theories underlying the CSF system in relation to neurological diseases in the brain and spinal cord. This will provide the basis for highlighting the knowledge gaps that should be addressed through further research.

CSF PRODUCTION AND ABSORPTION

The CSF is a clear, colorless fluid that occupies the ventricular system, the cerebral and spinal subarachnoid spaces, and the perivascular spaces in the CNS. The fluid is a mixture of water, proteins at low concentrations, ions, neurotransmitters, and glucose that is renewed three to four times per day (Damkier et al., 2013; Hladky and Barrand, 2014; Spector et al., 2015). Several theories have been proposed to explain how CSF is produced. The classic theory states that the choroid plexi are the primary sources of CSF production. The choroid plexi develop from the ependyma protruding from the pia mater into the lateral, third, and fourth ventricles

(Damkier et al., 2013; Hladky and Barrand, 2014). The plexi consist of a single layer of epithelial cells residing on a basement membrane, connective tissue, and fenestrated capillaries (**Figure 1A**). The epithelial cells are connected by tight junctions making the epithelial layer relatively tight, whereas the underlying fenestrated capillaries are relatively leaky. This enables the passage of compounds from the blood to the epithelial cells. The production of CSF depends on the transcellular movement of Na^+ primarily driven by the Na^+/K^+-ATPase expressed at the luminal membrane facing the CSF. The movement of Na^+ is accompanied by Cl^- and HCO_3^- as well as water that follows the solute gradient. The water transport is distributed from the blood system to the ventricular system through aquaporin-1 (AQP1) water channels (Nielsen et al., 1993; Jensen et al., 2015). CSF is therefore not simply an ultrafiltrate of the blood, but a product of a tightly regulated ion transport that generates osmotic gradients and water transport. The production of CSF by the choroid plexi is believed to be relatively constant; however, the CSF secretion varies over the duration of a day with an average production of 650 ml and maximal production after midnight (Nilsson et al., 1992). The classic theory of CSF production has been challenged by findings in AQP1 knockout mice, demonstrating that water permeability across the choroid plexi is reduced by 85%, while the CSF secretion is only reduced by 35% (Oshio et al., 2005), suggesting other means of water transport across the epithelia. It is generally believed that the choroid plexi are the main sites of CSF production with contribution from extrachoroidal sites (Orešković and Klarica, 2010; Khasawneh et al., 2018); however, it has been proposed that the extrachoroidal sites are the main sites of CSF production with contribution from the choroid plexi (Orešković et al., 2017; Klarica et al., 2019).

As for CSF production, several theories of CSF absorption have emerged. The classic theory of CSF absorption states that absorption takes place from the subarachnoid spaces into the venous blood system through dural venous sinuses *via* cranial arachnoid granulations and into the lymph system *via* the nasal cribriform plate and the perineural sheaths (Klarica et al., 2019). Additional absorption is suggested to occur through cranial meningeal lymphatics embedded in the dura mater alongside arterial and venous vessels (**Figures 1B,C**; Aspelund et al., 2015; Jensen et al., 2015; Louveau et al., 2015; Tamura et al., 2020). Additional absorption has also been suggested to occur through spinal arachnoid granulations and spinal meningeal lymphatics (Chen et al., 2015b; Benveinste et al., 2017). Others have proposed that absorption through dural venous sinuses and/or lymphatics is of minor importance compared to absorption through blood microvessels (Klarica et al., 2019).

Considering the classic theory, the variation in CSF production must be matched by a similar variation in CSF absorption; otherwise, CSF accumulation would arise.

CSF MOVEMENT

The CSF flow dynamics within the ventricular system and the subarachnoid spaces is thought to consist of two main types of movements: convective flow and pulsatile flow (Yildiz et al., 2017). Convective flow is a unidirectional motion from the choroid plexi in the lateral ventricles through the foramen of Monro into the third ventricle, passing through the cerebral aqueduct into the fourth ventricle. From the fourth ventricle, CSF exits the ventricular system through the three apertures where it enters the cerebral subarachnoid space, the spinal subarachnoid space, and the central canal of the spinal cord.

The driving force of convective flow is thought to be the result of hydrostatic pressure gradients between the choroid plexi (high pressure) and arachnoid granulations (low pressure). The movement of CSF from the spinal subarachnoid space to the perivascular spaces and the lymph system is poorly described, although similar routes have been suggested (Chen et al., 2015b; Benveinste et al., 2017). The unidirectional movement has, however, been questioned by studies showing constant CSF movement, but without net unidirectional CSF displacement, suggesting a pulsatile flow (Orešković and Klarica, 2010; Klarica et al., 2019). Contrary to the unidirectional movement of the convective flow, the pulsatile flow is a bidirectional movement in upward (cranial) and downward direction (caudal) along the spinal cord, and in varying directions in the brain. Prior theories assumed the origin of the pulsatile CSF motion was the choroid plexi (Takizawa et al., 2018); however, to date, two main theories exist: the cardiac-driven theory and the respiratory-driven theory (**Figure 2**). The cardiac-driven theory states that changes in the blood volume are transmitted directly and indirectly to the CSF, i.e., a direct transmission of blood vessel pulsations to the CSF and an indirect transmission of blood vessel pulsations through other tissues to the CSF (Haughton and Mardal, 2014; Daouk et al., 2017). The respiratory-driven theory states that changes in the intrathoracic pressure are transmitted *via* the venous system to the CSF (Daouk et al., 2017; Aktas et al., 2019; Lloyd et al., 2020). Natural respiration may not contribute to the respiratory-driving force with the same magnitude as forced respiration. It is generally believed that inspiration elicits a cranial movement of CSF, while expiration elicits a caudal movement (Yamada et al., 2013; Chen et al., 2015a; Dreha-Kulaczewski et al., 2017; Aktas et al., 2019). However, both cranial and caudal CSF movements have been observed during inspiration as a result of epidural venous blood return to the thoracic spine from the cervical and lumbar spine (Lloyd et al., 2020). The relationship between the cardiac- and respiratory-driving forces is debated as the driving forces influence arterial and venous blood flow differently, thereby contributing to CSF movement to a different extent; however, the cardiac-driven force is thought to be responsible for the basic pulsatile CSF flow, while the respiratory-driven force is responsible for the large pulsatile CSF flow (Takizawa et al., 2017). The variability in the relative influence of the cardiac and respiratory forces has been attributed to variations in musculature and respiratory capacity (Yildiz et al., 2017), and the anatomical differences between the cranial and spinal cavity (Yildiz et al., 2017; Aktas et al., 2019; Lloyd et al., 2020). Yet, the exact relationship between the cardiac- and respiratory-driving forces remains to be fully clarified.

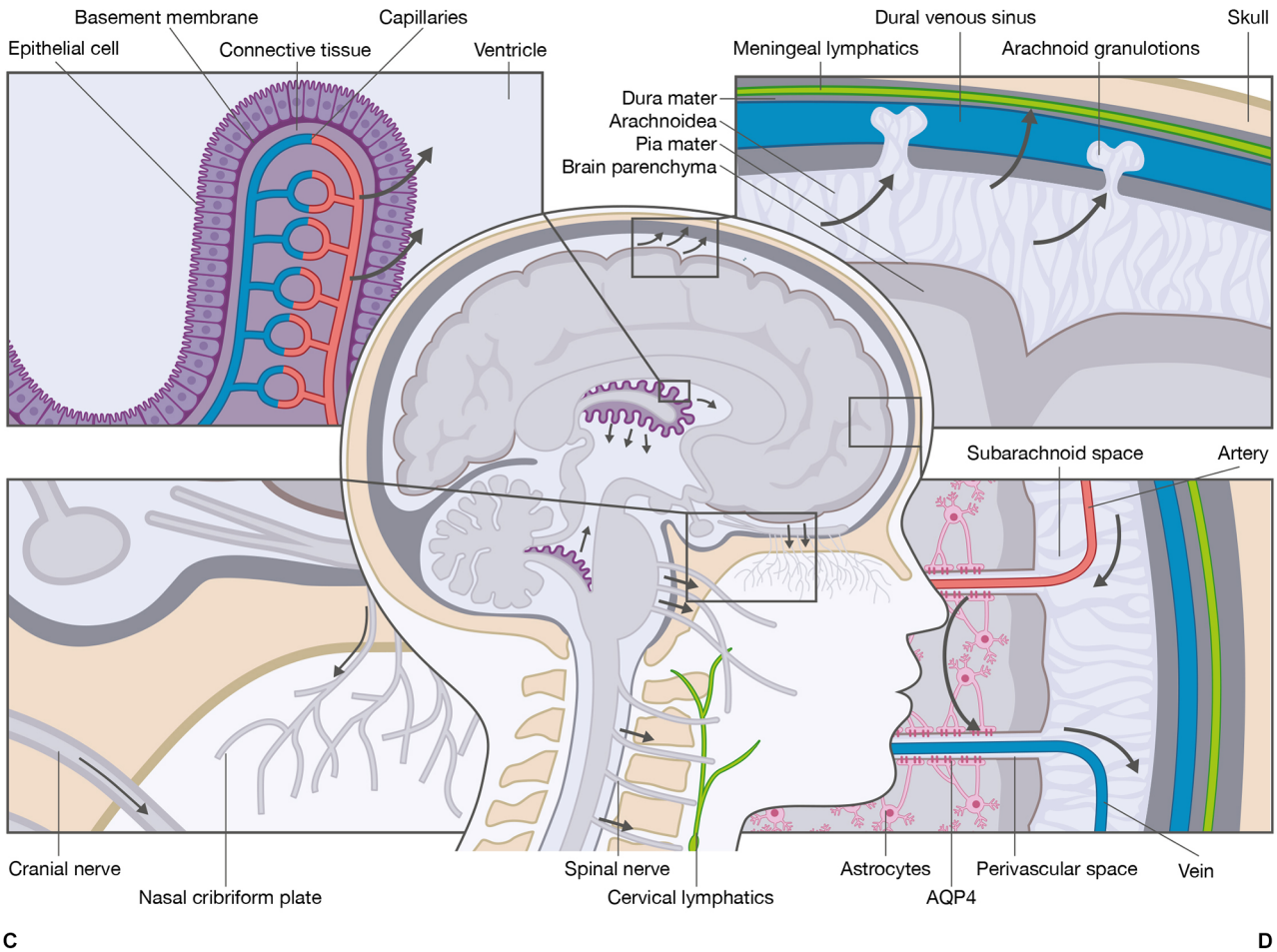

FIGURE 1 | Schematic overview of the cerebrospinal fluid system. The primary site of cerebrospinal fluid (CSF) production is the choroid plexi located within the lateral, third, and fourth ventricles of the brain. **(A)** The choroid plexi consist of leaky epithelial cells, a basement membrane, connective tissue, and fenestrated capillaries. The CSF production is mediated by ionic transport that generates osmotic gradients and water transport from the blood system to the ventricular system. **(B)** Several anatomical sites are responsible for CSF absorption e.g., arachnoid granulations, meningeal lymphatics, and **(C)** cranial nerve sheaths and nasal cribriform plate to the cervical lymphatics. **(D)** One essential function of CSF is the delivery of nutrients and the removal of waste products. The most recently proposed mechanism for removal of waste is the glymphatic system. The CSF enters from the perivascular spaces surrounding arteries into the brain parenchyma *via* mechanisms that include AQP4 water channels located at the astrocytic end-feet. Within the brain parenchyma, CSF disperses and intermixes with the interstitial fluid (ISF) and waste products. The mixture of CSF, ISF, and waste products enters the perivascular spaces surrounding veins by unknown mechanisms, e.g., AQP4 water channels. From the perivascular spaces, the mixture leaves the brain parenchyma.

FUNCTIONS OF THE CSF SYSTEM

An essential function of the CSF system is the maintenance of CNS homeostasis. As the CNS consists of highly active metabolic regions, waste products need to be cleared. The most recently proposed mechanism for waste clearance is the highly debated glymphatic system. The available literature primarily focuses on the mechanisms within the brain; thus, the mechanisms within the spinal cord remain largely elusive. The glymphatic system is a fluid conduit defined as an astrocyte-mediated fluid exchange of CSF and ISF in the brain (Iliff et al., 2012; Jensen et al., 2015; Rasmussen et al., 2018). Within the glymphatic system, CSF is thought to be driven from the subarachnoid space into the periarterial spaces surrounding penetrating arteries (Jensen et al., 2015), and along the periarterial spaces with a net convective flow following the direction of the blood flow (Mestre et al., 2018; Thomas, 2019; Kedarasetti et al., 2020). From the periarterial spaces, CSF enters the brain parenchyma. The water channels aquaporin-4 (AQP4) are expressed in the vascular endfeet of astrocytes (Trillo-Contreras et al., 2019) and have been implicated in the perivascular influx of water. AQP4 is a water channel with selective characteristics (Amasheh et al., 1995). The role of AQP4 is the most controversial part of the glymphatic system as convective transport through AQP4 is questionable from a physiological point of view. There is, however, consensus that

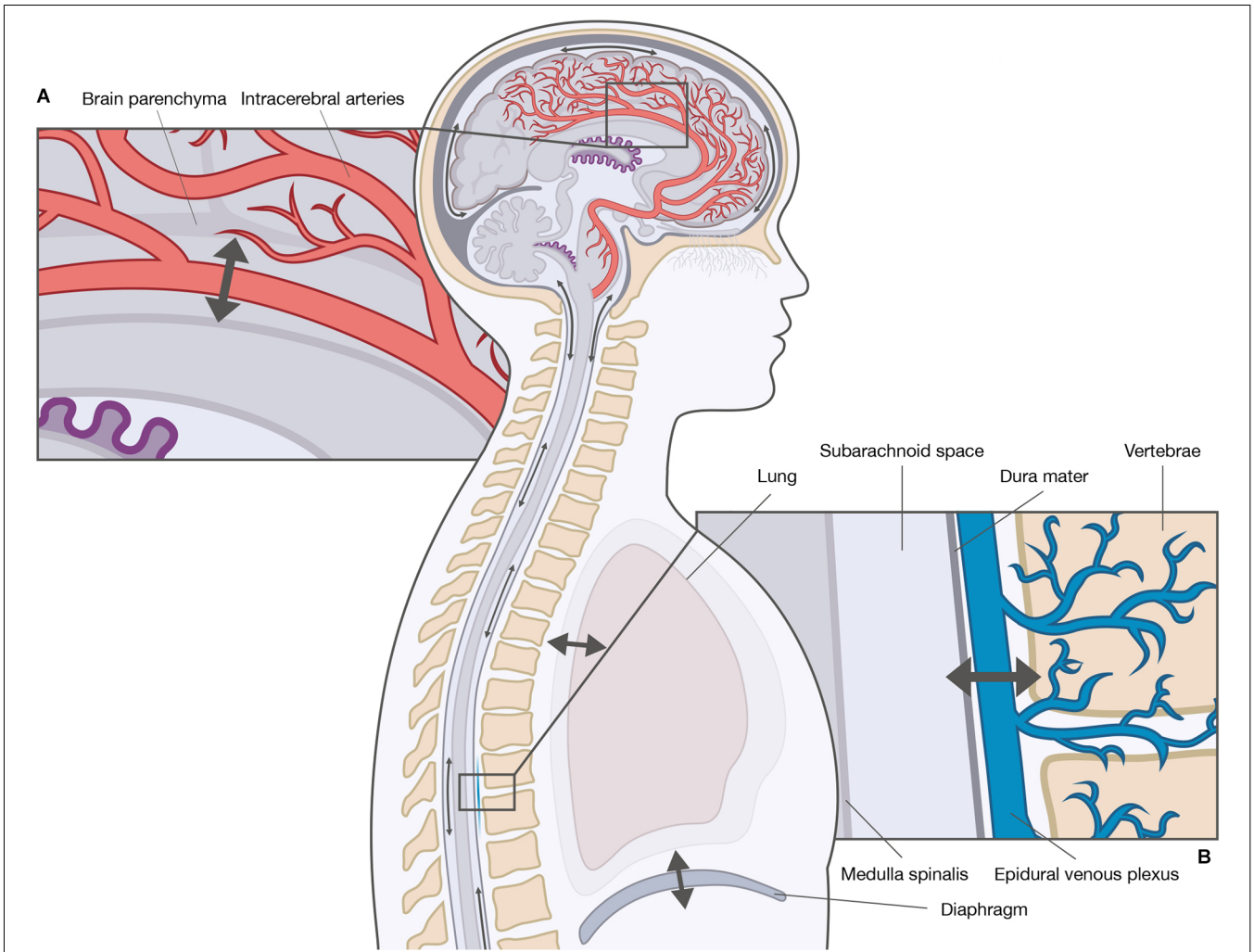

FIGURE 2 | Driving forces of cerebrospinal fluid (CSF) movement within the ventricles and subarachnoid spaces. The movement of CSF is convective and pulsatile. The two main driving forces of the pulsatile CSF movement are the cardiac-driven force and the respiratory-driven force. These forces influence the arterial blood and the venous blood differently, and thereby CSF movement to a different extent. **(A)** The cardiac-driven force causes a change in blood volume leading to pulsations that are transmitted directly or indirectly to the CSF. **(B)** The respiratory force consists of thoracic respiration and diaphragmatic respiration. Both types of respirations influence the CSF movement through the venous system, e.g., epidural venous plexus by changes in the intrathoracic pressure.

CSF has a convective flow along the perivascular spaces of the larger blood vessels (i.e., arteries and arterioles) and diffusion across the smaller blood vessels (i.e., capillaries) situated at the neurovascular unit including AQP4. As discussed by others (Abbott et al., 2018), it is likely that a convective force increases the availability of CSF at the basal lamina in the capillaries, thereby adding to the diffusion. Within the brain parenchyma, CSF disperses and mixes with ISF. The compositions of CSF and ISF are comparable, but the major difference between the two compartments is that ISF is surrounded by an extracellular matrix, thereby enabling alteration in the fluid composition of for instance ions (Syková, 2008). Due to compositional differences in CSF and ISF, it is generally accepted that the two entities can be recognized as two compartments that communicate. The mixture of CSF, ISF, and waste products enters the perivenous space by mechanisms that are poorly understood (Iliff et al., 2012). From the perivenous space, the mixture leaves the brain by returning to the vein itself across the vessel wall or by returning to the CSF in the subarachnoid space (**Figure 1D**). From here, the CSF mixed with ISF components may leave the subarachnoid space *via* the meningeal lymphatic vessels, nerve sheaths, and nasal cribriform plate into the deep cervical lymph nodes (Iliff et al., 2012; Mestre et al., 2020).

The existence of a lymphatic network within the meninges of the brain was first described by the Italian anatomist Paolo Mascagni in 1787; a description that recently has been translated and published (Sandrone et al., 2019). With the rediscovery of the lymphatic network, findings demonstrate that the meningeal lymphatic vessels are embedded within the dura mater alongside arteries, veins, and cranial nerves (Aspelund et al., 2015; Jensen et al., 2015; Tamura et al., 2020). Here they

create a network that facilitates waste clearance away from the brain and a direct link between the CNS and the peripheral immune system (Oliver et al., 2020). The entry of solutes and immune cells from the CSF to the meningeal lymphatics is proposed to occur through specific entry points along the vessels (Louveau et al., 2018).

Although considerable anatomical differences exist between the brain and the spinal cord, it seems reasonable to assume that the spinal cord has a waste clearance system and a lymphatic system resembling the systems proposed for the brain. In support of this assumption studies have demonstrated the existence of spinal perivascular spaces in rats (Lam et al., 2017; Liu et al., 2018), the existence of meningeal lymphatic vessels along the spinal cord in mice (Jacob et al., 2019), and expression of AQP1 and AQP4 water channels in the rodent spinal cord (Oklinski et al., 2014, 2016; Wei et al., 2017). As these findings are based upon animal studies, there is a need for human studies. These findings may have a vast impact on the emergence and progress of several CNS diseases, thus emphasizing the need for further research.

THE RELATIONSHIP BETWEEN THE CSF SYSTEM AND CNS DISEASES

Knowledge of the CSF system has significant implications for understanding diseases in the brain and the spinal cord. It is, however, of great importance to acknowledge that any alteration in the CSF system may be influenced by other factors, e.g., aging, hypertension, atherosclerosis, and sleep deprivation (Benveinste et al., 2017), and that any alteration in the CSF system may influence other parts of the CSF system. A greater understanding of the relationship between the CSF system and CNS diseases may provide a better understanding of these diseases' emergence and progress, and thereby reveal potential targets for treatment and intervention. A few examples of these relationships are given below.

CNS Diseases Associated With Altered CSF Production

A physiological hyposecretion of CSF occurs with age due to increased amounts of connective tissue between the vasculature and the epithelial cells (Preston, 2001). This physiological age-dependent hyposecretion is thought to be additive to the changes in the brain's waste clearance during the progression of dementia and Alzheimer's disease (AD) as mentioned later in the text. A pathophysiological hypersecretion of CSF is relatively rare and has mostly been described in connection to choroid plexus papillomas or neoplasms (Crawford and Isaacs, 2019; Crea et al., 2020). Yet, a common complication of subarachnoid hemorrhage is hydrocephalus (Chen et al., 2017). This type of hydrocephalus was previously believed to be caused by an obstruction of the CSF flow in the cerebral aqueduct or the arachnoid granulations; however, recent studies suggest that hemorrhage causes an inflammation-dependent hypersecretion of CSF by the choroid plexi (Karimy et al., 2017; Li et al., 2018). Knowledge of the mechanisms leading to hemorrhage-dependent hypersecretion could provide targets for inhibition of CSF secretion following subarachnoid hemorrhage.

CNS Diseases Associated With Altered CSF Clearance and Absorption

The progression of neurodegenerative diseases e.g., AD has been linked to attenuation of the waste clearance system. AD is an age-dependent disease marked by the accumulation of specific proteins, neurofibrillary tangles, and amyloid ß peptide, in the brain. These proteins are proposed to be cleared by the waste clearance system, thus reduced movement of CSF from the periarterial spaces to the brain parenchyma *via* AQP4 could facilitate protein accumulation in the brain (Rasmussen et al., 2018; Oliver et al., 2020). Supportive of this assumption, a study of human AD brains found that loss of AQP4 localized to the perivascular astrocytic endfeet was associated with AD (Zeppenfeld et al., 2017; Reeves et al., 2020). Altered AQP4 expression has been linked to the formation of edema following CNS injury (Sun et al., 2003; Nesic et al., 2006; Zhang et al., 2015). An early down-regulation and a late up-regulation of APQ4 expression have been found to correlate with an increased water content within spinal cord injured rats (Nesic et al., 2006).

As described previously, lymphatic vessels are essential for fluid balance and immune surveillance in tissues (Oliver et al., 2020), thus alterations in the lymphatic vessels may facilitate fluid imbalance and CNS-directed immune responses. These considerations have been addressed in mice with chemical-induced spinal cord injury, where the authors found spinal cord injury to cause lymphangiogenesis, which exacerbated immune-cell infiltration and demyelination of the spinal cord concomitant with reduced regeneration (Jacob et al., 2019). The CNS-directed immune responses have also been addressed in mice with experimental autoimmune encephalomyelitis, demonstrating that lymphatic ablation attenuated the immune response of reactive immune cells around demyelinated lesions (Louveau et al., 2018). The relationship between CNS diseases and CNS-directed immune responses as well as fluid imbalance facilitated by the lymphatic vessel may also have implications for other CNS diseases e.g., traumatic spinal cord injury.

CNS Diseases Associated With Altered CSF Movement

Disturbances in the CSF movement may influence the functioning of the waste clearance system. Thus, CNS diseases causing an obstruction in the brain or along the spinal cord, and thereby CSF movement disturbances, may promote the emergence and progress of secondary CNS diseases. This is demonstrated by the association between traumatic spinal cord injury and posttraumatic syringomyelia: a disease characterized by the formation of fluid-filled cysts within the spinal cord parenchyma (Vandertop, 2014). In mice suffering from posttraumatic syringomyelia, an increased AQP4 expression has been found, suggesting increased AQP4 expression as a driver of cyst formation (Hemley et al., 2013). Supportive of this finding, studies of traumatic spinal cord injured rats found increased APQ4 expression to be correlated with

water content within the spinal cord (Nesic et al., 2006; Pan et al., 2019). Thus, increased AQP4 expression might be implicated in CNS diseases with excessive parenchymal fluid accumulation; however, the exact mechanisms remain elusive.

As the preponderance of studies investigate the mechanisms of the CSF system and its implications for neurological diseases in the brain, our understanding is sparse when it comes to the mechanisms in the spinal cord. It does, however, seem reasonable to believe that the assumptions made in the brain, to some extent, are applicable to the spinal cord. Yet, the examples above highlight the complexity of the CSF system. Therefore, research is needed to evaluate the CSF system in a more integrative view to elucidate how changes in one part of the system lead to changes in other parts of the system.

CONCLUSION

Despite significant advances in our understanding of the CSF system, many processes remain to be elucidated. Notably, as the majority of studies focuson the brain, there is a significant knowledge gap regarding the spinal cord. Both the anatomical and physiological differences between the brain and spinal cord hamper the translation of findings found in the brain to the spinal cord, thus more research into the mechanisms in the spinal cord is warranted.

AUTHOR CONTRIBUTIONS

All authors contributed to conception and design of the work. TW and HD wrote sections of the manuscript. All authors contributed to the article and approved the submitted version.

REFERENCES

Abbott, N. J., Pizzo, M. E., Preston, J. E., Janigro, D., and Thorne, R. G. (2018). The role of brain barriers in fluid movement in the CNS: is there a 'glymphatic' system? *Acta Neuropathol.* 135, 387–407. doi: 10.1007/s00401-018-1812-4

Adigun, O.O., and Al-Dhahir, M.A. (2021). "Anatomy, head and neck, cerebrospinal fluid," *in StatPearls* [Internet], (Treasure Island, FL: StatPearls Publishing). Available online at: https://www.ncbi.nlm.nih.gov/books/NBK459286/.

Aktas , G., Kollmeier, J. M., Joseph, A. A., Merboldt, K. D., Ludwig, H. C., Gärtner, J., et al. (2019). Spinal CSF flow in response to forced thoracic and abdominal respiration. *Fluids Barriers CNS* 16:10. doi: 10.1186/s12987-019-0130-0

Amasheh, S., Wenzel, U., Boll, M., Dorn, D., Clauss, W., and Daniel, H. (1995). The proximal straight tubule (PST) basolateral cell membrane water channel: selectivity characteristics. *J. Membr. Biol.* 143, 189–197. doi: 10.1007/BF00233447

Aspelund, A., Antila, S., Proulx, S. T., Karlsen, T. V., Karaman, S., Detmar, M., et al. (2015). A dural lymphatic vascular system that drains brain interstitial fluid and macromolecules. *J. Exp. Med.* 212, 991–999. doi: 10.1084/jem.20142290

Benveinste, H., Lee, H., and Volkow, N. D. (2017). The glymphatic pathway: waste removal from the CNS *via* cerebrospinal fluid transport. *Neuroscientist* 23, 454–465. doi: 10.1177/1073858417691030

Chen, L., Beckett, A., Verma, A., and Feinberg, D. A. (2015a). Dynamics of respiratory and cardiac CSF motion revealed with real-time simultaneous multi-slice EPI velocity phase contrast imaging. *Neuroimage* 122, 281–287. doi: 10.1016/j.neuroimage.2015.07.073

Chen, L., Elias, G., Yostos, M. P., Stimec, B., Fasel, J., and Murphy, K. (2015b). Pathways of cerebrospinal fluid outflow: a deeper understanding of resorption. *Neuroradiology* 57, 139–147. doi: 10.1007/s00234-014-1461-9

Chen, Q., Feng, Z., Tan, Q., Guo, J., Tang, J., Tan, L., et al. (2017). Post-hemorrhagic hydrocephalus: recent advances and new therapeutic insights. *J. Neurol. Sci.* 375, 220–230. doi: 10.1016/j.jns.2017.01.072

Crawford, J. R., and Isaacs, H. (2019). Perinatal (fetal and neonatal) choroid plexus tumors: a review. *Child's Nerv. Syst.* 35, 937–944. doi: 10.1007/s00381-019-04135-x

Crea, A., Bianco, A., Cossandi, C., Forgnone, S., Fornaro, R., Crobeddu, E., et al. (2020). Choroid plexus carcinoma in adults: literature review and first report of a location into the third ventricle. *World Neurosurg.* 133, 302–307. doi: 10.1016/j.wneu.2019.10.051

Damkier, H. H., Brown, P. D., and Praetorius, J. (2013). Cerebrospinal fluid secretion by the choroid plexus. *Physiol. Rev.* 93, 1847–1892. doi: 10.1152/physrev.00004.2013

Daouk, J., Bouzerar, R., and Baledent, O. (2017). Heart rate and respiration influence on macroscopic blood and CSF flows. *Acta Radiol.* 58, 977–982. doi: 10.1177/0284185116676655

Dreha-Kulaczewski, S., Joseph, A. A., Merboldt, K. D., Ludwig, H. C., Gärtner, J., and Frahm, J. (2017). Identification of the upward movement of human CSF *in vivo* and its relation to the brain venous system. *J. Neurosci.* 37, 2395–2402. doi: 10.1523/JNEUROSCI.2754-16.2017

Haughton, V., and Mardal, K. A. (2014). Spinal fluid biomechanics and imaging: an update for neuroradiologists. *Am. J. Neuroradiol.* 35, 1864–1869. doi: 10.3174/ajnr.A4023

Hemley, S. J., Bilston, L. E., Cheng, S., Chan, J. N., and Stoodley, M. A. (2013). Aquaporin-4 expression in post-traumatic syringomyelia. *J. Neurotrauma* 30, 1457–1467. doi: 10.1089/neu.2012.2614

Hladky, S. B., and Barrand, M. A. (2014). Mechanisms of fluid movement into, through and out of the brain: evaluation of the evidence. *Fluids Barriers CNS* 11:26. doi: 10.1186/2045-8118-11-26

Iliff, J. J., Wang, M., Liao, Y., Plogg, B. A., Peng, W., Gundersen, G. A., et al. (2012). A paravascular pathway facilitates CSF flow through the brain parenchyma and the clearance of interstitial solutes, including amyloid β. *Sci. Transl. Med.* 4:147ra111. doi: 10.1126/scitranslmed.3003748

Jacob, L., Boisserand, L. S. B., Geraldo, L. H. M., de Brito Neto, J., Mathivet, T., Antila, S., et al. (2019). Anatomy and function of the vertebral column lymphatic network in mice. *Nat. Commun.* 10:4594. doi: 10.1038/s41467-019-12568-w

Jensen, N. A., Munk, A. S. F., Lundgaard, I., and Nedergaard, M. (2015). The glymphatic system - a beginner's guide. *Neurochem. Res.* 40, 2583–2599. doi: 10.1007/s11064-015-1581-6

Karimy, J. K., Zhang, J., Kurland, D. B., Theriault, B. C., Duran, D., Stokum, J. A., et al. (2017). Inflammation-dependent cerebrospinal fluid hypersecretion by the choroid plexus epithelium in posthemorrhagic hydrocephalus. *Nat. Med.* 23, 997–1003. doi: 10.1038/nm.4361

Kedarasetti, R. T., Drew, P. J., and Costanzo, F. (2020). Arterial pulsations drive oscillatory flow of CSF but not directional pumping. *Sci. Rep.* 10:10102. doi: 10.1038/s41598-020-66887-w

Khasawneh, A., Garling, R., and Harris, C. (2018). Cerebrospinal fluid circulation: what do we know and how do we know it? *Brain Circ.* 4, 14–18. doi: 10.4103/bc.bc_3_18

Klarica, M., Radoš, M., and Orešković, D. (2019). The movement of cerebrospinal fluid and its relationship with substances behavior in cerebrospinal and interstitial fluid. *Neuroscience* 414, 28–48. doi: 10.1016/j.neuroscience.2019.06.032

Lam, M. A., Hemley, S. J., Najafi, E., Vella, N. G. F., Bilston, L. E., and Stoodley, M. A. (2017). The ultrastructure of spinal cord perivascular spaces: implications for the circulation of cerebrospinal fluid. *Sci. Rep.* 7:12924. doi: 10.1038/s41598-017-13455-4

Li, Q., Ding, Y., Krafft, P., Wan, W., Yan, F., Wu, G., et al. (2018). Targeting germinal matrix hemorrhage-induced overexpression of sodium-coupled bicarbonate exchanger reduces posthemorrhagic hydrocephalus formation in neonatal rats. *J. Am. Heart Assoc.* 7:e007192. doi: 10.1161/JAHA.117.007192

Liu, S., Lam, M. A., Sial, A., Hemley, S. J., Bilston, L. E., and Stoodley, M. A. (2018). Fluid outflow in the rat spinal cord: the role of perivascular and paravascular pathways. *Fluids Barriers CNS* 15:13. doi: 10.1186/s12987-018-0098-1

Lloyd, R. A., Butler, J. E., Gandevia, S. C., Ball, I. K., Toson, B., Stoodley, M. A., et al. (2020). Respiratory cerebrospinal fluid flow is driven by the thoracic and lumbar spinal pressures. *J. Physiol.* 598, 5789–5805. doi: 10.1113/JP279458

Louveau, A., Herz, J., Alme, M. N., Salvador, A. F., Dong, M. Q., Viar, K. E., et al. (2018). CNS lymphatic drainage and neuroinflammation are regulated by meningeal lymphatic vasculature. *Nat. Neurosci.* 21, 1380–1391. doi: 10.1038/s41593-018-0227-9

Louveau, A., Smirnov, I., Keyes, T. J., Eccles, J. D., Sherin, J., Peske, J. D., et al. (2015). Structural and functional features of central nervous system lymphatics vessels. *Nature* 523, 337–341. doi: 10.1038/nature14432

Mestre, H., Mori, Y., and Nedergaard, M. (2020). The brain's glymphatic system: current controversies. *Trends Neurosci.* 43, 458–466. doi: 10.1016/j.tins.2020.04.003

Mestre, H., Tithof, J., Du, T., Song, W., Peng, W., Sweeney, A. M., et al. (2018). Flow of cerebrospinal fluid is driven by arterial pulsations and is reduced in hypertension. *Nat. Commun.* 9:4878. doi: 10.1038/s41467-018-07318-3

Nesic, O., Lee, J., Ye, Z., Unabia, G. C., Rafati, D., Hulsebosch, C. E., et al. (2006). Acute and chronic changes in aquaporin 4 expression after spinal cord injury. *Neuroscience* 143, 779–792. doi: 10.1016/j.neuroscience.2006.08.079

Nielsen, S., Smith, B. L., Christensen, E. I., and Agre, P. (1993). Distribution of the aquaporin CHIP in secretory and resorptive epithelia and capillary endothelia. *Proc. Natl. Acad. Sci. U S A* 90, 7275–7279. doi: 10.1073/pnas.90.15.7275

Nilsson, C., Stahlberg, F., Thomsen, C., Henriksen, O., Herning, M., and Owman, C. (1992). Circadian variation in human cerebrospinal fluid production measured by magnetic resonance imaging. *Am. J. Physiol.* 262, R20–24. doi: 10.1152/ajpregu.1992.262.1.R20

Oklinski, M. K., Lim, J. S., Choi, H. J., Oklinska, P., Skowronski, M. T., and Kwon, T. H. (2014). Immunolocalization of water channel proteins AQP1 and AQP4 in rat spinal cord. *J. Histochem. Cytochem.* 62, 598–611. doi: 10.1369/0022155414537495

Oklinski, M. K., Skowronski, M. T., Skowronska, A., Rützler, M., Nørgaard, K., Nieland, J. D., et al. (2016). Aquaporins in the spinal cord. *Int. J. Mol. Sci.* 17:2050. doi: 10.3390/ijms17122050

Oliver, G., Kipnis, J., Randolph, G. J., and Harvey, N. L. (2020). The lymphatic vasculature in the 21st century: novel functional roles in homeostasis and disease. *Cell* 182, 270–296. doi: 10.1016/j.cell.2020.06.039

Orešković, D., and Klarica, M. (2010). The formation of cerebrospinal fluid: nearly a hundred years of interpretations and misinterpretations. *Brain Res. Rev.* 64, 241–262. doi: 10.1016/j.brainresrev.2010.04.006

Orešković, D., Radoš, M., and Klarica, M. (2017). Role of choroid plexus in cerebrospinal fluid hydrodynamics. *Neuroscience* 354, 69–87. doi: 10.1016/j.neuroscience.2017.04.025

Oshio, K., Watanabe, H., Song, Y., Verkman, A. S., and Manley, G. T. (2005). Reduced cerebrospinal fluid production and intracranial pressure in mice lacking choroid plexus water channel Aquaporin-1. *FASEB J.* 19, 76–78. doi: 10.1096/fj.04-1711fje

Pan, Y. L., Guo, Y., Ma, Y., Wang, L., Zheng, S. Y., Liu, M. M., et al. (2019). Aquaporin-4 expression dynamically varies after acute spinal cord injury-induced disruption of blood spinal cord barrier in rats. *Neuropathology* 39, 181–186. doi: 10.1111/neup.12539

Preston, J. E. (2001). Ageing choroid plexus-cerebrospinal fluid system. *Microsc. Res. Tech.* 52, 31–37. doi: 10.1002/1097-0029(20010101)52:1<31::AID-JEMT5>3.0.CO;2-T

Reeves, B. C., Karimy, J. K., Kundishora, A. J., Mestre, H., Cerci, H. M., Matouk, C., et al. (2020). Glymphatic system impairment in Alzheimer's disease and idiopathic normal pressure hydrocephalus. *Trends Mol. Med.* 26, 285–295. doi: 10.1016/j.molmed.2019.11.008

Rasmussen, M. K., Mestre, H., and Nedergaard, M. (2018). The glymphatic pathway in neurological disorders. *Lancet Neurol.* 17, 1016–1024. doi: 10.1016/S1474-4422(18)30318-1

Sandrone, S., Moreno-Zambrano, D., Kipnis, J., and van Gijn, J. (2019). A (delayed) history of the brain lymphatic system. *Nat. Med.* 25, 538–540. doi: 10.1038/s41591-019-0417-3

Spector, R., Keep, R. F., Robert Snodgrass, S., Smith, Q. R., and Johanson, C. E. (2015). A balanced view of choroid plexus structure and function: Focus on adult humans. *Exp. Neurol.* 267, 78–86. doi: 10.1016/j.expneurol.2015.02.032

Sun, M. C., Honey, C. R., Berk, C., Wong, N. L. M., and Tsui, J. K. C. (2003). Regulation of aquaporin-4 in a traumatic brain injury model in rats. *J. Neurosurg.* 98, 565–569. doi: 10.3171/jns.2003.98.3.0565

Syková, E. (2008). Diffusion in brain extracellular space. *Physiol. Rev.* 88, 1277–1340. doi: 10.1152/physrev.00027.2007

Takizawa, K., Mattsumae, M., Hayashi, N., Hirayama, A., Sano, F., Yatsushiro, S., et al. (2018). The choroid plexus of the lateral ventricle as the origin of CSF pulsation is questionable. *Neurol. Med. Chir. (Tokyo)* 58, 23–31. doi: 10.2176/nmc.oa.2017-0117

Takizawa, K., Matsumae, M., Sunohara, S., Yatsushiro, S., and Kuroda, K. (2017). Characterization of cardiac and respiratory-driven cerebrospinal fluid motion based on asynchronous phase-contrast magnetic resonance imaging in volunteers. *Fluids Barriers CNS* 14:25. doi: 10.1186/s12987-017-0074-1

Tamura, R., Yoshida, K., and Toda, M. (2020). Current understanding of lymphatic vessels in the central nervous system. *Neurosurg. Rev.* 43, 1055–1064. doi: 10.1007/s10143-019-01133-0

Thomas, J. H. (2019). Fluid dynamics of cerebrospinal fluid flow in perivascular spaces. *J. R. Soc. Interface* 16:20190572. doi: 10.1098/rsif.2019.0572

Trillo-Contreras, J., Toledo-Aral, J., Echevarría, M., and Villadiego, J. (2019). AQP1 and AQP4 contribution to cerebrospinal fluid homeostasis. *Cells* 8:197. doi: 10.3390/cells8020197

Vandertop, W. P. (2014). Syringomyelia. *Neuropediatrics* 45, 3–9. doi: 10.1055/s-0033-1361921

Wei, F., Zhang, C., Xue, R., Shan, L., Gong, S., Wang, G., et al. (2017). The pathway of subarachnoid CSF moving into the spinal parenchyma and the role of astrocytic aquaporin-4 in this process. *Life Sci.* 182, 29–40. doi: 10.1016/j.lfs.2017.05.028

Yamada, S., Miyazaki, M., Yamashita, Y., Ouyang, C., Yui, M., Nakahashi, M., et al. (2013). Influence of respiration on cerebrospinal fluid movement using magnetic resonance spin labeling. *Fluids Barriers CNS* 10:36. doi: 10.1186/2045-8118-10-36

Yildiz, S., Thyagaraj, S., Jin, N., Zhong, X., Heidari Pahlavian, S., Martin, B. A., et al. (2017). Quantifying the influence of respiration and cardiac pulsations on cerebrospinal fluid dynamics using real-time phase-contrast MRI. *J. Magn. Reson. Imaging* 46, 431–439. doi: 10.1002/jmri.25591

Zeppenfeld, D. M., Simon, M., Haswell, J. D., D'Abreo, D., Murchison, C., Quinn, J. F., et al. (2017). Association of perivascular localization of aquaporin-4 with cognition and Alzheimer disease in aging brains. *JAMA Neurol.* 74, 91–99. doi: 10.1001/jamaneurol.2016.4370

Zhang, C., Chen, J., and Lu, H. (2015). Expression of aquaporin-4 and pathological characteristics of brain injury in a rat model of traumatic brain injury. *Mol. Med. Rep.* 12, 7351–7357. doi: 10.3892/mmr.2015.4372

Conflict of Interest: The authors declare that the research was conducted in the absence of any commercial or financial relationships that could be construed as a potential conflict of interest.

Publisher's Note: All claims expressed in this article are solely those of the authors and do not necessarily represent those of their affiliated organizations, or those of the publisher, the editors and the reviewers. Any product that may be evaluated in this article, or claim that may be made by its manufacturer, is not guaranteed or endorsed by the publisher.

frontiers | Frontiers in Human Neuroscience

REVIEW
published: 24 June 2022
doi: 10.3389/fnhum.2022.924155

The Role of Brain-Derived Neurotrophic Factor Signaling in Central Nervous System Disease Pathogenesis

*Shu-Hui Dou[1], Yu Cui[2], Shu-Ming Huang[1] and Bo Zhang[1]**

[1] Department of Neuroscience, Institute of Chinese Medicine, Heilongjiang University of Chinese Medicine, Harbin, China,
[2] Department of Veterinary Medicine, College of Agriculture, Hainan University, Haikou, China

OPEN ACCESS

Edited by:
Björn H. Schott,
Leibniz Institute for Neurobiology (LG), Germany

Reviewed by:
Sonia Canterini,
Sapienza University of Rome, Italy
Rainer Hellweg,
Charité – University Medicine Berlin, Germany

***Correspondence:**
Bo Zhang
hljzyyzb@163.com

Specialty section:
This article was submitted to Brain Health and Clinical Neuroscience, a section of the journal Frontiers in Human Neuroscience

Received: *20 April 2022*
Accepted: *31 May 2022*
Published: *24 June 2022*

Citation:
Dou S-H, Cui Y, Huang S-M and Zhang B (2022) The Role of Brain-Derived Neurotrophic Factor Signaling in Central Nervous System Disease Pathogenesis. Front. Hum. Neurosci. 16:924155. doi: 10.3389/fnhum.2022.924155

Recent studies have found abnormal levels of brain-derived neurotrophic factor (BDNF) in a variety of central nervous system (CNS) diseases (e.g., stroke, depression, anxiety, Alzheimer's disease, and Parkinson's disease). This suggests that BDNF may be involved in the pathogenesis of these diseases. Moreover, regulating BDNF signaling may represent a potential treatment for such diseases. With reference to recent research papers in related fields, this article reviews the production and regulation of BDNF in CNS and the role of BDNF signaling disorders in these diseases. A brief introduction of the clinical application status of BDNF is also provided.

Keywords: brain-derived neurotrophic factor, TrkB, stroke, depression, anxiety, neurodegenerative disease

INTRODUCTION

Brain-derived neurotrophic factor (BDNF) is a small molecule dimer protein, and the main member of the neurotrophic protein family in the brain (Song et al., 2017). BDNF is widely expressed in the central nervous system (CNS), endocrine system, bone and cartilage tissue, as is particularly highly concentrated within the hippocampus and cortex in the brain. BDNF plays an important role in the survival and proliferation and differentiation of neurons and glial cells, axon growth, synapse formation, and regulation of synaptic transmission and plasticity (Nagahara and Tuszynski, 2011; Kowiański et al., 2018). Conversely, disorder of BDNF signaling induces dysfunctions in CNS. Abnormal BDNF signaling has been found in many CNS diseases, and is considered to be involved in the pathological process of the disorders, affecting the occurrence, development and prognosis. Currently, researches on mental and neurological disease (e.g., stroke, mood disorders, and neurodegenerative diseases) found that abnormal BDNF signaling is involved in the diseases. In this article, the role of BDNF in the pathogenesis of a series of CNS diseases (including brain injury after stroke, depression, anxiety disorder, and neurodegenerative diseases, such as Alzheimer's disease (AD), Parkinson's disease (PD), Huntington's disease (HD), and cerebellar ataxia) was reviewed (**Figure 1**), and the current status of research in the clinical application of BDNF and proposed future research directions are discussed.

SOURCES AND PHYSIOLOGICAL FUNCTIONS OF BRAIN-DERIVED NEUROTROPHIC FACTOR

Molecular Structure of Brain-Derived Neurotrophic Factor

Brain-derived neurotrophic factor represents the most abundant and widely studied neurotrophic factor in the mammalian nervous system. Barde et al. (1982) first isolated and purified an alkaline protein from porcine cerebrospinal fluid, which had a very similar amino acid sequence and associated biological activity with the known nerve growth factor (NGF) structure. Consequently, BDNF is collectively known as the "neurotrophin family" together with NT-3, NT-4, and NT-5, which were later cloned. The BDNF gene is located in the p13–14 region of chromosome 11, with a full length of approximately 70 kb. This gene is composed of 11 exons at the 5′ end and contains 9 functional promoters specific for tissues and brain regions (Pruunsild et al., 2007). The BDNF molecular monomer is a secretory polypeptide composed of 119 amino acid residues. The isoelectric point of the protein is 9.99, and the molecular mass is 13.15 KDa. BDNF is primarily composed of a β folding and random coil secondary structure, contains three disulfide bonds, and exists in the form of dimer *in vivo*.

Production, Existence, and Physiological Function of Brain-Derived Neurotrophic Factor

Brain-derived neurotrophic factor is produced by neurons and glial cells in the mammalian brain and is mainly distributed throughout key brain regions (e.g., the cortex, hippocampus, and cerebellum). Astrocytes are also an important source of BDNF, and BDNF released from astrocytes has been demonstrated to exhibit neuroprotective and neuroregenerative effects, such as promotion of neogenesis and development of glial cells (Quesseveur et al., 2013). In addition, astrocytes promote microglia to express BDNF by releasing cytokines, inducing microglia transformation, and regulating their function (Clarke and Barres, 2013; Louveau et al., 2015). In several pathological conditions, glial cell-derived BDNF is involved in the recovery of disease and injury repair processes.

Brain-derived neurotrophic factor exists as two forms: precursor form of BDNF (pro-BDNF) and mature form of BDNF (m-BDNF). BDNF is first translated into the pro-BDNF in the endoplasmic reticulum. Pro-BDNF is subsequently cleaved by serine proteases in the Golgi and endoplasmic reticulum to form m-BDNF (Zhao et al., 2022). Early studies showed that only m-BDNF is biologically active, while pro-BDNF as an intermediate does not exert biological function. However, recent studies confirmed that pro-BDNF can exist as a precursor form of BDNF, and also can be directly secreted from synapses extracellularly exert a variety of biological effects. Both pro-BDNF and m-BDNF presenting in neurons are released following cell membrane depolarization. In addition, there is a dynamic balance between the different forms of BDNF, and the ratio of Pro-BDNF to m-BDNF varies between specific stages and regions of brain development. Although pro-BDNF exists at higher concentrations during the early stages of brain development, m-BDNF is dominant during the mature stage. Therefore, the ratio of pro-BDNF to m-BDNF during early development is considered to represent an important factor for the regulation of brain function (Zhou et al., 2013; Qiao et al., 2017; Li et al., 2019). In contrast, m-BDNF plays an essential role in neuroprotection and synaptic plasticity following maturation.

Brain-derived neurotrophic factor binds to two types of receptors: high-affinity receptor tyrosine kinase receptor B (TrkB) and low-affinity neurotrophin factor receptor (p75NTR). BDNF binds to the receptors to activate a series of downstream signaling pathways to promote neurogenesis, neuronal growth and survival, enhance synaptic plasticity, and exert neurotrophic effects (Andero et al., 2014). BDNF binding to TrkB promotes astrocyte development. It was found that the TrkB gene knockout mice showed an incomplete astrocyte morphology, which was not able to support normal synaptic function (Holt et al., 2019). Furthermore, BDNF/TrkB can mediate hippocampal plasticity and promote the survival and integration of the hippocampal newborn neurons (Li et al., 2008).

However, BDNF binds to p75NTR may promote apoptosis and accelerate pathological process. It has been reported that the increased expression of p75NTR in the brain can reduce the neuroprotective effects of BDNF mentioned above, and the expression of p75NTR is significantly increased in some pathological conditions associated with the decline in brain function including learning and memory (Chakravarthy et al., 2012). This suggests that BDNF is bound or reduced when p75NTR is highly expressed, resulting in the competitive inhibition of TrkB (Brito et al., 2013). In addition, it has reported that pro-BDNF mainly binding to p75NTR plays a role in neuronal apoptosis and promotes synaptic long-term depression (Woo et al., 2005). On the other hand, p75NTR expression was significantly elevated in some conditions of decreased brain function. This raises the question "why the nervous system induces a pro-apoptotic molecule to respond to damage" (Ibáñez and Simi, 2012), and therefore, it is argued that p75NTR can promote apoptosis after injury to eliminate damaged cells, minimize inflammation, and maintain suitable environment for the cells (Meeker and Williams, 2015). The detailed roles of p75NTR remains to be discovered in the future.

BRAIN-DERIVED NEUROTROPHIC FACTOR AND BRAIN INJURY FOLLOWING STROKE

Stroke is a type of acute cerebrovascular disease involving a group of diseases that damage brain tissue when blood vessels in the brain burst or become blocked, which prevent blood flow to the brain. Following a stroke, there is increased risk of abnormal remodeling of the hippocampus, decreased

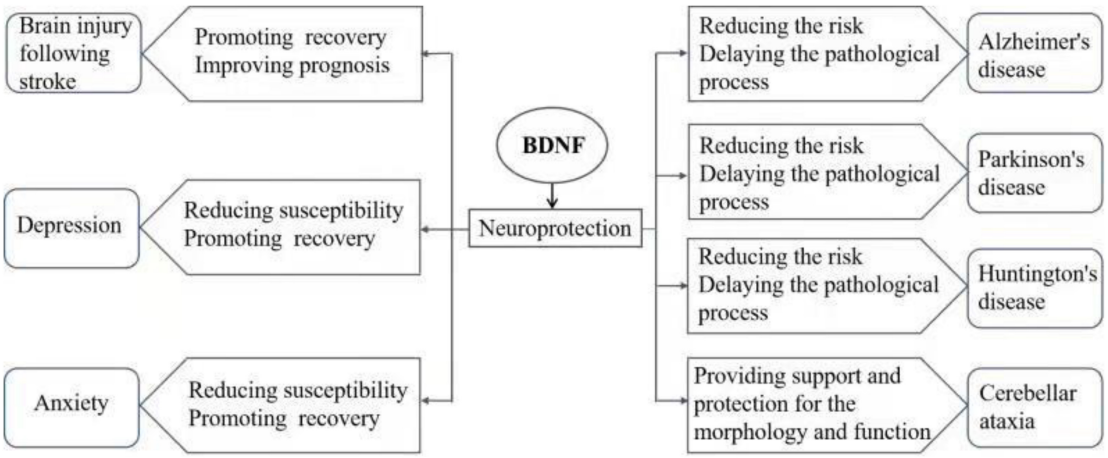

FIGURE 1 | The role of BDNF signaling in CNS disease pathogenesis.

neurogenesis and neuronal apoptosis, as well as neuron damage, which increases the risk of depression. The recovery of post-stroke injury was found to be promoted by an increase in BDNF levels (Chen et al., 2015). Furthermore, Hsu et al. (2020) found that the regulation of endogenous BDNF production could alleviate brain injury following stroke. At the same time, exogenous BDNF has been found to reduce the infarct size caused by local ischemia, protect neurons, as well as promote neuronal survival and differentiation (Kurozumi et al., 2004). BDNF improves cognitive function by improving neuronal plasticity and increasing acetylcholinesterase activity. Indeed, an intravenous injection of BDNF has been shown to enhance cognitive recovery and stimulate neurogenesis following a stroke (Schäbitz et al., 2007). In addition, BDNF supports the development, differentiation, growth, and regeneration of 5-hydroxy tryptamine (5-HT) and dopamine (DA) neurons (Levivier et al., 1995; Mamounas et al., 2000), and also promotes the generation and release of neurotransmitters and improves neurological function. The expression of BDNF was found to be triggered by brain injury as part of the neuroprotective response following a stroke (Kokaia et al., 1998). Moreover, pro-BDNF plays a role in apoptosis following its binding to the p75NTR receptor, which aggravates post-stroke depression (PSD) (Yang et al., 2021). These results indicate that regulation of the BDNF signaling pathway has the potential to treat brain injury after a stroke.

BRAIN-DERIVED NEUROTROPHIC FACTOR AND COMMON MOOD DISORDERS

Brain-Derived Neurotrophic Factor and Depression

Depression represents one of the most common emotional disorders and is characterized by an abnormal and persistent low mood. Depression is also accompanied by cognitive and physical changes, including anhedonia, slow response, and loss of appetite. Moreover, depression is associated with both a high recurrence and suicide rate. The neurotrophic factor hypothesis holds that a decrease in neurotrophic factors is the pathological basis of depression (Levy et al., 2018). Thus, increasing or restoring the content of BDNF can help reverse brain damage and promote the expression of nutritional proteins, which is an antidepressant effect. The study by Saarelainen et al. (2003) confirmed the role of endogenous BDNF, which was found increase of the release of BDNF and BDNF-TrkB signal transduction in the brain following the administration of antidepressants. Infusion of BDNF into the midbrain of mice with learned helplessness was found to improve depressive-like behavior; however, its antidepressant effect disappeared following the administration with a TrkB inhibitor (Siuciak et al., 1997; Shirayama et al., 2002). This finding confirms that alterations in the BDNF-TrkB pathway led to a reduction in neurogenesis, which indicated that BDNF-TrkB signaling plays a key role in the pathophysiology of depression and mechanism of antidepressant treatment (Shirayama et al., 2002). Hayley et al. (2015) reported that the level of BDNF in the brains of depressed patients with suicidal tendency was lower than that of patients without suicidal tendency, suggesting that the level of BDNF may be related to the severity of depression. More severe the depressive symptoms were associated with lower levels of BDNF in the brain. An imbalance of production and release of 5-HT is the main cause of major depressive disorder (MDD). Moreover, BDNF can promote the function and growth of 5-HT neurons in the brain (Mamounas et al., 2000), indicating that the level of BDNF in MDD is critical. Some scholars believe that levels of serum BDNF can represent the levels of BDNF in the brain to a certain extent, which may be used as an indicator to evaluate the severity of depressive symptoms (Peng et al., 2018). However, Hellweg et al. (2008) tested BDNF levels in depressed patients with

different antidepressants and found that changes in serum concentrations caused by antidepressants depended on the drugs rather than the general pathophysiological response of the subjects after antidepressant administration. Many studies have shown that BDNF is closely related to depression, however, the relationship between BDNF levels and the severity, remission, and recurrence of depression; the effect and enhanced expression of antidepressants on BDNF, the maintenance of long-term antidepressant treatment and the examination of ideal BDNF levels remain to be explored.

Brain-Derived Neurotrophic Factor and Anxiety

Anxiety, also known as anxiety neurosis, exists as two clinically common forms: generalized anxiety and panic disorder. Generalized anxiety is characterized by continuous nervousness, excessive alertness, and autonomic nervous dysfunction. Panic disorder is characterized by recurrent autonomic symptoms (e.g., palpitation, sweating, and tremors), as well as an irrational fear of unfortunate consequences. Epidemiological studies have revealed that approximately 30% anxiety disorder cases are hereditary. Anxiety disorder is an organic disease with physiological and biochemical abnormalities in the brain, particularly those associated with changes in the amygdala, hippocampus, hypothalamus, and frontal cortex (Mah et al., 2016). The BDNF Val66Met polymorphism is the most common structural variation of BDNF, in which a valine (Val) at codon 66 is replaced by methionine (Met). The Met allele affects the secretion and transportation of BDNF within cells (Egan et al., 2003). As a result, changes in the spatial conformation of the synaptic cleft and the growth morphology of neurons lead to the degeneration of the neural structure and an impairment in synaptic plasticity. In a study of BDNF polymorphisms, it was found that adults with the Met allele had poorer memory and smaller hippocampal volume compared with that of normal adults (Lim et al., 2017). Since BDNF is concentrated in the hippocampus and amygdala, the BDNF mononucleotide polymorphism, Val66Met, has been implicated in the pathogenesis of anxiety disorder (Mühlberger et al., 2014; Meier and Deckert, 2019). Chen et al. (2006) found that compared with normal mice, $BDNF_{Met}$ mice had impaired memory and reduced hippocampal volume due to changes in the dendritic shape of the dentate gyrus, confirming that decreased BDNF signaling can lead to damage to hippocampal morphology and function, and these changes may increase anxiety-related behavior. Therefore, the Val66Met polymorphism of the BDNF gene could affect both hippocampal structure and function (Bueller et al., 2006). Additionally, external factors (e.g., social stress) can lead to anxiety, as the levels of brain BDNF have been found to decrease under stressful environment (Berry et al., 2012). Although there is no definitive explanation for the relationship between these genes and anxiety, the discovery of BDNF Val66Met continues to hold promise for the development of effective drugs that target these genes for the treatment of anxiety disorders.

BRAIN-DERIVED NEUROTROPHIC FACTOR AND NEURODEGENERATIVE DISEASES

Brain-Derived Neurotrophic Factor and Alzheimer's Disease

Alzheimer's disease is the most common type of dementia, characterized by progressive cognitive decline (e.g., memory, language, and behavior), resulting in the loss of the ability to use tools of daily life and carry out basic activities (No authors listed, 2020). The pathological characteristics of AD consist of the senile plaques formed by the accumulation of β-amyloid peptide (Aβ) outside of brain neurons, neurofibrillary tangles produced by the hyperphosphorylation of tau protein in the neurons and loss of neurons (Soria Lopez et al., 2019). A study has shown that Aβ decreases the level of BDNF primarily by reducing phosphorylated cAMP response element binding protein (CREB) (Garzon and Fahnestock, 2007). Furthermore, the hyperphosphorylation of tau protein downregulates the BDNF transcription process both *in vivo* and *in vitro*, while tau protein knockdown partially rescues the Aβ induced BDNF downregulation (Rosa et al., 2016). Injection of BDNF into the hippocampus of AD model mice can rescue the deficits of hippocampal synaptic long term potentiation (Nagahara et al., 2009). There are pathological changes in the AD cerebellum including granule cell dendrites and dendritic spine loss and Purkinje cell loss (Larner, 1997), and it has been found that exogenous BDNF can improve the pathology in the cerebellum associated with AD (Carter et al., 2002). The above confirmed that BDNF expression is closely related to AD pathological process. The study by Buchman et al. (2016) evaluated the cognition of 535 elderly participants year by year, and the level of BDNF in their brain after death was measured. The rate of cognitive decline was negatively correlated with the level of BDNF expression in the brain. Further analysis showed that the relationship between AD pathology and the rate of cognitive decline differed due to the level of BDNF expression. Rex et al. (2006) considered that BDNF and its receptor (TrkB) were impaired with age in AD patients. It was also suggested that β-amyloid protein was detrimental to the production and signaling of BDNF. In addition, exercise helps to increase the levels of BDNF, which can improve AD performance to some extent (Laurin et al., 2001; Etnier et al., 2016; Choi et al., 2018). Taken together, BDNF can reduce the toxicity of Aβ to neurons and enhance learning and memory capability. Thus, the application of BDNF may potentially be used to prevent and treat AD.

Brain-Derived Neurotrophic Factor and Parkinson's Disease

Parkinson's disease is the second most common neurodegenerative disease after AD. The primary pathological change is the degeneration and death of dopamine (DA) neurons in the substantia nigra of the midbrain, which leads to a significant decrease in the level of DA in the striatum. The cause of DA neuron death is not fully understood, and the intracellular

accumulation of a-synuclein is thought to be mainly responsible for the loss of the neurons. The main histopathological features of PD are the presence of dystrophic neurons and Lewy bodies in the surviving neurons (Wakabayashi et al., 2007). Clinically, PD manifests primarily as static tremor, bradykinesia, myotonia, and postural gait disorder. Moreover, the prevalence rate increases with age (Frisardi et al., 2016). BDNF can promote the survival and differentiation of dopaminergic neurons and inhibit the degeneration of dopaminergic neurons caused by neurotoxicity, thereby improving PD (Kim et al., 2021). The study by Huang et al. (2019) found that the decrease in the level of peripheral BDNF/TrkB in PD patients was directly related to the degeneration of dopaminergic neurons. In an experiment involving monkeys, PD symptoms were significantly alleviated in the BDNF treatment group (Tsukahara et al., 1995). Moreover, BDNF Val66Met has also been indicated to be related to PD cognitive impairment (Altmann et al., 2016). Moreover, overexpression of a-synuclein downregulates the transcription and transport of BDNF in the neurons (Yuan et al., 2010). Levivier et al. (1995) used genetic engineering technology to study a rat model of PD and found that the transplantation of BDNF-producing fibroblasts into the brain could prevent the degeneration of dopamine neurons in the brain of adult rats. This finding provided direct evidence for the treatment of PD neurodegeneration by gene therapy and neurotrophic factors (e.g., BDNF).

Brain-Derived Neurotrophic Factor and Huntington's Disease

Huntington's disease, also known as chronic progressive dance disease, is a slow onset hereditary neurodegenerative disease, with an incidence of approximately 1 in 10,000 people. HD patients tend to appear between 30 and 40 years old and primarily manifest as involuntary dance-like body movements, cognitive dysfunction, and mental disorders. HD is an autosomal dominant neurodegenerative disease, which is primarily caused by a mutation in the Huntingtin (HTT) gene on chromosome 4, producing the mutated Huntingtin protein, which is widely expressed in neurons (No authors listed, 1993). Studies have shown that HTT is an antiapoptotic protein in striatum cells, which can prevent caspase activation. In the cells of the CNS, HTT expression can protect from lethal stimulation under normal condition (Bhide et al., 1996). However, this intracellular protein metabolic disorder causes an over-aggregation to form large molecular clusters, which will affect the normal function of nerve cells and lead to the occurrence of HD. HTT over-expression is particularly observed in damaged neurons in the striatum (Reiner et al., 1988). Yu et al. (2018) showed that the toxicity generated during the aggregation of small HTT fragments could lead to neuronal death, and BDNF expression in the striatum was also decreased. This was because BDNF was produced by the cerebral cortex and subsequently transported to the striatum. A mutation in HTT decreases the expression of BDNF, which is also associated with a reduction in the level of BDNF in the striatum (Zuccato et al., 2001). Furthermore, the activity of the BDNF/TrkB pathway was reduced by HTT and in turn aggravates striatum neuron injury, in human cerebral cortex samples, examined at postmortem, confirmed that the level of cerebral cortex BDNF in HD patients was found to be significantly lower (Zuccato et al., 2008). These findings suggest that BDNF signaling is involved in the occurrence and development of HD, and the regulation of BDNF signaling may have the potential to treat HD.

Brain-Derived Neurotrophic Factor and the Cerebellar Ataxia

The cerebellum is responsible for coordination and fine regulation of movement, and its dysfunction can cause motor ataxia. BDNF is highly expressed in cerebellar granule cells and Purkinje cells, and BDNF deficiency can result in abnormality of morphology of the cells, especially their synapses (Carter et al., 2002; Salomova et al., 2020). In BDNF knockout mice, migration of cerebellar granule cells is impaired, and is relieved after administration of exogenous BDNF (Borghesani et al., 2002). Stg mouse is a mutant mouse model with cerebellar ataxia, BDNF is significantly reduced in the cerebellum other than other brain regions of the mouse (Qiao et al., 1996). Meng et al. (2007) produced stg-BDNF double mutant mice by crossing stg mice with BDNF over-expression transgenic mice. Compared with stg mice, the coordination of movements of stg-BDNF mice was significantly improved. Moreover, a study showed that after human limbs had been trained, the volume of cerebellar gray matter and the level of BDNF in the saliva of the subjects increased, and a positive correlation was found between the two parameters (Ben-Soussan et al., 2015). All of these indicate that BDNF provides important support for the morphology and function of cerebellum.

CLINICAL APPLICATION OF BRAIN-DERIVED NEUROTROPHIC FACTOR

Although a large number of preclinical studies have provided evidence regarding the therapeutic potential of BDNF, it has been difficult to translate the work into clinical practice. The study by Benraiss et al. (2013) used an adeno-associated virus (AAV) vector to express BDNF in striatum neurons, and proved that AAV delivered BDNF-induced neurogenesis and promoted longer neuron survival in a mouse model of HD. Despite this success, the clinical use of AAV remains difficult due to the immunogenicity and biological distribution of the virus in the host (Hudry and Vandenberghe, 2019). Furthermore, BDNF has an extremely short half-life, which severely limits the effectiveness of recombinant proteins. The use of recombinant proteins is riddled with problems, including protein degradation, the immune response, and inability to cross the blood-brain barrier in large quantities. Currently, a variety of drug delivery methods have been explored in preclinical studies, including: (1) intracerebral perfusion or intracerebral injection; (2) route of viral gene therapy administration; (3) liposome encapsulated drugs; and (4) monoclonal antibody conjugated

drugs for intravenous administration. However, each method has its drawbacks, and there is currently a lack of safe and effective delivery methods in clinical practice.

OUTLOOK AND SUMMARY

Multiple studies have demonstrated that BDNF has therapeutic potential for promoting axonal regeneration, maintaining synaptic strength, preventing neuron loss in several neurodegenerative disease models, and inducing neuronal redifferentiation in acute CNS injury. However, the current understanding of the role and mechanism of BDNF in CNS diseases is not intensive, and many aspects must be explored further. Some examples of such questions include: what is the mechanism by which BDNF mediates structural and functional plasticity in the CNS under physiological circumstances? What is the specific mechanism of BDNF production, neuroprotective effect, and regulation of glial cell function in acute brain injury (e.g., stroke or brain trauma) and its recovery period? What are the changes that occur in the production and protective effects of BDNF in the pathological process of chronic ischemic brain injury (e.g., chronic hypoperfusion) and neurodegenerative diseases (e.g., AD and PD)? On the other hand, the establishment and improvement of the determination of the level of BDNF in the brain of patients in clinical application; the definition of clinical significance of peripheral and central BDNF levels in CNS disease pathogenesis; the methods by which exogenous BDNF efficiently permeates the blood-brain barrier and accurately reaches the lesion location remain to be further explored. Taken together, these findings indicate that BDNF and its downstream signaling play a key role under normal conditions, as well as in the pathological states of many neurological diseases. However, its detailed mechanism and application remains to be clarified and established in future studies.

This article discusses the role of BDNF in the pathogenesis of CNS diseases, providing a new theoretical reference for the exploration of the pathogenesis of CNS diseases, as well as their clinical diagnosis and treatment. Future in-depth studies on BDNF will be of great significance for determining the diagnosis and treatment of the neurological diseases mentioned in this article. It is believed that with further development of clinical application methods, BDNF will become an effective means of treating these diseases in the future.

AUTHOR CONTRIBUTIONS

S-HD wrote the manuscript. YC wrote part of the manuscript. S-MH and BZ provided the critical comments and revised the manuscript. All authors approved the final draft and agreed to be accountable for all aspects of the work.

FUNDING

This work was supported by National Natural Science Foundation of China (Nos. 81873108 and 81603321), University Nursing Program for Young Scholars with Creative Talents in Heilongjiang Province (No. UNPYSCT-2017216), Excellent Creative Talents Support Program of Heilongjiang University of Chinese Medicine (No. 2018RCQ08), and Research Foundation of Heilongjiang University of Chinese Medicine (No. 2019BJP02).

REFERENCES

Altmann, V., Schumacher-Schuh, A. F., Rieck, M., Callegari-Jacques, S. M., Rieder, C. R., and Hutz, M. H. (2016). Val66Met BDNF polymorphism is associated with Parkinson's disease cognitive impairment. *Neurosci. Lett.* 615, 88–91.

Andero, R., Choi, D. C., and Ressler, K. J. (2014). BDNF-TrkB receptor regulation of distributed adult neural plasticity, memory formation, and psychiatric disorders. *Prog. Mol. Biol. Transl. Sci.* 122, 169–192. doi: 10.1016/B978-0-12-420170-5.00006-4

Barde, Y. A., Edgar, D., and Thoenen, H. (1982). Purification of a new neurotrophic factor from mammalian brain. *EMBO J.* 1, 549–553. doi: 10.1002/j.1460-2075.1982.tb01207.x

Benraiss, A., Toner, M. J., Xu, Q., Bruel-Jungerman, E., Rogers, E. H., and Wang, F. (2013). Sustained mobilization of endogenous neural progenitors delays disease progression in a transgenic model of Huntington's disease. *Cell Stem Cell* 12, 787–799. doi: 10.1016/j.stem.2013.04.014

Ben-Soussan, T. D., Piervincenzi, C., Venditti, S., Verdone, L., Caserta, M., and Carducci, F. (2015). Increased cerebellar volume and BDNF level following quadrato motor training. *Synapse* 69, 1–6. doi: 10.1002/syn.21787

Berry, A., Bellisario, V., Capoccia, S., Tirassa, P., Calza, A., and Alleva, E. (2012). Social deprivation stress is a triggering factor for the emergence of anxiety- and depression-like behaviours and leads to reduced brain BDNF levels in C57BL/6J mice. *Psychoneuroendocrinology* 37, 762–772. doi: 10.1016/j.psyneuen.2011.09.007

Bhide, P. G., Day, M., Sapp, E., Schwarz, C., Sheth, A., and Kim, J. (1996). Expression of normal and mutant huntingtin in the developing brain. *J. Neurosci.* 16, 5523–5535. doi: 10.1523/JNEUROSCI.16-17-05523.1996

Borghesani, P. R., Peyrin, J. M., Klein, R., Rubin, J., Carter, A. R., and Schwartz, P. M. (2002). BDNF stimulates migration of cerebellar granule cells. *Development* 129, 1435–1442. doi: 10.1242/dev.129.6.1435

Brito, V., Puigdellívol, M., Giralt, A., del Toro, D., Alberch, J., and Ginés, S. (2013). Imbalance of p75(NTR)/TrkB protein expression in Huntington's disease: implication for neuroprotective therapies. *Cell Death Dis.* 4:e595. doi: 10.1038/cddis.2013.116

Buchman, A. S., Yu, L., Boyle, P. A., Schneider, J. A., De Jager, P. L., and Bennett, D. A. (2016). Higher brain BDNF gene expression is associated with slower cognitive decline in older adults. *Neurology* 86, 735–741. doi: 10.1212/WNL.0000000000002387

Bueller, J. A., Aftab, M., Sen, S., Gomez-Hassan, D., Burmeister, M., and Zubieta, J. K. (2006). BDNF Val66Met allele is associated with reduced hippocampal volume in healthy subjects. *Biol. Psychiatry* 59, 812–815. doi: 10.1016/j.biopsych.2005.09.022

Carter, A. R., Chen, C., Schwartz, P. M., and Segal, R. A. (2002). Brain-derived neurotrophic factor modulates cerebellar plasticity and synaptic ultrastructure. *J. Neurosci.* 22, 1316–1327. doi: 10.1523/JNEUROSCI.22-04-01316.2002

Chakravarthy, B., Ménard, M., Ito, S., Gaudet, C., Dal Prà, I., and Armato, U. (2012). Hippocampal membrane-associated p75NTR levels are increased in Alzheimer's disease. *J. Alzheimers Dis.* 30, 675–684. doi: 10.3233/JAD-2012-120115

Chen, H. H., Zhang, N., Li, W. Y., Fang, M. R., Zhang, H., and Fang, Y. S. (2015). Overexpression of brain-derived neurotrophic factor in the hippocampus protects against post-stroke depression. *Neural Regen. Res.* 10, 1427–1432. doi: 10.4103/1673-5374.165510

Chen, Z. Y., Jing, D., Bath, K. G., Ieraci, A., Khan, T., and Siao, C. J. (2006). Genetic variant BDNF (Val66Met) polymorphism alters anxiety-related behavior. *Science* 314, 140–143. doi: 10.1126/science.1129663

Choi, S. H., Bylykbashi, E., Chatila, Z. K., Lee, S. W., Pulli, B., and Clemenson, G. D. (2018). Combined adult neurogenesis and BDNF mimic exercise effects on cognition in an Alzheimer's mouse model. *Science* 361:6406. doi: 10.1126/science.aan8821

Clarke, L. E., and Barres, B. A. (2013). Emerging roles of astrocytes in neural circuit development. *Nat. Rev. Neurosci.* 14, 311–321. doi: 10.1038/nrn3484

Egan, M. F., Kojima, M., Callicott, J. H., Goldberg, T. E., Kolachana, B. S., and Bertolino, A. (2003). The BDNF val66met polymorphism affects activity-dependent secretion of BDNF and human memory and hippocampal function. *Cell* 112, 257–269.

Etnier, J. L., Wideman, L., Labban, J. D., Piepmeier, A. T., Pendleton, D. M., and Dvorak, K. K. (2016). The Effects of Acute Exercise on Memory and Brain-Derived Neurotrophic Factor (BDNF). *J. Sport Exerc. Psychol.* 38, 331–340. doi: 10.1123/jsep.2015-0335

Frisardi, V., Santamato, A., and Cheeran, B. (2016). Parkinson's Disease: New Insights into Pathophysiology and Rehabilitative Approaches. *Parkinsons Dis.* 2016:3121727. doi: 10.1155/2016/3121727

Garzon, D. J., and Fahnestock, M. (2007). Oligomeric amyloid decreases basal levels of brain-derived neurotrophic factor (BDNF) mRNA via specific downregulation of BDNF transcripts IV and V in differentiated human neuroblastoma cells. *J. Neurosci.* 27, 2628–2635. doi: 10.1523/JNEUROSCI.5053-06.2007

Hayley, S., Du, L., Litteljohn, D., Palkovits, M., Faludi, G., and Merali, Z. (2015). Gender and brain regions specific differences in brain derived neurotrophic factor protein levels of depressed individuals who died through suicide. *Neurosci. Lett.* 600, 12–16. doi: 10.1016/j.neulet.2015.05.052

Hellweg, R., Ziegenhorn, A., Heuser, I., and Deuschle, M. (2008). Serum concentrations of nerve growth factor and brain-derived neurotrophic factor in depressed patients before and after antidepressant treatment. *Pharmacopsychiatry* 41, 66–71. doi: 10.1055/s-2007-1004594

Holt, L. M., Hernandez, R. D., Pacheco, N. L., Torres Ceja, B., Hossain, M., and Olsen, M. L. (2019). Astrocyte morphogenesis is dependent on BDNF signaling via astrocytic TrkB.T1. *eLife* 8:e44667. doi: 10.7554/eLife.44667

Hsu, C. C., Kuo, T. W., Liu, W. P., Chang, C. P., and Lin, H. J. (2020). Calycosin Preserves BDNF/TrkB Signaling and Reduces Post-Stroke Neurological Injury after Cerebral Ischemia by Reducing Accumulation of Hypertrophic and TNF-α-Containing Microglia in Rats. *J. Neuroimmune Pharmacol.* 15, 326–339. doi: 10.1007/s11481-019-09903-9

Huang, Y., Huang, C., and Yun, W. (2019). Peripheral BDNF/TrkB protein expression is decreased in Parkinson's disease but not in Essential tremor. *J. Clin. Neurosci.* 63, 176–181. doi: 10.1016/j.jocn.2019.01.017

Hudry, E., and Vandenberghe, L. H. (2019). Therapeutic AAV Gene Transfer to the Nervous System: A Clinical Reality. *Neuron* 101, 839–862.

Ibáñez, C. F., and Simi, A. (2012). p75 neurotrophin receptor signaling in nervous system injury and degeneration: paradox and opportunity. *Trends Neurosci.* 35, 431–440. doi: 10.1016/j.tins.2012.03.007

Kim, H. I., Lee, S., Lim, J., Chung, S., Koo, T. S., and Ji, Y. G. (2021). ERRγ ligand HPB2 upregulates BDNF-TrkB and enhances dopaminergic neuronal phenotype. *Pharmacol. Res.* 165:105423. doi: 10.1016/j.phrs.2021.105423

Kokaia, Z., Andsberg, G., Yan, Q., and Lindvall, O. (1998). Rapid alterations of BDNF protein levels in the rat brain after focal ischemia: evidence for increased synthesis and anterograde axonal transport. *Exp. Neurol.* 154, 289–301. doi: 10.1006/exnr.1998.6888

Kowiański, P., Lietzau, G., Czuba, E., Waśkow, M., Steliga, A., and Moryś, J. (2018). BDNF: A Key Factor with Multipotent Impact on Brain Signaling and Synaptic Plasticity. *Cell. Mol. Neurobiol.* 38, 579–593. doi: 10.1007/s10571-017-0510-4

Kurozumi, K., Nakamura, K., Tamiya, T., Kawano, Y., Kobune, M., and Hirai, S. (2004). BDNF gene-modified mesenchymal stem cells promote functional recovery and reduce infarct size in the rat middle cerebral artery occlusion model. *Mol. Ther.* 9, 189–197. doi: 10.1016/j.ymthe.2003.10.012

Larner, A. J. (1997). The cerebellum in Alzheimer's disease: evaluating its role in cognitive decline. *Brain* 8, 203–209. doi: 10.1093/brain/awx194

Laurin, D., Verreault, R., Lindsay, J., MacPherson, K., and Rockwood, K. (2001). Physical activity and risk of cognitive impairment and dementia in elderly persons. *Arch. Neurol.* 58, 498–504. doi: 10.1001/archneur.58.3.498

Levivier, M., Przedborski, S., Bencsics, C., and Kang, U. J. (1995). Intrastriatal implantation of fibroblasts genetically engineered to produce brain-derived neurotrophic factor prevents degeneration of dopaminergic neurons in a rat model of Parkinson's disease. *J. Neurosci.* 15, 7810–7820. doi: 10.1523/JNEUROSCI.15-12-07810.1995

Levy, M. J. F., Boulle, F., Steinbusch, H. W., van den Hove, D. L. A., Kenis, G., and Lanfumey, L. (2018). Neurotrophic factors and neuroplasticity pathways in the pathophysiology and treatment of depression. *Psychopharmacology* 235, 2195–2220. doi: 10.1007/s00213-018-4950-4

Li, J., Chen, J., Ma, N., Yan, D., Wang, Y., and Zhao, X. (2019). Effects of corticosterone on the expression of mature brain-derived neurotrophic factor (mBDNF) and proBDNF in the hippocampal dentate gyrus. *Behav. Brain Res.* 365, 150–156. doi: 10.1016/j.bbr.2019.03.010

Li, Y., Luikart, B. W., Birnbaum, S., Chen, J., Kwon, C. H., and Kernie, S. G. (2008). TrkB regulates hippocampal neurogenesis and governs sensitivity to antidepressive treatment. *Neuron* 59, 399–412. doi: 10.1016/j.neuron.2008.06.023

Lim, Y. Y., Rainey-Smith, S., Lim, Y., Laws, S. M., Gupta, V., and Porter, T. (2017). BDNF Val66Met in preclinical Alzheimer's disease is associated with short-term changes in episodic memory and hippocampal volume but not serum mBDNF. *Int. Psychogeriatr.* 29, 1825–1834. doi: 10.1017/S1041610217001284

Louveau, A., Nerrière-Daguin, V., Vanhove, B., Naveilhan, P., Neunlist, M., and Nicot, A. (2015). Targeting the CD80/CD86 costimulatory pathway with CTLA4-Ig directs microglia toward a repair phenotype and promotes axonal outgrowth. *Glia* 63, 2298–2312. doi: 10.1002/glia.22894

Mah, L., Szabuniewicz, C., and Fiocco, A. J. (2016). Can anxiety damage the brain? *Curr. Opin. Psychiatry* 29, 56–63.

Mamounas, L. A., Altar, C. A., Blue, M. E., Kaplan, D. R., Tessarollo, L., and Lyons, W. E. (2000). BDNF promotes the regenerative sprouting, but not survival, of injured serotonergic axons in the adult rat brain. *J. Neurosci.* 20, 771–782. doi: 10.1523/JNEUROSCI.20-02-00771.2000

Meeker, R. B., and Williams, K. S. (2015). The p75 neurotrophin receptor: at the crossroad of neural repair and death. *Neural Regen. Res.* 10, 721–725. doi: 10.4103/1673-5374.156967

Meier, S. M., and Deckert, J. (2019). Genetics of Anxiety Disorders. *Curr. Psychiatry Rep.* 21:16.

Meng, H., Larson, S. K., Gao, R., and Qiao, X. (2007). BDNF transgene improves ataxic and motor behaviors in stargazer mice. *Brain Res.* 1160, 47–57. doi: 10.1016/j.brainres.2007.05.048

Mühlberger, A., Andreatta, M., Ewald, H., Glotzbach-Schoon, E., Tröger, C., and Baumann, C. (2014). The BDNF Val66Met polymorphism modulates the generalization of cued fear responses to a novel context. *Neuropsychopharmacology* 39, 1187–1195. doi: 10.1038/npp.2013.320

Nagahara, A. H., Merrill, D. A., Coppola, G., Tsukada, S., Schroeder, B. E., and Shaked, G. M. (2009). Neuroprotective effects of brain-derived neurotrophic factor in rodent and primate models of Alzheimer's disease. *Nat. Med.* 15, 331–337. doi: 10.1038/nm.1912

Nagahara, A. H., and Tuszynski, M. H. (2011). Potential therapeutic uses of BDNF in neurological and psychiatric disorders. *Nat. Rev. Drug Discov.* 10, 209–219. doi: 10.1038/nrd3366

No authors listed (1993). A novel gene containing a trinucleotide repeat that is expanded and unstable on Huntington's disease chromosomes. The Huntington's Disease Collaborative Research Group. *Cell* 72, 971–983.

No authors listed (2020). 2020 Alzheimer's disease facts and figures. *Alzheimers Dement.* [Epub online ahead of print]. doi: 10.1002/alz.12068

Peng, S., Li, W., Lv, L., Zhang, Z., and Zhan, X. (2018). BDNF as a biomarker in diagnosis and evaluation of treatment for schizophrenia and depression. *Discov. Med.* 26, 127–136.

Pruunsild, P., Kazantseva, A., Aid, T., Palm, K., and Timmusk, T. (2007). Dissecting the human BDNF locus: bidirectional transcription, complex splicing, and multiple promoters. *Genomics* 90, 397–406. doi: 10.1016/j.ygeno.2007.05.004

Qiao, H., An, S. C., Xu, C., and Ma, X. M. (2017). Role of proBDNF and BDNF in dendritic spine plasticity and depressive-like behaviors induced by an animal model of depression. *Brain Res.* 1663, 29–37. doi: 10.1016/j.brainres.2017.02.020

Qiao, X., Hefti, F., Knusel, B., and Noebels, J. L. (1996). Selective failure of brain-derived neurotrophic factor mRNA expression in the cerebellum of stargazer, a

mutant mouse with ataxia. *J. Neurosci.* 16, 640–648. doi: 10.1523/JNEUROSCI.16-02-00640.1996

Quesseveur, G., David, D. J., Gaillard, M. C., Pla, P., Wu, M. V., and Nguyen, H. T. (2013). BDNF overexpression in mouse hippocampal astrocytes promotes local neurogenesis and elicits anxiolytic-like activities. *Transl. Psychiatry* 3:e253. doi: 10.1038/tp.2013.30

Reiner, A., Albin, R. L., Anderson, K. D., D'Amato, C. J., Penney, J. B., and Young, A. B. (1988). Differential loss of striatal projection neurons in Huntington disease. *Proc. Natl. Acad. Sci. U.S.A.* 85, 5733–5737. doi: 10.1073/pnas.85.15.5733

Rex, C. S., Lauterborn, J. C., Lin, C. Y., Kramár, E. A., Rogers, G. A., and Gall, C. M. (2006). Restoration of long-term potentiation in middle-aged hippocampus after induction of brain-derived neurotrophic factor. *J. Neurophysiol.* 96, 677–685. doi: 10.1152/jn.00336.2006

Rosa, E., Mahendram, S., Ke, Y. D., Ittner, L. M., Ginsberg, S. D., and Fahnestock, M. (2016). Tau downregulates BDNF expression in animal and cellular models of Alzheimer's disease. *Neurobiol. Aging* 48, 135–142. doi: 10.1016/j.neurobiolaging.2016.08.020

Saarelainen, T., Hendolin, P., Lucas, G., Koponen, E., Sairanen, M., and MacDonald, E. (2003). Activation of the TrkB neurotrophin receptor is induced by antidepressant drugs and is required for antidepressant-induced behavioral effects. *J. Neurosci.* 23, 349–357. doi: 10.1523/JNEUROSCI.23-01-00349.2003

Salomova, M., Tichanek, F., Jelinkova, D., and Cendelin, J. (2020). Abnormalities in the cerebellar levels of trophic factors BDNF and GDNF in pcd and lurcher cerebellar mutant mice. *Neurosci. Lett.* 725:134870. doi: 10.1016/j.neulet.2020.134870

Schäbitz, W. R., Steigleder, T., Cooper-Kuhn, C. M., Schwab, S., Sommer, C., and Schneider, A. (2007). Intravenous brain-derived neurotrophic factor enhances poststroke sensorimotor recovery and stimulates neurogenesis. *Stroke* 38, 2165–2172. doi: 10.1161/STROKEAHA.106.477331

Shirayama, Y., Chen, A. C., Nakagawa, S., Russell, D. S., and Duman, R. S. (2002). Brain-derived neurotrophic factor produces antidepressant effects in behavioral models of depression. *J. Neurosci.* 22, 3251–3261. doi: 10.1523/JNEUROSCI.22-08-03251.2002

Siuciak, J. A., Lewis, D. R., Wiegand, S. J., and Lindsay, R. M. (1997). Antidepressant-like effect of brain-derived neurotrophic factor (BDNF). *Pharmacol. Biochem. Behav.* 56, 131–137.

Song, M., Martinowich, K., and Lee, F. S. (2017). BDNF at the synapse: why location matters. *Mol. Psychiatry* 22, 1370–1375. doi: 10.1038/mp.2017.144

Soria Lopez, J. A., González, H. M., and Léger, G. C. (2019). Alzheimer's disease. *Handb. Clin. Neurol.* 167, 231–255.

Tsukahara, T., Takeda, M., Shimohama, S., Ohara, O., and Hashimoto, N. (1995). Effects of brain-derived neurotrophic factor on 1-methyl-4-phenyl-1,2,3,6-tetrahydropyridine-induced parkinsonism in monkeys. *Neurosurgery* 37, 733–739. ; discussion 9-41. doi: 10.1227/00006123-199510000-00018

Wakabayashi, K., Tanji, K., Mori, F., and Takahashi, H. (2007). The Lewy body in Parkinson's disease: molecules implicated in the formation and degradation of alpha-synuclein aggregates. *Neuropathology* 27, 494–506. doi: 10.1111/j.1440-1789.2007.00803.x

Woo, N. H., Teng, H. K., Siao, C. J., Chiaruttini, C., Pang, P. T., and Milner, T. A. (2005). Activation of p75NTR by proBDNF facilitates hippocampal long-term depression. *Nat. Neurosci.* 8, 1069–1077. doi: 10.1038/nn1510

Yang, B., Wang, L., Nie, Y., Wei, W., and Xiong, W. (2021). proBDNF expression induces apoptosis and inhibits synaptic regeneration by regulating the RhoA-JNK pathway in an in vitro post-stroke depression model. *Transl. Psychiatry* 11:578. doi: 10.1038/s41398-021-01667-2

Yu, C., Li, C. H., Chen, S., Yoo, H., Qin, X., and Park, H. (2018). Decreased BDNF Release in Cortical Neurons of a Knock-in Mouse Model of Huntington's Disease. *Sci. Rep.* 8:16976. doi: 10.1038/s41598-018-34883-w

Yuan, Y., Sun, J., Zhao, M., Hu, J., Wang, X., and Du, G. (2010). Overexpression of alpha-synuclein down-regulates BDNF expression. *Cell. Mol. Neurobiol.* 30, 939–946. doi: 10.1007/s10571-010-9523-y

Zhao, X. P., Li, H., and Dai, R. P. (2022). Neuroimmune crosstalk through brain-derived neurotrophic factor and its precursor pro-BDNF: New insights into mood disorders. *World J. Psychiatry* 12, 379–392. doi: 10.5498/wjp.v12.i3.379

Zhou, L., Xiong, J., Lim, Y., Ruan, Y., Huang, C., and Zhu, Y. (2013). Upregulation of blood proBDNF and its receptors in major depression. *J. Affect. Disord.* 150, 776–784. doi: 10.1016/j.jad.2013.03.002

Zuccato, C., Ciammola, A., Rigamonti, D., Leavitt, B. R., Goffredo, D., and Conti, L. (2001). Loss of huntingtin-mediated BDNF gene transcription in Huntington's disease. *Science* 293, 493–498. doi: 10.1126/science.1059581

Zuccato, C., Marullo, M., Conforti, P., MacDonald, M. E., Tartari, M., and Cattaneo, E. (2008). Systematic assessment of BDNF and its receptor levels in human cortices affected by Huntington's disease. *Brain Pathol.* 18, 225–238. doi: 10.1111/j.1750-3639.2007.00111.x

Conflict of Interest: The authors declare that the research was conducted in the absence of any commercial or financial relationships that could be construed as a potential conflict of interest.

Publisher's Note: All claims expressed in this article are solely those of the authors and do not necessarily represent those of their affiliated organizations, or those of the publisher, the editors and the reviewers. Any product that may be evaluated in this article, or claim that may be made by its manufacturer, is not guaranteed or endorsed by the publisher.

frontiers | Frontiers in Surgery

TYPE Case Report
PUBLISHED 26 July 2022
DOI 10.3389/fsurg.2022.888558

OPEN ACCESS

EDITED BY
Lorelei Shoemaker,
Stanford University, United States

REVIEWED BY
Jose Cohen,
Hadassah Medical Center, Israel
Peicong Ge,
Capital Medical University, China

*CORRESPONDENCE
Bangkun Yang
bangkunyang@whu.edu.cn
Nanxiang Xiong
13971139959@163.com

†These authors have contributed equally to this work

SPECIALTY SECTION
This article was submitted to Neurosurgery, a section of the journal Frontiers in Surgery

RECEIVED 03 March 2022
ACCEPTED 12 July 2022
PUBLISHED 26 July 2022

CITATION
Wang L, Li J, Li Z, Chai S, Chen J, Xiong N and Yang B (2022) Hybrid surgery for coexistence of cerebral arteriovenous malformation and primitive trigeminal artery: A case report and literature review.
Front. Surg. 9:888558.
doi: 10.3389/fsurg.2022.888558

Hybrid surgery for coexistence of cerebral arteriovenous malformation and primitive trigeminal artery: A case report and literature review

Lesheng Wang[1,2†], Jieli Li[1†], Zhengwei Li[1], Songshan Chai[1], Jincao Chen[1], Nanxiang Xiong[1*] and Bangkun Yang[1*]

[1]Department of Neurosurgery, Zhongnan Hospital of Wuhan University, Wuhan, China, [2]Brain Research Center, Zhongnan Hospital of Wuhan University, Wuhan, China

The primitive trigeminal artery (PTA), an abnormal carotid-basilar anastomosis, forms the vascular anomaly connection between the internal carotid artery and vertebrobasilar system. Rarely, PTA can be complicated by several other cerebrovascular disease, including arteriovenous malformations (AVMs), intracranial aneurysms, moyamoya disease, and carotid-cavernous malformations. Herein, we reported a rare case of PTA combined with an AVM in a male patient. The patient was a 28-year-old male with epileptic seizures at the onset of symptoms. Magnetic resonance imaging showed abnormal signal foci and localized softening foci formation with gliosis in the right parietal temporal lobe. Furthermore, using a digital subtraction angiogram (DSA), it was found that an abnormal carotid-basilar anastomosis had developed through a PTA originating from the cavernous portion of the right internal carotid artery (ICA) and a large AVM on the surface of the right carotid artery. The lesion of AVM tightly developed and draining into superior sagittal sinus. A hybrid operating room was used for the surgery. The main feeding arteries of the AVM originating from three major arteries, including the right middle cerebral artery, the right anterior cerebral artery, and the right posterior cerebral artery, were clipped and subsequently, then the AVM was thoroughly removed. The intraoperative DSA showed that the AVM had been resected completely. Postoperative pathological examination of the resected specimen indicated the presence of an AVM. The patient recovered well after surgery and has been symptom-free for more than 3 months. In summary, the pathogenesis of the coexistence of PTA and AVM remains unknown. As highlighted in this case report, hybrid surgery can be used to remove AVMs and can improve the patients' prognosis. To our best knowledge, this is the first case in the literature of successful AVM treatment using hybrid surgery.

KEYWORDS

primitive trigeminal artery, cerebral arteriovenous malformation, hybrid surgery, case report, literature review

Introduction

The primitive trigeminal artery (PTA), also known as the persistent trigeminal artery is a relatively rare vascular anomaly characterized by the embryonic arteries that connect the internal carotid artery (ICA) to the vertebrobasilar system (1). To date, PTA has an incidence of 3–22 cases per 10,000 people (2) and an estimated incidence of 0.1%–1.0% on cerebral angiograms (3). Although the incidence of PTA is not high at present, it is commonly combined with other cerebrovascular diseases, including cerebral aneurysms (4–6), cavernous sinus fistula (7–9), trigeminal neuralgia (10, 11), and cerebral arteriovenous malformation (AVM) (12–17).

PTA is associated with a higher incidence of AVMs (approximately 4.5%) (14). Generally, patients who undergo PTA alone do not require surgery or other treatments. Other comorbidities including cerebral aneurysms and AVMs, require different management strategies and treatments. The prognosis of most patients is considered to be good. However, there have been relatively few reports of coexistence of AVMs and PTA. Herein, we present a rare case of temporal AVM with PTA in a patient who underwent hybrid surgery.

Case report

A 28-year-old male presented with sudden cerebral hemorrhage 5 years ago and underwent decompressive hemicraniectomy with hematoma evacuation. The patient recovered into a good condition after surgery. The patient experienced grand mal epileptic seizures at 5 years after surgery. The patient was treated with antiseizure medication and showed poor response. Following the onset of symptoms, the patient was admitted to our hospital. The right limbs moved freely, while the left limbs were reflexive (muscle strength grade IV). The positive Babinski sign was presented in the left lower limb. Magnetic resonance imaging showed abnormal signal foci and localized softening foci formation with gliosis in the right parietotemporal lobe (**Figures 1A–C**). Magnetic resonance angiography (MRA) indicated carotid-basilar anastomosis and the presence of vascular malformations in the right parietal temporal lobe (**Figure 1D**). Further evaluation using DSA revealed an abnormal anastomosis between the carotid and basilar arteries through a PTA originating from the cavernous portion of the right internal carotid artery (ICA) (**Figures 1E–H**). Vascular malformation is tight, and a large number of fine branching arteries from the frontotemporal branch of the right middle cerebral artery, the right anterior cerebral artery, the right posterior cerebral artery, and the right external carotid artery served as its blood supply (**Figures 1E–H**). The maximum size of the AVM was approximately 42.8 mm.

Headaches and dizziness restricted the patient's daily activities; therefore, he underwent hybrid surgery to completely resect the AVM. AVM resection was scheduled to be performed in a hybrid operating room. AVM resection and preoperative embolization were performed in a single stage. Emboli were performed *via* endovascular and intravascular embolization using a biplane flat-panel angiographic suite (UNIQ FD2020 Hybrid-OR, Philips, Eindhoven, the Netherlands) and 3D reconstruction under general anesthesia. After the incision of the skin, a 6-F guiding catheter (Medtronic, Irvine, CA, USA) was placed in the right femoral artery by a percutaneous puncture. The presurgical embolization procedure involved identifying the main supplying artery of the AVM, guiding superselective cannulation into the feeding artery with a microcatheter system, embolizing the vessels with an ethylene-vinyl copolymer (Onyx 18, Medtronic, Inc., Minneapolis, Minnesota, USA), and confirming continued injection until the feeding artery stasis (**Figure 2A**). Intraoperative DSA showed a residual AVM with an early draining vein (**Figure 2B**). Subsequently, a right-expanded subtemporal approach was adopted during surgery. The AVM is located on the surface of the right parietal temporal lobe. The AVM's major feeding artery was clipped, which arose from the right middle cerebral artery, the right anterior cerebral artery, and the right posterior cerebral artery (**Figure 2C**). The dura was cut under a microscope and observed to be tightly adherent to the brain surface tissue (**Figure 2D**). The lesion in the AVM was removed afterwards, resulting in obsolete hemorrhage in the AVM. There was an AVM with a tight venous end draining into the superior sagittal sinus. No focal regions were observed in the right hemisphere (**Figure 2E**). The final pathological examination after removal showed an irregular vascular shape consisting of various types of expanded and transparent veins and abnormal muscularized arteries. DSA was performed immediately after the AVM resection, which showed that the AVM was completely removed (**Figure 2F**). The patient recovered well postoperatively without complications. A 3e-day postoperative computed tomography scan showed good recovery of brain tissue (**Figure 2G**). The patient was in good condition without any episodes of seizures, had grade IV muscle strength in the left limb, and could take care of himself. On postoperative DSA rightward head rotation, the AVM lesion completely disappeared (**Figure 2H**).

Discussion

The PTA ranging from 0.1% to 0.6%, is an embryological anastomosis between the cavernous sinus segment of the ICA and the basilar artery and is the most common anomalous traffic between the ICA system and the vertebrobasilar system

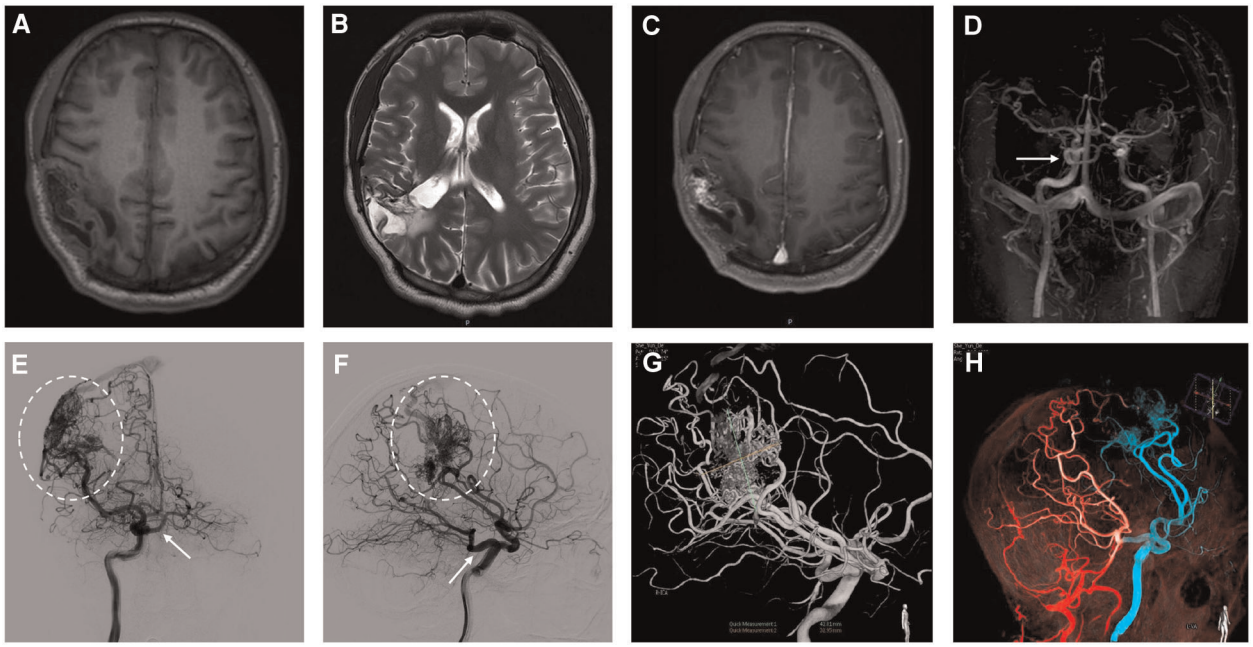

FIGURE 1
In the right parietotemporal lobe, an irregularly circular space-occupying lesion was found with slightly long T1 shadows (**A**). T2-weighted image shows a parietotemporal lesion with mixed signal characteristics (**B**). Enhanced MRI shows heterogeneous enhancement in the right parietotemporal lobe (**C**). The primitive trigeminal artery arose from the cavernous sinus segment of the right ICA (**D**). Initial right internal carotid artery injections, anteroposterior (**E**) and lateral views (**F**), show shunted flow to the cavernous sinus (arrow). Anteroposterior and lateral projection angiogram shows a right parietotemporal AVM supplied by the right middle cerebral artery drainage into the superior sagittal sinus (**E**, **F**, dashed oval). 3-dimensional (3D) DSA arterial phase indicates in the lateral projection showing AVM lesion with 42.8 mm in size and PTA obtained after right internal carotid artery injection (**G**). Fused image of 3D DSA demonstrates the flow of the right ICA (blue), VA (red) (**H**).

(18). Other anomalous anastomoses include the persistent subungual, auditory, and intersegmental arteries. The etiology of PTA may be due to the non-degeneration of the anastomosing branch between the embryonic aorta and the neural artery during the embryonic period; normally this vessel degenerates after the development of the posterior communicating artery. Some authors have suggested that the failure of trigeminal artery degeneration is due to occlusion of the proximal portion of the fetal internal carotid artery, resulting in the inevitable persistence of the trigeminal artery to maintain an adequate blood supply to the forebrain by retrograde transport of blood from the basilar artery to the carotid artery (19).

PTA was first proposed by Saltzman in 1958 and is divided into two main types (20). In Saltzman type 1, PTA supplies the vessels distal to the anastomosis, the posterior communicating arteries bilaterally, and the basilar arteries below the junction of the PTA and the basilar arteries are hypoplastic or absent. In Saltzman type II, PTA supplies the superior cerebellar arteries bilaterally, and the posterior cerebral arteries bilaterally are supplied by the ipsilateral posterior communicating arteries. Previous studies have indicated that the relative incidence of Saltzman types 1 and 2 is approximately equal (21). However, the typology proposed by Saltzman is rather general and does not elaborate on the anatomical features of PTA. Therefore, in 2011, Weon et al. proposed a new typology based on the Saltzman typology, namely the Weon typology (22). The definitions of types I and II remain consistent with those described by Saltzman et al. In the Weon type III, PTA supplies the contralateral posterior cerebral artery, and the ipsilateral posterior cerebral artery is supplied by the posterior communicating artery. In the Weon type IV, PTA supplies the ipsilateral posterior cerebral artery, and the posterior communicating artery supplies the contralateral posterior cerebral artery. In the Weon type V, all other variants of PTA, including those ending in the superior anterior inferior, and posterior inferior cerebellar arteries. Hence, according to the classification suggested by Weon et al., the case we reported belongs to Weon type V.

Associations between PTA and cerebrovascular diseases, especially with vertebrobasilar embolic ischemia, and with vascular nerve compression syndrome, have been reviewed (23–25). These could not be confirmed in large-scale studies and, therefore, represent more likely coincidental findings rather than true associations in the absence of other arterial vascular anomalies or syndromes (18). However, the pathogenesis underlying the coexistence of PPTA and MMD remains unknown.

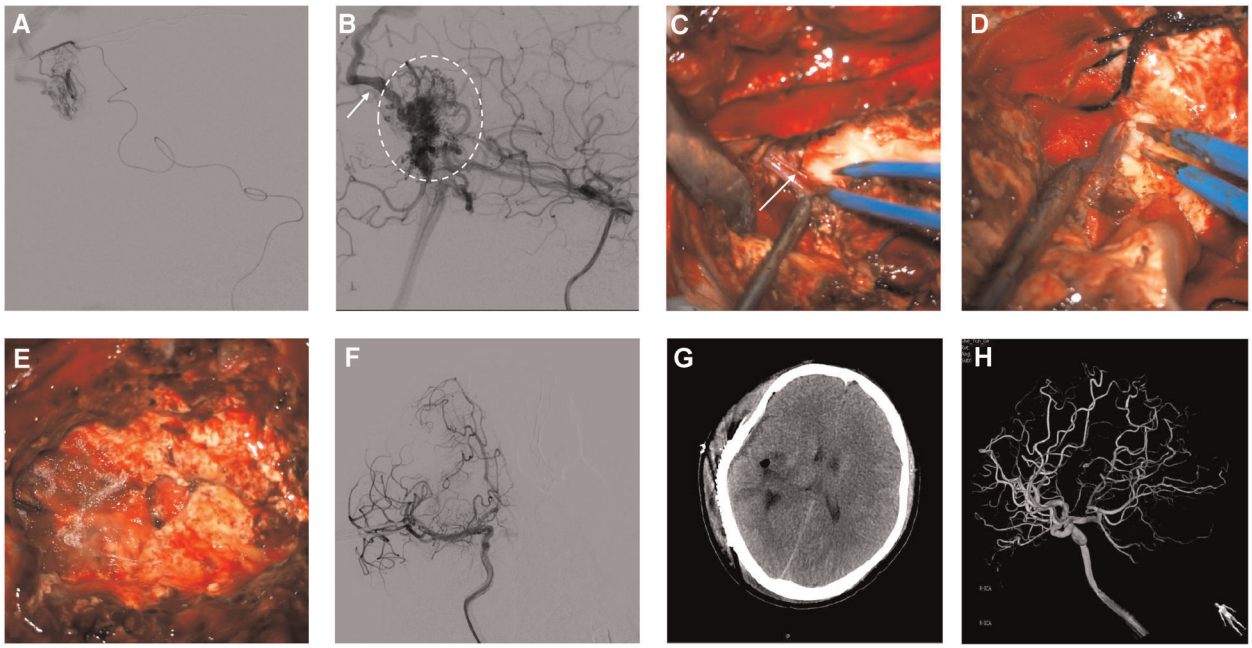

FIGURE 2
Intraoperative angiography demonstrates subsequent injection of Onyx18 with obliteration of the AVM (A). Lateral view of right ICA angiogram demonstrates the presence of residual arteriovenous malformation (dashed oval) with an early draining vein (arrow) (B). The feeding artery arteries and main draining veins were isolated and resected (C,D, arrows). Intra-operative image shows lesion excised during surgery (E). Postoperative anteroposterior projection angiograms following resection demonstrate the obliteration of the AVM (F). Postoperative Contrast CT shows no obvious significant ischemic or hemorrhage changes (G). Follow-up 3D DSA shows the complete disappearance of AVM (H).

TABLE 1 Summary of AVM associated with PTA.

No.	Author, year	Age/ Gender	Clinical Presentation	Location of PTA	Location of AVM	Treatment	Outcome
1	Jayaraman, 1977	27/Female	Subarachnoid hemorrhage	Left side	Left superior temporal lobe	Uncertain	Good
2	Uchino, 1989	16/Female	Sudden onset of severe headache and vomiting	Left side	Left Frontal lobe	Radiosurgery	Good
3	Matsko, 1991	22/Female	Unknown	Unknown	Unknown	Embolization	Good
4	Takumi, 1994	48/Female	Sudden loss of consciousness	Left side	Right parietal lobe	Microsurgery	Good
5	Nakai, 2000	58/Male	Sudden onset of headache and vomiting	Left side	Cerebellum	Conservative management	Good
6	Ohtakara, 2000	21/Female	Wallenberg's syndrome and Foville's syndrome	Left side	Brain stem and left cerebellum	Embolization and radiosurgery	Good
7	Igor, 2011	31/Female	Subarachnoid hemorrhage and cerebellar hematoma	Left side	Cerebellum	Microsurgery	Good
8	Kenichi, 2013	53/Male	Trigeminal neuralgia	Left side	Cerebellum	Embolization	Good
9	Present case	28/male	Hemmorrahge	Right side	Right temporo-parietal lobe	Hybrid surgery	Good

To our knowledge, only eight reported cases of AVM have occurred in association with PTA (**Table 1**) (12–14, 16, 26–29). In six out of the eight cases, the patients received different treatments, including microsurgery, conservative treatment, radiosurgery, embolization, and radiosurgery combined with embolization. In the remaining two cases, although the requested original texts could not be found, the good outcomes of the patients were described in their abstracts. Considering these results, the intervention would be the first option for AVMs associated with a PTA when

patients have indications of treatment. In our case, hybrid surgery was performed to remove the lesion, and the patient recovered well after the operation.

Recently, multimodality treatment, especially hybrid surgery, has received increasing attention as an effective treatment for intracranial AVMs (30, 31). Preoperative partial embolization of the malformation can assist surgical positioning, reduce blood flow to the malformation, and reduce the risk of intraoperative bleeding risk and surgical difficulty (32). Intraoperative angiography can detect the residual malformation immediately after one-stop resection, greatly reducing the residual rate of postoperative malformation and the risk of postoperative rebleeding (33–36). Despite the lack of a large number of randomized controlled trials have reported that the application of a hybrid operating room provides more satisfactory effectiveness than traditional surgery.

Conclusion

In summary, coexistence of AVM and PTA was successfully treated with hybrid surgery. A one-stop hybrid operation combining embolization and microsurgical resection could be performed as a safe and effective intervention strategy for AVMs. More follow-up data is required to determine the long-term effects of surgery.

Data availability statement

The raw data supporting the conclusions of this article will be made available by the authors, without undue reservation.

Ethics statement

Ethical review and approval was not required for the study on human participants in accordance with the local legislation and institutional requirements. The patients/participants provided their written informed consent to participate in this study.

Written informed consent was obtained from the individual(s) for the publication of any potentially identifiable images or data included in this article.

Author contributions

BY and NX contributed to the conception and design of the study. LW and JL wrote the manuscript. SC collected the patient's clinical data. JC and ZL reviewed the manuscript. All authors contributed to the article and approved the submitted version.

Funding

This article was supported by and the Science and Technology Innovation Cultivation Foundation of the Zhongnan Hospital of Wuhan University (znpy2018108).

Acknowledgments

The authors express their sincere appreciation to Ms Jianan Liu for editing the figures.

Conflict of interest

The authors declare that the research was conducted in the absence of any commercial or financial relationships that could be construed as a potential conflict of interest.

Publisher's note

References

1. Alcalá-Cerra G, Tubbs RS, Niño-Hernández LM. Anatomical features and clinical relevance of a persistent trigeminal artery. *Surg Neurol Int*. (2012) 3:111. doi: 10.4103/2152-7806.101798

2. Vasović L, Jovanović I, Ugrenović S, Vlajković S, Jovanović P, Stojanović V. Trigeminal artery: a review of normal and pathological features. *Childs Nerv Syst*. (2012) 28:33–46. doi: 10.1007/s00381-011-1622-7

3. Azab W, Delashaw J, Mohammed M. Persistent primitive trigeminal artery: a review. *Turk Neurosurg*. (2012) 22:399–406. doi: 10.5137/1019-5149.JTN.4427-11.1

4. Lam J, Shah M, Chung SL, Ho CL. Persistent primitive trigeminal artery associated with a cavernous carotid aneurysm. Case report and literature review. *J Radiol Case Rep*. (2018) 12:1–11. doi: 10.3941/jrcr.v12i11.3500

5. Ishikawa T, Yamaguchi K, Anami H, Sumi M, Ishikawa T, Kawamata T. Treatment of large or giant cavernous aneurysm associated with persistent trigeminal artery: case report and review of literature. *World Neurosurg*. (2017) 108:996.e11–e15. doi: 10.1016/j.wneu.2017.09.033

6. Sato H, Haraguchi K, Takahashi Y, Ohtaki S, Shimizu T, Matsuura N, et al. Flow-diverter stent for an unruptured aneurysm at the junction of the internal

carotid artery and persistent primitive trigeminal artery: case report and literature review. *World Neurosurg.* (2019) 132:329–32. doi: 10.1016/j.wneu.2019.08.199

7. Ishiguro T, Satow T, Okada A, Hamano E, Ikeda G, Chikuie H, et al. Spontaneous persistent primitive trigeminal artery-cavernous sinus fistula successfully treated by multipronged coil embolization: case report and literature review. *World Neurosurg.* (2019) 128:122–6. doi: 10.1016/j.wneu.2019.05.003

8. Fan Y, Li Y, Zhang T, Jiang C, Zhang P. Carotid-cavernous sinus fistula caused by persistent primitive trigeminal artery aneurysm rupture: a case report. *J Stroke Cerebrovasc Dis.* (2019) 28:104306. doi: 10.1016/j.jstrokecerebrovasdis.2019.104306

9. Shiomi K, Yamao Y, Ishii A, Kikuchi T, Okawa M, Yamada K, et al. Carotid-cavernous fistula associated with a ruptured persistent primitive trigeminal artery aneurysm: a case report and review of literature. *NMC Case Rep J.* (2021) 8:691–6. doi: 10.2176/nmccrj.cr.2021-0084

10. Sadashiva N. Microvascular decompression for trigeminal neuralgia with concomitant persistent primitive trigeminal artery. *Neurol India.* (2021) 69:826–8. doi: 10.4103/0028-3886.325353

11. Kato N, Tanaka T, Sakamoto H, Arai T, Hasegawa Y, Abe T. Identification of a persistent primitive trigeminal artery following the transposition technique for trigeminal neuralgia: a case report. *Pain Res Manage.* (2011) 16:357–9. doi: 10.1155/2011/987865

12. Abe T, Matsumoto K, Aruga T. Primitive trigeminal artery variant associated with intracranial ruptured aneurysm and cerebral arteriovenous malformation–case report. *Neurol Med Chir (Tokyo).* (1994) 34:104–7. doi: 10.2176/nmc.34.104

13. Nakai Y, Yasuda S, Hyodo A, Yanaka K, Nose T. Infratentorial arteriovenous malformation associated with persistent primitive trigeminal artery–case report. *Neurol Med Chir (Tokyo).* (2000) 40:572–4. doi: 10.2176/nmc.40.572

14. Uchino A, Matsunaga M, Ohno M. Arteriovenous malformation of the corpus callosum associated with persistent primitive trigeminal artery–case report. *Neurol Med Chir (Tokyo).* (1989) 29:429–32. doi: 10.2176/nmc.29.429

15. Uzawa A, Aotsuka A, Terano T. Cerebellar haemorrhage associated with persistent primitive trigeminal artery. *J Clin Neurosci.* (2009) 16:152–4. doi: 10.1016/j.jocn.2008.03.012

16. Ohtakara K, Kuga Y, Murao K, Kojima T, Taki W, Waga S. Posterior fossa arteriovenous malformation associated with persistent primitive trigeminal artery–case report. *Neurol Med Chir (Tokyo).* (2000) 40:169–72. doi: 10.2176/nmc.40.169

17. Garza-Mercado R, Cavazos E, Urrutia G. Persistent hypoglossal artery in combination with multifocal arteriovenous malformations of the brain: case report. *Neurosurgery.* (1990) 26:871–6. doi: 10.1097/00006123-199005000-00024

18. Meckel S, Spittau B, McAuliffe W. The persistent trigeminal artery: development, imaging anatomy, variants, and associated vascular pathologies. *Neuroradiology.* (2013) 55:5–16. doi: 10.1007/s00234-011-0995-3

19. Okuno T, Nishiguchi T, Hayashi S, Miyamoto K, Terashita T, Itakura T, et al. A case of carotid superior cerebellar artery anastomosis associated with bilateral hypoplasia of the internal carotid artery represented as the rupture of posterior cerebral artery-posterior communicating artery aneurysm. *No Shinkei Geka.* (1988) 16:1211–7.

20. Saltzman GF. Patent primitive trigeminal artery studied by cerebral angiography. *Acta Radiol.* (1959) 51:329–36. doi: 10.3109/00016925909171103

21. McKenzie JD, Dean BL, Flom RA. Trigeminal-cavernous fistula: saltzman anatomy revisited. *Am J Neuroradiol.* (1996) 17:280–2.

22. Weon YC, Choi SH, Hwang JC, Shin SH, Kwon WJ, Kang BS. Classification of persistent primitive trigeminal artery (PPTA): a reconsideration based on MRA. *Acta Radiol.* (2011) 52:1043–51. doi: 10.1258/ar.2011.110191

23. Li MH, Li WB, Pan YP, Fang C, Wang W. Persistent primitive trigeminal artery associated with aneurysm: report of two cases and review of the literature. *Acta Radiol.* (2004) 45:664–8. doi: 10.1080/02841850410001196

24. Guglielmi G, Viñuela F, Dion J, Duckwiler G, Cantore G, Delfini R. Persistent primitive trigeminal artery-cavernous sinus fistulas: report of two cases. *Neurosurgery.* (1990) 27:805–8; discussion 808–9. doi: 10.1097/00006123-199011000-00021

25. Jackson IJ, Garza-Mercado R. Persistent carotidbasilar artery anastomosis: occasionally a possible cause of tic douloureux. *Angiology.* (1960) 11:103–7. doi: 10.1177/000331976001100203

26. Jayaraman A, Garofalo M, Brinker RA, Chusid JG. Cerebral arteriovenous malformation and the primitive trigeminal artery. *Arch Neurol.* (1977) 34:96–8. doi: 10.1001/archneur.1977.00500140050009

27. Jovanović IB, Samardzić M, Nagulić M, Bascarević V, Mićović M, Milosević S. [Primitive trigeminal artery associated (corrected) with arteriovenous malformation of cerebellum]. *Vojnosanit Pregl.* (2011) 68:699–704. doi: 10.2298/vsp1108699j

28. Matsko DE, IuN Z. [Primitive trigeminal artery combined with arteriovenous malformation of the brain]. *Arkh Patol.* (1991) 53:57–60.

29. Kono K, Matsuda Y, Terada T. Resolution of trigeminal neuralgia following minimal coil embolization of a primitive trigeminal artery associated with a cerebellar arteriovenous malformation. *Acta Neurochir (Wien).* (2013) 155:1699–701. doi: 10.1007/s00701-013-1753-6

30. Grüter BE, Mendelowitsch I, Diepers M, Remonda L, Fandino J, Marbacher S. Combined endovascular and microsurgical treatment of arteriovenous malformations in the hybrid operating room. *World Neurosurg.* (2018) 117:e204–14. doi: 10.1016/j.wneu.2018.05.241

31. Fandino J, Taussky P, Marbacher S, Muroi C, Diepers M, Fathi AR, et al. The concept of a hybrid operating room: applications in cerebrovascular surgery. *Acta Neurochir Suppl.* (2013) 115:113–7. doi: 10.1007/978-3-7091-1192-5_24

32. Chen Y, Li R, Ma L, Zhao Y, Yu T, Wang H, et al. Single-stage combined embolization and resection for spetzler-martin grade III/IV/V arteriovenous malformations: a single-center experience and literature review. *Front Neurol.* (2020) 11:570198. doi: 10.3389/fneur.2020.570198

33. Lawton MT, Rutledge WC, Kim H, Stapf C, Whitehead KJ, Li DY, et al. Brain arteriovenous malformations. *Nat Rev Dis Primers.* (2015) 1:15008. doi: 10.1038/nrdp.2015.8

34. Kotowski M, Sarrafzadeh A, Schatlo B, Boex C, Narata AP, Pereira VM, et al. Intraoperative angiography reloaded: a new hybrid operating theater for combined endovascular and surgical treatment of cerebral arteriovenous malformations: a pilot study on 25 patients. *Acta Neurochir (Wien).* (2013) 155:2071–8. doi: 10.1007/s00701-013-1873-z

35. Murayama Y, Arakawa H, Ishibashi T, Kawamura D, Ebara M, Irie K, et al. Combined surgical and endovascular treatment of complex cerebrovascular diseases in the hybrid operating room. *J Neurointerv Surg.* (2013) 5:489–93. doi: 10.1136/neurintsurg-2012-010382

36. Tian J, Lin Z, Zhang J, Yang Q, Huang J, Zhang H, et al. [Combined surgical and endovascular treatments of complex cerebral arteriovenous malformation in hybrid operating room]. *Zhonghua Yi Xue Za Zhi.* (2014) 94:3763–6.

frontiers | Frontiers in Human Neuroscience

TYPE Original Research
PUBLISHED 06 September 2022
DOI 10.3389/fnhum.2022.974033

OPEN ACCESS

EDITED BY
Marcus Stoodley,
Macquarie University, Australia

REVIEWED BY
Peter Mukli,
University of Oklahoma Health Sciences Center, United States
Eugenia Eloísa Isasi,
University of the Republic, Uruguay
Davide Maselli,
King's College London, United Kingdom

*CORRESPONDENCE
Corinne M. Nielsen
nielsenc@ohio.edu

†These authors have contributed equally to this work and share first authorship

SPECIALTY SECTION
This article was submitted to Brain Health and Clinical Neuroscience, a section of the journal Frontiers in Human Neuroscience

RECEIVED 20 June 2022
ACCEPTED 15 August 2022
PUBLISHED 06 September 2022

CITATION
Selhorst S, Nakisli S, Kandalai S, Adhicary S and Nielsen CM (2022) Pathological pericyte expansion and impaired endothelial cell-pericyte communication in endothelial Rbpj deficient brain arteriovenous malformation.
Front. Hum. Neurosci. 16:974033.
doi: 10.3389/fnhum.2022.974033

Pathological pericyte expansion and impaired endothelial cell-pericyte communication in endothelial Rbpj deficient brain arteriovenous malformation

Samantha Selhorst[1,2†], Sera Nakisli[1,3†], Shruthi Kandalai[1,2], Subhodip Adhicary[1,4] and Corinne M. Nielsen[1,3,5*]

[1]Department of Biological Sciences, Ohio University, Athens, OH, United States, [2]Honors Tutorial College, Ohio University, Athens, OH, United States, [3]Neuroscience Program, Ohio University, Athens, OH, United States, [4]Translational Biomedical Sciences Program, Ohio University, Athens, OH, United States, [5]Molecular and Cellular Biology Program, Ohio University, Athens, OH, United States

Pericytes, like vascular smooth muscle cells, are perivascular cells closely associated with blood vessels throughout the body. Pericytes are necessary for vascular development and homeostasis, with particularly critical roles in the brain, where they are involved in regulating cerebral blood flow and establishing the blood-brain barrier. A role for pericytes during neurovascular disease pathogenesis is less clear—while some studies associate decreased pericyte coverage with select neurovascular diseases, others suggest increased pericyte infiltration in response to hypoxia or traumatic brain injury. Here, we used an endothelial loss-of-function Recombination signal binding protein for immunoglobulin kappa J region (Rbpj)/Notch mediated mouse model of brain arteriovenous malformation (AVM) to investigate effects on pericytes during neurovascular disease pathogenesis. We tested the hypothesis that pericyte expansion, via morphological changes, and Platelet-derived growth factor B/Platelet-derived growth factor receptor β (Pdgf-B/Pdgfrβ)-dependent endothelial cell-pericyte communication are affected, during the pathogenesis of Rbpj mediated brain AVM in mice. Our data show that pericyte coverage of vascular endothelium expanded pathologically, to maintain coverage of vascular abnormalities in brain and retina, following endothelial deletion of Rbpj. In Rbpj-mutant brain, pericyte expansion was likely attributed to cytoplasmic process extension and not to increased pericyte proliferation. Despite expanding overall area of vessel coverage, pericytes from Rbpj-mutant brains showed decreased expression of *Pdgfr*β, *Neural (N)-cadherin*, and *cluster of differentiation* (*CD)146*, as compared to controls, which likely affected Pdgf-B/Pdgfrβ-dependent communication and appositional associations between endothelial cells and pericytes in Rbpj-mutant brain microvessels. By contrast, and perhaps by compensatory

mechanism, endothelial cells showed increased expression of *N-cadherin*. Our data identify cellular and molecular effects on brain pericytes, following endothelial deletion of Rbpj, and suggest pericytes as potential therapeutic targets for Rbpj/Notch related brain AVM.

KEYWORDS

brain, endothelial, Notch, pericyte, Rbpj, vascular, arteriovenous malformation (AVM)

Introduction

Brain arteriovenous malformation (AVM) is a neurovascular disease characterized by multiple vascular abnormalities, including arteriovenous (AV) shunting—formation of direct connections between arteries and veins at the expense of capillary networks. Blood flows rapidly through these abnormal connections; thus, AVM vessels are prone to rupture, which can lead to devastating outcomes (Do Prado et al., 2019). Treatment methods for brain AVM are limited (Raper et al., 2020); therefore, it is important to understand the mechanisms of disease pathogenesis in order to develop novel therapies. Molecular and genetic studies from human tissue and animal models have revealed several signaling pathways involved in brain AVM pathogenesis, namely TGFβ (Bourdeau et al., 1999; Satomi et al., 2003; Park et al., 2009), Ras/Raf/MEK/ERK (Nikolaev et al., 2018; Fish et al., 2020), and Notch (Murphy et al., 2014; Nielsen et al., 2014). Collectively, these data support the emerging view that diverse mechanisms underlie brain AVM pathologies and diverse therapies must be developed to treat brain AVM patients safely and effectively.

Endothelial Notch signaling plays an essential role in vessel remodeling, angiogenesis, and endothelial cell specification in many vascular beds, including those in the central nervous system (CNS) (Krebs et al., 2000; Fernández-Chacón et al., 2021). We previously developed a mouse model of brain AVM, by selectively deleting Rbpj—a transcriptional regulator of canonical Notch signaling—from early postnatal endothelium in mice. Mutant mice developed AV shunts, displayed abnormal endothelial cell (EC) gene expression (suggesting disruption of arterial vs. venous EC identity), and showed altered smooth muscle cell coverage on the abnormal AV connections. In this mouse model, advanced brain AVM pathologies and 50% lethality were reported just 2 weeks post EC-Rbpj deletion (Nielsen et al., 2014); thus, endothelial Rbpj is required to prevent brain AVM formation in the early postnatal brain vasculature. Interestingly, careful regulation of Notch signaling is critical, as both loss and gain of function mutations in Notch signaling molecules result in abnormal vasculature in mice (Krebs et al., 2004; Murphy et al., 2014; Nielsen et al., 2014; Cuervo et al., 2016).

Pericytes are specialized perivascular cells closely associated with microvessels throughout the body. Pericytes and ECs are separated by a shared basement membrane, except at points of closer apposition called peg-and-socket contacts, which are typically found at the pericyte cytosolic processes that enwrap microvessels. Pericytes vary in morphology, function, and molecular signature, depending on where and when they are present (Uemura et al., 2020). Pericytes are necessary for vascular development and homeostasis and are particularly critical to brain capillaries for regulating cerebral blood flow (Bell et al., 2010, 2020; Gonzales et al., 2020) and establishing the blood-brain barrier (BBB) (Armulik et al., 2010; Daneman et al., 2010). Such developmental and functional influences on microvessels rely on intercellular signaling events between ECs and pericytes, permitting a "molecular crosstalk" that regulates vascular homeostasis.

Notch signaling is involved in EC-pericyte communication and association, by influencing pericyte maturation and recruitment to vessels (Liu et al., 2010; Gu et al., 2012). Notch achieves this, in part, by regulating Pdgf-B-Pdgfrβ signaling (Jin et al., 2008; Yao et al., 2011). In vasculature, Pdgf-B ligands are expressed and secreted by ECs (Battegay et al., 1994), while their membrane-localized Pdgf receptors are expressed primarily by pericytes (Winkler et al., 2010). In the CNS, impaired Pdgf-B-Pdgfrβ signaling leads to reduced pericyte coverage, vessel instability, and compromised BBB function (Armulik et al., 2010; Daneman et al., 2010; Nikolakopoulou et al., 2017). N-cadherin, another molecule involved in EC-pericyte interaction, is a membrane-spanning protein expressed on both ECs and pericytes (Gerhardt et al., 2000). N-cadherin mediates EC-pericyte communication, downstream of Pdgf-B-Pdgfrβ signaling, via direct contact between neighboring cells, and one study has implicated Notch and TGFβ as co-activators of N-cadherin (Li et al., 2011). Thus, Notch signaling promotes pericyte recruitment and adhesion to microvessels during normal neurovascular morphogenesis.

While pericytes are important for development and maintenance of the neurovascular system, a role for pericytes during neurovascular disease pathogenesis is

less clear. Pericyte response to neurovascular disease (e.g., cerebrovascular and neurodegenerative diseases) varies, and pericytes adapt to their environment by changing morphology, undergoing differentiation, secreting growth factors, and altering vessel permeability to allow select solutes to reach affected brain tissue (Hirunpattarasilp et al., 2019; Lendahl et al., 2019). While several studies associate decreased pericyte coverage with neurovascular diseases like brain AVM (Chen et al., 2013; Tual-Chalot et al., 2014; Crist et al., 2018; Winkler et al., 2018; Diéguez-Hurtado et al., 2019; Nadeem et al., 2020), others demonstrate pericyte hypertrophy, tissue infiltration, and proliferation in response to hypoxia, ischemic stroke, or traumatic brain injury (Tagami et al., 1990; Bonkowski et al., 2011; Cai et al., 2017; Birbrair, 2019). Despite disparate consequences to pericytes during CNS diseases, these important vascular cells are indeed affected and may play actively pathogenic roles; thus, targeting pericytes in neurovascular anomalies, like brain AVM, is a promising therapeutic avenue (Lebrin et al., 2010; Thalgott et al., 2015; Geranmayeh et al., 2019).

We investigated consequences to pericytes in our endothelial Rbpj mediated model of brain AVM, and we found that CNS pericytes pathologically expanded in a regionally and temporally regulated manner, as compared to controls. In Rbpj mutant cerebellum and cortex (but not brain stem), increased pericyte area kept pace with increased endothelial area, thus maintaining pericyte coverage of microvessels. Pathological pericyte expansion increased in severity as features of brain AVM (AV shunting) progressed; however, there was no evidence for early pericyte reduction, indicating temporal regulation of brain pericytes by endothelial Rbpj. Pericyte expansion was not caused by increased cell proliferation, but rather by hypertrophy of cytosolic pericyte processes on enlarging AV connections. Rbpj dependent EC-pericyte communication was affected in mutant brain vasculature, as isolated brain pericytes showed decreased expression of *Pdgfrβ*, *N-cadherin*, and *CD146*—all of which are molecules involved in pericyte recruitment to and association with microvessels. By contrast, isolated brain ECs showed increased expression of *N-cadherin*, perhaps in response to downregulation by pericytes. Our results indicate that pathological pericyte expansion progresses in concert with AV shunt formation, during Rbpj mediated brain AVM; thus, our data challenge a working hypothesis in the field, which posits that decreased pericyte coverage necessarily precedes brain AVM formation. Collectively, our findings define a novel role for Rbpj in postnatal brain endothelium—to prevent pathological pericyte expansion and to maintain pericyte morphology. Our study also refines the current view of pericyte involvement in neurovascular disease and the therapeutic potential of targeting and manipulating pericytes in brain AVM.

Materials and methods

Mice

All experiments were completed in accordance with Ohio University's Institutional Animal Care and Use Committee (IACUC) protocol number 16-H-024. Mouse lines *Cdh5(PAC)-CreER*^{T2} (Sörensen et al., 2009), *Rbpj*^{flox} (Tanigaki et al., 2002), *Rosa26*$^{mT/mG}$ (Muzumdar et al., 2007), and *Cspg4(NG2)-DsRed* (Zhu et al., 2008) were, respectively, provided by Taconic Biosciences (in accord with Breeding Agreement), Tasuku Honjo (Kyoto University), and the last two by Jackson Laboratory [*GT(Rosa)26Sor*$^{TM4(ACTB-tdTomato-EGFP)Luo}$: JAX stock #007576 and *Tg(Cspg4-DsRed.T1)1Akik:* JAX stock #008241]. At P1 and P2, 100 μg of Tamoxifen (Sigma) in 50 μL of peanut oil (Planters) was injected intragastrically, as previously described (Nielsen et al., 2014). PCR based genotyping was performed, as previously described (Nielsen et al., 2014), except *Rosa26*$^{mT/mG}$ and *Cspg4(NG2)-DsRed* genotyping was determined by tail biopsy tissue fluorescence, using a Nikon NiU microscope.

Tissue harvest and preparation

Brain and retina tissue was harvested following intracardial perfusion and simultaneous euthanasia by exsanguination. Perfusion solution depended on subsequent analysis, as follows: 1% paraformaldehyde (PFA) for anti-CD13, anti-N-cadherin, anti-Pdgfrβ, NG2-DsRed; phosphate buffered saline (PBS) for anti-desmin. Endothelial cells were genetically labeled with mGFP or were perfusion labeled with intravenous Dylight488 *Lycopersicon esculentum* (tomato) lectin (Vector Laboratories) (50 μg lectin/125–150 μL PBS). For tissue sections, brains were hemisected, cryopreserved in 30% sucrose, and stored at −80°C. Mid-sagittal cryosections, 10–12 μm thick, were collected with a CM-1350 cryostat (Leica) and stored at −80°C. For mid-sagittal sections, the following brain regions were imaged: (i) frontal cortex near the pial surface was imaged; (ii) cerebellum lobule V, VIA, VIB, or VII was imaged, as these lobules are consistently affected in Rbpj$^{i\Delta EC}$ mutants (Chapman et al., 2022); (iii) brain stem immediately caudal to the pons (as identified by the pontine flexure) was imaged. For whole cortex preparation, a 2–3 mm thick slice of frontal cortex was removed with a scalpel. For whole retina preparation, retinae were dissected and splayed, according to published methods (Tual-Chalot et al., 2013).

Immunostaining and 5-ethynyl-2′-deoxyuridine incorporation

Immunostaining was performed with modifications from standard protocol previously described (Nielsen and Dymecki, 2010). Primary antibody dilutions: rat anti-CD13 (MCA2183GA) (1:500) (AbD Serotec); mouse anti-desmin (D33) (1:50) (DAKO/Agilent); mouse anti-N-cadherin (3B9) (1:300) (Invitrogen); rat anti-Pdgfrβ (CD140b) (1:50) (Invitrogen). Secondary antibodies: Cy3 donkey anti-rat; Alexa647 donkey anti-mouse; Alexa647 donkey anti-rat (all dilutions 1:500) (Jackson ImmunoResearch). For EdU incorporation assay, mice were injected intraperitoneally with 10 μg/gram of body weight with EdU at P5–7 or P8–10 or P12–14. On the day of harvest (P7 or P10 or P14), tissue was harvested 2 h post-injection. Detection of EdU used Click-iT™ Plus chemistry, with AlexaFluor® 647 component following manufacturer's instructions (Invitrogen). Cell nuclei were counterstained with 4′,6′-diamidino-2-phenylindole (DAPI). Tissue sections were mounted with ProLong Gold™ (Invitrogen) and coverslipped for imaging.

Single cell suspension and cell isolation

Whole brain tissue was mechanically and chemically dissociated by Neutral Protease (Worthington), Collagenase Type II (Worthington), Deoxyribonuclease (Worthington), and Complete 1X DMEM (Gibco) with 5% heat inactivated Fetal Bovine Serum (Gibco) and 1% PenStrep (Gibco). 70% Percoll (Cytiva) density gradient was used to separate single cell suspension into cellular fractions. Endothelial cells were labeled with CD31 microbeads (1:10) (mouse, Miltenyi Biotec). Pericytes were labeled with primary antibody rat anti-mouse CD13 (1:50) (Bio-Rad) and secondary anti-rat IgG MicroBeads (1:10) (Miltenyi Biotec). Select cell populations were isolated *via* magnetic activated cell sorting using LS separation columns (QuadroMACS™ Starting Kit, Miltenyi Biotec). To reduce endothelial cell contamination in the pericyte samples, endothelial cells were removed prior to collecting pericytes. Cell pellets were stored at −80°C until RNA extraction.

Reverse transcription quantitative PCR

Total RNA was extracted from isolated cells using RNeasy Plus Micro Kit (including genomic DNA removal columns) (Qiagen), and concentration was measured using NanoDrop One spectrophotometer. For Reverse transcription quantitative PCR (RT-Qpcr), RNA input was 10 ng per well (96-well plate format). qScript One-Step SYBR Green RT-qPCR (Quantabio) was used to run qPCR with cycling in a CFX Connect Real-Time PCR Detection System (BioRad), using CFX Maestro 2.0 Software for Windows PC (BioRad). Tissue from 3 to 5 brains was pooled for each biological sample. Each biological sample was run in technical triplicate. Cycling conditions were as follows: (1) 49°C 10 min; (2) 95°C 5 min; (3) 95°C 10 s; (4) 58°C 30 s; (5) repeat steps 3–4 39 times; (6) melt curve 55–95°C 5 s, in 0.5°C increments. Quantification was performed using the comparative C_T method with Microsoft Excel software (Schmittgen and Livak, 2008). Values were normalized to expression of reference genes β-*actin* for ECs and *Rplpo* for pericytes. Reference genes were selected based on test runs for three reference genes (β-*actin*, *Gapdh*, *Rplpo*) per cell type—genes with consistent results across triplicate runs were selected. All sample replicates were used in quantification analyses (outliers were not identified; no samples were removed from analysis). Primer sequences and information relevant to MIQE Guidelines are listed in **Supplementary Table 1**.

Western blotting

Protein lysates were prepared in 1X RIPA buffer from isolated cells (see above). Protein concentration was estimated using Precision Red (Cytoskeleton, Inc.) and NanoDrop One spectrophotometer. Proteins were separated using an 8% polyacrylamide separating/resolving gel, 4% stacking gel, and electrophoresis. Protein was transferred to PVDF membrane, and membrane was blocked with 3% bovine serum albumin in tris-buffered saline with Tween-20, before incubating with primary antibodies. Primary antibody dilutions: rabbit anti-gapdh (1:1,000) (Cell Signaling Technologies); mouse anti-N-cadherin (3B9) (1:1,000) (Invitrogen); rat anti-Pdgfrβ (CD140b) (1:1,000) (Invitrogen); rabbit anti-Rbpj (1:1,000) (Cell Signaling Technologies). HRP-conjugated secondary antibody dilutions: anti-mouse (1:1,000); anti-rabbit (1:1,000); anti-rat (1:1,000) (Cell Signaling Technologies). Chemiluminescent substate was applied to the membrane and bands were detected and quantified with BioRad ChemiDoc XRS+ and ImageLab software.

Fluorescence imaging

Epifluorescent images were acquired using a Nikon NiU microscope and NIS Elements software. Confocal fluorescent images were acquired using a Zeiss LSM 510 laser scanning microscope system and Upright Zen software. Confocal Z-stacks ranged from 36 to 40 slices, at 2 μm steps, and were projected at maximum intensity.

Quantification and statistical analysis

For pericyte ensheathment ratio, following retina imaging, a 10 by 10 grid was overlayed with the mGFP+ endothelial cell images and desmin+ or CD13+ pericyte images in Adobe Photoshop (Creative Cloud). Points of intersection between the grid and positive cells were counted, modified from previously published protocols (Chan-Ling et al., 2004; Hughes et al., 2007), as a proxy for measuring changes to cell area or direct pericyte coverage of endothelium. Statistical analysis was completed using Prism software (GraphPad). Except for qPCR data (see above), unpaired Student's *t*-tests with Welch's correction were used to compare values between control and mutant mice. *P*-values < 0.05 were considered significant ($^{*}P < 0.05$, $^{**}P < 0.01$, $^{***}P < 0.001$, $^{****}P < 0.0001$, ns = not significant).

Results

Central nervous system pericyte area was pathologically expanded by P10 in cerebellum and by P14 in frontal cortex and retina, following endothelial deletion of Rbpj from birth

To delete Rbpj from ECs in a temporally restricted manner, we bred *Cdh5(PAC)-CreER^{T2}; Rbpj$^{flox/wt}$* and *Cdh5(PAC)-CreER^{T2}; Rbpj$^{flox/flox}$*, hereafter referred to as control and Rbpj$^{i\Delta EC}$ mutant mice, and we administered Tamoxifen to induce endothelial Rbpj deletion at postnatal day (P) 1 and P2 (Nielsen et al., 2014). Effective deletion of Rbpj from ECs was confirmed by P7 in brain ECs isolated from Rbpj$^{i\Delta EC}$ mice, as compared to controls (**Supplementary Figure 1**). This corroborated published data that showed loss of Rbpj protein from cortical ECs and cerebellum ECs (Nielsen et al., 2014; Chapman et al., 2022) in P14 Rbpj$^{i\Delta EC}$ brain tissue, as compared to controls. To determine whether total pericyte bed area, within mid-sagittal section through brain tissue, was altered in Rbpj$^{i\Delta EC}$ mice, we immunostained against the pericyte marker CD13 and measured CD13+ area per tissue area. To determine total endothelial area, we genetically labeled ECs with mGFP from the Cre-responsive *Rosa26$^{mT/mG}$* (*mTmG*) allele (Nielsen et al., 2014) and measured mGFP+ area per tissue area. By P14, CD13+ pericyte area and mGFP+ endothelial area (per brain tissue area) increased in Rbpj$^{i\Delta EC}$ mutant cerebellum (**Figures 1A–D**) and cortex (**Figures 1E–H**), but not in brain stem (**Figures 1I–L**), as compared to controls [note that our endothelial area results were similar to previously published results that showed increased vascular density in P14 Rbpj$^{i\Delta EC}$ mutants, as compared to controls (Nielsen et al., 2014)]. Interestingly, the percentage of pericyte area per endothelial area was not changed in mutant vs. control (right graphs in **Figures 1D,H,L**), suggesting that overall pericyte coverage of brain vessels did not change. Rather, pericyte expansion kept pace with pathological endothelial expansion. To illustrate pericyte-microvessel congruency and coverage of microvessels, we acquired higher magnification images of CD13+ pericytes and mGFP+ microvessels in P14 control and mutant cerebellum (**Supplementary Figures 2B,C**), cortex (**Supplementary Figures 2D,E**), and brain stem (**Supplementary Figures 2F,G**). Because no pan-pericyte marker has been identified to date, we repeated our pericyte-positive area measurements using tissue immunostained against the pericyte marker desmin. Using desmin+ pericytes and Dylight488-lectin+ ECs for area measurements, we found similarly increased pericyte and endothelial expansion in P14 Rbpj$^{i\Delta EC}$ mutant cerebellum (**Supplementary Figures 3A–D**) and frontal cortex (**Supplementary Figures 3E–H**), but not brain stem (**Supplementary Figures 3I–L**), as compared to controls. Percentage pericyte/endothelial area was not changed in any brain region, indicating desmin+ pericyte expansion kept pace with endothelial expansion (right graphs in **Supplementary Figures 3D,H,L**). These data suggest that endothelial Rbpj is required, in different brain regions, to prevent pericytes from expanding along with expanding endothelium in the early postnatal brain.

Because brain AVM has been correlated with pericyte reduction in other studies, and to examine pericyte coverage at different timepoints post-endothelial Rbpj deletion, we analyzed pericyte area from pre-brain AVM (P7) and from earlier (P10)- and later (P21)-stage brain AVM. While the precise onset of Rbpj$^{i\Delta EC}$ brain AVM in mice has not been reported, previous work showed that increased AV connection (microvessel) diameter appeared around P8–P10 (Nielsen et al., 2014). Thus, we decided to analyze brain pericyte area at P7, a timepoint before features of brain AVM developed. In P7 Rbpj$^{i\Delta EC}$ mutants, as compared to controls, endothelial area was not increased (**Supplementary Figures 4A–C,E–G**, quantified in left graphs in D,H), suggesting that endothelial expansion, a feature of brain AVM onset, had not yet occurred. At P7, CD13+ pericytes were observed in cerebellum and cortex of controls and Rbpj$^{i\Delta EC}$ mutants (**Supplementary Figures 4A–C,E–G**, middle graphs in D,H), and pericyte coverage of microvessels was similar in controls and Rbpj$^{i\Delta EC}$ mutants (**Supplementary Figure 4**, right graphs in D,H). These data indicate that brain pericytes were present, prior to the onset of brain AV features, and suggest that pericyte reduction is likely not necessary for Rbpj$^{i\Delta EC}$ brain AVM to form. In P10 Rbpj$^{i\Delta EC}$ mutants, as compared to controls, pericytes were present in all brain regions analyzed; however, increased CD13+ pericyte area and mGFP+ endothelial area was only seen in cerebellum, with pericyte expansion in pace with endothelial expansion (**Supplementary Figures 5A–D**). Increased CD13+ pericyte area and mGFP+ endothelial area was not observed in P10 Rbpj$^{i\Delta EC}$ mutant cortex (**Supplementary Figures 5E–H**)

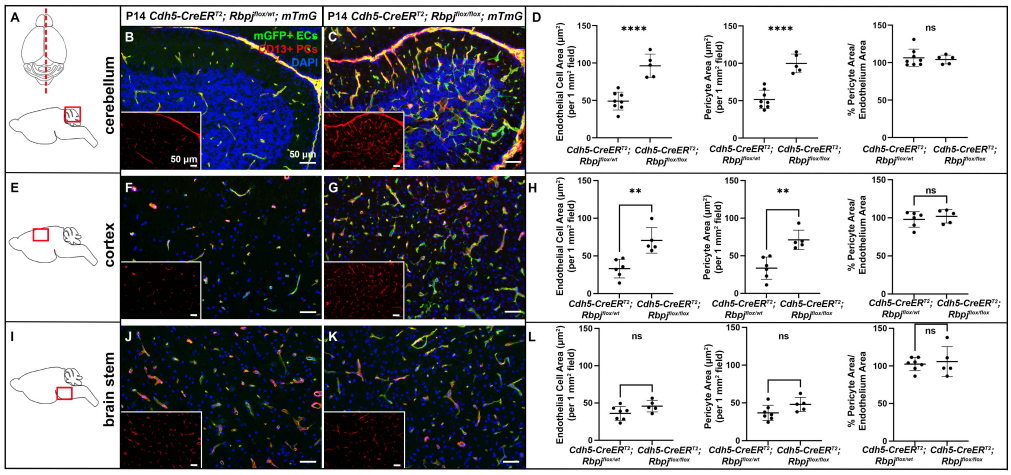

FIGURE 1

CD13-positive cortex and cerebellum pericyte area expanded and kept pace with expanded endothelium at P14, following endothelial deletion of Rbpj. In all tissue panels, CD13+ pericytes (PCs) (red), mGFP+ ECs (green), DAPI+ nuclei (blue); insets show CD13+ pericytes only. **(A)** Upper schematic indicates mid-sagittal plane of section through brain. Lower schematic indicates cerebellum region shown. **(B,C)** mGFP+ endothelial area and CD13+ pericyte area pathologically expanded in P14 Rbpj$^{i\Delta EC}$ cerebellum, as compared to controls. Quantified in **(D)** endothelial area $P < 0.0001$; pericyte area $P < 0.0001$. Percentage of pericyte area/endothelial area did not change (right graph in **D**; $P = 0.7048$. $N = 8$ controls and $N = 5$ mutants. **(E)** Schematic indicates cortex region shown. **(F,G)** mGFP+ endothelial area and CD13+ pericyte area pathologically expanded in P14 Rbpj$^{i\Delta EC}$ cortex, as compared to controls. Quantified in **(H)** endothelial area $P = 0.0022$; pericyte area $P = 0.0016$. Percentage of pericyte area/endothelial area did not change (right graph in **H**; $P = 0.5015$). $N = 6$ controls and $N = 5$ mutants. **(I)** Schematic indicates brainstem region shown. **(J,K)** mGFP+ endothelial area and CD13+ pericyte area did not change in P14 Rbpj$^{i\Delta EC}$ brain stem, as compared to controls. Quantified in **(L)** endothelial area $P = 0.0835$; pericyte area $P = 0.0799$. Percentage of pericyte area/endothelial area did not change (right graph in **L**; $P = 0.6973$). $N = 7$ controls and $N = 5$ mutants. $^{**}P < 0.01$; $^{****}P < 0.0001$; ns, not significant.

or brain stem (**Supplementary Figures 5I–L**), as compared to controls. Using desmin as a marker for P10 pericytes, we did not measure any changes in desmin+ pericyte area in any brain region from Rbpj$^{i\Delta EC}$ mutant vs. control (**Supplementary Figures 6A–L**). To determine whether pericytes were still present (and pathologically expanded) on vessels after advanced AV shunts have formed, we next analyzed P21 brain tissue. We found increased mGFP+ endothelial area and CD13+ pericyte area in Rbpj$^{i\Delta EC}$ cerebellum (**Supplementary Figures 7A–D**) and cortex (**Supplementary Figures 7E–H**), but not in brain stem (**Supplementary Figures 7I–L**), as compared to controls. Pericyte area expanded in concert with endothelial area, as the percentage of pericyte area/endothelial area did not change in Rbpj$^{i\Delta EC}$ vs. control brain tissue (right graph in **Supplementary Figure 7L**). A summary of Rbpj$^{i\Delta EC}$ brain pericyte expansion, over time and in select brain regions, is included in **Table 1**. These data, coupled with the previous finding that only 50% of Rbpj$^{i\Delta EC}$ mice survive to P14 (Nielsen et al., 2014), highlighted P14 as a timepoint for further analyses. Together, our findings suggest a temporal requirement for endothelial Rbpj to prevent pathological pericyte expansion in the early postnatal brain.

The mouse retina is often used in vascular studies as part of the CNS and as a proxy for studies in the brain. While retinal AVM have not been reported in endothelial Rbpj mutants, previous studies showed that loss of Notch signaling molecules from ECs leads to increased angiogenic sprouting and branch points in the leading edge of early postnatal retinal vasculature (Hellström et al., 2007). Given our results from brain vasculature, we hypothesized that endothelial Rbpj may also be required in the neonatal retinal vasculature to prevent pericyte expansion. We dissected eyes from P10 to P14 control and Rbpj$^{i\Delta EC}$ mice and used a whole mount preparation to splay the eye and expose the retina for immunostaining and tissue mounting (**Supplementary Figure 8A**). We labeled pericytes with CD13 and desmin markers, and because we stained whole tissue, we measured a pericyte ensheathment ratio (PER) as a proxy for pericyte+ and endothelium+ area measurements. Our PER method was adapted from previous studies with retinal ECs and pericytes (Chan-Ling et al., 2004; Hughes et al., 2007). We overlayed a 10x10 grid onto a retina image (**Supplementary Figure 8B**) and counted the number of intersection points at which pericyte+ or EC+ marker was observed (**Supplementary Figures 8C,D,F,G**). At P10, we did not observe increased number of EC+ intersection points in control vs. Rbpj$^{i\Delta EC}$ (left graphs in **Supplementary Figures 8E,H**), in agreement with previous data suggesting that endothelium had not yet expanded in Rbpj$^{i\Delta EC}$ brain. At P10, we observed increased number of desmin+ pericyte intersection points but not CD13+ points (middle graphs in **Supplementary Figures 8E,H**). Consistent with data from brain vessels, the ratio of pericyte+/EC+ intersection points in Rbpj$^{i\Delta EC}$ vs. controls was not affected by P10 (right graphs in **Supplementary Figures 8E,H**). In P14 retina, the number of EC+ and pericyte+ intersection points significantly increased in Rbpj$^{i\Delta EC}$, as

TABLE 1 Summary of regional and temporal pericyte expansion (as measured by different pericyte markers) in the CNS vasculature, following endothelial deletion of Rbpj.

Central nervous system region	Degree of postnatal (P) pericyte expansion in Rbpj$^{i\Delta EC}$ vs. control		
	P10	P14	P21
Cerebellum	↑ CD13	↑↑↑↑ CD13	↑↑ CD13
	no desmin	↑↑ desmin	
Cortex (frontal)	no CD13	↑↑ CD13	↑ CD13
	no desmin	↑↑ desmin	
Brain stem	no CD13	no CD13	no CD13
	no desmin	no desmin	
Retina	no CD13	↑ CD13	
	↑↑↑ desmin	↑↑↑ desmin	

↑ represents *($P < 0.05$) statistical significance.
↑↑ represents **($P < 0.01$) statistical significance.
↑↑↑ represents ***($P < 0.001$) statistical significance.
↑↑↑↑ represents ****($P < 0.0001$) statistical significance.

compared to controls, using either CD13 (**Supplementary Figures 8I–K**) or desmin (**Supplementary Figures 8L–N**) to label pericytes. However, the ratio of pericyte+/EC+ intersection points in Rbpj$^{i\Delta EC}$ vs. controls was not affected (right graphs in **Supplementary Figures 8K,N**). A summary of Rbpj$^{i\Delta EC}$ retinal pericyte expansion, over time, is included in **Table 1**. These data suggest that pericyte expansion kept pace with endothelial expansion in the early postnatal retinae, following endothelial deletion of Rbpj.

The number of pericytes per brain vessel length increased by P14, without increased cell proliferation, following endothelial deletion of Rbpj from birth

To determine whether pericyte expansion resulted from an increased number of pericytes, we counted the number of pericytes, per vessel length, on AV connections (4–6 μm diameter capillaries in control and > 12 μm diameter AV shunts in Rbpj$^{i\Delta EC}$ brains). We used another pericyte marker, the transgene *Cspg4(NG2)-DsRed* (Zhu et al., 2008), which does not label pericyte processes, so that individual pericytes could be readily distinguished. We bred the transgene into our P14 control and Rbpj$^{i\Delta EC}$ mice and counted Cspg4(NG2)-DsRed+ pericytes per Dylight488-lectin+ vessel length (mm). Using a whole mount cortical preparation so that intact vessels and pericytes could be visualized, described in Nielsen et al. (2014), we found an increased number of pericytes per mm of vessel in Rbpj$^{i\Delta EC}$ cortex at P14, as compared to controls (**Figures 2A–C**). Because *Cspg4(NG2)* is highly expressed by oligodendrocyte precursor cells (Polito and Reynolds, 2005; Zhu et al., 2008), we wanted to validate that the cells we identified as Cspg4(NG2)+ and directly juxtaposed to vessels were indeed pericytes. We immunostained Dylight488-lectin-injected, *Cspg4(NG2)-DsRed* brain tissue against CD13 in P14 controls. We found CD13+/Cspg4(NG2)-DsRed+ pericytes were identified adjacent to lectin+ microvessels (**Figures 2D–I**), while CD13-/Cspg4(NG2)-DsRed+ oligodendrocyte precursor cells were not found near vessels (**Figures 2E,G,I**).

To assess pericyte proliferation during AV shunt formation, we initiated EdU incorporation experiments during incremental time periods before P14. We administered EdU on three consecutive days at P5–7, P8–10, P12–14, and harvested tissue on P7, P10, P14, 2 h post-EdU. We counted double-labeled EdU+ and CD13+ pericytes in mid-sagittal brain tissue sections. Overall, we found very few proliferative pericytes in control and mutant brain tissue. Our analysis did not detect a significant difference in the number of proliferative pericytes (per brain tissue field) between Rbpj$^{i\Delta EC}$ and control mice, in cerebellum or cortex, and at all timepoints analyzed (P14 cortex, **Figures 3A–C**; P14 cerebellum **Figures 3D–F**) (P7 cortex, **Supplementary Figures 9A–C**; P7 cerebellum **Supplementary Figures 9D–F**; P10 cortex, **Supplementary Figures 9G–I**; P10 cerebellum **Supplementary Figures 9J–L**). Taken together, these results suggest that the increased number of pericytes per vessel length was not caused by increased cell proliferation but by another mechanism, perhaps related to another cellular change to pericytes and/or to changes in the Rbpj$^{i\Delta EC}$ microvessels.

Brain pericytes extended processes to enwrap late-stage arteriovenous shunts, following endothelial deletion of Rbpj

To determine whether pericyte morphology was affected on Rbpj$^{i\Delta EC}$ brain AV connections, we combined our whole

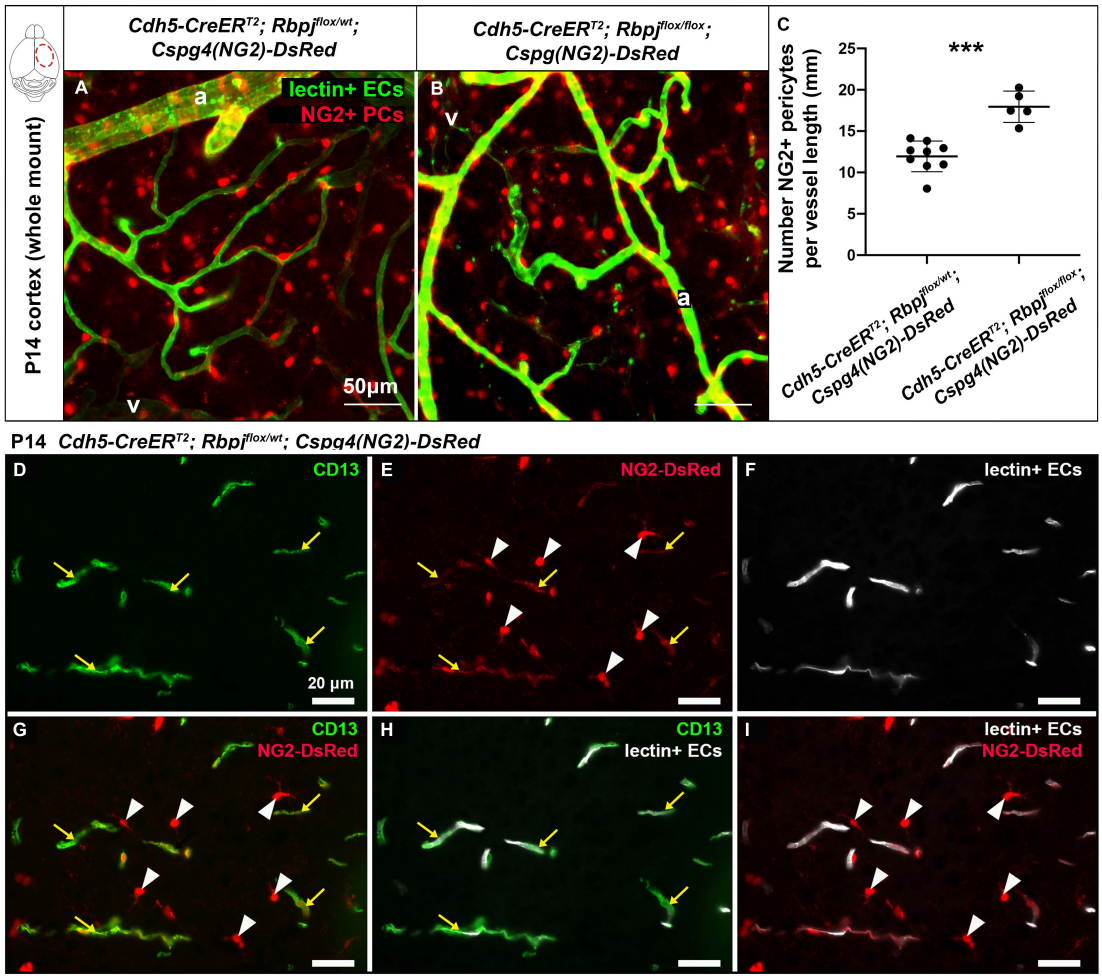

FIGURE 2
Endothelial Rbpj deficiency led to increased number of NG2-positive pericytes per vessel length by P14. **(A,B)** In P14 whole mount cortex, pericytes were labeled by the *Cspg4(NG2)-DsRed* transgene (red). ECs were labeled by Dylight488-lectin (green). NG2+ pericytes (PCs) were counted, and the corresponding lectin+ vessel length [between arteries (a) and veins (v)] was measured. The number of NG2+ pericytes per millimeter of vessel length significantly increased in Rbpj$^{i\Delta EC}$ mutants, as compared to controls (quantified in **C**; $P = 0.0004$, $N = 9$ controls and $N = 5$ mutants). **(D–I)** P14 *Cspg4(NG2)-DsRed* (red) mid-sagittal brain tissue sections were immunostained against CD13 (green), and vessels were highlighted with Dylight488-lectin (white). **(D)** CD13 labeled pericytes; **(E)** *Cspg4(NG2)-DsRed* genetically labeled pericytes (yellow arrows) and oligodendrocyte precursor cells (white arrowheads); **(F)** Perfused Dylight488-lectin labeled ECs within blood vessels. **(G)** Co-labeling showed CD13+/Cspg4(NG2)-DsRed+ pericytes (yellow arrows) and CD13-/Cspg4(NG2)-DsRed+ oligodendrocyte precursor cells (white arrowheads). **(H,I)** Pericytes were found adjacent to lectin+ vessel, while oligodendrocyte precursor cells were not found near vessels. ***$P < 0.001$.

mount cortical prep with anti-desmin immunostaining. Desmin expression spanned the cytosolic pericyte processes and offered a view of desmin+ pericyte ensheathment on mGFP+ brain vessels. In P14 control cortex, pericytes on AV connections (4–6 µm diameter capillaries) extended thin cytoplasmic processes to enwrap vessels (Figures 4A–A"'), while in Rbpj$^{i\Delta EC}$ cortex, pericyte processes appeared thickened and ring-like in abnormal AV vessel segments (>12 µm diameter AV shunts) (Figures 4B–B"'). In P21 control cortex, pericytes were similar to P14 controls, with thin and elongated processes (Figures 4C–C"'). In P21 Rbpj$^{i\Delta EC}$ cortex, thickened, ring-like pericytes began to resemble the concentric morphology characteristic of vascular smooth muscle cells (Figures 4D–D"'). These findings suggest that endothelial Rbpj is required to maintain healthy pericyte morphology on brain microvessels.

Endothelial Rbpj deficiency led to decreased Pdgfrβ expression in pericytes and decreased vessel coverage by Pdgfrβ+ pericytes

Based on previous reports of Notch dependent Pdgfrβ expression in pericytes, we next hypothesized that endothelial

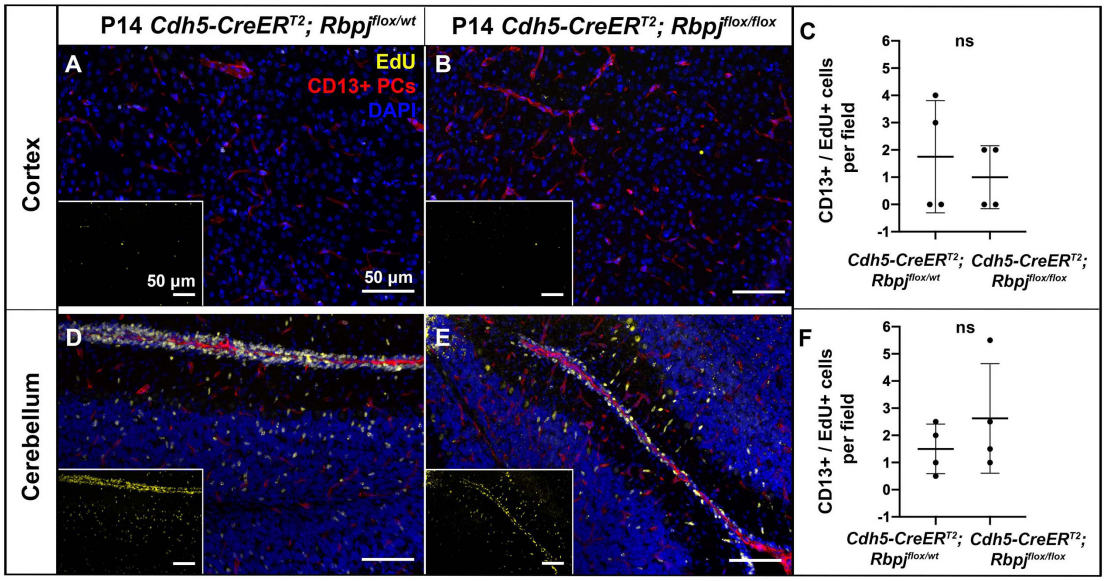

FIGURE 3
Endothelial deletion of Rbpj did not lead to increased CD13-positive pericyte proliferation from P12 to P14 in cortex or cerebellum. In all tissue panels, CD13+ pericytes (PCs) (red), EdU+ nuclei (yellow), DAPI+ nuclei (blue). **(A,B)** Mice were administered EdU at P12, P13, P14. Mid-sagittal sections through P14 control and Rbpj$^{i\Delta EC}$ cortex. CD13+ pericytes and CD13+/EdU+ double positive pericytes were counted at P14 harvest. **(C)** Quantification of CD13+ pericytes per CD13+/EdU+ pericytes showed no significant change (P = 0.555). N = 4 controls and N = 4 mutants. **(D,E)** Mid-sagittal sections through P14 control and Rbpj$^{i\Delta EC}$ cerebellum. CD13+ pericytes and CD13+/EdU+ double positive pericytes were counted at P14 harvest. **(F)** Quantification of CD13+ pericytes per CD13+/EdU+ pericytes showed no significant change (P = 0.364). N = 4 controls and N = 4 mutants. ns, not significant.

Rbpj deficiency from birth would lead to decreased Pdgfrβ expression in pericytes by P14. We first examined Pdgfrβ+ pericyte area to determine whether Rbpj$^{i\Delta EC}$ pericyte expansion included predominately Pdgfrβ+ or Pdgfrβ- pericytes. We measured Pdgfrβ+ and mGFP+ areas in P14 cerebellum and cortex. As expected, and consistent with previous data, mGFP+ endothelial area was increased in both P14 cerebellum and cortex (cerebellum **Figures 5A–C**, left graph in D; cortex **Figures 5E–G**, left graph in H). In P14 cerebellum and cortex, we found slight but significantly increased Pdgfrβ+ area in mutants, as compared to controls (**Figures 5A–H**). By contrast to our CD13+ and desmin+ area data, the percentage of Pdgfrβ+ area/endothelial area was significantly decreased in P14 Rbpj$^{i\Delta EC}$ cerebellum and cortex (right graphs in **Figures 5D,H**). These data suggest that while total pericyte area increased in Rbpj$^{i\Delta EC}$ brains, a significant number of pericytes expressed Pdgfrβ abnormally. To determine whether endothelial deletion of Rbpj affected pericyte *Pdgfrβ* expression at the transcript and/or protein level, we isolated pericytes from P14 control and Rbpj$^{i\Delta EC}$ brains for transcript and Western blot analyses. As compared to controls, Rbpj$^{i\Delta EC}$ brain pericytes showed decreased expression of *Pdgfrβ* transcript (**Figure 5Q**) and protein (**Figures 5R,S**) by P14, indicating that endothelial Rbpj regulates expression of *Pdgfrβ* in pericytes in the early postnatal brain.

Endothelial Rbpj deficiency led to decreased N-cadherin and *CD146* expression in pericytes, but increased N-cadherin expression in endothelial cells

We next tested whether endothelial deletion of Rbpj affected expression of other factors involved in EC-pericyte communication—specifically, molecules predicted to be regulated by (N-cadherin) or molecules predicted to be regulators of (CD146) Pdgf-B/Pdgfrβ signaling. We immunostained against N-cadherin, a molecule expressed by ECs and pericytes and involved in direct cell-cell association. We measured N-cadherin+ and mGFP+ areas in P14 cerebellum and cortex. As expected, and consistent with previous data, mGFP+ endothelial area was increased in both P14 cerebellum and cortex (cerebellum **Figures 5I–K**, left graph in L; cortex Figures 5M–O, left graph in P). Total N-cadherin+ area was significantly increased in both cerebellum (**Figure 5L**, middle graph) and cortex (**Figure 5P**, middle graph). The percentage of N-cadherin+ area/endothelial area was significantly increased in P14 Rbpj$^{i\Delta EC}$ cerebellum and cortex (right graphs in **Figures 5L,P**); however, it must be noted that N-cadherin expression was not exclusive to pericytes, so the percentage did not represent pericyte/endothelial coverage exclusively.

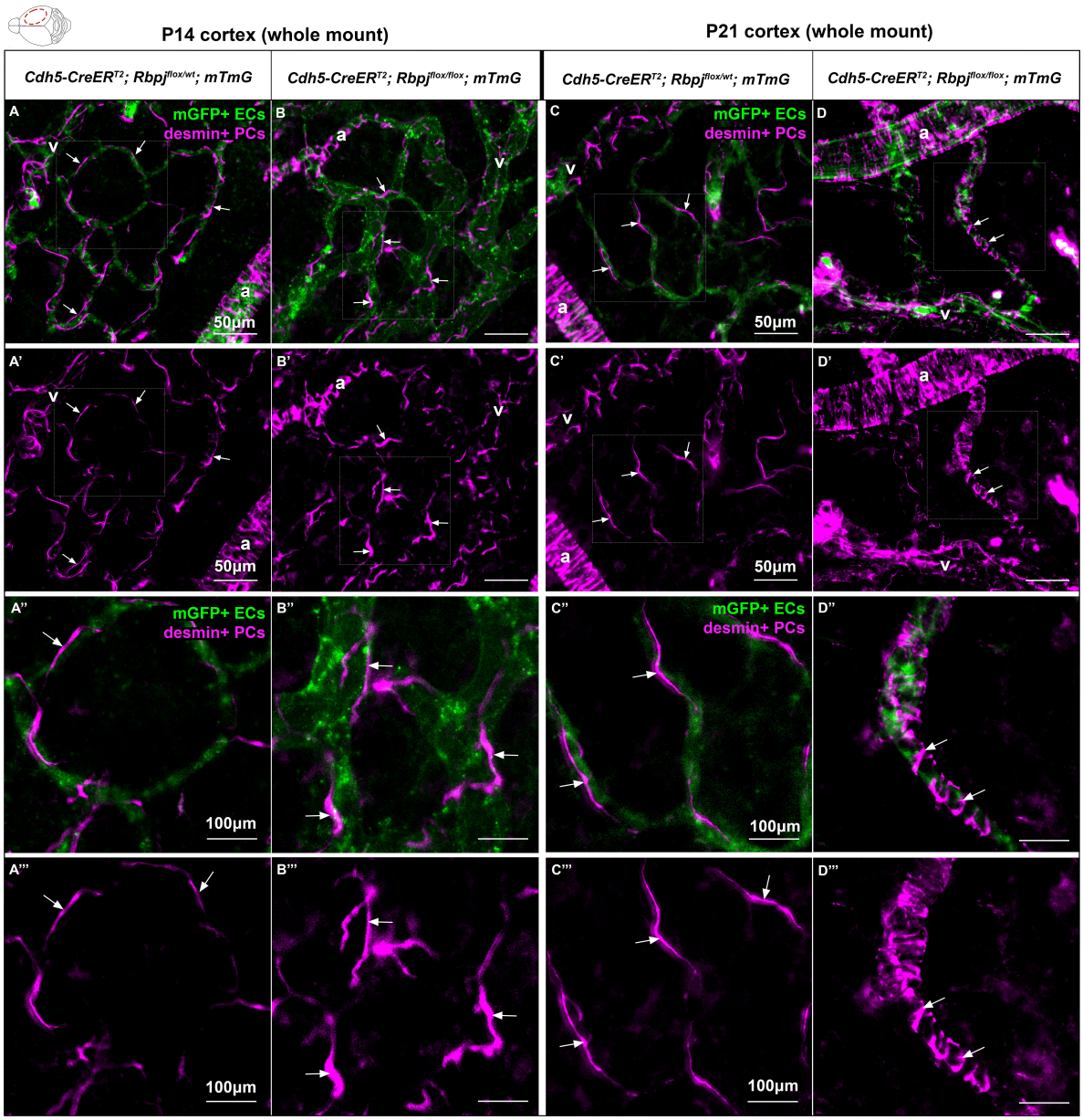

FIGURE 4
Desmin-positive pericytes showed abnormal morphology on P14 and P21 brain microvessels, following endothelial deletion of Rbpj. Whole mount immunostaining against desmin highlighted pericyte processes (PCs) (magenta) on mGFP+ brain AV connections (ECs) (green). By P14 **(A–B″)** and P21 **(C–D″)**, pericyte processes enwrapped brain capillaries in controls and AV shunts in Rbpj$^{i\Delta EC}$ mutants (arrows). **(B′,B‴,D′,D″)** Pericytes extended their cytosolic processes to maintain coverage of expanding endothelium. By P21, pericytes on AV shunts appeared to acquire a ring-like morphology to enwrap the expanded microvessel. A, artery; V, vein. P14, *N* = 9 controls and *N* = 9 mutants; P21, *N* = 3 controls and *N* = 3 mutants.

To determine whether endothelial deletion of Rbpj affected EC and/or pericyte expression of *N-cadherin* at the transcript and/or protein level, we isolated ECs and pericytes from P14 control and Rbpj$^{i\Delta EC}$ brains. As compared to controls, P14 Rbpj$^{i\Delta EC}$ brain pericytes showed decreased expression of *N-cadherin* transcript (**Figure 5Q**) and protein (**Figures 5R,T**). By contrast, P14 Rbpj$^{i\Delta EC}$ brain ECs showed increased expression of *N-cadherin* transcript (**Figure 5U**) and protein (**Figures 5R,V**), indicating that endothelial Rbpj regulates expression of *N-cadherin* differentially in pericytes and ECs in the early postnatal brain.

CD146 is expressed dynamically by ECs and pericytes in the developing brain, where it has been shown to promote pericyte association with ECs, in part by regulating Pdgf-B/Pdgfrβ

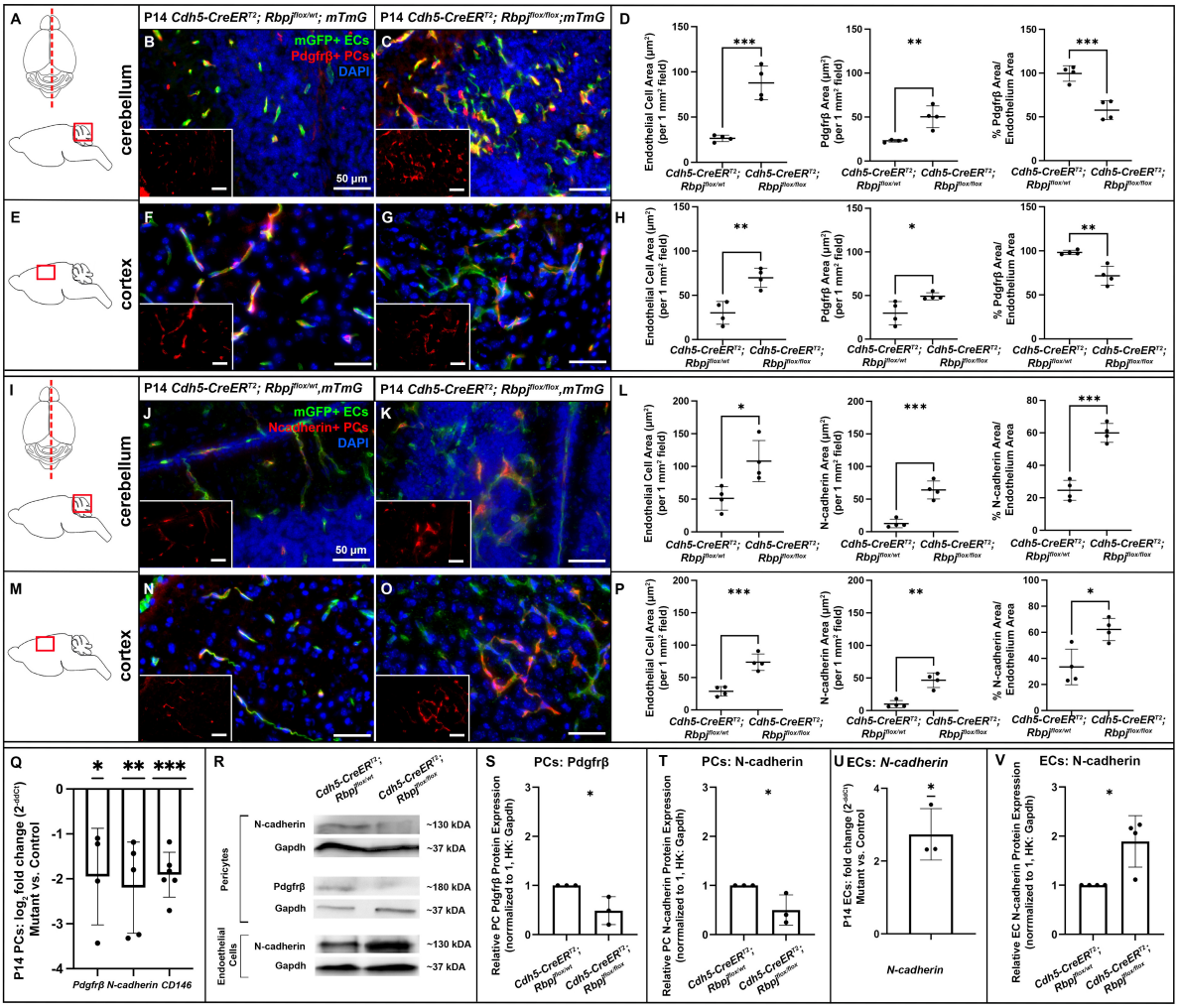

FIGURE 5

By P14, endothelial Rbpj deficiency led to decreased expression of *Pdgfrβ*, *N-cadherin*, and *CD146* by brain pericytes and increased expression of *N-cadherin* by brain endothelial cells. **(A,I)** Upper, schematic of brain mid-sagittal section cerebellum; lower, schematic of cerebellum brain region shown. **(E,M)** schematic of cortex brain region shown. **(B,C,F,G)** Pdgfrβ+ pericytes (PCs) (red), mGFP+ ECs (green), DAPI+ nuclei (blue). **(B,C)** mGFP+ endothelial area and Pdgfrβ+ pericyte area increased in P14 Rbpj$^{i\Delta EC}$ cerebellum, as compared to control. Quantified in **(D)** endothelial area $P = 0.0007$; Pdgfrβ+ area $P = 0.0048$. Percentage of Pdgfrβ+ area/endothelial area was decreased in Rbpj$^{i\Delta EC}$ cerebellum, as compared to controls (right graph in **D**; $P = 0.0010$). $N = 4$ controls and $N = 4$ mutants. **(F,G)** mGFP+ endothelial area and Pdgfrβ+ pericyte area increased in P14 Rbpj$^{i\Delta EC}$ cortex, as compared to control. Quantified in **(H)** endothelial area $P = 0.0033$; Pdgfrβ+ area $P = 0.0317$. Percentage of Pdgfrβ+ area/endothelial area was decreased in Rbpj$^{i\Delta EC}$ cerebellum, as compared to controls (right graph in **H**; $P = 0.0032$). $N = 4$ controls and $N = 4$ mutants. **(J,K,N,O)** N-cadherin+ cells (red), mGFP+ ECs (green), DAPI+ nuclei (blue). **(J,K)** mGFP+ endothelial area and N-cadherin+ area increased in P14 Rbpj$^{i\Delta EC}$ cerebellum, as compared to control. Quantified in **(L)** endothelial area $P = 0.0204$; N-cadherin+ area $P = 0.0005$. Percentage of N-cadherin+ area/endothelial area decreased in Rbpj$^{i\Delta EC}$ cerebellum, as compared to controls (right graph in **L**; $P = 0.0002$). $N = 4$ controls and $N = 4$ mutants. **(N,O)** mGFP+ endothelial area and N-cadherin+ area increased in P14 Rbpj$^{i\Delta EC}$ cortex, as compared to control. Quantified in **(P)** endothelial area $P = 0.0009$; N-cadherin+ area $P = 0.0011$. Percentage of N-cadherin+ area/endothelial area decreased in Rbpj$^{i\Delta EC}$ cortex, as compared to controls (right graph in **P**; $P = 0.0119$). $N = 4$ controls and $N = 4$ mutants. **(Q)** RT-qPCR analysis of transcript expression from isolated P14 brain pericytes showed decreased expression of *Pdgfrβ* ($p = 0.0360$), *N-cadherin* ($P = 0.0084$) and *CD146* ($P = 0.0002$) in Rbpj$^{i\Delta EC}$ mutants as compared to controls. **(R)** Western blot analysis of protein expression from isolated brain pericytes and ECs showed decreased expression of Pdgfrβ ($P = 0.0349$) and N-cadherin ($P = 0.0487$) in Rbpj$^{i\Delta EC}$ pericytes [quantified in **(S,T)**, respectively; $N = 3$ controls and $N = 3$ mutants] and increased expression of N-cadherin ($P = 0.0143$) in Rbpj$^{i\Delta EC}$ ECs [quantified in **(V)**; $N = 4$ controls and $N = 4$ mutants]. **(U)** RT-qPCR analysis of transcript expression from isolated P14 brain ECs showed increased expression of *N-cadherin* ($P = 0.0216$) in Rbpj$^{i\Delta EC}$ ECs. $N = 3$ controls and $N = 3$ mutants. $^*P < 0.05$; $^{**}P < 0.01$; $^{***}P < 0.001$.

signaling. In brain microvessels, CD146 is expressed primarily by pericytes, where it has been shown to act as a co-receptor for Pdgfrβ (Chen et al., 2017). To test whether expression of *CD146* was affected by endothelial Rbpj deficiency, we analyzed *CD146* expression in pericytes isolated from P14 control and Rbpj$^{i\Delta EC}$ brains. We found decreased expression of *CD146* by Rbpj$^{i\Delta EC}$

brain pericytes, as compared to controls (**Figure 5Q**), suggesting that endothelial Rbpj regulates expression of *CD146*. Together, our data suggest that Rbpj is required in early postnatal endothelium, to regulate expression of molecules involved in EC-pericyte communication and association.

Discussion

Endothelial Rbpj regulates pericyte bed area and maintains pericyte morphology in the early postnatal central nervous system

Our data indicate that endothelial Rbpj is required to prevent pathological pericyte expansion in the early postnatal brain vasculature (**Figures 6A,B**). Consistent with our data, previous studies have shown increased pericyte area or coverage in abnormal CNS or non-CNS vascular beds. Loss of *Foxf2* from neuronal progenitor cells leads to a twofold increase in pericyte coverage of forebrain cortical microvessels in late-gestation mouse embryos (Reyahi et al., 2015), suggesting genetic regulation to prevent pericyte expansion in the developing CNS. Depletion of astrocytes in perinatal mouse brain leads to increased cortical vessel and luminal diameter, with increased desmin+ pericyte expression, suggesting that newly born astrocytes influence the early postnatal brain microvessels and pericytes (Ma et al., 2012). Outside of the CNS vasculature, increased pericyte coverage has been reported in bone marrow samples from myelofibrosis patients (Zetterberg et al., 2007), in PDGF-BB induced non-small cell lung xenograft tumors (Song et al., 2009), in an *in vitro* pulmonary hypertension model (Khoury and Langleben, 1996), and in mice and guinea pig cochlear capillaries following auditory trauma (Shi, 2009). Our pericyte expansion data are consistent with these previous findings, which demonstrate increased pericyte area and/or coverage, in the context of microvessel abnormalities.

In the early postnatal brain, endothelial Rbpj likely plays a role in maintaining pericyte morphology and regulating the number of pericytes per vessel length. Our EdU incorporation data indicate that pericyte proliferation was not increased in $Rbpj^{i\Delta EC}$ brain vasculature, yet total pericyte area and pericyte number per vessel length were increased. Based on our whole-mount observations of desmin+ pericyte processes enwrapping abnormal AV connections in $Rbpj^{i\Delta EC}$ brain, it is likely that pericytes abnormally extend processes, in response to endothelial Rbpj deficiency and pathological endothelial expansion. As brain AVM pathology progressed, pericytes on $Rbpj^{i\Delta EC}$ AV shunts began to resemble the band-like morphology characteristic of smooth muscle cells. However, previous data showed that α-smooth muscle actin (αSMA, a smooth muscle marker) was not expressed by brain AV shunts in P14 $Rbpj^{i\Delta EC}$ mice, while αSMA was expressed by arterioles (Nielsen et al., 2014). Since the band-like desmin+ pericytes spanned the entire length of the AV shunt in **Figure 4**, it is not likely that these are smooth muscle cells, but rather pericytes that have altered band-like morphology.

What then accounts for the increased number of pericytes on AV shunts, as compared to control capillaries? As brain pericytes are capable of microvascular migration (Dore-Duffy et al., 2000) and of cellular trans-differentiation (Dore-Duffy et al., 2006; Bonkowski et al., 2011) within the CNS, it is possible that affected pericytes migrate from healthy vessel segments to abnormal AV connections and/or initiate differentiation into another neural cell type, yet retain pericyte marker expression and position adjacent to blood vessels. Because mesenchymal cells, bone marrow cells, and ECs are capable of trans-differentiating into pericytes—either *in vitro* or under pathological conditions (DeRuiter et al., 1997; Rajantie et al., 2004; Kokovay et al., 2006)—it is possible that these origins contribute to increased pericyte number per vessel length in $Rbpj^{i\Delta EC}$ brains. Another possibility is that the nature of brain AV shunt formation in $Rbpj^{i\Delta EC}$ mice influences pericyte number per vessel length. For example, in healthy early postnatal brain vasculature, vascular remodeling is required to form a functionally mature vascular bed (Wang et al., 1992; Wälchli et al., 2015). At P0–P5, mouse neurovasculature resembles a primitive vascular plexus (similar to the yolk sac vasculature) in which arteries and veins can be identified, but in which AV connections have not yet refined to capillary-diameter vessels (Wang et al., 1992; Nielsen et al., 2014). By P14, capillary beds can be seen joining arterial to venous vessels (Nielsen et al., 2014). While pericyte dynamics during this postnatal morphogenesis have not been studied, it is possible that impaired vascular remodeling affects pericyte number in $Rbpj^{i\Delta EC}$ neonatal brain tissue. For example, AV connection remodeling may involve EC rearrangement by which vessels narrow and "stretch out," and this may affect pericyte number per given vessel length. Thus, endothelial Rbpj may be required in the early postnatal brain to maintain healthy pericyte number and morphology.

Endothelial Rbpj regulates central nervous system pericyte bed area in a regionally and temporally regulated manner

Our findings show that abnormal pericyte expansion began in cerebellum and retina by P10 and in frontal cortex by P14, and pericyte area expansion continued until P21 in both brain regions; thus, endothelial Rbpj influences pericytes differentially as postnatal brain morphogenesis proceeds. Pericyte expansion paralleled endothelial expansion at all timepoints, in both

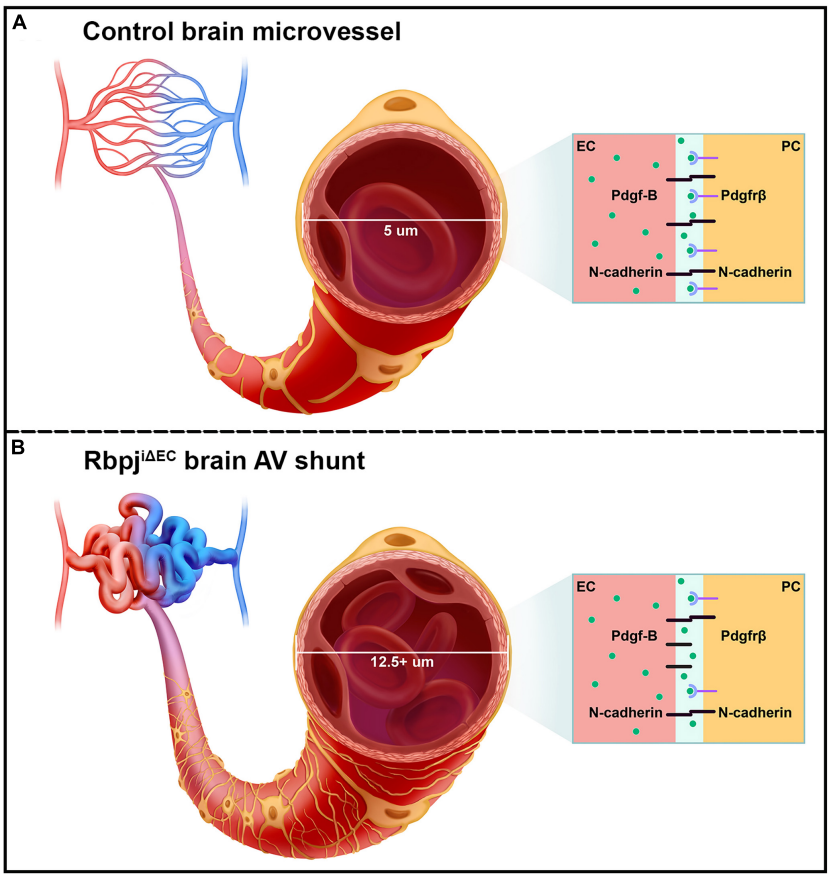

FIGURE 6
Schematic of the pathological consequences to brain pericytes, following endothelial deletion of Rbpj. **(A)** Top cartoon illustrates healthy brain microvessels. In controls, ~5 μm capillaries are enwrapped by pericyte processes (gold). Capillary ECs and pericytes are tightly apposed and share a basement membrane. Box represents an adjacent EC and pericyte (PC), which remain tightly associated via Pdgf-B/Pdgfrβ signaling and downstream N-cadherin expression. **(B)** Bottom cartoon illustrates Rbpj$^{i\Delta EC}$ AV connections. Vessel diameter is enlarged (12.5+ μm), and pericytes pathologically expand to keep pace with the increased endothelium. Box shows effects on EC-pericyte communication, following endothelial deletion of Rbpj: pericytes down-regulate Pdgfrβ and N-cadherin, while ECs up-regulate N-cadherin.

cerebellum and cortex, indicating that pericyte area keeps pace with pathological endothelial area, following endothelial deletion of Rbpj. Cerebellum pericytes were preferentially affected in mutants, pericyte expansion began earliest (P10) and was most severe by P14 in the cerebellum (**Table 1**). These findings are consistent with significant abnormalities to cerebellum tissue itself, following endothelial deletion of Rbpj (Chapman et al., 2022). During the early postnatal period, endothelial Rbpj is critical for cerebellar vascular development and proper tissue lobulation and growth (Chapman et al., 2022). Our findings show that endothelial Rbpj is also critical for pericyte maintenance during this period of cerebellar morphogenesis and outward growth. By contrast, pericyte area was not affected in the brain stem at any timepoint analyzed, suggesting that endothelial Rbpj regulates pericyte expansion in a regionally restricted manner. Consistent with this, (1) endothelial area in brain stem was not affected, following endothelial deletion of Rbpj in postnatal brain (Nielsen et al., 2014), and (2) brain stem AVM in human patients are rare, comprising 2–6% of all brain AVM (Chen et al., 2021) and often presenting superficially in the meninges rather than deep within brain parenchyma (Han et al., 2015). It is not known whether or how the brain stem is physiologically refractory to and/or protected from brain AVM. Together, our data demonstrate spatial and temporal regulation of CNS pericyte area by endothelial Rbpj.

Endothelial Rbpj regulates expression of factors that promote brain pericyte recruitment and association with endothelial cells

Decreased expression of *Pdgfrβ*, *N-cadherin*, and *CD146* by Rbpj$^{i\Delta EC}$ brain pericytes suggests that intercellular

communication between ECs and pericytes was affected. For example, Pdgf-B/Pdgfrβ signaling between ECs and pericytes is critical for recruiting pericytes to microvessels and maintaining the cells' close juxtaposition (Armulik et al., 2010; Daneman et al., 2010; Chen et al., 2017; Nikolakopoulou et al., 2017). Despite the expanded pericyte area in Rbpj$^{i\Delta EC}$ neurovasculature, Pdgf-B/Pdgfrβ signaling was likely affected and pericyte association with microvessels may have been impaired. Consistent with previous studies (Jin et al., 2008; Li et al., 2011; Yao et al., 2011), our data suggest a role for endothelial Rbpj/Notch signaling to regulate pericyte expression of *Pdgfrβ*. Interestingly, our results showed that while pericytes decreased *N-cadherin* expression, following endothelial deletion of Rbpj, ECs increased *N-cadherin* expression. This differential regulation of *N-cadherin* by endothelial Rbpj may be an attempt by ECs to compensate for decreased Pdgf-B/Pdgfrβ signaling and N-cadherin expression and thereby restore vessel stability, in the context of Rbpj$^{i\Delta EC}$ microvessel and pericyte abnormalities. Collectively, our data suggest that endothelial Rbpj regulates Pdgf-B/Pdgfrβ signaling, including expression of genes encoding the Pdgfrβ co-receptor CD146 and downstream target N-cadherin (**Figures 6A,B**).

As proper pericyte coverage of microvessels is involved in regulating vascular permeability, it is possible that the pathologically expanded pericyte bed in Rbpj$^{i\Delta EC}$ brain may affect pericyte function and vessel stability. However, given the abnormalities to ECs, following endothelial deletion of Rbpj, it would be difficult to tease apart whether abnormal function of pericytes and/or ECs might contribute to altered vessel permeability. By P14, Rbpj$^{i\Delta EC}$ brains show signs of intracerebral hemorrhage (Nielsen et al., 2014); however, the cellular mechanism by which blood leaks from Rbpj$^{i\Delta EC}$ vessels remains unknown. One hypothesis raised by our data is that brain pericytes expand in concert with Rbpj$^{i\Delta EC}$ vessels, as an attempt to stabilize mutant microvessels.

Recent evidence suggests there is a variety of pericyte subtypes that differ in morphology, molecular signature, and vascular function (Hartmann et al., 2015; Sweeney et al., 2016; Geranmayeh et al., 2019; Lendahl et al., 2019; Uemura et al., 2020; Bennett and Kim, 2021; Nadeem et al., 2022); therefore, the different pericyte populations may be differentially affected by Rbpj mediated brain AVM. We observed differences in pericyte area measurements, based on the which pericyte marker was used for analyses. While this alone underscores the importance of using multiple pericyte markers, this may also provide insight regarding how—and perhaps which—pericytes were pathologically expanded. CD13 is a metalloprotease and considered a selective surface marker for pericytes (Crouch and Doetsch, 2018), while desmin is present in intermediate filaments commonly found in pericyte processes (Armulik et al., 2011). As such, thin desmin+ processes may have been less detectable in mid-sagittal area measurements but gave insight about morphological changes to abnormal pericytes in Rbpj$^{i\Delta EC}$ brain.

Pericyte reduction or loss from brain microvessels is not associated with Rbpj mediated brain arteriovenous malformation

To our knowledge, this report is the first to demonstrate pathological pericyte expansion in a mouse model of brain AVM. Our data contrast findings from other genetic models of CNS AVMs and from human brain AVM tissue and thus emphasize the heterogeneity among AVM pathologies and mechanisms. For example, reduced pericyte number and coverage of endothelium was reported in sporadic brain AVM samples from human patients (Winkler et al., 2018); however, these correlative studies could not reveal whether pericyte reduction was a cause or consequence of human brain AVM. Using mouse models of TGFβ related brain AVM, studies have similarly shown reduced pericyte coverage of brain microvessels (Chen et al., 2013; Tual-Chalot et al., 2014). In a genetic model of retina AVM, endothelial Smad4 deficiency led to decreased pericytes associated with retinal vessels (Crist et al., 2018). Two recent studies genetically deleted Rbpj from pericytes, in the early postnatal period, and found CNS AVM with pericyte deficiency (Diéguez-Hurtado et al., 2019; Nadeem et al., 2020). Further, Nadeem et al. (2020) showed that pericyte deficiency preceded vessel enlargement, suggesting that intact pericytes prevent AV shunting in retina vasculature. Differences in pericyte coverage among AVM models may reflect different mechanisms in AVM pathogenesis. For example, some AVMs are triggered by increased EC proliferation, serving to populate the increasing-diameter vessel growth. Such angiogenic AVMs are associated with reduced pericyte coverage, possibly as a mechanism to accommodate proliferative ECs and growth. By contrast, some AVMs, including Rbpj$^{i\Delta EC}$ mediated brain AVMs, develop without increased EC proliferation (Murphy et al., 2014; Nielsen et al., 2014)—perhaps non-angiogenic ECs on microvessels elicit different pericyte responses during AVM pathogenesis. Despite the contrasting data for pericytes and CNS AVMs, our findings show that pericyte deficiency is not required for brain AVM formation. Thus, our study underscores the importance of probing mechanisms of genetically distinct brain AVM and of developing specific and appropriate therapies.

A question remains regarding the functional implications of pericyte abnormalities during brain AVM. In models of pericyte reduction during brain AVM, one working hypothesis is that the loss of pericytes loosens contractile constraints on microvessels and permits vessel dilation (Nadeem et al., 2020). Following even a slight increase in vessel diameter, increased blood flow is directed toward that path of least resistance and triggers continued vessel dilation, resulting in

AV shunting. Loss of pericytes in brain AVM has also been suggested to disrupt vessel stability, which may be related to intracranial hemorrhages associated with brain AVM tissue (Winkler et al., 2018). Data from our Rbpj mediated brain AVM model showed that pericyte expansion was accompanied by abnormalities to pericyte morphology and disruptions to EC-pericyte communication. Thus, these abnormal pericytes may also contribute to microvascular instability. Because endothelial Rbpj deletion leads to endothelial, pericyte, cerebellar, and motor behavioral abnormalities (Nielsen et al., 2014; Chapman et al., 2022), a future challenge will be to tease apart which brain AVM pathologies are a consequence of endothelial vs. pericyte vs. tissue morphogenetic impairments, or of some combination thereof.

Data availability statement

The original contributions presented in this study are included in the article/**Supplementary material**, further inquiries can be directed to the corresponding author.

Ethics statement

This animal study was reviewed and approved by the Ohio University IACUC, Animal Protocol # 16-H-024.

Author contributions

SS, SN, SK, and CN conceptualized and designed the experiments. SS, SN, SK, SA, and CN performed the experiments and analyzed the data. CN wrote the manuscript. All authors contributed to the article and approved the submitted version.

Funding

This research was supported by the President's Undergraduate Research Funding and John J. Kopchick/Molecular and Cellular Biology/Translational Biomedical Sciences Undergraduate Research Support Funding to SS. By Ohio University Honors Tutorial College Research Apprenticeships and Summer Neuroscience Undergraduate Research Fellowships to SS and SK; and by start-up funding (Ohio University College of Arts and Sciences) and NIH R15 NS111376 to CN.

Acknowledgments

We thank Emi Olin (www.abieto.com) for artistic rendering in **Figure 6**. We also thank Ohio University IACUC and Laboratory for Animal Research for Animal Care; Ohio University Histopathology Core for access to cryostat; Ohio University Neuroscience Program for training and access to confocal microscope.

Conflict of interest

The authors declare that the research was conducted in the absence of any commercial or financial relationships that could be construed as a potential conflict of interest.

Publisher's note

Supplementary material

The Supplementary Material for this article can be found online at: https://www.frontiersin.org/articles/10.3389/fnhum.2022.974033/full#supplementary-material

References

Armulik, A., Genové, G., and Betsholtz, C. (2011). Pericytes: developmental, physiological, and pathological perspectives, problems, and promises. *Dev. Cell* 21, 193–215. doi: 10.1016/j.devcel.2011.07.001

Armulik, A., Genové, G., Mäe, M., Nisancioglu, M. H., Wallgard, E., Niaudet, C., et al. (2010). Pericytes regulate the blood-brain barrier. *Nature* 468, 557–561. doi: 10.1038/nature09522

Battegay, E. J., Rupp, J., Iruela-Arispe, L., Sage, E. H., and Pech, M. (1994). PDGF-BB modulates endothelial proliferation and angiogenesis in vitro via PDGF B-Receptors. *J. Cell Biol.* 125, 917–928.

Bell, A. H., Miller, S. L., Castillo-Melendez, M., and Malhotra, A. (2020). The neurovascular unit: effects of brain insults during the perinatal period. *Front. Neurosci.* 13:1452. doi: 10.3389/fnins.2019.01452

Bell, R. D., Winkler, E. A., Sagare, A. P., Singh, I., LaRue, B., Deane, R., et al. (2010). Pericytes control key neurovascular functions and neuronal phenotype in the adult brain and during brain aging. *Neuron* 68, 409–427. doi: 10.1016/j.neuron.2010.09.043

Bennett, H. C., and Kim, Y. (2021). Pericytes across the lifetime in the central nervous system. *Front. Cell. Neurosci.* 15:627291. doi: 10.3389/fncel.2021.627291

Birbrair, A. (2019). "Pericyte biology in disease," in *Advances in Experimental Medicine and Biology*, ed. A. Birbrair (Cham: Springer International Publishing), doi: 10.1007/978-3-030-16908-4

Bonkowski, D., Katyshev, V., Balabanov, R. D., Borisov, A., and Dore-Duffy, P. (2011). The CNS microvascular pericyte: pericyte-astrocyte crosstalk in the regulation of tissue survival. *Fluids Barriers CNS* 8:8. doi: 10.1186/2045-8118-8-8

Bourdeau, A., Dumont, D. J., and Letarte, M. (1999). A murine model of hereditary hemorrhagic telangiectasia. *J. Clin. Invest.* 104, 1343–1351. doi: 10.1172/JCI8088

Cai, W., Liu, H., Zhao, J., Chen, L. Y., Chen, J., Lu, Z., et al. (2017). Pericytes in brain injury and repair after ischemic stroke. *Transl. Stroke Res.* 8, 107–121. doi: 10.1007/s12975-016-0504-4

Chan-Ling, T., Page, M. P., Gardiner, T., Baxter, L., Rosinova, E., and Hughes, S. (2004). Desmin ensheathment ratio as an indicator of vessel stability. *Am. J. Pathol.* 165, 1301–1313. doi: 10.1016/S0002-9440(10)63389-5

Chapman, A. D., Selhorst, S., LaComb, J., LeDantec-Boswell, A., Wohl, T. R., Adhicary, S., et al. (2022). Endothelial Rbpj is required for cerebellar morphogenesis and motor control in the early postnatal mouse brain. *Cerebellum* Online ahead of print. doi: 10.1007/s12311-022-01429-w

Chen, J., Luo, Y., Hui, H., Cai, T., Huang, H., Yang, F., et al. (2017). CD146 coordinates brain endothelial cell-pericyte communication for blood-brain barrier development. *Proc. Natl. Acad. Sci. U S A.* 114, E7622–E7631. doi: 10.1073/pnas.1710848114

Chen, W., Guo, Y., Walker, E. J., Shen, F., Jun, K., Oh, S. P., et al. (2013). Reduced mural cell coverage and impaired vessel integrity after angiogenic stimulation in the Alk1 -deficient brain. *Arterioscler. Thromb. Vasc. Biol.* 33, 305–310. doi: 10.1161/ATVBAHA.112.300485

Chen, Y., Li, R., Ma, L., Meng, X., Yan, D., Wang, H., et al. (2021). Long-term outcomes of brainstem arteriovenous malformations after different management modalities: a single-centre experience. *Stroke Vasc. Neurol.* 6, 65–73. doi: 10.1136/svn-2020-000407

Crist, A. M., Lee, A. R., Patel, N. R., Westhoff, D. E., and Meadows, S. M. (2018). Vascular deficiency of Smad4 causes arteriovenous malformations: a mouse model of hereditary hemorrhagic telangiectasia. *Angiogenesis* 21, 363–380. doi: 10.1007/s10456-018-9602-0

Crouch, E. E., and Doetsch, F. (2018). FACS isolation of endothelial cells and pericytes from mouse brain microregions. *Nat. Protoc.* 13, 738–751. doi: 10.1038/nprot.2017.158

Cuervo, H., Nielsen, C. M., Simonetto, D. A., Ferrell, L., Shah, V. H., and Wang, R. A. (2016). Endothelial notch signaling is essential to prevent hepatic vascular malformations in mice: notch signaling prevents hepatic vascular malformations in mice. *Hepatology* 64, 1302–1316. doi: 10.1002/hep.28713

Daneman, R., Zhou, L., Kebede, A. A., and Barres, B. A. (2010). Pericytes are required for blood-brain barrier integrity during embryogenesis. *Nature* 468, 562–566. doi: 10.1038/nature09513

DeRuiter, M. C., Poelmann, R. E., VanMunsteren, J. C., Mironov, V., Markwald, R. R., and Gittenberger-de Groot, A. C. (1997). Embryonic endothelial cells transdifferentiate into mesenchymal cells expressing smooth muscle actins in vivo and in vitro. *Circulation Res.* 80, 444–451. doi: 10.1161/01.RES.80.4.444

Diéguez-Hurtado, R., Kato, K., Giaimo, B. D., Nieminen-Kelhä, M., Arf, H., Ferrante, F., et al. (2019). Loss of the transcription factor RBPJ induces disease-promoting properties in brain pericytes. *Nat. Commun.* 10:2817. doi: 10.1038/s41467-019-10643-w

Dore-Duffy, P., Katychev, A., Wang, X., and Van Buren, E. (2006). CNS microvascular pericytes exhibit multipotential stem cell activity. *J. Cereb. Blood Flow Metab.* 26, 613–624. doi: 10.1038/sj.jcbfm.9600272

Dore-Duffy, P., Owen, C., Balabanov, R., Murphy, S., Beaumont, T., and Rafols, J. A. (2000). Pericyte migration from the vascular wall in response to traumatic brain injury. *Microvasc. Res.* 60, 55–69. doi: 10.1006/mvre.2000.2244

Do Prado, L. B., Han, C., Oh, S. P., and Su, H. (2019). Recent advances in basic research for brain arteriovenous malformation. *IJMS* 20:5324. doi: 10.3390/ijms20215324

Fernández-Chacón, M., García-González, I., Mühleder, S., and Benedito, R. (2021). Role of notch in endothelial biology. *Angiogenesis* 24, 237–250. doi: 10.1007/s10456-021-09793-7

Fish, J. E., Flores Suarez, C. P., Boudreau, E., Herman, A. M., Gutierrez, M. C., Gustafson, D., et al. (2020). Somatic gain of KRAS function in the endothelium is sufficient to cause vascular malformations that require MEK but not PI3K signaling. *Circ. Res.* 127, 727–743. doi: 10.1161/CIRCRESAHA.119.316500

Geranmayeh, M. H., Rahbarghazi, R., and Farhoudi, M. (2019). Targeting pericytes for neurovascular regeneration. *Cell Commun. Signal.* 17:26. doi: 10.1186/s12964-019-0340-8

Gerhardt, H., Wolburg, H., and Redies, C. (2000). N-cadherin mediates pericytic-endothelial interaction during brain angiogenesis in the chicken. *Dev. Dyn.* 218, 472–479. doi: 10.1002/1097-0177(200007)218:3<472::AID-DVDY1008>3.0.CO;2-#

Gonzales, A. L., Klug, N. R., Moshkforoush, A., Lee, J. C., Lee, F. K., Shui, B., et al. (2020). Contractile pericytes determine the direction of blood flow at capillary junctions. *Proc. Natl. Acad. Sci. U S A.* 117, 27022–27033. doi: 10.1073/pnas.1922755117

Gu, X., Liu, X.-Y., Fagan, A., Gonzalez-Toledo, M. E., and Zhao, L.-R. (2012). Ultrastructural changes in cerebral capillary pericytes in aged notch3 mutant transgenic mice. *Ultrastructural Pathol.* 36, 48–55. doi: 10.3109/01913123.2011.620220

Han, S. J., Englot, D. J., Kim, H., and Lawton, M. T. (2015). Brainstem arteriovenous malformations: anatomical subtypes, assessment of "occlusion in situ" technique, and microsurgical results. *JNS* 122, 107–117. doi: 10.3171/2014.8.JNS1483

Hartmann, D. A., Underly, R. G., Grant, R. I., Watson, A. N., Lindner, V., and Shih, A. Y. (2015). Pericyte structure and distribution in the cerebral cortex revealed by high-resolution imaging of transgenic mice. *Neurophoton* 2:041402. doi: 10.1117/1.NPh.2.4.041402

Hellström, M., Phng, L.-K., Hofmann, J. J., Wallgard, E., Coultas, L., Lindblom, P., et al. (2007). Dll4 signalling through Notch1 regulates formation of tip cells during angiogenesis. *Nature* 445, 776–780. doi: 10.1038/nature05571

Hirunpattarasilp, C., Attwell, D., and Freitas, F. (2019). The role of pericytes in brain disorders: from the periphery to the brain. *J. Neurochem.* 150, 648–665. doi: 10.1111/jnc.14725

Hughes, S., Gardiner, T., Baxter, L., and Chan-Ling, T. (2007). Changes in pericytes and smooth muscle cells in the kitten model of retinopathy of prematurity: implications for plus disease. *Invest. Ophthalmol. Vis. Sci.* 48:1368. doi: 10.1167/iovs.06-0850

Jin, S., Hansson, E. M., Tikka, S., Lanner, F., Sahlgren, C., Farnebo, F., et al. (2008). Notch signaling regulates platelet-derived growth factor receptor-β expression in vascular smooth muscle cells. *Circ. Res.* 102, 1483–1491. doi: 10.1161/CIRCRESAHA.107.167965

Khoury, J., and Langleben, D. (1996). Platelet-activating factor stimulates lung pericyte growth in vitro. *Am. J. Physiology-Lung Cell. Mol. Physiol.* 270, L298–L304. doi: 10.1152/ajplung.1996.270.2.L298

Kokovay, E., Li, L., and Cunningham, L. A. (2006). Angiogenic recruitment of pericytes from bone marrow after stroke. *J. Cereb. Blood Flow Metab.* 26, 545–555. doi: 10.1038/sj.jcbfm.9600214

Krebs, L. T., Shutter, J. R., Tanigaki, K., Honjo, T., Stark, K. L., and Gridley, T. (2004). Haploinsufficient lethality and formation of arteriovenous malformations in Notch pathway mutants. *Genes Dev.* 18, 2469–2473. doi: 10.1101/gad.1239204

Krebs, L. T., Xue, Y., Norton, C. R., Shutter, J. R., Maguire, M., Sundberg, J. P., et al. (2000). Notch signaling is essential for vascular morphogenesis in mice. *Genes Dev.* 14, 1343–1352. doi: 10.1101/gad.14.11.1343

Lebrin, F., Srun, S., Raymond, K., Martin, S., van den Brink, S., Freitas, C., et al. (2010). Thalidomide stimulates vessel maturation and reduces epistaxis in individuals with hereditary hemorrhagic telangiectasia. *Nat. Med.* 16, 420–428. doi: 10.1038/nm.2131

Lendahl, U., Nilsson, P., and Betsholtz, C. (2019). Emerging links between cerebrovascular and neurodegenerative diseases—a special role for pericytes. *EMBO Rep.* 20:e48070. doi: 10.15252/embr.201948070

Li, F., Lan, Y., Wang, Youliang, Wang, J., Yang, G., et al. (2011). Endothelial Smad4 maintains cerebrovascular integrity by activating N-Cadherin through cooperation with notch. *Dev. Cell* 20, 291–302. doi: 10.1016/j.devcel.2011.01.011

Liu, H., Zhang, W., Kennard, S., Caldwell, R. B., and Lilly, B. (2010). Notch3 is critical for proper angiogenesis and mural cell investment. *Circ. Res.* 107, 860–870. doi: 10.1161/CIRCRESAHA.110.218271

Ma, S., Kwon, H. J., and Huang, Z. (2012). A functional requirement for astroglia in promoting blood vessel development in the early postnatal brain. *PLoS One* 7:e48001. doi: 10.1371/journal.pone.0048001

Murphy, P. A., Kim, T. N., Huang, L., Nielsen, C. M., Lawton, M. T., Adams, R. H., et al. (2014). Constitutively active Notch4 receptor elicits brain

arteriovenous malformations through enlargement of capillary-like vessels. *Proc. Natl. Acad. Sci. U S A.* 111, 18007–18012. doi: 10.1073/pnas.1415316111

Muzumdar, M. D., Tasic, B., Miyamichi, K., Li, L., and Luo, L. (2007). A global double-fluorescent Cre reporter mouse. *Genesis* 45, 593–605. doi: 10.1002/dvg.20335

Nadeem, T., Bogue, W., Bigit, B., and Cuervo, H. (2020). Deficiency of Notch signaling in pericytes results in arteriovenous malformations. *JCI Insight* 5:e125940. doi: 10.1172/jci.insight.125940

Nadeem, T., Bommareddy, A., Bolarinwa, L., and Cuervo, H. (2022). Pericyte dynamics in the mouse germinal matrix angiogenesis. *FASEB J.* 36:e22339. doi: 10.1096/fj.202200120R

Nielsen, C. M., Cuervo, H., Ding, V. W., Kong, Y., Huang, E. J., and Wang, R. A. (2014). Deletion of Rbpj from postnatal endothelium leads to abnormal arteriovenous shunting in mice. *Development* 141, 3782–3792. doi: 10.1242/dev.108951

Nielsen, C. M., and Dymecki, S. M. (2010). Sonic hedgehog is required for vascular outgrowth in the hindbrain choroid plexus. Developmental Biology 340, 430–437. doi: 10.1016/j.ydbio.2010.01.032

Nikolaev, S. I., Vetiska, S., Bonilla, X., Boudreau, E., Jauhiainen, S., Rezai Jahromi, B., et al. (2018). Somatic activating KRAS mutations in arteriovenous malformations of the brain. *N. Engl. J. Med.* 378, 250–261. doi: 10.1056/NEJMoa1709449

Nikolakopoulou, A. M., Zhao, Z., Montagne, A., and Zlokovic, B. V. (2017). Regional early and progressive loss of brain pericytes but not vascular smooth muscle cells in adult mice with disrupted platelet-derived growth factor receptor-β signaling. *PLoS One* 12:e0176225. doi: 10.1371/journal.pone.0176225

Park, S. O., Wankhede, M., Lee, Y. J., Choi, E.-J., Fliess, N., Choe, S.-W., et al. (2009). Real-time imaging of de novo arteriovenous malformation in a mouse model of hereditary hemorrhagic telangiectasia. *J. Clin. Invest.* 119, 3487–3496. doi: 10.1172/JCI39482

Polito, A., and Reynolds, R. (2005). NG2-expressing cells as oligodendrocyte progenitors in the normal and demyelinated adult central nervous system. *J. Anatomy* 207, 707–716. doi: 10.1111/j.1469-7580.2005.00454.x

Rajantie, I., Ilmonen, M., Alminaite, A., Ozerdem, U., Alitalo, K., and Salven, P. (2004). Adult bone marrow-derived cells recruited during angiogenesis comprise precursors for periendothelial vascular mural cells. *Blood* 104, 2084–2086. doi: 10.1182/blood-2004-01-0336

Raper, D. M. S., Winkler, E. A., Rutledge, C. W., Cooke, D. L., and Abla, A. A. (2020). An update on medications for brain arteriovenous malformations. *Neurosurgery* 87, 871–878. doi: 10.1093/neuros/nyaa192

Reyahi, A., Nik, A. M., Ghiami, M., Gritli-Linde, A., Pontén, F., Johansson, B. R., et al. (2015). Foxf2 is required for brain pericyte differentiation and development and maintenance of the blood-brain barrier. *Dev. Cell* 34, 19–32. doi: 10.1016/j.devcel.2015.05.008

Satomi, J., Mount, R. J., Toporsian, M., Paterson, A. D., Wallace, M. C., Harrison, R. V., et al. (2003). Cerebral vascular abnormalities in a murine model of hereditary hemorrhagic telangiectasia. *Stroke* 34, 783–789. doi: 10.1161/01.STR.0000056170.47815.37

Schmittgen, T. D., and Livak, K. J. (2008). Analyzing real-time PCR data by the comparative CT method. *Nat. Protoc.* 3, 1101–1108. doi: 10.1038/nprot.2008.73

Shi, X. (2009). Cochlear pericyte responses to acoustic trauma and the involvement of hypoxia-inducible factor-1α and vascular endothelial growth factor. *Am. J. Pathol.* 174, 1692–1704. doi: 10.2353/ajpath.2009.080739

Song, N., Huang, Y., Shi, H., Yuan, S., Ding, Y., Song, X., et al. (2009). Overexpression of platelet-derived growth factor-bb increases tumor pericyte content via stromal-derived factor-1α/CXCR4 axis. *Cancer Res.* 69, 6057–6064. doi: 10.1158/0008-5472.CAN-08-2007

Sörensen, I., Adams, R. H., and Gossler, A. (2009). DLL1-mediated Notch activation regulates endothelial identity in mouse fetal arteries. *Blood* 113, 5680–5688. doi: 10.1182/blood-2008-08-174508

Sweeney, M. D., Ayyadurai, S., and Zlokovic, B. V. (2016). Pericytes of the neurovascular unit: key functions and signaling pathways. *Nat. Neurosci.* 19, 771–783. doi: 10.1038/nn.4288

Tagami, M., Nara, Y., Kubota, A., Fujino, H., and Yamori, Y. (1990). Ultrastructural changes in cerebral pericytes and astrocytes of stroke-prone spontaneously hypertensive rats. *Stroke* 21, 1064–1071. doi: 10.1161/01.STR.21.7.1064

Tanigaki, K., Han, H., Yamamoto, N., Tashiro, K., Ikegawa, M., Kuroda, K., et al. (2002). Notch-RBP-J signaling is involved in cell fate determination of marginal zone B cells. *Nat. Immunol.* 3, 443–450. doi: 10.1038/ni793

Thalgott, J., Dos-Santos-Luis, D., and Lebrin, F. (2015). Pericytes as targets in hereditary hemorrhagic telangiectasia. *Front. Genet.* 6:37. doi: 10.3389/fgene.2015.00037

Tual-Chalot, S., Allinson, K. R., Fruttiger, M., and Arthur, H. M. (2013). Whole mount immunofluorescent staining of the neonatal mouse retina to investigate angiogenesis in vivo. *JoVE* 77:50546. doi: 10.3791/50546

Tual-Chalot, S., Mahmoud, M., Allinson, K. R., Redgrave, R. E., Zhai, Z., Oh, S. P., et al. (2014). Endothelial depletion of acvrl1 in mice leads to arteriovenous malformations associated with reduced endoglin expression. *PLoS One* 9:e98646. doi: 10.1371/journal.pone.0098646

Uemura, M. T., Maki, T., Ihara, M., Lee, V. M. Y., and Trojanowski, J. Q. (2020). Brain microvascular pericytes in vascular cognitive impairment and dementia. *Front. Aging Neurosci.* 12:80. doi: 10.3389/fnagi.2020.00080

Wälchli, T., Mateos, J. M., Weinman, O., Babic, D., Regli, L., Hoerstrup, S. P., et al. (2015). Quantitative assessment of angiogenesis, perfused blood vessels and endothelial tip cells in the postnatal mouse brain. *Nat. Protoc.* 10, 53–74. doi: 10.1038/nprot.2015.002

Wang, D.-B., Blocher, N. C., Spence, M. E., Rovainen, C. M., and Woolsey, T. A. (1992). Development and remodeling of cerebral blood vessels and their flow in postnatal mice observed with in vivo videomicroscopy. *J. Cereb. Blood Flow Metab.* 12, 935–946. doi: 10.1038/jcbfm.1992.130

Winkler, E. A., Bell, R. D., and Zlokovic, B. V. (2010). Pericyte-specific expression of PDGF beta receptor in mouse models with normal and deficient PDGF beta receptor signaling. *Mol. Neurodegeneration* 5:32. doi: 10.1186/1750-1326-5-32

Winkler, E. A., Birk, H., Burkhardt, J.-K., Chen, X., Yue, J. K., Guo, D., et al. (2018). Reductions in brain pericytes are associated with arteriovenous malformation vascular instability. *J. Neurosurg.* 129, 1464–1474. doi: 10.3171/2017.6.JNS17860

Yao, H., Duan, M., Hu, G., and Buch, S. (2011). Platelet-Derived growth factor b chain is a novel target gene of cocaine-mediated notch1 signaling: implications for hiv-associated neurological disorders. *J. Neurosci.* 31, 12449–12454. doi: 10.1523/JNEUROSCI.2330-11.2011

Zetterberg, E., Vannucchi, A. M., Migliaccio, A. R., Vainchenker, W., Tulliez, M., Dickie, R., et al. (2007). Pericyte coverage of abnormal blood vessels in myelofibrotic bone marrows. *Haematologica* 92, 597–604. doi: 10.3324/haematol.11013

Zhu, X., Bergles, D. E., and Nishiyama, A. (2008). NG2 cells generate both oligodendrocytes and gray matter astrocytes. *Development* 135, 145–157. doi: 10.1242/dev.004895

frontiers | Frontiers in Human Neuroscience

TYPE Original Research
PUBLISHED 16 September 2022
DOI 10.3389/fnhum.2022.946349

OPEN ACCESS

EDITED BY
Lorelei Shoemaker,
Stanford University, United States

REVIEWED BY
Li Chuanhui,
Capital Medical University, China
Ting-yu Yi,
Zhangzhou Affiliated Hospital of Fujian Medical University, China

*CORRESPONDENCE
Guohui Jiang
neurodoctor@163.com
Youlin Wu
suriv007@126.com

†These authors have contributed equally to this work and share first authorship

SPECIALTY SECTION
This article was submitted to Brain Health and Clinical Neuroscience, a section of the journal Frontiers in Human Neuroscience

RECEIVED 17 May 2022
ACCEPTED 15 August 2022
PUBLISHED 16 September 2022

CITATION
Zhou J, Peng D, Sun D, Dai W, Long C, Meng R, Wang J, Yan Z, Wang T, Wang L, Yue C, Li L, Zi W, Wang L, Wang X, Wu Y and Jiang G (2022) Effect of vertebrobasilar dolichoectasia on endovascular therapy in acute posterior circulation infarction. *Front. Hum. Neurosci.* 16:946349. doi: 10.3389/fnhum.2022.946349

Effect of vertebrobasilar dolichoectasia on endovascular therapy in acute posterior circulation infarction

Jing Zhou[1,2†], Daizhou Peng[3†], Dong Sun[4], Weipeng Dai[5], Ceng Long[6], Renliang Meng[7], Jing Wang[8], Zhizhong Yan[9], Tao Wang[10], Li Wang[11], Chengsong Yue[12], Linyu Li[12], Wenjie Zi[12], Lingling Wang[1,2], Xiaoming Wang[1,2], Youlin Wu[13*] and Guohui Jiang[1,2*]

[1]Department of Neurology, Affiliated Hospital of North Sichuan Medical College, Nanchong, China, [2]Institute of Neurological Diseases, North Sichuan Medical College, Nanchong, China, [3]Department of Neurology, Qianxinan People's Hospital, Wuhan, China, [4]Department of Neurology, Zhongnan Hospital, Wuhan University, Wuhan, China, [5]Department of Neurology, Jiangmen Central Hospital, Jiangmen, China, [6]Department of Emergency, Xiangtan Central Hospital, Xiangtan, China, [7]Department of Neurology Affiliated Hospital of Southwest Medical University, Luzhou, China, [8]Department of Neurology, Shanxi Provincial People's Hospital, Taiyuan, China, [9]Department of Neurosurgery, The 904th Hospital of the People's Liberation Army, Wuxi, China, [10]Department of Neurology, Huainan First People's Hospital, Huainan, China, [11]Department of Neurology, The First Affiliated Hospital of University of Science and Technology of China, Hefei, China, [12]Department of Neurology, Xinqiao Hospital and the Second Affiliated Hospital, Army Medical University (Third Military Medical University), Chongqing, China, [13]Department of Neurology, Chongzhou People's Hospital, Chongzhou, China

Background and purpose: This study aimed to analyze the feasibility and safety of endovascular therapy (EVT) in patients with acute posterior circulation stroke and vertebrobasilar dolichoectasia (VBD).

Materials and methods: BASILAR was a national prospective registry of consecutive patients with symptomatic and imaging-confirmed acute stroke in the posterior circulation within 24 h of symptom onset. We evaluated EVT feasibility and safety in patients with VBD. Primary outcomes included improvement in modified Rankin Scale scores (mRS) at 90 days and mortality within 90 days. The secondary outcome was the rate of favorable functional outcome, defined as mRS $\leq$ 3 (indicating independent ambulation) at 90 days. Safety outcomes included surgery-related complications and other serious adverse events.

Results: A total of 534 cases were included: 159 with VBD and 375 controls. No significant difference in mRS at 90 days was found between groups, but patients with VBD had a higher baseline National Institutes of Health Stroke Scale (NIHSS) score [30 (19–33) vs. 25 (15–32)] and were older [65 (59–74) vs. 63 (55–72) year]. After propensity score matching, there were no significant differences in baseline NIHSS score between the two groups, and the efficacy and safety of EVT were similar between patients with or without VBD. Furthermore, the

prognostic effect of puncture-to-recanalization time on the probability of mortality within 90 days in EVT-treated patients with VBD was significant {adjusted odds ratio, 1.008 [95% confidence interval (1.001–1.015)]}.

Conclusion: Endovascular therapy is safe and feasible in patients with acute posterior circulation stroke and VBD. The puncture-to-recanalization time is important for predicting the prognosis of EVT-treated patients with VBD.

KEYWORDS

vertebrobasilar dolichoectasia, endovascular therapy, posterior circulation infarction, acute ischemic stroke, clinical outcome

Introduction

Vertebrobasilar dolichoectasia (VBD) is a rare disease characterized by elongation, dilation, and tortuosity of the vertebrobasilar artery. Its prevalence is inaccurate and variable, ranging from 0.05 to 18%, based on several different study populations (Samim et al., 2016). For instance, in stroke patients, it ranges from 2.6 to 17.1% (Wolters et al., 2013). Despite the low prevalence of VBD, several serious clinical syndromes are associated with it, including combined brainstem and cranial nerve syndrome, cervicomedullary junction compression, temporary or permanent motor impairment, cerebellar dysfunction, central sleep apnea, hydrocephalus, ischemic stroke, and subarachnoid hemorrhage (Moss and West, 1996; Hongo et al., 1999). Despite various reports of combined compression of brainstem structures in patients with VBD, few studies focused on ischemic stroke complications and whether the treatment of vascular events associated with VBD must differ from standard treatment.

Recently, endovascular therapy (EVT) has been applied for its efficacy and safety. Several studies have shown better functional outcomes in patients with acute basilar artery occlusion (BAO) treated with EVT than patients treated with standard medical therapy alone and that EVT is effective in reducing mortality and improving activities of daily function in stroke patients (Kang et al., 2018; Kwak and Park, 2020). The BASILAR study found among patients with acute BAO, EVT administered within 24 h of estimated occlusion time is associated with better functional outcomes and reduced mortality (Writing Group for the et al., 2020). In other words, EVT is an effective treatment option for patients with ischemic stroke in the posterior circulation; however, the effect of EVT on patients with ischemic stroke and VBD is unclear.

Based on the largest multicenter consecutive BAO-cohort undergoing EVT, this study investigated for the first time whether EVT affects outcomes in patients with VBD and ischemic stroke in the posterior circulation.

Materials and methods

Data supporting this study may be provided by the corresponding author upon reasonable request.

The BASILAR registry and patient selection

The BASILAR study enrolled patients with symptomatic and radiologically confirmed acute stroke in the posterior circulation within 24 h of symptom onset from 47 comprehensive stroke centers in China between January 2014 and May 2019. Study centers were required to have performed at least 30 endovascular procedures annually, including at least 15 thrombectomy procedures using stent retriever devices. All interventionists had to be certified in EVT of large vessel occlusion strokes. The study protocol was approved by the ethics committee of the Xinqiao Hospital, Army Medical University, in Chongqing, China, and each subcenter. BASILAR is registered on the Chinese Clinical Trial Registry (Writing Group for the et al., 2020).

Currently, there are no uniform quantitative imaging criteria for VBD diagnosis. It usually relies on the practical experience of clinicians and radiologists, combined with the assessment of clinical symptoms on vascular images. Patients are diagnosed with VBD depending on the extrapolation of the established computed tomography (CT) criteria by Smoker (Smoker et al., 1986) and magnetic resonance imaging (MRI) criteria by Giang et al. (1988). According to the imaging diagnostic criteria, we included data of patients with VBD if they fulfilled the following criteria: (1) aged $\geq$ 18 years; (2) presentation within 24 h of estimated time of acute stroke in the posterior circulation; (3) being able to provide informed consent; (4) EVT had to be initiated within 24 h of estimated time of acute stroke in the posterior circulation; (5)diameter of the vertebral artery or BA $>$ 4.5 mm; (6) for the basilar artery (BA), bifurcation above the suprasellar cistern or evidence

10.3389/fnhum.2022.946349

TABLE 1 Baseline characteristics of patients with or without VBD.

	No./Total No. (%)			Propensity Score Matching No./No. (%)		
Characteristic	**Non-VBD, *n* = 375**	**VBD, *n* = 159**	***P*-value**	**Non-VBD, *n* = 159**	**VBD, *n* = 159**	***P*-value**
Age, median (IQR), y	63 (55–72)	65 (59–74)	< 0.015	64 (57–74)	65 (59–74)	0.306
Male, *n*/total *n* (%)	277 (73.9)	130 (81.8)	0.05	121 (76.1)	130 (81.8)	0.216
Baseline NIHSS, median (IQR)	25 (15–32)	30 (19–33)	0.03	29 (20–34)	30 (19–34)	0.793
pc-ASPECT baseline	8 (7–9)	8 (7–9)	0.7	8 (7–9)	8 (7–9)	0.627
ASITN/SIR grade			0.23			0.478
Grade 0–1	220 (58.7)	100 (62.9)		100 (62.9)	100 (62.9)	
Grade 2	99 (26.4)	44 (27.7)		38 (23.9)	44 (27.7)	
Grade 3–4	56 (14.9)	15 (9.4)		21 (13.2)	15 (9.4)	
Medical history *n*/total *n* (%)						
Ischemic stroke	85 (22.7)	35 (22.0)	0.868	39 (24.5)	35 (22.0)	0.596
Hypertension	263 (70.1)	103 (64.8)	0.223	119 (74.8)	103 (64.8)	0.051
Hyperlipidemia	132 (35.2)	47 (29.6)	0.207	50 (31.4)	47 (29.6)	0.715
Diabetes	89 (23.7)	31 (19.5)	0.283	42 (26.4)	31 (19.5)	0.142
Smoking	147 (39.2)	52 (32.7)	0.156	70 (44)	52 (32.7)	0.038
Dringking	95 (25.3)	31 (19.5)	0.146	43 (27)	31 (19.5)	0.111
Coronary heart disease	54 (14.4)	20 (12.6)	0.577	28 (17.6)	20 (12.6)	0.21
Atrial fibrillation	76 (20.3)	29 (18.2)	0.590	38 (23.9)	29 (18.2)	0.216
Location of occlusion, *n*/total *n* (%)			0.732			0.4
Distal BA	115 (30.7)	45 (28.3)		50 (31.4)	45 (28.3)	
Middle BA	113 (30.1)	53 (33.3)		45 (28.3)	53 (33.3)	
Proximal BA	64 (17.1)	32 (20.1)		24 (44.8)	32 (20.1)	
VA-V4	73 (19.5)	25 (15.7)		35 (58.3)	25 (15.7)	
Time metrics, min, median (IQR)						
Onset-puncture time	315 (216–459)	355 (208–510)	0.184	319 (219–490)	355 (208–510)	0.486
Onset-imaging time	190 (80–332)	232 (102–410)	0.048	220 (100–389)	232 (102–410)	0.802
Puncture-recanalization time	100 (69–141)	110 (77–160)	0.032	102 (67–141)	110 (77–160)	0.032
mTICI score 2b/3, *n*/total *n* (%)	303 (80.8)	131 (82.4)	0.667	125 (78.6)	131 (82.4)	0.396

IQR, interquartile range; VBD, vertebrobasilar dolichoectasia; Non-VBD, patients without vertebrobasilar dolichoectasia; NIHSS, National Institutes of Health Stroke Scale; pc-ASPECTS, posterior circulation Alberta Stroke Program Early Computed Tomography Score; VA-V4, V4 of vertebral artery; mTICI, modified Thrombolysis in Cerebral Infarction Score. ASITN/SIR grade indicates the American Society of Interventional and Therapeutic Neuroradiology/Society of Interventional Radiology collateral score.

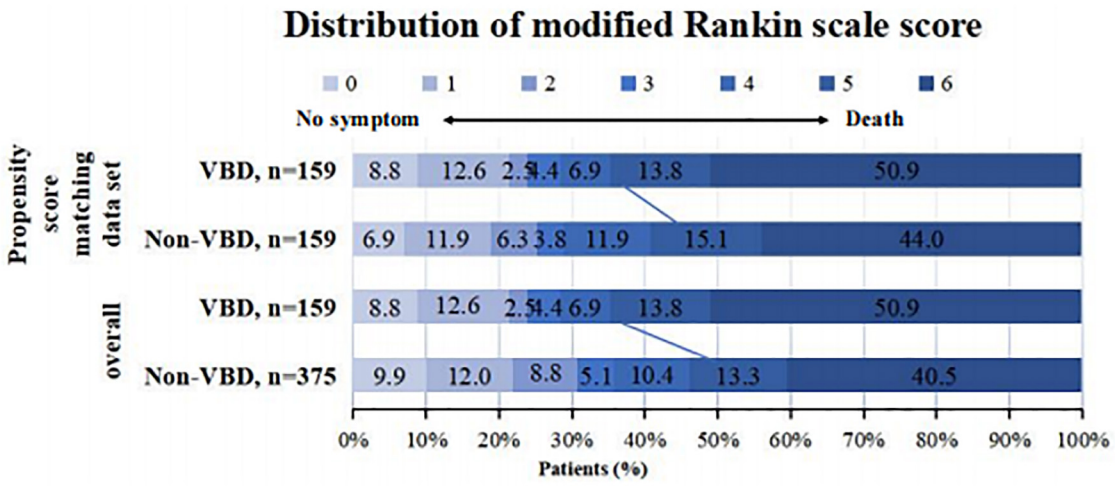

FIGURE 1
Distribution of the modified Rankin scale score at 90 days in the VBD and Non-VBD.

of any portion lateral to the margin of the clivus or dorsum sellae considered elongated; (7) length of the BA > 29.5 mm or lateral deviation at 10 mm from the vertical line between the origin and bifurcation of the BA; and (8) if the length of the intracranial segment of the vertebral artery is > 23.5 mm or any vertebral artery deviates > 10 mm from the vertical

line at the beginning of the BA, the vertebral artery will be lengthened. We included data of patients without VBD if they fulfilled the first four criteria. Exclusion criteria were: (1) lack of follow-up information, (2) incomplete baseline critical imaging data, (3) patients with occlusion in the BA on angiography, (4) neuroimaging evidence of cerebral hemorrhage on presentation, (5) current pregnancy or lactation, and (6) a serious, advanced, or terminal illness.

All participating centers' ethics committees approved the study protocol. Written informed consent was obtained from all patients or their legal representatives.

Variables and imaging analysis

Patients were divided into two groups based on initial enrollment criteria: the VBD and non-VBD groups. Stroke severity was assessed at admission using the National Institutes of Health Stroke Scale (NIHSS) score. Imaging scans were separately reviewed by two trained neuroradiologists (Dr. Chen and Dr. Qiu). In case of discrepancies in the assessment, a third neurologist (Dr. Zi) made the final decision, and a final retrospective analysis was performed. Vascular risk factors (diabetes, hypertension, smoking, hypercholesterolemia, and coronary artery disease) were compared with those in non-VBD patients.

Outcome measurement

Modified Rankin Scale scores (mRS) is a 7-point scale for neurological disability [ranging from 0 (asymptomatic) to 6 (death)] and is assessed by a local neurologist.

The secondary clinical endpoints included functional independence mRS $\leq$ 3 at 90 days, while other outcomes included changes in the NIHSS score from baseline at 24 h and at 5–7 days (or discharge, if earlier).

Safety outcomes included symptomatic intracranial hemorrhage (sICH) within 48 h, confirmed by CT or MRI, and procedure-related complications or other serious adverse events. sICH was defined as an NIHSS score $\geq$ 4 or any parenchymal intracerebral hemorrhage.

Statistical analysis

We compared baseline characteristics, outcomes, and severe adverse events between the VBD and non-VBD groups. Statistical analyses were performed using SPSS version 26 (IBM Corp., Armonk, NY, United States) and STATA version 15.2 (Stata Corp LLC, TX, United States). A two-tailed $P < 0.05$ was considered statistically significant. Univariate comparisons were performed using Fisher's exact test or χ^2 test for categorical variables and Kruskal Wallis test or Mann–Whitney U test for continuous variables. VBD cases were matched in a 1:1 ratio to controls based on the propensity score. To assess the prognostic impact of EVT, propensity score matching was applied to achieve a balance at baseline. We performed a 1:1 matching based on the nearest-neighbor matching algorithm using a caliper width of 0.2 of the propensity score, with age and baseline NIHSS as covariates (Methods in **Supplementary material**).

The second part of the analysis included only patients in the VBD group. A binary logistic regression model was used to assess the variables independently associated with 90-days favorable functional outcomes. The association of puncture-to-recanalization time with outcome is shown in the adjusted margin plots.

Results

Patients' characteristics

Based on the inclusion and exclusion criteria, we initially screened 829 patients from 47 comprehensive stroke centers in China. Among these patients, 179 patients were excluded because the data couldn't be measured due to basilar artery remained closed after surgery and 116 patients were excluded because of lack of imaging data, leaving 534 patients as the current study population.

Baseline characteristics

A total of 534 cases were reviewed, revealing 159 patients with VBD and 375 patients without VBD who met the inclusion criteria. **Table 1** shows the baseline patients' characteristics. VBD was more common in men (81.8%). Hypertension was present in 103 cases (64.8%) and diabetes mellitus in 31 patients (19.5%). Hyperlipidemia and coronary heart disease were present in 47 (29.6%) and 20 (12.6%) patients, respectively. Compared with the non-VBD group, patients in the VBD group were older [65 (59–74) vs. 63 (55–72)] and had higher baseline NIHSS scores [30 (19–33) vs. 25 (15–32)]. Other baseline characteristics were not significantly different between the two groups.

Primary efficacy outcome

The Distribution of the modified Rankin scale score at 90 days is shown in **Figure 1**. The analysis of the primary outcome is shown in **Table 2**. The median 90-day mRS score was 6 [interquartile range (IQR) (3–6)] in the VBD group and 5 [IQR (2–6)] in the non-VBD group ($P < 0.05$; **Table 2**). However, after adjusting for confounding factors, there was no statistical

TABLE 2 Primary and secondary efficacy outcomes and safety outcomes.

Characteristic	No./Total No. (%)							Propensity score matching No./No. (%)		
	Non-VBD *n* = 375	VBD *n* = 159	*P*-value	Unadjusted odds ratio (95% CI)	*P*-value	Adjused odds[a] ratio (95% CI)	*P*-value[b]	Non-VBD *n* = 159	VBD *n* = 159	*P*-value
Primary outcome										
mRS score at 90 days (ordinal)	5 (2–6)	6 (3–6)	0.042	0.696 (0.493–0.983)	0.04	0.9 (0.626–1.293)	0.569	5 (3–6)	6 (3–6)	0.689
Mortality at 90 days	152 (40.5)	81 (50.9)	0.027	1.542 (1.049–2.212)	0.027	1.162 (0.768–1.759)	0.477	74 (46.5)	81 (50.9)	0.432
Secondary outcome										
mRS 0-3 at 90 days	134 (35.7%)	45 (28.3)	0.096					49 (30.8)	45 (28.3)	0.623
mRS 0-2 at 90 days	115 (30.7)	38 (23.9)	0.114					38 (23.9)	38 (23.9)	1
mTICI			0.667							0.369
0–2a	72 (19.2)	28 (17.6)						33 (21.4)	28 (17.6)	
2b–3	303 (80.8)	131 (82.4)						125 (78.6)	131 (82.4)	
NIHSS score, median (IQR)										
NIHSS score after 24 h	26 (11–35)	30 (16–35)	0.036	1.176 (1.144–1.210)	0.001	1.179 (1.145–1.215)	0.001	30 (17–36)	30 (16–35)	0.483
NIHSS score at 5–7 days	18 (5.5–35)	25 (7.3–35)	0.074					24 (8–36)	25 (7.3–35)	0.713
Safety outcome										
sICH	24 (6.5)	14 (9.0)	0.512					12 (7.6)	14 (9)	0.88
Respiratory Failure	151 (40.3)	66 (41.5)	0.789					73 (45.9)	66 (41.5)	0.429
Reocclusion	12 (8.7)	6 (15)	0.244					5 (9.8)	6 (15)	0.45
Venous Thrombosis	31 (8.3)	7 (4.4)	0.112					12 (7.5)	7 (4.4)	0.237

[a]The multiple logistic regression test was used to analyze odds ratios. Adjusted variables: age, baseline NIHSS score, and time from puncture to recanalization.

[b]The Bonferroni correction method was applied to multiple comparisons using a *P*-value < 0.05/number of comparisons as a threshold for statistical significance.

CI, confidence interval; mRS, modified Rankin Scale; sICH, symptomatic intracranial hemorrhage; mTICI, modified Thrombolysis in Cerebral Infarction Score; NIHSS, National Institutes of Health Stroke Scale; IQR, interquartile range; VBD, vertebrobasilar dolichoectasia; Non-VBD, patients without vertebrobasilar dolichoectasia.

10.3389/fnhum.2022.946349

TABLE 3 Factors associated with favorable outcomes at 90 days of VBD patients.

	Favorable outcome (n = 45)	Unfavorable outcome (n = 114)	P-value	Adjusted OR (95% CI)[a]	P-value[b]
Age, years, median (IQR)	63 (54.5–70.5)	67 (60.8–75.3)	0.24	0.948 (0.910–0.989)	0.013
Male, no./total no. (%)	35 (77.8)	95 (83.3)	0.414	0.519 (0.173–1.554)	0.241
Baseline NIHSS, median (IQR)	21 (9–30)	30.5 (24–35)	< 0.001	0.938 (0.893–0.985)	0.01
Baseline ASPECTS, media (IQR)	9 (8–10)	7 (6–8)	< 0.001	1.839 (1.325–2.553)	< 0.001
History, no./total no. (%)					
Diabetes	5 (11.1)	26 (22.8)	0.094	0.512 (0.143–1.839)	0.305
Coronary heart disease	5 (11.1)	15 (13.2)	0.726	0.618 (0.160–2.380)	0.484
Atrial fibrillation	9 (20)	20 (17.5)	0.718	1.178 (0.387–3.591)	0.773
Location of occlusion, no./total no. (%)			0.139		
Distal BA	19 (42.2)	30 (26.3)		Reference	Reference
Middle BA	12 (26.7)	41 (36)		0.180 (0.055–0.592)	0.005
Proximal BA	10 (22.2)	22 (19.3)		0.586 (0.173–1.987)	0.391
VA-V4	4 (8.9)	21 (18.4)		0.117 (0.020–0.689)	0.018
Intravenous thrombolysis, no./total no. (%)	8 (17.8)	16 (14)	0.553	1.277 (0.410–3.974)	0.673
Onset-Imaging Time, min, median (IQR)	212 (87–406.5)	240 (104.3–417)	0.511	1.000 (0.998–1.002)	0.728
Puncture-Recanalization Time, min, median (IQR)	99 (66.5–133.5)	113 (86–167.5)	0.028	0.996 (0.988–1.004)	0.319
Collateral grade, n (%)			< 0.001		
ASTIN/SIR grade 0	5 (11.1)	38 (33.3)		Reference	Reference
ASTIN/SIR grade 1	11 (24.4)	46 (40.4)		1.181 (0.341–4.096)	0.793
ASTIN/SIR grade 2	18 (40)	26 (22.8)		1.938 (0.527–7.130)	0.319
ASTIN/SIR grade 3	11 (24.4)	4 (3.5)		5.538 (0.960–31.941)	0.056
ASTIN/SIR grade 4	NA	NA	NA	NA	NA

[a]The multiple logistic regression test was used to analyze ORs. Adjusted variables: baseline NIHSS score, Baseline ASPECTS, Puncture-Recanalization Time, Collateral grade.
[b]The Bonferroni correction method was applied to multiple comparisons using a p-value < 0.05/number of comparisons as a threshold for statistical significance.
NIHSS, National Institutes of Health Stroke Scale; ASITN/SIR grade indicates the American Society of Interventional and Therapeutic Neuroradiology/Society of Interventional Radiology collateral score; ASPECTS, Acute Stroke Prognosis Early Computed Tomography Score; IQR, interquartile range; CI, confidence interval.

difference between groups in mRS at 90 days. Mortality at 90 days was significantly higher in the VBD group than in the non-VBD group [81 of 159 patients (50.9%) vs. 152 of 357 patients (40.5%)]. Similarly, there was no significant difference between the two groups after adjusting for confounding factors.

Secondary efficacy outcomes

The secondary outcomes are shown in Table 2. There was no significant difference in the proportion of favorable prognosis (mRS $\leq$ 3) at 90 days between the two groups; the baseline NIHSS score at 24 h was significantly higher in the VBD group than in the non-VBD group [30 (16–35) vs. 26 (11–35); $P < 0.05$], with an adjusted odds ratio (OR) of 1.179 [95% confidence interval (CI) (1.145–1.215), $P < 0.05$], there was no significant difference between the two groups after adjusting for confounding factors.

Propensity score matching analysis

Table 1 shows that baseline characteristics were well balanced between the two groups after 1:1 propensity score matching. The median 90–day mRS was 6 [IQR (3–6)] in the VBD group and 5 [IQR (3–6)] in the non-VBD group ($P = 0.689$); there was no significant difference between the two groups, and mortality within 90 days occurred in 81 of 159 patients (50.9%) in the VBD group and 74 of 159 patients (46.5%) in the non-VBD group [81 (50.9%) vs. 74 (46.5%), $P = 0.432$]. The rate of sICH was 9% (14 of 159 patients) in the VBD group and 7.6% in the non-VBD group (12 of 159 patients; $P = 0.429$). There was no significant difference between surgery-related complications and other severe adverse events.

Outcomes of vertebrobasilar dolichoectasia with endovascular therapy

Restricting the analysis to only the VBD group, the results of univariate and logistic regression analyses are presented in Tables 3, 4. Patients were divided into favorable and unfavorable outcome groups based on prognosis (mRS $\leq$ 3) at 90 days.

The odds of baseline NIHSS score significantly decreased by 9% in the favorable outcome group [adjusted OR 0.938, 95% CI (0.893–0.985)]. Similarly, the odds of baseline NIHSS score significantly increased by 11.2% in the probability of mortality within 90 days in the unfavorable outcome group [adjusted OR 1.121, 95% CI (1.064–1.181)]. We observed a significant detrimental effect of prolonging the puncture-to-recanalization time on the probability of mortality within 90 days [adjusted OR 1.008,

TABLE 4 Factors associated with mortality at 90 days of VBD patients.

	Death ($n = 81$)	*P*-value	Adjusted OR (95% CI)[a]	*P*-value[b]
Age, years, median (IQR)	66 (59–75.5)	0.742	1.005 (0.971–1.040)	0.777
Male, no./total no. (%)	65 (80.2)	0.614	0.577 (0.212–1.567)	0.281
Baseline NIHSS, median (IQR)	32 (26.5–35)	< 0.001	1.121 (1.064–1.181)	< 0.001
Baseline ASPECTS, media (IQR)	7.5 (6–9)	0.008	0.804 (0.637–1.015)	0.066
History, no./total no. (%)				
Diabetes	20 (24.7)	0.092	2.358 (0.828–6.719)	0.108
Coronary heart disease	7 (8.6)	0.127	0.372 (0.121–1.142)	0.084
Atrial fibrillation	15 (18.5)	0.926	0.911 (0.351–2.367)	0.848
Location of occlusion, no./total no. (%)		0.775		
Distal BA	22 (27.2)		Reference	Reference
Middle BA	28 (34.6)		1.713 (0.651–4.506)	0.275
Proximal BA	17 (21)		1.753 (0.599–5.131)	0.306
VA-V4	14 (17.3)		2.144 (0.650–7.069)	0.21
Intravenous thrombolysis, no./total no. (%)	12 (14.8)	0.92	1.250 (0.451–3.463)	0.668
Onset-Imaging Time, min, median (IQR)	237 (103.5–398.2)	0.973	1.000 (0.998–1.001)	0.657
Puncture-Recanalization Time, min, median (IQR)	123 (95.5–171)	0.003	1.008 (1.001–1.015)	0.02
Collateral grade, *n* (%)		0.001		
ASTIN/SIR grade 0	26 (32.1)		Reference	Reference
ASTIN/SIR grade 1	35 (43.2)		1.749 (0.684–4.473)	0.243
ASTIN/SIR grade 2	19 (23.5)		1.755 (0.594–5.187)	0.309
ASTIN/SIR grade 3	1 (1.2)		0.189 (0.019–1.881)	0.155
ASTIN/SIR grade 4	NA	NA	NA	NA

[a]The multiple logistic regression test was used to analyze odds ratios. Adjusted variables: baseline NIHSS score, Baseline ASPECTS, Puncture-Recanalization Time, Collateral grade.
[b]The Bonferroni correction method was applied to multiple comparisons using a *P*-value < 0.05/number of comparisons as a threshold for statistical significance.
NIHSS, National Institutes of Health Stroke Scale; ASITN/SIR grade indicates the American Society of Interventional and Therapeutic Neuroradiology/Society of Interventional Radiology collateral score; IQR, interquartile range; CI, confidence interval.

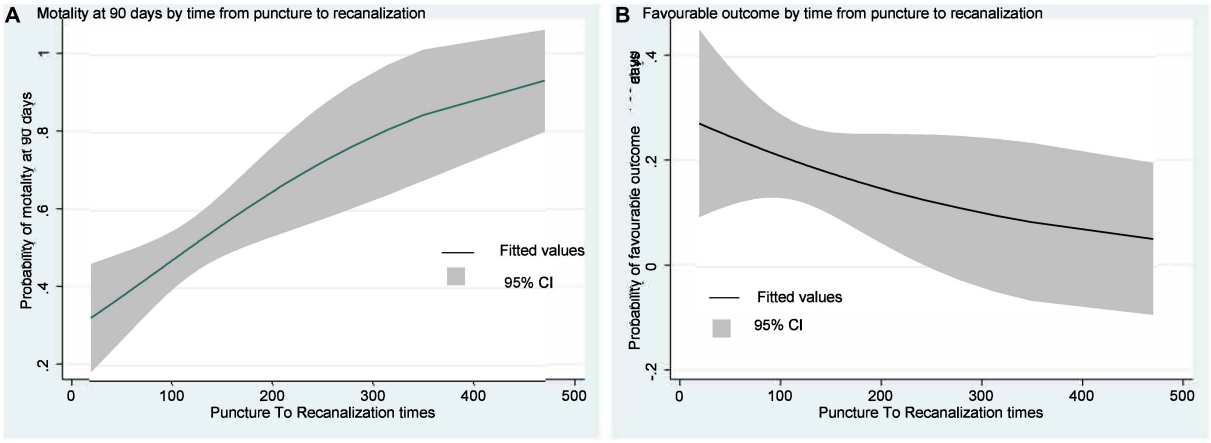

FIGURE 2
Curves show the increase in predicted motality probabilities with increases in puncture-to-recanalization time and **(A)**. The decreases in predicted favorable outcome probabilities with increases in puncture-to-recanalization time **(B)**.

95% CI (1.001–1.015)] (Table 4). Figure 2 illustrates the predicted outcome probabilities with puncture-to-recanalization time increment as a continuous variable. Figure 3 illustrates the effects of baseline NIHSS score and puncture-to-recanalization time on the probability of favorable outcomes with EVT.

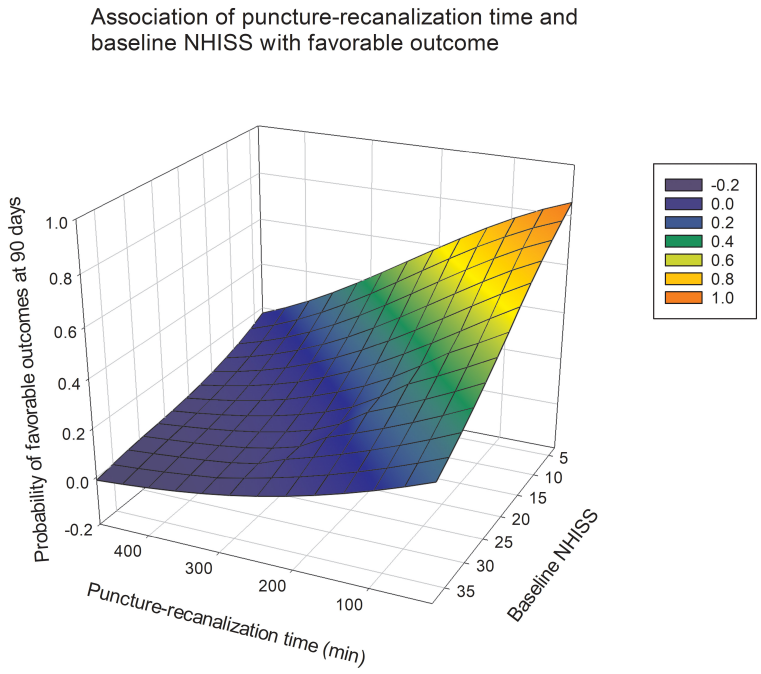

FIGURE 3
The gray shading indicates 95% CIs. Association of NIHSS and time from puncture to recanalization with the probability of a favorable outcome at 90 days after endovascular thrombectomy.

Discussion

To our knowledge, this study is the first and largest prospective multicenter registry of patients with VBD. The main finding of the study was the correlation between EVT and the feasibility and safety in patients with acute posterior circulation stroke and VBD. And there was no statistical difference in the incidence of adverse events between the EVT and non-EVT group. The findings provide extensive evidence for the choice of EVT for patients with VBD and for clinicians.

Many studies have confirmed the efficacy and safety of EVT after intervention in patients with acute BAO (Gory et al., 2016; Kang et al., 2018; Kwak and Park, 2020). Mechanical thrombectomy for acute ischemic stroke caused by anterior or posterior circulation occlusion of large vessels is safe and effective in a recent randomized controlled trial (Berkhemer et al., 2015; Writing Group for the et al., 2020). To our knowledge, no other trials have evaluated the safety and efficacy of mechanical embolization in stroke patients with VBD. Our results clearly demonstrate the feasibility and safety of EVT in patients with VBD. Our study retrospectively analyzed the clinical and imaging data of 159 VBD patients with mechanical embolization in the acute phase of cerebral infarction to investigate the feasibility and safety of this technique in preventing ischemic events in patients with VBD. Our study showed that patients with VBD had a higher NIHSS score and probability of death at 90 days; after adjusting for confounding factors, there was no significant difference in mortality at 90 days between the two groups. This may be because EVT treatment can relieve symptoms in patients with acute posterior circulation infarction combined with VBD. In addition, we found no significant differences in any safety endpoints between groups. Our study did not find evidence of differences in neurological outcomes between VBD and non-VBD patients. Therefore, EVT may be acceptable for patients with acute cerebral infarction associated with VBD.

However, there are few reports on the puncture-to-recanalization time; therefore, we also paid attention to the effect of operation time on the prognosis of EVT. Recent studies reporting the effect of procedural time on EVT outcomes have shown that prolonged procedural time not only decreases functional independence but also increases the incidence of complications (Spiotta et al., 2014; Hassan et al., 2019). Furthermore, as our results and those of other studies have shown, patients with good outcomes typically had a much shorter puncture-to-recanalization time, supporting that a shorter puncture-to-recanalization time may reduce the risk of death. Therefore, finding a more appropriate method during surgery may also be a key factor affecting the prognosis of patients.

Vertebrobasilar dolichoectasia is a potentially serious disease that can lead to severe disability due to ischemic or compressive disease of the posterior circulation. Symptomatic VBD is generally considered to have a poor outcome and

to be a challenging disease for which there are no effective treatment modalities. No effective treatment is available for some asymptomatic patients. Previous studies have found patients with VBD and hypertension, previous anterior or posterior stroke, and lack of warfarin therapy may have a higher risk of all-cause mortality. Patients with VBD and diabetes mellitus, smoking, and BA involvement may have a higher risk of posterior circulation dysfunction; (Wolfe et al., 2008) therefore, the prognosis of patients with VBD appears more dependent on traditional vascular risk factors. However, we were unable to find the correlation between these risk factors with prognostic factors. It may be that EVT was not involved in previous studies, but in our study, EVT intervention was performed after the onset of the patients with VBD. However, as this is a retrospective study, no additional information was available to assess the effectiveness of the treatment for VBD or onset of ischemia. As mentioned previously, our study confirmed the safety of EVT in patients with acute posterior circulation infarction associated with VBD, and further studies are required to develop safe and feasible treatments to prevent ischemic events in patients with VBD.

Limitations

Our study has all the inherent limitations of a non-randomized study. The major ones were its retrospective nature, selection bias, and the self-assessed angiographic evaluation. Because we lacked data on the mechanism of stroke death, our study did not yet answer whether VBD is a direct cause of death or a marker of high risk of death from cerebrovascular disease. Additionally, the lack of properly validated diagnostic criteria for VBD is a potential limitation. Nevertheless, this is the largest study published to date on VBD This study could provide additional information on treatment strategies for this subgroup of cerebral infarction, and further prospective studies are required to evaluate the best treatment options for VBD.

Conclusion

In conclusion, patients with VBD can benefit from EVT after acute cerebral infarction. In addition, prolonging procedural time may reduce the likelihood of a favorable functional outcome in patients with VBD treated with EVT. Strategies that reduce surgery duration may provide opportunities for improving patient prognosis.

Data availability statement

The raw data supporting the conclusions of this article will be made available by the authors, without undue reservation.

Ethics statement

The studies involving human participants were reviewed and approved by the Medical Ethics Committee of Second Affiliated Hospital of Third Military Medical University. The patients/participants provided their written informed consent to participate in this study.

Author contributions

JZ and DP analyzed and interpreted the data and drafted the manuscript. DS, WD, CL, RM, JW, ZY, TW, LW, and CY assisted to promote data collection. LIW and GJ completed the statistical work. WZ, YW, and XW conceived and designed the research. All authors contributed to the article and approved the submitted version.

Funding

This work was supported by funding from the National Natural Science Foundation of China (Nos. 81971220 and 81830039).

Conflict of interest

The authors declare that the research was conducted in the absence of any commercial or financial relationships that could be construed as a potential conflict of interest.

Publisher's note

Supplementary material

The Supplementary Material for this article can be found online at: https://www.frontiersin.org/articles/10.3389/fnhum.2022.946349/full#supplementary-material

References

Berkhemer, O. A., Fransen, P. S., Beumer, D., van den Berg, L. A., Lingsma, H. F., Yoo, A. J., et al. (2015). A randomized trial of intraarterial treatment for acute ischemic stroke. *N. Engl. J. Med.* 372, 11–20. doi: 10.1056/NEJMoa1411587

Giang, D. W., Perlin, S. J., Monajati, A., Kido, D. J., and Hollander, J. (1988). Vertebrobasilar dolichoectasia: Assessment using MR. *Neuroradiology* 30, 518–523. doi: 10.1007/BF00339693

Gory, B., Eldesouky, I., Sivan-Hoffmann, R., Rabilloud, M., Ong, E., Riva, R., et al. (2016). Outcomes of stent retriever thrombectomy in basilar artery occlusion: An observational study and systematic review. *J. Neurol. Neurosurg. Psychiatry.* 87, 520–525. doi: 10.1136/jnnp-2014-310250

Hassan, A. E., Shariff, U., Saver, J. L., Goyal, M., Liebeskind, D., Jahan, R., et al. (2019). Impact of procedural time on clinical and angiographic outcomes in patients with acute ischemic stroke receiving endovascular treatment. *J. Neurointerv. Surg.* 11, 984–988. doi: 10.1136/neurintsurg-2018-014576

Hongo, K., Nakagawa, H., Morota, N., and Isobe, M. (1999). Vascular compression of the medulla oblongata by the vertebral artery: Report of two cases. *Neurosurgery* 45, 907–910. doi: 10.1097/00006123-199910000-00039

Kang, D. H., Jung, C., Yoon, W., Kim, S. K., Baek, B. H., Kim, J. T., et al. (2018). Endovascular Thrombectomy for Acute Basilar Artery Occlusion: A Multicenter Retrospective Observational Study. *J. Am. Heart Assoc.* 7:e009419. doi: 10.1161/JAHA.118.009419

Kwak, H. S., and Park, J. S. (2020). Mechanical Thrombectomy in Basilar Artery Occlusion: Clinical Outcomes Related to Posterior Circulation Collateral Score. *Stroke* 51, 2045–2050. doi: 10.1161/STROKEAHA.120.029861

Moss, M. S., and West, R. J. (1996). Ectasia of the vertebral artery as a cause of isolated pyramidal tract signs: Case report and a review of the literature. *Br. J. Neurosurg.* 10, 497–499. doi: 10.1080/02688699647159

Samim, M., Goldstein, A., Schindler, J., and Johnson, M. H. (2016). Multimodality Imaging of Vertebrobasilar Dolichoectasia: Clinical Presentations and Imaging Spectrum. *Radiographics* 36, 1129–1146. doi: 10.1148/rg.2016150032

Smoker, W. R., Price, M. J., Keyes, W. D., Corbett, J. J., and Gentry, L. R. (1986). High-resolution computed tomography of the basilar artery: 1. Normal size and position. *AJNR Am. J. Neuroradiol.* 7, 55–60.

Spiotta, A. M., Vargas, J., Turner, R., Chaudry, M. I., Battenhouse, H., Turk, A. S., et al. (2014). The golden hour of stroke intervention: Effect of thrombectomy procedural time in acute ischemic stroke on outcome. *J. Neurointerv. Surg.* 6, 511–516. doi: 10.1136/neurintsurg-2013-010726

Wolfe, T., Ubogu, E. E., Fernandes-Filho, J. A., and Zaidat, O. O. (2008). Predictors of clinical outcome and mortality in vertebrobasilar dolichoectasia diagnosed by magnetic resonance angiography. *J. Stroke Cerebrovasc. Dis.* 17, 388–393. doi: 10.1016/j.jstrokecerebrovasdis.2008.06.006

Wolters, F. J., Rinkel, G. J., and Vergouwen, M. D. (2013). Clinical course and treatment of vertebrobasilar dolichoectasia: A systematic review of the literature. *Neurol. Res.* 35, 131–137. doi: 10.1179/1743132812Y.0000000149

Writing Group for the, B. G., Zi, W., Qiu, Z., Wu, D., Li, F., Liu, H., et al. (2020). Assessment of Endovascular Treatment for Acute Basilar Artery Occlusion *via* a Nationwide Prospective Registry. *JAMA Neurol.* 77, 561–573. doi: 10.1001/jamaneurol.2020.0156

frontiers | Frontiers in Human Neuroscience

TYPE Review
PUBLISHED 21 September 2022
DOI 10.3389/fnhum.2022.968369

OPEN ACCESS

EDITED BY
Richard Daneman,
University of California, San Diego,
United States

REVIEWED BY
Tom Gardiner,
Queen's University Belfast,
United Kingdom
Carmen Muñoz-Ballester,
University of Alabama at Birmingham,
United States
Luciana Mateus Gonçalves,
University of Miami, United States

*CORRESPONDENCE
Hua Su
hua.su@ucsf.edu

SPECIALTY SECTION
This article was submitted to
Brain Health and Clinical
Neuroscience,
a section of the journal
Frontiers in Human Neuroscience

RECEIVED 13 June 2022
ACCEPTED 31 August 2022
PUBLISHED 21 September 2022

CITATION
Shabani Z, Schuerger J and Su H
(2022) Cellular loci involved
in the development of brain
arteriovenous malformations.
Front. Hum. Neurosci. 16:968369.
doi: 10.3389/fnhum.2022.968369

Cellular loci involved in the development of brain arteriovenous malformations

Zahra Shabani[1,2], Joana Schuerger[1,2] and Hua Su [1,2]*

[1]Center for Cerebrovascular Research, University of California, San Francisco, San Francisco, CA, United States, [2]Department of Anesthesia and Perioperative Care, University of California, San Francisco, San Francisco, CA, United States

Brain arteriovenous malformations (bAVMs) are abnormal vessels that are prone to rupture, causing life-threatening intracranial bleeding. The mechanism of bAVM formation is poorly understood. Nevertheless, animal studies revealed that gene mutation in endothelial cells (ECs) and angiogenic stimulation are necessary for bAVM initiation. Evidence collected through analyzing bAVM specimens of human and mouse models indicate that cells other than ECs also are involved in bAVM pathogenesis. Both human and mouse bAVMs vessels showed lower mural cell-coverage, suggesting a role of pericytes and vascular smooth muscle cells (vSMCs) in bAVM pathogenesis. Perivascular astrocytes also are important in maintaining cerebral vascular function and take part in bAVM development. Furthermore, higher inflammatory cytokines in bAVM tissue and blood demonstrate the contribution of inflammatory cells in bAVM progression, and rupture. The goal of this paper is to provide our current understanding of the roles of different cellular loci in bAVM pathogenesis.

KEYWORDS

brain arteriovenous malformations, endothelial cells, pericytes, smooth muscle cells, astrocyte, inflammatory cells

Introduction

An abnormal mass of blood vessels named "nidus" is a main characteristic of brain arteriovenous malformations (bAVM), leading to the direct shunting of blood from the arteries to veins. There is no intervening capillary bed in the nidus (Rodrigues de Oliveira et al., 2020). The Patients with bAVM are at risk of intracranial hemorrhage (ICH) (Kim et al., 2011). Overall, bAVMs account for 25% of hemorrhagic strokes in adults < 50 years of age (Cordonnier et al., 2010), and up to 40% of bAVM patients die or remain functionally impaired within one-year after ICH (van Beijnum et al., 2009). The treatment of unruptured lesions has become controversial because the natural history of these patients may be less morbid than invasive therapies (Stapf et al., 2006; Mohr et al., 2010, 2012, 2014; Cockroft et al., 2012; Derdeyn et al., 2017). However, the mechanism

of bAVM development is not fully understood and there is no specific medical therapy available for bAVM patients.

Mouse model studies identified several key factors that are crucial for bAVM initiation and progression (Walker et al., 2011a; Choi et al., 2012, 2014; Chen et al., 2013a, 2014a,b; Zhang et al., 2016a). Angiogenesis and AVM causative gene mutation in endothelial cells (ECs) are necessary for AVM development. Arterial and venous specification of ECs is a crucial step for development of normal vascular bed, which is determined by genetic factors, although surrounding cells and hemodynamic forces may also contribute to vascular remodeling (Liu et al., 2020). Among those genes that are involved in EC arteriovenous specification, abnormal NOTCH signaling has been detected in human bAVMs and both gain or loss of function of Notch in mouse lead to bAVM formation (Murphy et al., 2009; ZhuGe et al., 2009; Li et al., 2014). Although ECs have been identified as the primary cellular locus for AVM initiation (Walker et al., 2011b; Choi et al., 2012; Garrido-Martin et al., 2014; Park H. et al., 2021; Shaligram et al., 2021), other cellular loci, such as pericytes and microglia/macrophages, have also been shown to play roles in bAVM pathogenesis (Chen et al., 2013a; Zhang et al., 2016a; Winkler et al., 2018; Krithika and Sumi, 2021; Scherschinski et al., 2022). Both human and mouse bAVM vessels have less mural cell coverage than normal vessels, which is associated with vessel leakage and hemorrhage (Chen et al., 2013a; Winkler et al., 2018). Inflammation may promote bAVM progression. An abnormally high numbers of inflammatory cells like macrophages, neutrophils, and T lymphocytes have been detected in human and mouse bAVMs, even in unruptured specimens (Guo et al., 2012, 2014). Both Cx3cr1^{+} microglia and Ccr2^{+} macrophages are present in bAVM lesions of an *Alk1* deficient mouse model indicating that both microglia and macrophages are involved in bAVM pathogenesis (Zhang et al., 2016a).

Astrocytes respond to multiple insults and diseases by a process called reactive astrogliosis or astrocytosis (Hamby and Sofroniew, 2010; Liddelow et al., 2017; Escartin et al., 2021). Abnormal astrocytes with increased expression of glial fibrillary acidic protein (GFAP) and vimentin have been observed in human sporadic bAVMs which is associated with deregulated retinoic acid signaling (Thomas et al., 2021). Astrocytes are essential cellular component of neurovascular unit which surround brain vascular ECs by their endfeet, resulting in generation of a penetrable membrane named the glial limitans and induction of capillary formation (Winkler et al., 2019).

To date, the roles of different cellular loci in bAVM initiation and progression have not been fully studied. In this review, we have summarized what we know based on studies conducted on animal models and surgical resected bAVM specimens. Understanding the roles of each cellular locus will help us to design targeted therapeutic strategies to treat bAVM or prevent bAVM hemorrhage.

Endothelial cells

Endothelial cells form the lumen of the capillaries, arteries, and veins. Brain ECs form a control barrier between blood and brain parenchyma and influence the blood vessel formation, coagulation, fibrinolysis, as well as regulation of vascular tone and neuroinflammation process. Furthermore, ECs take part in the pathogenesis of bAVMs.

Gene mutation in Endothelial cells is necessary for brain arteriovenous malformations initiation

Gene mutations in ECs are essential for bAVM initiation. Mutation of genes in transforming growth factor beta (TGF-β) family and RAS-MAPK pathway have been linked to bAVM development.

Familial AVM

The majority of brain AVMs are sporadic; however, some evidence supports a familial component to the AVM phenotype, and that genetic variation is relevant to the disease course. Hereditary Hemorrhagic Telangiectasia (HHT) is an autosomal dominant disease. Majority of HHT patients have loss of function mutations of endoglin (*ENG*) or activin receptor like kinase 1 (*ALK1* also known as *ACVR1*) (**Figure 1**). ENG and ALK1 are receptors of TGF-β and bone morphogenetic proteins (BMPs), that are predominantly expressed in ECs. Some HHT patients have mutation in *SMAD4* or *BMP9*. TGF-β1 receptors, ALK 1 play an important role in the endothelial TGF-β signaling. Administration of low-dose TGF-β stimulates proliferation and migration of ECs through ALK1, whereas high doses of TGF-β result in quiescent endothelium (Lebrin et al., 2005).

Mouse studies showed that the lesional phenotypes are different between mice with heterozygous and homozygous *Alk1* or *Eng* mutation. In the Ad-Cre-treated brain of *Eng*$^{f/f}$ mice, homozygous deletion of *Eng* is assumed because Eng-null ECs were detected. VEGF induced more severe vascular dysplasia in the Ad-Cre-treated *Eng*$^{f/f}$ mice compared with the *Eng*$^{+/-}$ mice (Choi et al., 2012). A robust and reproducible bAVM phenotype in adult mice were induced through brain focal angiogenic stimulation and *Eng* or *Alk1* conditional knockout (iKO) specifically in ECs (Chen et al., 2014b; Choi et al., 2014). Deletion of *Eng* or *Alk1* in pericytes or macrophages did not cause bAVM development (Chen et al., 2014b; Choi et al., 2014). Gene mutation in a small portion of ECs and in bone marrow derived ECs also are sufficient to cause bAVM formation (Walker et al., 2011b; Choi et al., 2012; Shaligram et al., 2021). Recently, Kim et al. (2020) demonstrated that overexpression of Alk1 can rescue the AVM phenotypes in *Alk1*- and *Eng* (iKO) mice *via* normalizing the expression of Notch and Smad

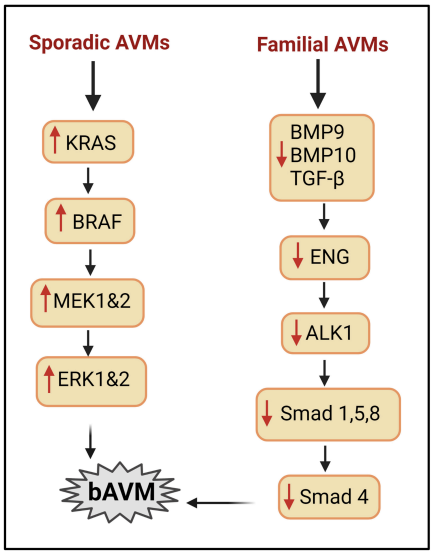

FIGURE 1
Signaling pathways involved in bAVM development. Right column: mechanisms implicated in HHT AVMs. BMP9/BMP10/TGFβ can regulate angiogenesis *via* interacting with ALK1/ENG to phosphorylate SMAD. Mutation of ALK1 or ENG reduces SMAD, leading to AVM development. Left column: mechanisms involved in sporadic bAVM. Mutations in genes of KRAS, BRAF pathway enhance the level of MEK and ERK and lead to bAVM development.

target genes and restoring the effect of BMP9 on suppression of pAkt in *Eng*-deficient ECs. In normal physiological conditions, overexpression of Alk1 globally or in pan ECs does not cause vascular malformation (Kim et al., 2020). Therefore, reduction of endothelial Eng or Alk1 levels can lead to bAVM development in the presence of angiogenic stimulation.

Alk1 signaling regulates Notch ligands and its target genes, but Alk1-overexpression in normal ECs does not generate any changes in the expression of Notch targets. Notch signaling have been shown to play a critical role in normal vasculogenesis and angiogenesis, as well as in abnormal vascular remodeling. Increased expression of NOTCH-1 and downstream target HES-1 was observed in human bAVM tissue compared to control vessels (Murphy et al., 2009; ZhuGe et al., 2009; Li et al., 2014). Both activation and repression of Notch have been implicated in AVM development (Zhang et al., 2016b). Endothelial-specific activation of Notch-4 induced AVMs in mouse brain (Murphy et al., 2008). Like Notch-4, EC-specific, constitutively active Notch-1 results in vascular defects and AVM formation (Krebs et al., 2010). Deletion of recombination signal binding protein for immunoglobulin kappa J region (Rbpj), which block Notch signaling in ECs of postnatal mice, also caused bAVM phenotype (Nielsen et al., 2014). Decreased Notch signaling was found in *Alk1* knockout mouse models. These data suggest that there is a connection between the Alk1 and the Notch signaling during vascular morphogenesis (Larrivee et al., 2012).

A soluble form of ENG can be shed off from the ECs membrane affecting the TGF-β signaling required for angiogenesis by scavenging TGF-β ligands. Chen et al. (2009) showed that overexpression of soluble ENG caused bAVMs in mice. Soluble ENG also specifically binds to BMP9, leading to the inhibition of blood vessel formation (Castonguay et al., 2011) and participates in bAVM inflammation (Park E. S. et al., 2022).

BMPs also play an important role in ECs function and angiogenesis. Blocking BMP9 and BMP10 induced AVMs in the retina (Ruiz et al., 2016). Recent studies have indicated that BMP9 and BMP10 are probably the natural ligands for the ENG/ALK1 signaling pathway (Tillet and Bailly, 2015). BMP9 has high-affinity binding sites for both ENG and ALK1. When they bind ALK1, mRNA expression of ALK1 receptor signaling-dependent gene; transmembrane protein 100 (Tmem100) is induced within the arteries (Somekawa et al., 2012). Furthermore, disorganized arteries and downregulated Notch/Akt signaling were demonstrated in the Tmem100-deficient mice (Somekawa et al., 2012). It is thought that BMP9 and BMP10 promote the Notch pathway and thus suppress the arterial development and inhibit endothelial tube elongation (Roca and Adams, 2007). It appears that ENG competes with ACVR2B (type II receptor) for BMP9 binding site, and that ENG can be re-positioned by the type II receptor, possibly leading to activation of the type 1 receptor ALK1 and down-regulation of its targets like SMAD. Thus, it confirms the assumption that a deficiency of BMP9/10-ENG-ALK1-SMAD4 pathway is a possible mechanism of bAVMs development in HHT patients (Townson et al., 2012; Saito et al., 2017).

Moreover, recent studies have shown that neuropilin-1 (NRP-1) inhibits ALK1- and ALK5-mediated SMAD2/3 phosphorylation in ECs and modulates tip and stalk cell phenotypes in vascular sprouting and stretch-induced TGF-β1/ALK1 signaling in ECs when cocultured with SMCs (Korff et al., 2007; Aspalter et al., 2015). Neuropilin-1 (NRP-1) inhibits ALK1 signaling in tip cells during vascular sprouting (Aspalter et al., 2015). NRP-1 level is reduced in perivascular SMCs in the livers from patients with ALK1 mutation (Kilari et al., 2022). The mice with Nrp1 deletion in vSMCs and cardiomyocytes are viable, and present with decreased blood pressure, cardiac hypertrophy, and infiltration of perivascular inflammatory cells into the lungs (Wang et al., 2015). Another study reported that NRP-1 is involved in vSMC differentiation *via* platelet-derived growth factor (PDGF) signaling (Kofler and Simons, 2016). Nrp1 knockdown impairs PDGF-B driven vSMC migration (Pellet-Many et al., 2011). NRP-1 has a direct interaction with ENG and ALK1. NRP-1 deletion in vSMC leads to a decrease in ALK1/ENG signaling and to a decrease in pSMAD1/5/8 in vSMCs contributing to the formation of AVMs associated with HHT2 phenotype (Kilari et al., 2022). Although NRP-1 mutation has not be identified in HHT patient, it may involve in HHT

pathogenesis through interaction with genes in TGF-β family and PDGF.

Sporadic AVMs

More than 95% bAVM cases are sporadic. Somatic mutations have been found in *KRAS*/ MAPK pathway genes in the lesions of sporadic bAVM and peripheral AVMs (Couto et al., 2017; Al-Olabi et al., 2018; Nikolaev et al., 2018; Goss et al., 2019; Hong et al., 2019; Priemer et al., 2019). Expression of $KRAS^{G12V}$ (a somatic mutation identified in sporadic bAVMs) in ECs *in vitro* stimulated ERK activity, and activated specific genes involved in angiogenesis and NOTCH signaling and enhanced EC migratory behavior. These effects of $KRAS^{G12V}$ were reversed by inhibition of MAPK-ERK signaling using MEK inhibitor (Nikolaev et al., 2018). Further work is needed to understand the interplay between the MAPK-ERK pathway with VEGF and other angiogenic pathways.

Sporadic bAVMs models have been generated in mouse and zebrafish recently through somatic ECs-specific gain of function mutation in *Kras* (Fish et al., 2020). Fish et al. demonstrated that ECs-specific gain of function mutations in *Kras* (G12D or G12V) are sufficient to induce bAVMs in mice (**Figure 1**). Park et al. confirmed that *Kras* mutations promote bAVM development *via* the MEK/ERK pathway using a brain ECs – specific adeno-associated viral vector (AAVBR1) mediated brain ECs transfer of $Kras^{G12D}$ (Park E. S. et al., 2021).

Endothelial inflammation

Endothelial cell inflammation in bAVM can be induced by multiple factors including hemodynamic changes as well as increased levels of angiogenic factors and cytokines in the lesion. Abnormally high flow rates and cerebral venous hypertension (VH) are common hemodynamic abnormalities in bAVM (Young et al., 1994). In rats, non-ischemic levels (15-23 mmHg) of VH cause expression of hypoxia-inducible factor 1 (HIF–1α) and its downstream signal, VEGF (Zhu et al., 2006). Further, HIF–1α, VEGF, SDF-1 expression, and neutrophils, macrophage, and MMP-9 activity are increased in the brain of the mice with VH. As shown in diabetic retinopathy, increased blood flow and vessel wall pressure in bAVM can cause EC damage and trigger EC inflammation (Stitt et al., 1995). ECs in bAVMs express cytokines and chemokines, which attract leukocyte infiltration causing vascular instability. The cellular adhesion molecules (CAMs), including E-selectin, intercellular CAM-1 (ICAM-1), and vascular CAM-1 (VCAM-1) are increased in ECs of human bAVMs and arteriovenous fistular in a rat model (Karunanyaka et al., 2008; Storer et al., 2008). Further receptors which are important in the inflammatory cascade like receptors for prostaglandin E2, a COX2-derived mediator of vascular remodeling, were found in the ECs and vSMCs and perivascular inflammatory cells (Keranen et al., 2021).

Endothelial-to-mesenchymal transition

In bAVMs, endothelial-to-mesenchymal transition (EndMT) has been observed (Shoemaker et al., 2020; Li et al., 2021). EndMT is a process where mature ECs transform into mesenchymal cells by acquiring the characteristics of mesenchymal cells, characterized by invasiveness and proliferation, disorganization of ECs junctions and a spindle like morphology.

In cardiovascular, pulmonary, and hepatic developments, and some fibrotic diseases, such as renal, pulmonary, and hepatic fibrosis, TGF-β pathway plays a major role in regulating the EndMT (Perez et al., 2017). EndMT could not be defined by single protein. Shoemaker et al. found evidence of EndMT in bAVM through detection of the expression of EndMT-associated transcription factors (TFs) and mesenchymal markers including KLF4, SNAI1/2, VIM, ACTA2, and S100A4 (Pardali et al., 2017; Shoemaker et al., 2020). SMAD-dependent TGF-β signaling was not strongly activated in bAVMs and this pathway may be only partially involved in mediating bAVM EndMT. Other signaling pathways, such as Wnt/β-catenin (He et al., 2010), NOTCH (Nielsen et al., 2014), MAPK-ERK (Nikolaev et al., 2018; Li et al., 2021), and Sonic Hedgehog (Giarretta et al., 2021), may play roles. Upregulation of EndMT-associated genes was also reported in human umbilical cord ECs (HUVECs) over-expressing mutated KRAS ($KRAS^{G12V}$), a somatic mutation that is associated with AVMs (Nikolaev et al., 2018).

In bAVMs that have microhemorrhage, immunohistochemical staining showed that the vascular endothelium exhibited decreased SMAD6 expression. Functional assays revealed that SMAD6 downregulation promoted the formation of ECs tubes with deficient cell-cell junctions (reduced the levels of VE-cadherin, occludin and ZO-1, and increased the level of N-Cadherin), and facilitated the acquisition of mesenchymal behavior (enhanced proliferation and migration) by ECs. Masson trichrome and immunofluorescence staining demonstrated that mesenchymal phenotype of ECs (increasing in the levels of the mesenchymal markers N-cadherin, α-SMA, SM22α, and CNN1 and reducing in the levels of the EC markers VE-cadherin, von Willebrand factor, Tie2, and CD31) is enhanced in bAVMs with microhemorrhage. TGF-β/BMP signaling mediated by SMAD6 in vascular ECs is associated with microhemorrhage in bAVMs. Therefore, mesenchymal behavior of ECs induced by SMAD6 downregulation is associated with bAVM microhemorrhage (Fu et al., 2020).

Pericytes and vascular smooth muscle cells

Pericytes and vSMCs are mural cells located at the abluminal side of small and large vessels, respectively (Armulik et al., 2011). Mural cells have a crucial role in vascular stability. Reduction of vascular pericytes impairs vascular integrity (Armulik et al., 2010; Bell et al., 2010). Pericytes modulate and maintain the BBB integrity through releasing signaling factors, such as angiopoietin 1 (ANGPT1), to determine the number of EC tight junctions and direct the polarization of astrocyte endfeet (Armulik et al., 2010). A reduction in pericyte numbers can cause a loss of tight junctions between EC, leading to increased BBB permeability (Winkler et al., 2013; Sengillo et al., 2013; Brown et al., 2019). In addition, PDGFB-PDGF receptor β (PDGFR-β), TGF-β, basement membrane and extracellular matrix (ECM) proteins, and pericyte differentiation have been shown to maintain normal brain vascular structure and function (**Figure 2**).

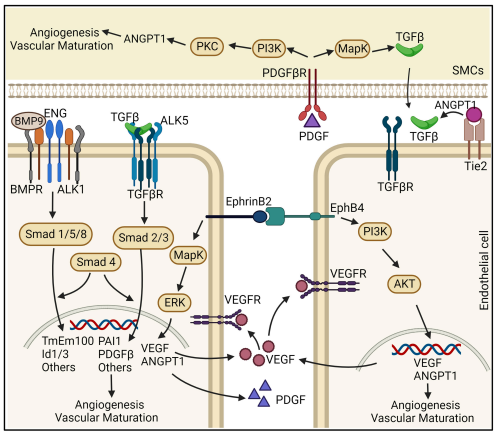

FIGURE 2
Schematic representation of the effects ECs and vSMCs on bAVM development. ENG and ALK1 are receptors of BMPs. TGF-β interacts with ALK5 and TGF-βR that are predominantly expressed in ECs. BMP9/10-ENG-ALK1 by triggering SMAD1,5,8, and 4 regulate angiogenesis and vascular maturation. Disruption of this pathway can cause the development of bAVMs. ANGPT/Tie2 are linked to TGF-β activation and binding to TGF-βR, which through SMAD2,3, and 4 induces angiogenesis. EphrinB2/EphrinB4 are differentially expressed in arterial and venous ECs. PDGFB and PDGFR-β both have an essential role in pericyte recruitment during angiogenesis. In the vSMCs, PDGFB upregulates ANGPT-1 through PI3K and PKC pathway and upregulates TGF-β1 expression through the MAPK pathway. ANGPT-1: angiopoietin 1, PDGFB: platelet derived growth factor B, PDGFR-β: PDGF receptor β, ECs: endothelial cells, SMCs: smooth muscle cells.

Pericytes and vascular smooth muscle cells are reduced in brain arteriovenous malformations vessels

Mural cells including pericytes and vSMCs are considered as key components of the vascular wall and operate in maintaining healthy homeostasis. Pericytes cover almost 90% of brain vascular abluminal side. The vSMCs are placed in the tunica media. Together, they offer vessel stabilization and control blood flow *via* regulating dilation and contraction of vessels (Frosen and Joutel, 2018). The decreased mural cells in bAVM vessels makes them vulnerable to vascular leakage and subsequent microhemorrhage (Pan et al., 2021). Reduction of mural cell coverage in the bAVM vessels in mouse models and human specimens is associated with reduction of PDGFB and PDGFR-β protein levels in bAVM lesions and AVM bleeding (Walker et al., 2011b; Chen et al., 2013a; Winkler et al., 2018). Compared with normal brain angiogenic foci, the lesion in bAVM mouse models have more vessels with diameters larger than 15 μm that lack α-SMA positive cells. However, α-SMA positive cells in human bAVMs have yet to be fully characterized, and the functional consequences of other described abnormalities such as cytoskeleton and contractile proteins remain unclear (Wong et al., 2000; Uranishi et al., 2001; Kim et al., 2018).

Pathways regulating mural cell coverage of brain arteriovenous malformations

Currently, the reasons of mural cells reduction in bAVM are unknown. Tie2/ANGPT-1 and PDGFB/PDGFR-β are two important pathways regulate mural cell-recruitment during vascular remodeling. We found that *ALK1* mutation decreases PDGFB expression in human and mouse brain ECs (Chen et al., 2013b). PDGFB upregulates ANGPT-1 in vSMCs through PI3K and PKC pathway and upregulates TGF-β1 expression through the MAPK pathway in vSMCs (Nishishita and Lin, 2004). In this section, we discussed three major pathways that regulate mural cell recruitment during angiogenesis and their involvement in AVM pathogenesis.

PDGFB and PDGFR-β

Both PDGFB and PDGFR-β have an essential role in pericyte recruitment during angiogenesis. PDGFB is secreted from the endothelium as a disulfide-linked homodimer and retained within the ECM as the result of electrostatic interactions (Abramsson et al., 2007; Andrae et al., 2008). This creates a steep perivascular concentration gradient of PDGFB which is essential for the recruitment of mural cells (Enge et al., 2002; Abramsson et al., 2007; Armulik et al., 2010). PDGFB upregulates ANGPT-1 in vSMCs through PI3K and PKC pathway and upregulates TGF-β1 expression through the MAPK pathway in vSMCs (Nishishita and Lin, 2004) (**Figure 2**).

Both pericytes and vSMCs express PDGFR-β (Tallquist et al., 2003). Global knockout *Pdgfb* or *Pdgfr*-β in mice results in the loss of pericytes from the microvessels (Lindahl et al., 1997)

and cerebral hemorrhage (Hellstrom et al., 2001). Homozygous deletion of *Pdgfb* or *Pdgfr*-β in rodents results *in utero* death due to widespread hemorrhage (Hellstrom et al., 2001).

Abnormal expression of PGDFB and PDGFR-β has been described in bAVMs in rodent models and patients (Yildirim et al., 2010; Winkler et al., 2018; Zhu et al., 2018). Knockdown ALK1 in human brain microvascular ECs reduced PDGFB expression (Zhu et al., 2018). Pdgfr-β expression is reduced in the bAVM lesions of *Alk1*-deficient mice (Chen et al., 2013a).

Thalidomide and lenalidomide (one of the newer analogs of thalidomide) treatment improved mural cell-coverage of bAVM vessels and reduced bAVM hemorrhage (Zhu et al., 2018). Thalidomide restored Pdgfb expression in bAVMs. Overexpression of PDGFB in bAVM lesion mimicked the effects of thalidomide, suggesting that thalidomide reduces bAVM hemorrhage through upregulation of Pdgfb in bAVM.

ANGPT/TIE2

ANGPT is part of a family of vascular growth factors that are implicated in embryonic and postnatal angiogenesis. ANGPT is involved with controlling microvascular permeability, vasodilation, and vasoconstriction by signaling in vSMCs surrounding the vessels. There are four identified angiopoietins: ANGPT-1, ANGPT-2, ANGPT-3, and ANGPT-4 (Valenzuela et al., 1999). ANGPT/TIE2 signaling plays a role in the recruitment of peri-endothelial support structures, including pericytes and vSMCs (**Figure 2**). ANGPT-1, expressed by pericytes and vSMCs, is critical for vessel maturation, as well as cell adhesion, migration, and survival. ANGPT-2, expressed by ECs, promotes cell death, and disrupts vascularization. When it is in conjunction with VEGF, it can promote neovascularization (Hegen et al., 2004; Fagiani and Christofori, 2013).

Alternations of ANGPT/TIE2 expression have been found in human sporadic bAVM specimens (Hashimoto et al., 2001). ANGPT-2, which allows loosening of cell-to-cell contacts, is overexpressed in the perivascular region in bAVM vascular channels, while ANGPT-1 expression is not changed (Hashimoto et al., 2001). Therefore, imbalance of ANGPT/TIE2 signaling could be another cause of vessel wall defects in bAVM.

ANGPT-2 expression is also increased in HHT AVMs. *Alk1* germline deletion increase Angpt-2 expression in brain and spinal AVMs (Milton et al., 2012). PMP9/10 inhibition let to overexpression of Angpt-2 in the neonate retina (Ruiz et al., 2016). Angpt-2 expression was also increased in the postnatal retinal of *Smad4* mutant mice (Crist et al., 2019). Endothelial specific deletion of *Smad4* increased embryonic Angpt-2 expression (Lan et al., 2007). Administration of Angpt-2 monoclonal antibodies prevent and resolved retinal AVMs of *Smad4* mutant mice (Crist et al., 2019). Therefore, ANGPT/Tie2 may link to TGF-β pathway through SMAD4 (Crist et al., 2019).

However, some other studies showed that ANGPT-2 levels in the blood of HHT2 patients were decrease and unchanged in HHT1 patients (Ojeda-Fernandez et al., 2010). ANGPT-2 expression was also lower in outgrowth ECs of HHT1 and 2 patients than normal ECs (Fernandez-Lopez et al., 2007). This difference could be due to the changes of cultured cells and the different levels of ANGPT-2 in tissues and blood. In addition, ANGPT/Tie can signal through autocrine/paracrine (Takahara et al., 2004), their levels in the circulation may not influence their effects on AVM vessels. Taken together, Angpt/Tie2 pathway may play a key role in regulating mural cell plasticity. Dysregulation of this pathway contributes to the pathogenesis of bAVMs (Pan et al., 2021).

EphrinB2/EphB4

EphrinB2/EphB4 are differentially expressed in arterial and venous ECs, through angiogenic stimulation by VEGF and NOTCH (Adams and Alitalo, 2007). This signaling has been implicated in the regulation of vascular events, including sprouting angiogenesis, vascular morphogenesis, arteriovenous differentiation, and vascular homeostasis (Luxan et al., 2019). EphB4 is specifically expressed in ECs while EphrinB2 is expressed in ECs and their surrounding mesenchymal and mural cells including pericytes (Gerety and Anderson, 2002). EphrinB2 and EphB4 have been deemed as the primary molecular markers for endothelial arteriovenous specification and are responsible for the pericyte function and regulates the switch between normal and aberrant angiogenesis. It has been shown that diabetes increases the expression of Ephrin-B2 in the cerebrovasculature and pericytes. Concomitant increases in cerebral neovascularization parameters including vascular density, tortuosity and branching density in diabetic rats were accompanied by deterioration of cognitive function. Inhibition of Ephrin-B2 expression in pericytes significantly restored cerebral vascularization and improved cognitive functions (Coucha et al., 2019). EphrinB2/EphB4 is also a key regulator of intussusceptive angiogenesis (**Figure 2**; Groppa et al., 2018) through controlling the outcome of intussusceptive angiogenesis by fine-tuning the degree of ECs-proliferation caused by specific VEGF doses, without directly affecting VEGFR2 activity, but rather modulating its downstream signaling through MAPK/ERK. EphrinB2 is a crucial regulator of PDGFR-β expression in vSMCs, and thereby acts as a molecular switch regulating the downstream signaling activity induced by PDGFB/PDGFR-β.

Ephs are among few receptor tyrosine kinases known to attenuate MAPK signaling downstream of mitogens (Miao et al., 2001; Pasquale, 2008; Ottone et al., 2014). EphrinB2 suppresses VEGF- and ANGPT-1-induced RAS-MAPK activities (Kim et al., 2002). In skeletal muscles, inhibition of EphrinB2/EphB4 in the present of low level of VEGF increased vessel-diameters and pErk in ECs (Groppa et al., 2018).

Accumulating evidence suggest that EphrinB2/EphB4 signaling plays a crucial role in AVMs development and other cerebrovascular disorders (Bai et al., 2014). Embryos harboring homozygous mutations in *EphrineB2* and *EphB4* exhibited vascular defects and AVMs (Krebs et al., 2010). It was shown in an *in vitro* model of HHT2 that loss of *ALK1* gene blocked BMP9 signaling, resulting in reduced EphrinB2 expression, enhanced VEGFR2 expression and dysregulated ECs sprouting and anastomosis (Feghali et al., 2019).

Astrocytes

Astrocytes are the most abundant cell type in the brain that are mainly involved in neuronal growth and survival, and reparation of nervous system by allowing the removal of dead neurons and pathogens (Rahman et al., 2021). Astrocytes have a key role in up taking and releasing the neurotransmitters, regulating ion homeostasis, and preserving the BBB integrity by secreting basement membrane proteins, such as laminin (Heithoff et al., 2021). Astrocytes also play roles in neuroinflammation (Colombo and Farina, 2016). Reactive astrocytes are astrocytes that go through morphological, molecular, and functional alterations around injured tissue following pathological conditions. Depending on context, reactive astrocytes may have fraction of simple changes between different states (Escartin et al., 2021).

Role in normal brain function

Astrocyte is a cellular component of neurovascular unit. Brain vascular ECs are bordered by astrocyte endfeet, which build a penetrable membrane named the glial limitans, and have a role in the induction of capillary formation (Winkler et al., 2019). Astrocytes extend processes that physically link neighboring neurons with blood vessels (Hawkins and Davis, 2005; Vangilder et al., 2011), allowing them to sense changes in the neuronal microenvironment and adjust the microvasculature accordingly (Hawkins and Davis, 2005; Attwell et al., 2010; Gordon et al., 2011; He et al., 2012). Due to the anatomical and physiological contacts between astrocytes and ECs, any stimuli from pathological astrocytes can influence EC function (Zhou et al., 2019).

Roles in brain arteriovenous malformations pathogenesis

The effects of astrocytes on bAVM pathogenesis are summarized in **Figure 3**. Several lines of evidence suggest that the astrocytes are involved in pathogeneses of bAVM. The expression of γ-glutamyl transpeptidase GGTP and glucose transporter 1 (GLUT1) protein expressed by ECs and astrocytes are increased in AVM nidus structures compared to control vessels confirming the contribution of astrocytes in bAVM pathogenesis (Thomas et al., 2018). Accumulation of albumin in astrocytes surrounding the AVM lesion has been noticed, which motivates the conversion of astrocytes from a resting state to a reactivate stage *via* triggering TGF-β signaling (Raabe et al., 2012). Li et al. reported that astrocytes in bAVM lesion have a higher level of VEGF and illustrated that the VEGF released by astrocytes can be delivered to the vascular ECs *via* perivascular pedunculus structures (Li et al., 2018). Patients with recurrent bAVM have an increased VEGF expression in astrocytes compared to non-recurrent bAVM cases, suggesting that astrocytes play roles in bAVM development (Zhou et al., 2019).

In a recent study, immunohistochemical analysis detected irregular astrocytes in and around bAVM nidus. The retinoic acid signaling pathway, which leads to the expression of angiogenic gene CYR61, was upregulated in the astrocytes in and around the bAVM structure. These data shows that astrocytes can modulate angiogenesis around the AVMs (Thomas et al., 2021). Notably, CYR61 gene takes part in angiogenesis through activating several growth factors, enhancing the migration and adhesion of ECs, as well as over-expression of αv integrin subunit and MMP, and other genes that are responsible for angiogenesis (Chen et al., 2001).

It has shown that the foot processes of perivascular astrocytes in adult mice and rats express integrin αvβ8, which interacts with latency-associated peptide (LAP) and activates TGF-β promoting differentiation and maintenance of vessels (Cambier et al., 2005). The level of integrin β8 protein in perivascular astrocytes in human bAVM lesion is lower compared to normal brain tissue (Su et al., 2010). In addition, elimination of integrin αv or β8 in astrocytes disrupts the suitable contacts between astrocyte endfeet and the vascular ECs (Proctor et al., 2005). As well, elimination of integrin β8 increased dysplastic vessels and hemorrhage in the *Alk1*$^{+/-}$ mouse brain (Ma et al., 2016).

Astrocyte crosstalk with brain ECs and pericytes by releasing soluble factors, including cytokines (Banks et al., 2018). Vasoactive molecules like arachidonic acid (AA), prostaglandin E2 (PGE2) and K+ generated by astrocytes endfeet onto the vSMCs, can regulate vascular tone (Watkins et al., 2014).

In addition, astrocytes are important contributors in normal structural integrity of newly formed vessels. During vascular tube generation, tight junction development is strongly associated with the cellular interactions between ECs and pericytes, followed by astrocytes (Bonkowski et al., 2011). In this regard, the interaction between pericytes and ECs is partially regulated by ECM. Both ECs and pericytes secrete MMPs which are important not only for ECM remodeling, but also for tight junction cleavage (Thanabalasundaram et al., 2011). Additionally, the endfeets of astrocytes, in association with

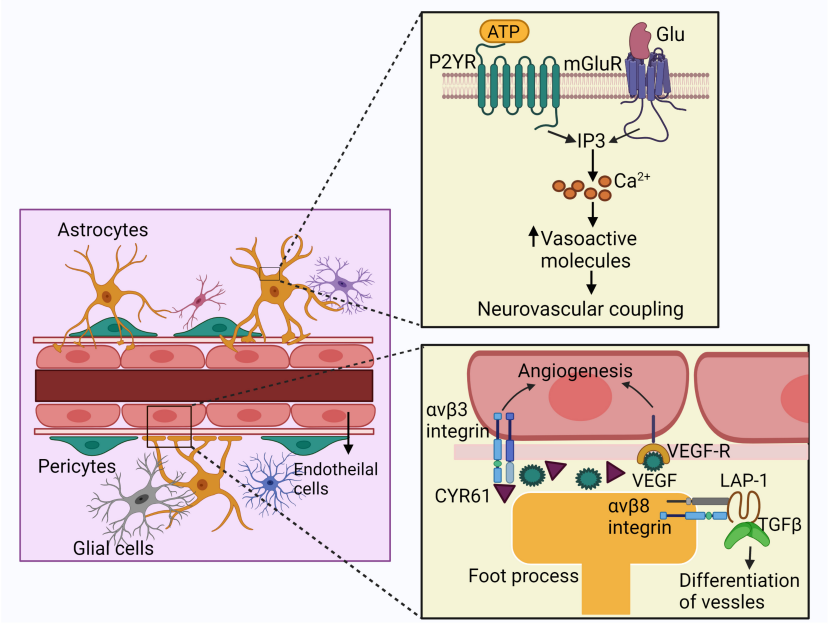

FIGURE 3
Schematic representation of the effects of astrocytes on bAVM pathogenesis. Astrocytes express mGluR and P2YR which interact with glutamate or ATP. Activation of these receptors trigger IP3 signaling cascade and the intracellular calcium currents, leading to the release of vasoactive molecules. These agents finally contribute to neurovascular coupling. Astrocytes also release VEGF in bAVM, which delivered to the ECs enhancing angiogenesis. Astrocytes also express CYR61, which takes part in angiogenesis. Foot processes of astrocytes express integrin αvβ8, interacting with LAP and activates TGF-β which promotes differentiation and maintenance of vessels. ECs: endothelial cells, mGluR: metabotropic glutamate receptors, P2YR: purinergic receptors, ATP: adenosine triphosphate, LAP: latency-associated peptide, IP3: inositol triphosphate.

pericytes, preserve the expression of ECs tight junction proteins, transporters and enzymes (Watkins et al., 2014). Therefore, the crosstalk among brain ECs, pericytes, and astrocytes results in tight junction formation during vascular tube development, which finally increases vessel wall integrity.

The above-mentioned data confirms the crucial effects of perivascular astrocytes in the neurovascular coupling. Astrocyte malfunction can lead toprogression of bAVM through impairment of BBB structure as well as the function of ECs, pericytes and vSMCs by cross talking among these cells.

Inflammatory cells

Typically, host immune system is divided into innate and adaptive immunity. Innate immune cells contain macrophages, neutrophils, monocytes, plasmacytoid dendritic cells, natural killer (NK) cells, and other myeloid and lymphoid cells. Adaptive immune reaction is mediated by the immunoglobulin family and cells such as B- and T-lymphocytes (Netea et al., 2019). Present evidence shows higher inflammatory cytokines in bAVM tissues and blood, suggesting the contribution of inflammation in the pathogenesis, progression, and rupture of bAVM (Zhang et al., 2016a). The overall roles of inflammatory cells in bAVM pathogenesis are summarized in **Figure 4**.

Microglia and macrophages

The normal function of microglia/macrophages

Microglia are ubiquitously distributed within the brain maintaining brain homeostasis. During disease or trauma, microglia may become activated, and the degree of microglia activation is directly correlated to the type and severity of brain injury (Speth et al., 2005). Activation of microglia is directly associated with dysfunction of the BBB by changing tight junction protein expression and increasing BBB permeability (Zlokovic, 2008). Macrophages are the primary BM-derived cells infiltrate into the brain angiogenic foci (Hao et al., 2008). These cells are primarily involved in phagocytosis and attracting peripheral immune cells to the injury site.

The microglia and macrophages are accumulated in and around brain arteriovenous malformations lesion

Macrophages are main inflammatory components that reside in and around vascular walls in human and animal bAVM samples with or without hemorrhage, indicating that macrophage burden is not a result of hemorrhage (Guo et al., 2014). A recent report shown that mononuclear cells (macrophages, T cells, B cells) were the dominant types of

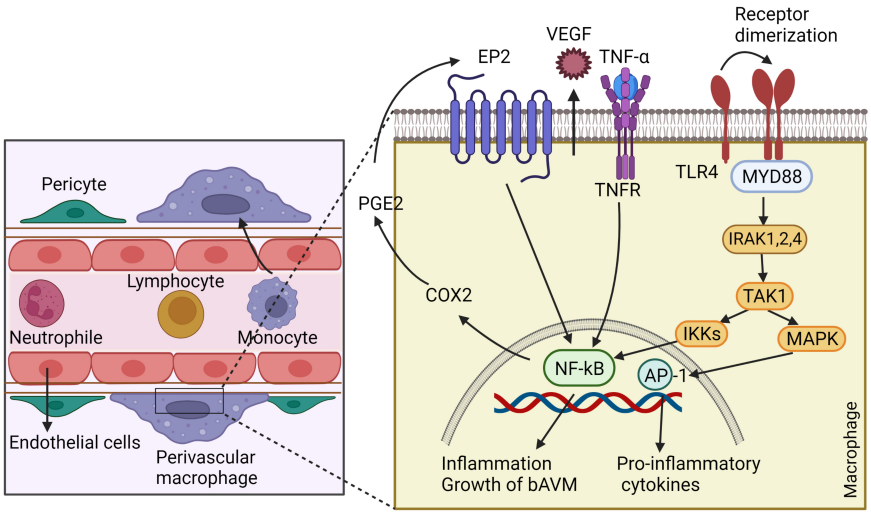

FIGURE 4
The involvement of inflammatory cells in bAVM growth. Macrophages release VEGF, which regulates the development of ECs and vessel sprouting. By generating matrix proteases, macrophages degrade ECM to create a guiding pathway for proliferation and migration of ECs and facilitating vascular branching. Macrophages also have crucial role in recruitment of pericytes around new blood vessels by expressing high levels of PDGFB. Macrophages through triggering autocrine feedback loop of COX2, PGE2, EP2-NF-kB-COX2 results in bAVM progression. Likewise, macrophages express TLR4, which binds to myeloid differentiation primary response gene 88 (MyD88) and leads to the generation of complex with IRAKs and activation of inhibitor kappa B kinase β (IKKβ). This process leads to translocation of NF-κB into the macrophage nucleus and overexpressing genes involved in inflammation. ECs: endothelial cells, COX2: cyclo-oxygenase 2, PGE2: Prostaglandin E2- EP2: prostaglandin E receptor subtype 2, MyD88: myeloid differentiation primary response gene 88, PDGFB: Platelet-derived growth factor B, TLR4: toll-like receptor 4, IRAKs: IL-1R-associated kinases, IKKβ: inhibitor kappa B kinase β.

inflammatory cells in bAVMs (Wright et al., 2020). In addition, the macrophage migration inhibitory factor (MIF), a main activation factor of macrophages, is highly expressed in bAVM and participates in the vascular cell proliferation and apoptosis (Chen et al., 2012).

It must be noted that, although *Eng* deficient mice show impaired monocyte migration toward injured site (Zhu et al., 2017), the macrophage burden is increased in bAVM in both *Eng*- and *Alk1*-deleted animal models (Chen et al., 2013b; Choi et al., 2014). The persistent infiltration and pro-inflammatory differentiation of monocytes might cause increase of macrophage in bAVM (Zhang et al., 2016a). Accordingly, a study by Zhang et al. (2016a) confirmed the recruitment of fewer macrophages to the brain angiogenic area at the initial step after angiogenic stimulation and more macrophages burden in the later stage of bAVM development. Moreover, Eng-null macrophages showed slower but more persistent infiltration into the brain angiogenic regions compared to the normal macrophages; therefore, macrophages burden could be partially due to the continues infiltration and late clearance of BM-derived macrophages (Shen et al., 2014; Zhang et al., 2016a). Moreover, an *in vitro* system mimicking angiogenic niches using the co-culture of ECs and vSMCs illustrated that the HHT $CD34^+$ monocytes have tendency to be differentiated into macrophages compared to normal $CD34^+$ monocytes, indicating a pro-inflammatory feature of HHT monocytes (Zhang et al., 2016a).

Notably, a recent study revealed enhanced soluble ENG in human bAVMs. The soluble ENG motivates microglia to express angiogenic/inflammatory mediators like VEGF, TNF-α, IL-6, NLRP3, ASC, Caspase-1, and IL-1β, and proteolytic enzyme of MMP-2 and MMP-9, which mediate dysplastic vessel formation. This study indicates that microglia may contribute to soluble ENG-induced EC dysfunction *via* expressing inflammatory and angiogenic factors (Park E. S. et al., 2022). The microglia-mediated EC dysfunction can be a mechanism underlying soluble ENG-induced bAVMs observed in a previous study (Chen et al., 2009).

Another data suggested the high wall shear stress (WSS) as a critical parameter in aggregation of macrophages by activating proinflammatory signaling in ECs, mostly through activation of NF-κB, macrophage chemoattractant protein 1 (MCP1), and VCAM-1 (Ahn et al., 2016). As a result, macrophage aggregation in bAVM leads to uncontrolled inflammation, which increases abnormal vascular remodeling and worsens bAVM phenotype (Zhu et al., 2017). Therefore, addressing the mechanisms of macrophages action in vascular remodeling, bAVM pathogenesis and progression can improve therapeutic strategies alternate to surgery.

Macrophages enhance bAVM phenotype severity through stimulating angiogenesis, activating EP2-NF-KB-COX2 and TLR4/MyD88 pathways and secreting ECM-degrading proteases. During development and tissue healing or regeneration, macrophages stimulate angiogenesis, and

facilitate tissue remodeling by secreting a number of proteases and growth factors (Krenkel and Tacke, 2017). The functions of macrophages in tissue and vessel repair include (i) secretion of pro-inflammatory cytokines and chemokines to maintain initial leukocytes infiltration, (ii) removal of invading pathogen and necrotic cell debris through phagocytosis, (iii) releasing MMP for ECM remodeling, (iv) promoting angiogenesis through guiding the sprouting of new blood vessels and stimulating the proliferation of EC and smooth muscle cells (SMC) (la Sala et al., 2012). The TIE2-expressing macrophage is a subtype of highly angiogenic macrophages that is able to influence angiogenesis *via* the ANGPT-TIE pathway (la Sala et al., 2012). It has been found recently that; microglia and macrophage promote angiogenesis by regulating EC subsets through SPP and IGF signaline pathways following spinal cord injury (Yao et al., 2022). Macrophages also have crucial role in recruitment of pericytes around new blood vessels by expressing high levels of PDGFB (Spiller et al., 2014).

Alternative to angiogenesis regulation, macrophages can act through an autocrine feedback loop of Cyclo-oxygenase 2 (COX2)- prostaglandin E2 (PGE2)- prostaglandin E receptor subtype 2 (EP2)-NF-kB-COX2 signaling pathway (Keranen et al., 2021). COX2, an inflammation-associated enzyme, is a main modulator of creation and progression of aneurysms (Keranen et al., 2021). In addition, the expression of COX2 in the vessels' lumen or medial layer of human bAVMs is increased and exerts an important role in the growth and remodeling of the bAVM vessels. Further, COX2-derived PGE2, a key mediator of vascular remodeling, is enhanced in the vSMCs, ECs, and perivascular inflammatory cells of bAVMs (Keranen et al., 2021). On the other side, the expression of COX2 intensifies the inflammatory response through the loop of COX2-PGE2-EP2-NF-kB-COX2 signaling in macrophages (Keranen et al., 2021). In this context, a recent data illustrated a link between EP2 and COX-2 with macrophage burden in human intracranial aneurysm (Aoki et al., 2017). Administration of EP2 antagonist dramatically decreased macrophage infiltration and reduced the progression of intracranial aneurysm, suggesting the therapeutic potential of EP2 antagonists in vascular lesions (Aoki et al., 2017).

Likewise, macrophages are implicated in bAVM pathogenesis by acting through toll-like receptor 4 (TLR4), which is strongly expressed on macrophages (Mitsui et al., 2020). Binding of TLR4 to MyD88 leads to the generation of complex with IL-1R-associated kinases (IRAKs). This complex increases the formation of inflammatory cytokines, including IL-1β, IL-6, MCP-1, and C-X-C motif ligand (CXCL) (Michelsen et al., 2004). The secreted inflammatory cytokines and chemokines are implicated in the progress of aneurysmal rupture by compelling macrophages toward the pro-inflammatory phenotype (Mitsui et al., 2020). Totally, the signaling cascade *via* MyD88 activates inhibitor kappa B kinase β (IKKβ), which finally induces the phosphorylation and degradation of inhibitor kappa B (IκB). This process leads to translocation of NF-κB into the macrophage nucleus and overexpressing several genes involved in inflammation (Aoki et al., 2017).

Given the previous findings, macrophages have strong role in bAVM pathogenesis promoting progression in several ways, therefore, blocking the signaling pathways may promisingly be used for treatment of bAVM.

Neutrophils

Neutrophils, the innate immune phagocytes, are critical effectors of the acute immune response against infection and tissue injury, with the capability to adjust their phenotype in accord with the microenvironment (Scalerandi et al., 2018).

Although the role of neutrophils in bAVM have been investigated in only a handful of studies so far, the presence of very large number of neutrophils in the vascular walls of bAVM indicate the involvement of these inflammatory cells in bAVM pathogenesis (Chen et al., 2008). Furthermore, the histological examination of surgically resected bAVMs tissue samples (n = 85) illustrated perivascular neutrophil recruitment and adhesion of neutrophils to the vessels' walls of bAVM nidal in 60% (51/85) of the samples (Jarvelin et al., 2020). Neutrophil-lymphocyte ratio (NLR) is considered as an efficient way for assessment of the inflammatory action in the vessels. A recent study reported the significantly association between the higher NLR with poor outcome of cases with ruptured AVMs (Zhang et al., 2018). Neutrophils could promote bAVM progression through formation of neutrophil extracellular traps (Bonaventura et al., 2020; Shimada et al., 2021) and promoting angiogenesis (Massena et al., 2015; Wang J. et al., 2017). In addition, the complex of MMP-9/neutrophil gelatinase-associated lipocalin (NGAL) is increased in AVM samples. NGAL secreted by the neutrophils protects the MMP-9 from degradation and thus enhances the activity of MMP-9 (Ardi et al., 2007).

Lymphocytes

It has been indicated that several kinds of inflammatory cells such as neutrophils, eosinophils, macrophages, and lymphocytes are present in bAVM samples (Wright et al., 2020). Of note, few studies focused on the involvement of lymphocytes in bAVM pathogenesis. Chen et al. (2008) showed that the bAVM specimens had minimal T-cells or B cells compared to macrophages and neutrophils. An another study (Guo et al., 2014) showed that the macrophages were dispersed frequently in the vessel walls and intervening stromal areas. T-lymphocytes were predominantly detected in unruptured bAVM tissue. However, rare B-lymphocytes and plasma cells were detected in the samples. They were generally appeared in samples with

a large quantity of T-lymphocytes and were co-localized with the T-lymphocytes. Regardless the existence of lymphocytes in bAVM tissue, the effects of these cells on the bAVM development and progression are remained blurred and there is a need to be discovered.

Discussion/summary

Much progress has been made in understanding bAVM pathogenesis. However, the effect of cellular population on development and progression of bAVM is still in its nascent stages. Although gene mutation in ECs seems essential for bAVM initiation, different cell types of the neurovascular unit and inflammatory cells are involved in bAVM pathogenesis. In this review, we systemically reviewed the cell types that present in bAVMs and their possible role in bAVM initiation, progression and hemorrhage.

The importance of EC in bAVM initiation has been supported by both animal study and analyzing human bAVM samples. Homozygous mutation of *Alk1* or *Eng* in a portion of somatic ECs (Walker et al., 2011b; Choi et al., 2012) is sufficient to trigger *de novo* bAVM in the presence of angiogenic stimulation in **adult** mice. Sporadic bAVM and extra-neural AVM harbor mutations of genes in RAS-MAPK pathways in a small number of ECs (Couto et al., 2017; Al-Olabi et al., 2018; Nikolaev et al., 2018). Transducing $Kras^{G12D}$ *and* $Kras^{G12V}$ into brain ECs induced bAVM in mice (Fish et al., 2020; Park E. S. et al., 2021). Other abnormalities of ECs such as EC inflammation, and EndMT also contribute to bAVM progression and hemorrhage.

Although mutation of HHT causative genes in pericytes, vSMCs or macrophages did not trigger AVM initiation (Chen et al., 2014b; Choi et al., 2014; Garrido-Martin et al., 2014), abnormalities of these cells have been observed in bAVMs. Both human and mouse bAVM vessels have fewer mural cell coverage, which is associated with vessel leakage and hemorrhage (Chen et al., 2013b; Winkler et al., 2018), suggesting roles of pericytes and vSMCs in bAVM pathogenesis. In addition, pathways, including PDGFB/PDGFR-β, ANGPT/TIE2 and EPHRINB2/EPHB4 play roles in the reduction of the mural cell coverage on bAVM vessels.

An abnormally high number of inflammatory cells including macrophages, neutrophils, and T lymphocytes have been detected in human and mouse bAVMs, even in unruptured specimens (Guo et al., 2012, 2014). Abnormal astrocytes with increased expression of GFAP and vimentin have been observed in human sporadic bAVMs, which is associated with deregulated expression of genes in retinoic acid signaling, (Thomas et al., 2021). Their role in bAVMs pathogenesis also discussed in this review paper.

In summary, we have discussed roles of different cell-types present in bAVM in bAVM pathogenesis and possible underlying mechanisms. We hope the information provided in this review will help in identifying targets for developing new therapies for treating bAVM or preventing bAVM hemorrhage.

Author contributions

ZS, JS, and HS drafted the manuscript. HS critically read the final manuscript. All authors contributed to the article and approved the submitted version.

Funding

This study was supported by grants to HS from the National Institutes of Health (NS027713 and NS112819) and from the Michael Ryan Zodda Foundation.

Conflict of interest

The authors declare that the research was conducted in the absence of any commercial or financial relationships that could be construed as a potential conflict of interest.

Publisher's note

All claims expressed in this article are solely those of the authors and do not necessarily represent those of their affiliated organizations, or those of the publisher, the editors and the reviewers. Any product that may be evaluated in this article, or claim that may be made by its manufacturer, is not guaranteed or endorsed by the publisher.

References

Abramsson, A., Kurup, S., Busse, M., Yamada, S., Lindblom, P., Schallmeiner, E., et al. (2007). Defective N-sulfation of heparan sulfate proteoglycans limits PDGF-BB binding and pericyte recruitment in vascular development. *Genes Dev.* 21, 316–331. doi: 10.1101/gad.398207

Adams, R. H., and Alitalo, K. (2007). Molecular regulation of angiogenesis and lymphangiogenesis. *Nat. Rev. Mol. Cell Biol.* 8, 464–478. doi: 10.1038/nrm2183

Ahn, S. M., Kim, Y. R., Kim, H. N., Shin, Y. I., Shin, H. K., and Choi, B. T. (2016). Electroacupuncture ameliorates memory impairments by enhancing oligodendrocyte regeneration in a mouse model of prolonged cerebral hypoperfusion. *Sci. Rep.* 6:28646. doi: 10.1038/srep28646

Al-Olabi, L., Polubothu, S., Dowsett, K., Andrews, K. A., Stadnik, P., Joseph, A. P., et al. (2018). Mosaic RAS/MAPK variants cause sporadic vascular

malformations which respond to targeted therapy. *J. Clin. Invest.* 128, 1496–1508. doi: 10.1172/JCI98589

Andrae, J., Gallini, R., and Betsholtz, C. (2008). Role of platelet-derived growth factors in physiology and medicine. *Genes Dev.* 22, 1276–1312. doi: 10.1101/gad.1653708

Aoki, T., Frosen, J., Fukuda, M., Bando, K., Shioi, G., Tsuji, K., et al. (2017). Prostaglandin E2-EP2-NF-kappaB signaling in macrophages as a potential therapeutic target for intracranial aneurysms. *Sci. Signal* 10:eaah6037. doi: 10.1126/scisignal.aah6037

Ardi, V. C., Kupriyanova, T. A., Deryugina, E. I., and Quigley, J. P. (2007). Human neutrophils uniquely release TIMP-free MMP-9 to provide a potent catalytic stimulator of angiogenesis. *Proc. Natl. Acad. Sci. U. S. A.* 104, 20262–20267. doi: 10.1073/pnas.0706438104

Armulik, A., Genove, G., and Betsholtz, C. (2011). Pericytes: developmental, physiological, and pathological perspectives, problems, and promises. *Dev. Cell* 21, 193–215. doi: 10.1016/j.devcel.2011.07.001

Armulik, A., Genove, G., Mae, M., Nisancioglu, M. H., Wallgard, E., Niaudet, C., et al. (2010). Pericytes regulate the blood-brain barrier. *Nature* 468, 557–561. doi: 10.1038/nature09522

Aspalter, I. M., Gordon, E., Dubrac, A., Ragab, A., Narloch, J., Vizan, P., et al. (2015). Alk1 and Alk5 inhibition by Nrp1 controls vascular sprouting downstream of Notch. *Nat. Commun.* 6:7264. doi: 10.1038/ncomms8264

Attwell, D., Buchan, A. M., Charpak, S., Lauritzen, M., Macvicar, B. A., and Newman, E. A. (2010). Glial and neuronal control of brain blood flow. *Nature* 468, 232–243. doi: 10.1038/nature09613

Bai, J., Wang, Y. J., Liu, L., and Zhao, Y. L. (2014). Ephrin B2 and EphB4 selectively mark arterial and venous vessels in cerebral arteriovenous malformation. *J. Int. Med. Res.* 42, 405–415. doi: 10.1177/0300060513478091

Banks, W. A., Kovac, A., and Morofuji, Y. (2018). Neurovascular unit crosstalk: pericytes and astrocytes modify cytokine secretion patterns of brain endothelial cells. *J. Cereb. Blood Flow Metab.* 38, 1104–1118. doi: 10.1177/0271678X17740793

Bell, R. D., Winkler, E. A., Sagare, A. P., Singh, I., LaRue, B., Deane, R., et al. (2010). Pericytes control key neurovascular functions and neuronal phenotype in the adult brain and during brain aging. *Neuron* 68, 409–427. doi: 10.1016/j.neuron.2010.09.043

Bonaventura, A., Vecchie, A., Abbate, A., and Montecucco, F. (2020). Neutrophil extracellular traps and cardiovascular diseases: an update. *Cells* 9:231. doi: 10.3390/cells9010231

Bonkowski, D., Katyshev, V., Balabanov, R. D., Borisov, A., and Dore-Duffy, P. (2011). The CNS microvascular pericyte: pericyte-astrocyte crosstalk in the regulation of tissue survival. *Fluids Barriers CNS* 8, 1–12. doi: 10.1186/2045-8118-8-8

Brown, L. S., Foster, C. G., Courtney, J. M., King, N. E., Howells, D. W., and Sutherland, B. A. (2019). Pericytes and neurovascular function in the healthy and diseased brain. *Front. Cell Neurosci.* 13:282. doi: 10.3389/fncel.2019.00282

Cambier, S., Gline, S., Mu, D., Collins, R., Araya, J., Dolganov, G., et al. (2005). Integrin alpha(v)beta8-mediated activation of transforming growth factor-beta by perivascular astrocytes: an angiogenic control switch. *Am. J. Pathol.* 166, 1883–1894. doi: 10.1016/s0002-9440(10)62497-2

Castonguay, R., Werner, E. D., Matthews, R. G., Presman, E., Mulivor, A. W., Solban, N., et al. (2011). Soluble endoglin specifically binds BMP9/BMP10 *via* its orphan domain, inhibits blood vessel formation and suppresses tumor growth. *J. Biol. Chem.* 286, 30034–30046. doi: 10.1074/jbc.M111.260133

Chen, C. C., Mo, F. E., and Lau, L. F. (2001). The angiogenic factor Cyr61 activates a genetic program for wound healing in human skin fibroblasts. *J. Biol. Chem.* 276, 47329–47337. doi: 10.1074/jbc.M107666200

Chen, G., Zheng, M., Shu, H., Zhan, S., Wang, H., Zhou, D., et al. (2012). Macrophage migration inhibitory factor reduces apoptosis in cerebral arteriovenous malformations. *Neurosci. Lett.* 508, 84–88. doi: 10.1016/j.neulet.2011.12.024

Chen, W., Guo, Y., Jun, K., Wankhede, M., Su, H., and Young, W. L. (2013a). Alk1 deficiency impairs mural cell recruitment during brain angiogenesis [Abstract]. *Stroke* 44:ATM118.

Chen, W., Guo, Y., Walker, E. J., Shen, F., Jun, K., Oh, S. P., et al. (2013b). Reduced mural cell coverage and impaired vessel integrity after angiogenic stimulation in the *Alk1*-deficient brain. *Arterioscler Thromb. Vasc. Biol.* 33, 305–310. doi: 10.1161/ATVBAHA.112.300485

Chen, W., Choi, E. J., McDougall, C. M., and Su, H. (2014a). Brain arteriovenous malformation modeling, pathogenesis, and novel therapeutic targets. *Transl. Stroke Res.* 5, 316–329. doi: 10.1007/s12975-014-0343-0

Chen, W., Sun, Z., Han, Z., Jun, K., Camus, M., Wankhede, M., et al. (2014b). De novo cerebrovascular malformation in the adult mouse after endothelial Alk1 deletion and angiogenic stimulation. *Stroke* 45, 900–902. doi: 10.1161/STROKEAHA.113.003655

Chen, Y., Hao, Q., Kim, H., Su, H., Letarte, M., Karumanchi, S. A., et al. (2009). Soluble endoglin modulates aberrant cerebral vascular remodeling. *Ann. Neurol.* 66, 19–27. doi: 10.1002/ana.21710

Chen, Y., Zhu, W., Bollen, A. W., Lawton, M. T., Barbaro, N. M., Dowd, C. F., et al. (2008). Evidence of inflammatory cell involvement in brain arteriovenous malformations. *Neurosurgery* 62, 1340–1349. doi: 10.1227/01.neu.0000333306.64683.b5

Choi, E. J., Chen, W., Jun, K., Arthur, H. M., Young, W. L., and Su, H. (2014). Novel brain arteriovenous malformation mouse models for type 1 hereditary hemorrhagic telangiectasia. *PLoS One* 9:e88511. doi: 10.1371/journal.pone.0088511

Choi, E. J., Walker, E. J., Shen, F., Oh, S. P., Arthur, H. M., Young, W. L., et al. (2012). Minimal homozygous endothelial deletion of Eng with VEGF stimulation is sufficient to cause cerebrovascular dysplasia in the adult mouse. *Cerebrovasc. Dis.* 33, 540–547. doi: 10.1159/000337762

Cockroft, K. M., Jayaraman, M. V., Amin-Hanjani, S., Derdeyn, C. P., McDougall, C. G., and Wilson, J. A. (2012). A perfect storm: how a randomized trial of unruptured brain arteriovenous malformations' (ARUBA's) trial design challenges notions of external validity. *Stroke* 43, 1979–1981. doi: 10.1161/STROKEAHA.112.652032

Colombo, E., and Farina, C. (2016). Astrocytes: key regulators of neuroinflammation. *Trends Immunol.* 37, 608–620. doi: 10.1016/j.it.2016.06.006

Cordonnier, C., Klijn, C. J., van Beijnum, J., and Al-Shahi Salman, R. (2010). Radiological investigation of spontaneous intracerebral hemorrhage: systematic review and trinational survey. *Stroke* 41, 685–690. doi: 10.1161/STROKEAHA.109.572495

Coucha, M., Barrett, A. C., Elgebaly, M., Ergul, A., and Abdelsaid, M. (2019). Inhibition of Ephrin-B2 in brain pericytes decreases cerebral pathological neovascularization in diabetic rats. *PLoS One* 14:e0210523. doi: 10.1371/journal.pone.0210523

Couto, J. A., Huang, A. Y., Konczyk, D. J., Goss, J. A., Fishman, S. J., Mulliken, J. B., et al. (2017). Somatic MAP2K1 mutations are associated with extracranial arteriovenous malformation. *Am. J. Hum. Genet.* 100, 546–554. doi: 10.1016/j.ajhg.2017.01.018

Crist, A. M., Zhou, X., Garai, J., Lee, A. R., Thoele, J., Ullmer, C., et al. (2019). Angiopoietin-2 inhibition rescues arteriovenous malformation in a smad4 hereditary hemorrhagic telangiectasia mouse model. *Circulation* 139, 2049–2063. doi: 10.1161/CIRCULATIONAHA.118.036952

Derdeyn, C. P., Zipfel, G. J., Albuquerque, F. C., Cooke, D. L., Feldmann, E., Sheehan, J. P., et al. (2017). Management of brain arteriovenous malformations: a scientific statement for healthcare professionals from the American Heart Association/American Stroke Association. *Stroke* 48, e200–e224. doi: 10.1161/STR.0000000000000134

Enge, M., Bjarnegard, M., Gerhardt, H., Gustafsson, E., Kalen, M., Asker, N., et al. (2002). Endothelium-specific platelet-derived growth factor-B ablation mimics diabetic retinopathy. *Embo J.* 21, 4307–4316. doi: 10.1093/emboj/cdf418

Escartin, C., Galea, E., Lakatos, A., O'Callaghan, J. P., Petzold, G. C., Serrano-Pozo, A., et al. (2021). Reactive astrocyte nomenclature, definitions, and future directions. *Nat. Neurosci.* 24, 312–325. doi: 10.1038/s41593-020-00783-4

Fagiani, E., and Christofori, G. (2013). Angiopoietins in angiogenesis. *Cancer Lett.* 328, 18–26. doi: 10.1016/j.canlet.2012.08.018

Feghali, J., Yang, W. Y., Xu, R. S., Liew, J., McDougall, C. G., Caplan, J. M., et al. (2019). R(2)eD AVM score a novel predictive tool for arteriovenous malformation presentation with hemorrhage. *Stroke* 50, 1703–1710. doi: 10.1161/Strokeaha.119.025054

Fernandez-Lopez, A., Garrido-Martin, E. M., Sanz-Rodriguez, F., Pericacho, M., Rodriguez-Barbero, A., Eleno, N., et al. (2007). Gene expression fingerprinting for human hereditary hemorrhagic telangiectasia. *Hum. Mol. Genet.* 16, 1515–1533. doi: 10.1093/hmg/ddm069

Fish, J. E., Flores Suarez, C. P., Boudreau, E., Herman, A. M., Gutierrez, M. C., Gustafson, D., et al. (2020). Somatic Gain of KRAS function in the endothelium is sufficient to cause vascular malformations that require MEK but Not PI3K signaling. *Circ. Res.* 127, 727–743. doi: 10.1161/CIRCRESAHA.119.316500

Frosen, J., and Joutel, A. (2018). Smooth muscle cells of intracranial vessels: from development to disease. *Cardiovasc. Res.* 114, 501–512. doi: 10.1093/cvr/cvy002

Fu, W., Huo, R., Yan, Z., Xu, H., Li, H., Jiao, Y., et al. (2020). Mesenchymal behavior of the endothelium promoted by SMAD6 downregulation is associated

with brain arteriovenous malformation microhemorrhage. *Stroke* 51, 2197–2207. doi: 10.1161/STROKEAHA.120.030046

Garrido-Martin, E. M., Nguyen, H. L., Cunningham, T. A., Choe, S. W., Jiang, Z., Arthur, H. M., et al. (2014). Common and distinctive pathogenetic features of arteriovenous malformations in hereditary hemorrhagic telangiectasia 1 and hereditary hemorrhagic telangiectasia 2 animal models–brief report. *Arterioscler Thromb. Vasc. Biol.* 34, 2232–2236. doi: 10.1161/ATVBAHA.114.303984

Gerety, S. S., and Anderson, D. J. (2002). Cardiovascular ephrinB2 function is essential for embryonic angiogenesis. *Development* 129, 1397–1410.

Giarretta, I., Sturiale, C. L., Gatto, I., Pacioni, S., Gaetani, E., Porfidia, A., et al. (2021). Sonic hedgehog is expressed in human brain arteriovenous malformations and induces arteriovenous malformations in vivo. *J. Cereb. Blood Flow Metab.* 41, 324–335. doi: 10.1177/0271678X20912405

Gordon, G. R., Howarth, C., and MacVicar, B. A. (2011). Bidirectional control of arteriole diameter by astrocytes. *Exp. Physiol.* 96, 393–399. doi: 10.1113/expphysiol.2010.053132

Goss, J. A., Huang, A. Y., Smith, E., Konczyk, D. J., Smits, P. J., Sudduth, C. L., et al. (2019). Somatic mutations in intracranial arteriovenous malformations. *PLoS One* 14:e0226852. doi: 10.1371/journal.pone.0226852

Groppa, E., Brkic, S., Uccelli, A., Wirth, G., Korpisalo-Pirinen, P., Filippova, M., et al. (2018). EphrinB2/EphB4 signaling regulates non-sprouting angiogenesis by VEGF. *EMBO Rep.* 19:e45045. doi: 10.15252/embr.201745054

Guo, Y., Saunders, T., Su, H., Kim, H., Akkoc, D., Saloner, D. A., et al. (2012). Silent intralesional microhemorrhage as a risk factor for brain arteriovenous malformation rupture. *Stroke* 43, 1240–1246. doi: 10.1161/STROKEAHA.111.647263

Guo, Y., Tihan, T., Kim, H., Hess, C., Lawton, M. T., Young, W. L., et al. (2014). Distinctive distribution of lymphocytes in unruptured and previously untreated brain arteriovenous malformation. *Neuroimmunol. Neuroinflamm.* 1, 147–152. doi: 10.4103/2347-8659.143674

Hamby, M. E., and Sofroniew, M. V. (2010). Reactive astrocytes as therapeutic targets for CNS disorders. *Neurotherapeutics* 7, 494–506. doi: 10.1016/j.nurt.2010.07.003

Hao, Q., Liu, J., Pappu, R., Su, H., Rola, R., Gabriel, R. A., et al. (2008). Contribution of bone marrow-derived cells associated with brain angiogenesis is primarily through leukocytes and macrophages. *Arterioscler Thromb. Vasc. Biol.* 28, 2151–2157. doi: 10.1161/ATVBAHA.108.176297

Hashimoto, T., Lam, T., Boudreau, N. J., Bollen, A. W., Lawton, M. T., and Young, W. L. (2001). Abnormal balance in the angiopoietin-tie2 system in human brain arteriovenous malformations. *Circ. Res.* 89, 111–113. doi: 10.1161/hh1401.094281

Hawkins, B. T., and Davis, T. P. (2005). The blood-brain barrier/neurovascular unit in health and disease. *Pharmacol. Rev.* 57, 173–185. doi: 10.1124/pr.57.2.4

He, L., Linden, D. J., and Sapirstein, A. (2012). Astrocyte inositol triphosphate receptor type 2 and cytosolic phospholipase A2 alpha regulate arteriole responses in mouse neocortical brain slices. *PLoS One* 7:e42194. doi: 10.1371/journal.pone.0042194

He, W., Tan, R., Dai, C., Li, Y., Wang, D., Hao, S., et al. (2010). Plasminogen activator inhibitor-1 is a transcriptional target of the canonical pathway of Wnt/beta-catenin signaling. *J. Biol. Chem.* 285, 24665–24675. doi: 10.1074/jbc.M109.091256

Hegen, A., Koidl, S., Weindel, K., Marme, D., Augustin, H. G., and Fiedler, U. (2004). Expression of angiopoietin-2 in endothelial cells is controlled by positive and negative regulatory promoter elements. *Arterioscler Thromb. Vasc. Biol.* 24, 1803–1809. doi: 10.1161/01.ATV.0000140819.81839.0e

Heithoff, B. P., George, K. K., Phares, A. N., Zuidhoek, I. A., Munoz-Ballester, C., and Robel, S. (2021). Astrocytes are necessary for blood-brain barrier maintenance in the adult mouse brain. *Glia* 69, 436–472. doi: 10.1002/glia.23908

Hellstrom, M., Gerhardt, H., Kalen, M., Li, X., Eriksson, U., Wolburg, H., et al. (2001). Lack of pericytes leads to endothelial hyperplasia and abnormal vascular morphogenesis. *J. Cell Biol.* 153, 543–553. doi: 10.1083/jcb.153.3.543

Hong, T., Yan, Y., Li, J., Radovanovic, I., Ma, X., Shao, Y. W., et al. (2019). High prevalence of KRAS/BRAF somatic mutations in brain and spinal cord arteriovenous malformations. *Brain* 142, 23–34. doi: 10.1093/brain/awy307

Jarvelin, P., Wright, R., Pekonen, H., Keranen, S., Rauramaa, T., and Frosen, J. (2020). Histopathology of brain AVMs part I: microhemorrhages and changes in the nidal vessels. *Acta Neurochir.* 162, 1735–1740. doi: 10.1007/s00701-020-04391-w

Karunanyaka, A., Tu, J., Watling, A., Storer, K. P., Windsor, A., and Stoodley, M. A. (2008). Endothelial molecular changes in a rodent model of arteriovenous malformation. *J. Neurosurg.* 109, 1165–1172. doi: 10.3171/JNS.2008.109.12.1165

Keranen, S., Suutarinen, S., Mallick, R., Laakkonen, J. P., Guo, D., Pawlikowska, L., et al. (2021). Cyclo-oxygenase 2, a putative mediator of vessel remodeling, is expressed in the brain AVM vessels and associates with inflammation. *Acta Neurochir.* 163, 2503–2514. doi: 10.1007/s00701-021-04895-z

Kilari, S., Wang, Y., Singh, A., Graham, R. P., Iyer, V., Thompson, S. M., et al. (2022). Neuropilin-1 deficiency in vascular smooth muscle cells is associated with hereditary hemorrhagic telangiectasia arteriovenous malformations. *JCI Insight* 7:e155565. doi: 10.1172/jci.insight.155565

Kim, H., Su, H., Weinsheimer, S., Pawlikowska, L., and Young, W. L. (2011). Brain arteriovenous malformation pathogenesis: a response-to-injury paradigm. *Acta Neurochir. Suppl.* 111, 83–92. doi: 10.1007/978-3-7091-0693-8_14

Kim, I., Ryu, Y. S., Kwak, H. J., Ahn, S. Y., Oh, J. L., Yancopoulos, G. D., et al. (2002). EphB ligand, ephrinB2, suppresses the VEGF- and angiopoietin 1-induced Ras/mitogen-activated protein kinase pathway in venous endothelial cells. *FASEB J.* 16, 1126–1128. doi: 10.1096/fj.01-0805fje

Kim, Y. H., Choe, S. W., Chae, M. Y., Hong, S., and Oh, S. P. (2018). SMAD4 deficiency leads to development of arteriovenous malformations in neonatal and adult mice. *J. Am. Heart Assoc.* 7:e009514. doi: 10.1161/JAHA.118.009514

Kim, Y. H., Phuong, N. V., Choe, S. W., Jeon, C. J., Arthur, H. M., Vary, C. P., et al. (2020). Overexpression of activin receptor-like kinase 1 in endothelial cells suppresses development of arteriovenous malformations in mouse models of hereditary hemorrhagic telangiectasia. *Circ. Res.* 127, 1122–1137. doi: 10.1161/CIRCRESAHA.119.316267

Kofler, N., and Simons, M. (2016). The expanding role of neuropilin: regulation of transforming growth factor-beta and platelet-derived growth factor signaling in the vasculature. *Curr. Opin. Hematol.* 23, 260–267. doi: 10.1097/MOH.0000000000000233

Korff, T., Aufgebauer, K., and Hecker, M. (2007). Cyclic stretch controls the expression of CD40 in endothelial cells by changing their transforming growth factor-beta1 response. *Circulation* 116, 2288–2297. doi: 10.1161/CIRCULATIONAHA.107.730309

Krebs, L. T., Starling, C., Chervonsky, A. V., and Gridley, T. (2010). Notch 1 activation in mice causes arteriovenous malformations phenocopied by EphrinB2 and EphB4 mutants. *Genesis* 48, 146–150. doi: 10.1002/dvg.20599

Krenkel, O., and Tacke, F. (2017). Liver macrophages in tissue homeostasis and disease. *Nat. Rev. Immunol.* 17, 306–321. doi: 10.1038/nri.2017.11

Krithika, S., and Sumi, S. (2021). Neurovascular inflammation in the pathogenesis of brain arteriovenous malformations. *J. Cell Physiol.* 236, 4841–4856. doi: 10.1002/jcp.30226

la Sala, A., Pontecorvo, L., Agresta, A., Rosano, G., and Stabile, E. (2012). Regulation of collateral blood vessel development by the innate and adaptive immune system. *Trends Mol. Med.* 18, 494–501. doi: 10.1016/j.molmed.2012.06.007

Lan, Y., Liu, B., Yao, H., Li, F., Weng, T., Yang, G., et al. (2007). Essential role of endothelial Smad4 in vascular remodeling and integrity. *Mol. Cell Biol.* 27, 7683–7692. doi: 10.1128/MCB.00577-07

Larrivee, B., Prahst, C., Gordon, E., Del Toro, R., Mathivet, T., Duarte, A., et al. (2012). ALK1 signaling inhibits angiogenesis by cooperating with the Notch pathway. *Dev. Cell* 22, 489–500. doi: 10.1016/j.devcel.2012.02.005

Lebrin, F., Deckers, M., Bertolino, P., and Ten Dijke, P. (2005). TGF-beta receptor function in the endothelium. *Cardiovasc. Res.* 65, 599–608. doi: 10.1016/j.cardiores.2004.10.036

Li, H., Nam, Y., Huo, R., Fu, W., Jiang, B., Zhou, Q., et al. (2021). De novo germline and somatic variants convergently promote endothelial-to-mesenchymal transition in simplex brain arteriovenous malformation. *Circ. Res.* 129, 825–839. doi: 10.1161/CIRCRESAHA.121.319004

Li, P., Zhang, L., Chen, D., Zeng, M., and Chen, F. (2018). Focal neurons: another source of vascular endothelial growth factor in brain arteriovenous malformation tissues? *Neurol. Res.* 40, 122–129. doi: 10.1080/01616412.2017.1405574

Li, S., Wang, R., Wang, Y., Li, H., Zheng, J., Duan, R., et al. (2014). Receptors of the Notch signaling pathway are associated with hemorrhage of brain arteriovenous malformations. *Mol. Med. Rep.* 9, 2233–2238. doi: 10.3892/mmr.2014.2061

Liddelow, S. A., Guttenplan, K. A., Clarke, L. E., Bennett, F. C., Bohlen, C. J., Schirmer, L., et al. (2017). Neurotoxic reactive astrocytes are induced by activated microglia. *Nature* 541, 481–487. doi: 10.1038/nature21029

Lindahl, P., Johansson, B. R., Leveen, P., and Betsholtz, C. (1997). Pericyte loss and microaneurysm formation in PDGF-B-deficient mice. *Science* 277, 242–245. doi: 10.1126/science.277.5323.242

Liu, F., Yao, Z., Lü, P., Jiao, Q.-B., Liu, Q., Wu, H.-X., et al. (2020). Pathophysiologic role of molecules determining arteriovenous differentiation in adult life. *J. Vasc. Res.* 57, 245–253. doi: 10.1159/000507627

Luxan, G., Stewen, J., Diaz, N., Kato, K., Maney, S. K., Aravamudhan, A., et al. (2019). Endothelial EphB4 maintains vascular integrity and transport function in adult heart. *Elife* 8:e45863. doi: 10.7554/eLife.45863

Ma, L., Shen, F., Jun, K., Bao, C., Kuo, R., Young, W. L., et al. (2016). Integrin beta8 deletion enhances vascular dysplasia and hemorrhage in the brain of adult alk1 heterozygous mice. *Transl. Stroke Res.* 7, 488–496. doi: 10.1007/s12975-016-0478-2

Massena, S., Christoffersson, G., Vagesjo, E., Seignez, C., Gustafsson, K., Binet, F., et al. (2015). Identification and characterization of VEGF-A-responsive neutrophils expressing CD49d, VEGFR1, and CXCR4 in mice and humans. *Blood* 126, 2016–2026. doi: 10.1182/blood-2015-03-631572

Miao, H., Wei, B. R., Peehl, D. M., Li, Q., Alexandrou, T., Schelling, J. R., et al. (2001). Activation of EphA receptor tyrosine kinase inhibits the Ras/MAPK pathway. *Nat. Cell Biol.* 3, 527–530. doi: 10.1038/35074604

Michelsen, K. S., Wong, M. H., Shah, P. K., Zhang, W., Yano, J., Doherty, T. M., et al. (2004). Lack of Toll-like receptor 4 or myeloid differentiation factor 88 reduces atherosclerosis and alters plaque phenotype in mice deficient in apolipoprotein E. *Proc. Natl. Acad. Sci. U. S. A.* 101, 10679–10684. doi: 10.1073/pnas.0403249101

Milton, I., Ouyang, D., Allen, C. J., Yanasak, N. E., Gossage, J. R., Alleyne, C. H. Jr., et al. (2012). Age-dependent lethality in novel transgenic mouse models of central nervous system arteriovenous malformations. *Stroke* 43, 1432–1435. doi: 10.1161/STROKEAHA.111.647024

Mitsui, K., Ikedo, T., Kamio, Y., Furukawa, H., Lawton, M. T., and Hashimoto, T. (2020). TLR4 (Toll-Like Receptor 4) mediates the development of intracranial aneurysm rupture. *Hypertension* 75, 468–476. doi: 10.1161/HYPERTENSIONAHA.118.12595

Mohr, J. P., Moskowitz, A. J., Parides, M., Stapf, C., and Young, W. L. (2012). Hull down on the horizon: a randomized trial of unruptured brain arteriovenous malformations (ARUBA) trial. *Stroke* 43, 1744–1745. doi: 10.1161/STROKEAHA.112.653584

Mohr, J. P., Moskowitz, A. J., Stapf, C., Hartmann, A., Lord, K., Marshall, S. M., et al. (2010). The ARUBA trial: current status, future hopes. *Stroke* 41, e537–e540. doi: 10.1161/STROKEAHA.110.580274

Mohr, J. P., Parides, M. K., Stapf, C., Moquete, E., Moy, C. S., Overbey, J. R., et al. (2014). Medical management with or without interventional therapy for unruptured brain arteriovenous malformations (ARUBA): a multicentre, non-blinded, randomised trial. *Lancet* 383, 614–621. doi: 10.1016/S0140-6736(13)62302-8

Murphy, P. A., Lam, M. T., Wu, X., Kim, T. N., Vartanian, S. M., Bollen, A. W., et al. (2008). Endothelial Notch4 signaling induces hallmarks of brain arteriovenous malformations in mice. *Proc. Natl. Acad. Sci. U. S. A.* 105, 10901–10906. doi: 10.1073/pnas.0802743105

Murphy, P. A., Lu, G., Shiah, S., Bollen, A. W., and Wang, R. A. (2009). Endothelial Notch signaling is upregulated in human brain arteriovenous malformations and a mouse model of the disease. *Lab. Invest* 89, 971–982. doi: 10.1038/labinvest.2009.62

Netea, M. G., Schlitzer, A., Placek, K., Joosten, L. A. B., and Schultze, J. L. (2019). Innate and adaptive immune memory: an evolutionary continuum in the host's response to pathogens. *Cell Host Microbe* 25, 13–26. doi: 10.1016/j.chom.2018.12.006

Nielsen, C. M., Cuervo, H., Ding, V. W., Kong, Y., Huang, E. J., and Wang, R. A. (2014). Deletion of Rbpj from postnatal endothelium leads to abnormal arteriovenous shunting in mice. *Development* 141, 3782–3792. doi: 10.1242/dev.108951

Nikolaev, S. I., Vetiska, S., Bonilla, X., Boudreau, E., Jauhiainen, S., Rezai Jahromi, B., et al. (2018). Somatic activating KRAS mutations in arteriovenous malformations of the brain. *N. Engl. J. Med.* 378, 250–261. doi: 10.1056/NEJMoa1709449

Nishishita, T., and Lin, P. C. (2004). Angiopoietin 1, PDGF-B, and TGF-beta gene regulation in endothelial cell and smooth muscle cell interaction. *J. Cell Biochem.* 91, 584–593. doi: 10.1002/jcb.10718

Ojeda-Fernandez, L., Barrios, L., Rodriguez-Barbero, A., Recio-Poveda, L., Bernabeu, C., and Botella, L. M. (2010). Reduced plasma levels of Ang-2 and sEng as novel biomarkers in hereditary hemorrhagic telangiectasia (HHT). *Clin. Chim. Acta* 411, 494–499. doi: 10.1016/j.cca.2009.12.023

Ottone, C., Krusche, B., Whitby, A., Clements, M., Quadrato, G., Pitulescu, M. E., et al. (2014). Direct cell-cell contact with the vascular niche maintains quiescent neural stem cells. *Nat. Cell Biol.* 16, 1045–1056. doi: 10.1038/ncb3045

Pan, P., Shaligram, S. S., Do Prado, L. B., He, L., and Su, H. (2021). The role of mural cells in hemorrhage of brain arteriovenous malformation. *Brain Hemorrhages* 2, 49–56.

Pardali, E., Sanchez-Duffhues, G., Gomez-Puerto, M. C., and Ten Dijke, P. (2017). TGF-beta-induced endothelial-mesenchymal transition in fibrotic diseases. *Int. J. Mol. Sci.* 18:2157. doi: 10.3390/ijms18102157

Park, E. S., Kim, S., Huang, S., Yoo, J. Y., Korbelin, J., Lee, T. J., et al. (2021). Selective endothelial hyperactivation of oncogenic KRAS induces brain arteriovenous malformations in mice. *Ann. Neurol.* 89, 926–941. doi: 10.1002/ana.26059

Park, H., Furtado, J., Poulet, M., Chung, M., Yun, S., Lee, S., et al. (2021). Defective flow-migration coupling causes arteriovenous malformations in hereditary hemorrhagic telangiectasia. *Circulation* 144, 805–822. doi: 10.1161/CIRCULATIONAHA.120.053047

Park, E. S., Kim, S., Yao, D. C., Savarraj, J. P. J., Choi, H. A., Chen, P. R., et al. (2022). Soluble endoglin stimulates inflammatory and angiogenic responses in microglia that are associated with endothelial dysfunction. *Int. J. Mol. Sci.* 23:1225. doi: 10.3390/ijms23031225

Pasquale, E. B. (2008). Eph-ephrin bidirectional signaling in physiology and disease. *Cell* 133, 38–52. doi: 10.1016/j.cell.2008.03.011

Pellet-Many, C., Frankel, P., Evans, I. M., Herzog, B., Junemann-Ramirez, M., and Zachary, I. C. (2011). Neuropilin-1 mediates PDGF stimulation of vascular smooth muscle cell migration and signalling *via* p130Cas. *Biochem. J.* 435, 609–618. doi: 10.1042/BJ20100580

Perez, L., Munoz-Durango, N., Riedel, C. A., Echeverria, C., Kalergis, A. M., Cabello-Verrugio, C., et al. (2017). Endothelial-to-mesenchymal transition: cytokine-mediated pathways that determine endothelial fibrosis under inflammatory conditions. *Cytokine Growth Factor Rev.* 33, 41–54. doi: 10.1016/j.cytogfr.2016.09.002

Priemer, D. S., Vortmeyer, A. O., Zhang, S., Chang, H. Y., Curless, K. L., and Cheng, L. (2019). Activating KRAS mutations in arteriovenous malformations of the brain: frequency and clinicopathologic correlation. *Hum. Pathol.* 89, 33–39. doi: 10.1016/j.humpath.2019.04.004

Proctor, J. M., Zang, K., Wang, D., Wang, R., and Reichardt, L. F. (2005). Vascular development of the brain requires beta8 integrin expression in the neuroepithelium. *J. Neurosci.* 25, 9940–9948. doi: 10.1523/JNEUROSCI.3467-05.2005

Raabe, A., Schmitz, A. K., Pernhorst, K., Grote, A., von der Brelie, C., Urbach, H., et al. (2012). Cliniconeuropathologic correlations show astroglial albumin storage as a common factor in epileptogenic vascular lesions. *Epilepsia* 53, 539–548. doi: 10.1111/j.1528-1167.2012.03405.x

Rahman, M. A., Cho, Y., Nam, G., and Rhim, H. (2021). Antioxidant compound, oxyresveratrol, inhibits APP production through the AMPK/ULK1/mTOR-mediated autophagy pathway in mouse cortical astrocytes. *Antioxidants* 10:408. doi: 10.3390/antiox10030408

Roca, C., and Adams, R. H. (2007). Regulation of vascular morphogenesis by Notch signaling. *Genes Dev.* 21, 2511–2524. doi: 10.1101/gad.1589207

Rodrigues de Oliveira, L. F., Castro-Afonso, L. H., Freitas, R. K., Colli, B. O., and Abud, D. G. (2020). De novo intracranial arteriovenous malformation-case report and literature review. *World Neurosurg.* 138, 349–351. doi: 10.1016/j.wneu.2020.03.109

Ruiz, S., Zhao, H., Chandakkar, P., Chatterjee, P. K., Papoin, J., Blanc, L., et al. (2016). A mouse model of hereditary hemorrhagic telangiectasia generated by transmammary-delivered immunoblocking of BMP9 and BMP10. *Sci. Rep.* 5:37366. doi: 10.1038/srep37366

Saito, T., Bokhove, M., Croci, R., Zamora-Caballero, S., Han, L., Letarte, M., et al. (2017). Structural basis of the human endoglin-BMP9 interaction: insights into BMP signaling and HHT1. *Cell Rep.* 19, 1917–1928. doi: 10.1016/j.celrep.2017.05.011

Scalerandi, M. V., Peinetti, N., Leimgruber, C., Cuello Rubio, M. M., Nicola, J. P., Menezes, G. B., et al. (2018). Inefficient N2-like neutrophils are promoted by androgens during infection. *Front. Immunol.* 9:1980. doi: 10.3389/fimmu.2018.01980

Scherschinski, L., Rahmani, R., Srinivasan, V. M., Catapano, J. S., and Lawton, M. T. (2022). Genetics and emerging therapies for brain arteriovenous malformations. *World Neurosurg.* 159, 327–337. doi: 10.1016/j.wneu.2021.10.127

Sengillo, J. D., Winkler, E. A., Walker, C. T., Sullivan, J. S., Johnson, M., and Zlokovic, B. V. (2013). Deficiency in mural vascular cells coincides with blood-brain barrier disruption in Alzheimer's disease. *Brain Pathol.* 23, 303–310. doi: 10.1111/bpa.12004

Shaligram, S. S., Zhang, R., Zhu, W., Ma, L., Luo, M., Li, Q., et al. (2021). Bone marrow derived Alk1 mutant endothelial cells and clonally expanded somatic Alk1 mutant endothelial cells contribute to the development of brain arteriovenous malformations in mice. *Transl. Stroke Res.* 13, 494–504. doi: 10.1007/s12975-021-00955-9

Shen, F., Degos, V., Chu, P. L., Han, Z., Westbroek, E. M., Choi, E. J., et al. (2014). Endoglin deficiency impairs stroke recovery. *Stroke* 45, 2101–2106. doi: 10.1161/STROKEAHA.114.005115

Shimada, K., Yamaguchi, I., Ishihara, M., Miyamoto, T., Sogabe, S., Miyake, K., et al. (2021). Involvement of neutrophil extracellular traps in cerebral arteriovenous malformations. *World Neurosurg.* 155, e630–e636. doi: 10.1016/j.wneu.2021.08.118

Shoemaker, L. D., McCormick, A. K., Allen, B. M., and Chang, S. D. (2020). Evidence for endothelial-to-mesenchymal transition in human brain arteriovenous malformations. *Clin. Transl. Med.* 10:e99. doi: 10.1002/ctm2.99

Somekawa, S., Imagawa, K., Hayashi, H., Sakabe, M., Ioka, T., Sato, G. E., et al. (2012). Tmem100, an ALK1 receptor signaling-dependent gene essential for arterial endothelium differentiation and vascular morphogenesis. *Proc. Natl. Acad. Sci. U. S. A.* 109, 12064–12069. doi: 10.1073/pnas.1207210109

Speth, C., Dierich, M. P., and Sopper, S. (2005). HIV-infection of the central nervous system: the tightrope walk of innate immunity. *Mol. Immunol.* 42, 213–228. doi: 10.1016/j.molimm.2004.06.018

Spiller, K. L., Anfang, R. R., Spiller, K. J., Ng, J., Nakazawa, K. R., Daulton, J. W., et al. (2014). The role of macrophage phenotype in vascularization of tissue engineering scaffolds. *Biomaterials* 35, 4477–4488. doi: 10.1016/j.biomaterials.2014.02.012

Stapf, C., Mohr, J. P., Choi, J. H., Hartmann, A., and Mast, H. (2006). Invasive treatment of unruptured brain arteriovenous malformations is experimental therapy. *Curr. Opin. Neurol.* 19, 63–68. doi: 10.1097/01.wco.0000200546.14668.78

Stitt, A. W., Gardiner, T. A., and Archer, D. B. (1995). Histological and ultrastructural investigation of retinal microaneurysm development in diabetic patients. *Br. J. Ophthalmol.* 79, 362–367. doi: 10.1136/bjo.79.4.362

Storer, K. P., Tu, J., Karunanayaka, A., Morgan, M. K., and Stoodley, M. A. (2008). Inflammatory molecule expression in cerebral arteriovenous malformations. *J. Clin. Neurosci.* 15, 179–184. doi: 10.1016/j.jocn.2006.10.013

Su, H., Kim, H., Pawlikowska, L., Kitamura, H., Shen, F., Cambier, S., et al. (2010). Reduced expression of integrin alphavbeta8 is associated with brain arteriovenous malformation pathogenesis. *Am. J. Pathol.* 176, 1018–1027. doi: 10.2353/ajpath.2010.090453

Takahara, K., Iioka, T., Furukawa, K., Uchida, T., Nakashima, M., Tsukazaki, T., et al. (2004). Autocrine/paracrine role of the angiopoietin-1 and –2/Tie2 system in cell proliferation and chemotaxis of cultured fibroblastic synoviocytes in rheumatoid arthritis. *Hum. Pathol.* 35, 150–158. doi: 10.1016/j.humpath.2003.11.010

Tallquist, M. D., French, W. J., and Soriano, P. (2003). Additive effects of PDGF receptor beta signaling pathways in vascular smooth muscle cell development. *PLoS Biol.* 1:E52. doi: 10.1371/journal.pbio.0000052

Thanabalasundaram, G., El-Gindi, J., Lischper, M., and Galla, H.-J. (2011). Methods to assess pericyte-endothelial cell interactions in a coculture model. *Methods Mol. Biol.* 686, 379–399. doi: 10.1007/978-1-60761-938-3_19

Thomas, J. M., Sasankan, D., Surendran, S., Abraham, M., Rajavelu, A., and Kartha, C. C. (2021). Aberrant regulation of retinoic acid signaling genes in cerebral arterio venous malformation nidus and neighboring astrocytes. *J. Neuroinflammation* 18:61. doi: 10.1186/s12974-021-02094-2

Thomas, J. M., Surendran, S., Abraham, M., Sasankan, D., Bhaadri, S., Rajavelu, A., et al. (2018). Gene expression analysis of nidus of cerebral arteriovenous malformations reveals vascular structures with deficient differentiation and maturation. *PLoS One* 13:e0198617. doi: 10.1371/journal.pone.0198617

Tillet, E., and Bailly, S. (2015). Emerging roles of BMP9 and BMP10 in hereditary hemorrhagic telangiectasia. *Front. Genet* 5:456. doi: 10.3389/fgene.2014.00456

Townson, S. A., Martinez-Hackert, E., Greppi, C., Lowden, P., Sako, D., Liu, J., et al. (2012). Specificity and structure of a high affinity activin receptor-like kinase 1 (ALK1) signaling complex. *J. Biol. Chem.* 287, 27313–27325. doi: 10.1074/jbc.M112.377960

Uranishi, R., Baev, N. I., Kim, J. H., and Awad, I. A. (2001). Vascular smooth muscle cell differentiation in human cerebral vascular malformations. *Neurosurgery* 49, 671–679. doi: 10.1097/00006123-200109000-00027

Valenzuela, D. M., Griffiths, J. A., Rojas, J., Aldrich, T. H., Jones, P. F., Zhou, H., et al. (1999). Angiopoietins 3 and 4: diverging gene counterparts in mice and humans. *Proc. Natl. Acad. Sci. U. S. A.* 96, 1904–1909. doi: 10.1073/pnas.96.5.1904

van Beijnum, J., Lovelock, C. E., Cordonnier, C., Rothwell, P. M., Klijn, C. J., and Salman, R. A. (2009). Outcome after spontaneous and arteriovenous malformation-related intracerebral haemorrhage: population-based studies. *Brain* 132(Pt 2), 537–543. doi: 10.1093/brain/awn318

Vangilder, R. L., Rosen, C. L., Barr, T. L., and Huber, J. D. (2011). Targeting the neurovascular unit for treatment of neurological disorders. *Pharmacol. Ther.* 130, 239–247. doi: 10.1016/j.pharmthera.2010.12.004

Walker, E. J., Shen, F., Young, W. L., and Su, H. (2011a). Cerebrovascular casting of the adult mouse for 3D imaging and morphological analysis. *J. Vis. Exp.* 57:e2958. doi: 10.3791/2958

Walker, E. J., Su, H., Shen, F., Choi, E. J., Oh, S. P., Chen, G., et al. (2011b). Arteriovenous malformation in the adult mouse brain resembling the human disease. *Ann. Neurol.* 69, 954–962. doi: 10.1002/ana.22348

Wang, J., Hossain, M., Thanabalasuriar, A., Gunzer, M., Meininger, C., and Kubes, P. (2017). Visualizing the function and fate of neutrophils in sterile injury and repair. *Science* 358, 111–116. doi: 10.1126/science.aam9690

Wang, Y., Cao, Y., Yamada, S., Thirunavukkarasu, M., Nin, V., Joshi, M., et al. (2015). Cardiomyopathy and worsened ischemic heart failure in SM22-alpha Cre-mediated neuropilin-1 null mice: dysregulation of PGC1alpha and mitochondrial homeostasis. *Arterioscler Thromb. Vasc. Biol.* 35, 1401–1412. doi: 10.1161/ATVBAHA.115.305566

Watkins, S., Robel, S., Kimbrough, I. F., Robert, S. M., Ellis-Davies, G., and Sontheimer, H. (2014). Disruption of astrocyte-vascular coupling and the blood-brain barrier by invading glioma cells. *Nat. Commun.* 5:4196. doi: 10.1038/ncomms5196

Winkler, E. A., Birk, H., Burkhardt, J. K., Chen, X., Yue, J. K., Guo, D., et al. (2018). Reductions in brain pericytes are associated with arteriovenous malformation vascular instability. *J. Neurosurg.* 129, 1464–1474. doi: 10.3171/2017.6.JNS17860

Winkler, E. A., Lu, A. Y., Raygor, K. P., Linzey, J. R., Jonzzon, S., Lien, B. V., et al. (2019). Defective vascular signaling & prospective therapeutic targets in brain arteriovenous malformations. *Neurochem. Int.* 126, 126–138. doi: 10.1016/j.neuint.2019.03.002

Winkler, E. A., Sengillo, J. D., Sullivan, J. S., Henkel, J. S., Appel, S. H., and Zlokovic, B. V. (2013). Blood-spinal cord barrier breakdown and pericyte reductions in amyotrophic lateral sclerosis. *Acta Neuropathol.* 125, 111–120. doi: 10.1007/s00401-012-1039-8

Wong, J. H., Awad, I. A., and Kim, J. H. (2000). Ultrastructural pathological features of cerebrovascular malformations: a preliminary report. *Neurosurgery* 46, 1454–1459. doi: 10.1097/00006123-200006000-00027

Wright, R., Jarvelin, P., Pekonen, H., Keranen, S., Rauramaa, T., and Frosen, J. (2020). Histopathology of brain AVMs part II: inflammation in arteriovenous malformation of the brain. *Acta Neurochir.* 162, 1741–1747. doi: 10.1007/s00701-020-04328-3

Yao, C., Cao, Y., Wang, D., Lv, Y., Liu, Y., Gu, X., et al. (2022). Single-cell sequencing reveals microglia induced angiogenesis by specific subsets of endothelial cells following spinal cord injury. *FASEB J.* 36:e22393. doi: 10.1096/fj.202200337R

Yildirim, O., Bicer, A., Ozkan, A., Kurtkaya, O., Cirakoglu, B., and Kilic, T. (2010). Expression of platelet-derived growth factor ligand and rece ptor in cerebral arteriovenous and cavernous malformations. *J. Clin. Neurosci.* 17, 1557–1562. doi: 10.1016/j.jocn.2010.04.028

Young, W. L., Kader, A., Pile-Spellman, J., Ornstein, E., Stein, B. M., and Columbia University Avm Study Project. (1994). Arteriovenous malformation draining vein physiology and determinants of transnidal pressure gradients. *Neurosurgery* 35, 389–395. doi: 10.1227/00006123-199409000-00005

Zhang, R., Han, Z., Degos, V., Shen, F., Choi, E. J., Sun, Z., et al. (2016a). Persistent infiltration and pro-inflammatory differentiation of monocytes cause unresolved inflammation in brain arteriovenous malformation. *Angiogenesis* 19, 451–461. doi: 10.1007/s10456-016-9519-4

Zhang, R., Zhu, W., and Su, H. (2016b). Vascular integrity in the pathogenesis of brain arteriovenous malformation. *Acta Neurochir. Suppl.* 121, 29–35. doi: 10.1007/978-3-319-18497-5_6

Zhang, S., Zing, J., Ren, Q., He, M., Shan, B., Zeng, Y., et al. (2018). Prognostic role of neutrophil-to-lymphocyte ratio in patients with brain arteriovenous malformations. *Oncotarget* 8, 77752–77760.

Zhou, D., Huang, X., Xie, Y., Deng, Z., Guo, J., and Huang, H. (2019). Astrocytes-derived VEGF exacerbates the microvascular damage of late delayed RBI. *Neuroscience* 408, 14–21. doi: 10.1016/j.neuroscience.2019.03.039

Zhu, W., Chen, W., Zou, D., Wang, L., Bao, C., Zhan, L., et al. (2018). Thalidomide reduces hemorrhage of brain arteriovenous malformations in a mouse model. *Stroke* 49, 1232–1240. doi: 10.1161/STROKEAHA.117.020356

Zhu, W., Ma, L., Zhang, R., and Su, H. (2017). The roles of endoglin gene in cerebrovascular diseases. *Neuroimmunol. Neuroinflamm.* 4, 199–210. doi: 10.20517/2347-8659.2017.18

Zhu, Y., Lawton, M. T., Du, R., Shwe, Y., Chen, Y., Shen, F., et al. (2006). Expression of hypoxia-inducible factor-1 and vascular endothelial growth factor in response to venous hypertension. *Neurosurgery* 59, 687–696. doi: 10.1227/01.NEU.0000228962.68204.CF

ZhuGe, Q., Zhong, M., Zheng, W., Yang, G. Y., Mao, X., Xie, L., et al. (2009). Notch-1 signalling is activated in brain arteriovenous malformations in humans. *Brain* 132(Pt 12), 3231–3241. doi: 10.1093/brain/awp246

Zlokovic, B. V. (2008). The blood-brain barrier in health and chronic neurodegenerative disorders. *Neuron* 57, 178–201. doi: 10.1016/j.neuron.2008.01.003

frontiers | Frontiers in Human Neuroscience

TYPE Review
PUBLISHED 03 November 2022
DOI 10.3389/fnhum.2022.1006027

OPEN ACCESS

EDITED BY
Lorelei Shoemaker,
Stanford University, United States

REVIEWED BY
Eulalia Baselga,
Sant Joan de Déu Barcelona Hospital, Spain
Mitsuhiro Kato,
Showa University, Japan

*CORRESPONDENCE
William K. Van Trigt
william.vantrigt@uci.edu
Christopher C. W. Hughes
cchughes@uci.edu

SPECIALTY SECTION
This article was submitted to Brain Health and Clinical Neuroscience, a section of the journal Frontiers in Human Neuroscience

RECEIVED 28 July 2022
ACCEPTED 12 October 2022
PUBLISHED 03 November 2022

CITATION
Van Trigt WK, Kelly KM and Hughes CCW (2022) GNAQ mutations drive port wine birthmark-associated Sturge-Weber syndrome: A review of pathobiology, therapies, and current models.
Front. Hum. Neurosci. 16:1006027.
doi: 10.3389/fnhum.2022.1006027

GNAQ mutations drive port wine birthmark-associated Sturge-Weber syndrome: A review of pathobiology, therapies, and current models

William K. Van Trigt[1]*, Kristen M. Kelly[2] and Christopher C. W. Hughes[1]*

[1]Department of Molecular Biology and Biochemistry, School of Biological Sciences, University of California, Irvine, Irvine, CA, United States, [2]Department of Dermatology, School of Medicine, University of California, Irvine, Irvine, CA, United States

Port-wine birthmarks (PWBs) are caused by somatic, mosaic mutations in the G protein guanine nucleotide binding protein alpha subunit q (GNAQ) and are characterized by the formation of dilated, dysfunctional blood vessels in the dermis, eyes, and/or brain. Cutaneous PWBs can be treated by current dermatologic therapy, like laser intervention, to lighten the lesions and diminish nodules that occur in the lesion. Involvement of the eyes and/or brain can result in serious complications and this variation is termed Sturge-Weber syndrome (SWS). Some of the biggest hurdles preventing development of new therapeutics are unanswered questions regarding disease biology and lack of models for drug screening. In this review, we discuss the current understanding of GNAQ signaling, the standard of care for patients, overlap with other GNAQ-associated or phenotypically similar diseases, as well as deficiencies in current *in vivo* and *in vitro* vascular malformation models.

KEYWORDS

GNAQ, guanine nucleotide binding protein alpha subunit q, $G\alpha_q$, port wine birthmark, Sturge-Weber syndrome, brain vascular malformation, capillary malformation

Introduction

Port-wine birthmark (PWB; also known as nevus flammeus and Port Wine Stain) is a congenital, progressive blood vessel disease that manifests as regions of skin that darken and thicken with age (**Figure 1**; Yin et al., 2017). Approximately one in 350 newborns is born with capillary malformations (CMs) like PWB (Kanada et al., 2012;

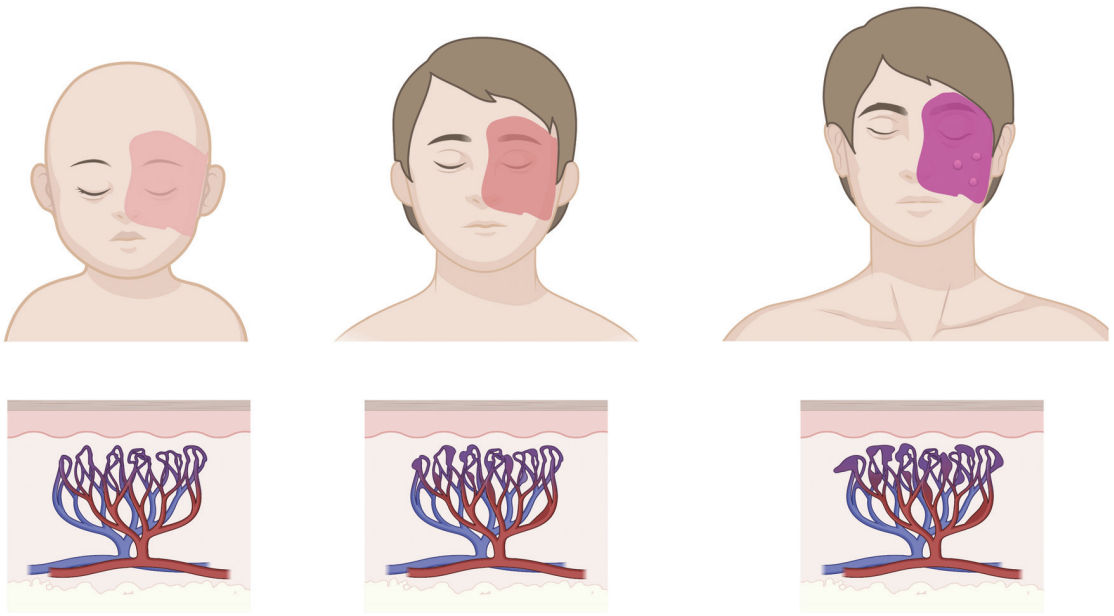

FIGURE 1
Age progression of cutaneous PWB. Birthmark is usually apparent from birth as a light pink patch that can get darker with age, corresponding to progressive dilation of affected capillaries in the dermis. Patients in adulthood may develop soft tissue hypertrophy or nodularity in the absence of clinical intervention. Images created using BioRender.

Higueros et al., 2017). PWB lesions are usually apparent from birth as a unilateral light pink to red patch typically on the face or neck, although PWB can occur on any area of the body (Martins et al., 2017). CMs that are also found in the eyes and/or the brain are commonly referred to as Sturge-Weber syndrome (SWS). SWS has also been described as an over-arching syndrome with three types – Type I with neurological and skin involvement, with or without glaucoma; Type II with skin, but no neurological involvement, with or without glaucoma; and, Type III neurological only (Sturge Weber Foundation). In this review we will discuss cutaneous CMs as PWB and CMs with neurological involvement as SWS.

The CMs associated with PWB/SWS are caused by a somatic activating mutation in guanine nucleotide binding protein alpha subunit q (GNAQ) (although sometimes found in the paralog GNA11) that results in an arginine to glutamine substitution at the 183 amino acid residue (p.R183Q) (Couto et al., 2016). Disease appears to be manifested by expression of this mutant protein primarily, perhaps exclusively, in endothelial cells (ECs) leading to an increase in proliferation and capillary overgrowth, as summarized in **Figure 2**. A glutamine to leucine (p.Q209L) GNAQ mutation can also cause CMs and cancer, although this mutation has not yet been reported in PWB patients (Bichsel and Bischoff, 2019; Schneider et al., 2019; Jain et al., 2020). It has been included in this review in discussions of possible overlap with p.R183Q GNAQ constitutive activity. PWB and SWS are typically differentiated from other types of capillary vascular lesions through genetic tests that confirm the presence of mutant GNAQ in these lesions.

Since the mutations are somatically acquired, no difference in disease prevalence is expected or known to occur between sexes or races, although there are discrepancies in diagnosis and treatment.

Port-wine birthmark

As noted above, PWB lesions can occur anywhere on the body but are particularly prevalent around the head and neck. Without treatment (or with treatment-resistant PWB), cutaneous lesions have the potential to progress with vascular hyperplasia, increasing prevalence of ectatic (dilated) vessels that cause the skin to darken in color (from pink or red to purple), and in some cases nodularity can develop (Yin et al., 2017; Lee et al., 2019). Perivascular cell disorganization is also observed (Couto et al., 2016). Disease progression is slow, however, so patients may not experience serious pathologies until late teens or adulthood.

Nodules are predicted to occur in about 40 percent of untreated PWB, with a mean onset of 22 years, and soft-tissue hypertrophy is seen in about 60% of cutaneous PWB patients (Lee et al., 2015; Higueros et al., 2017). Early laser intervention is thought to significantly delay onset of nodularity, however nodularity and hypertrophy can be difficult to treat with lasers and may require excisional surgical intervention

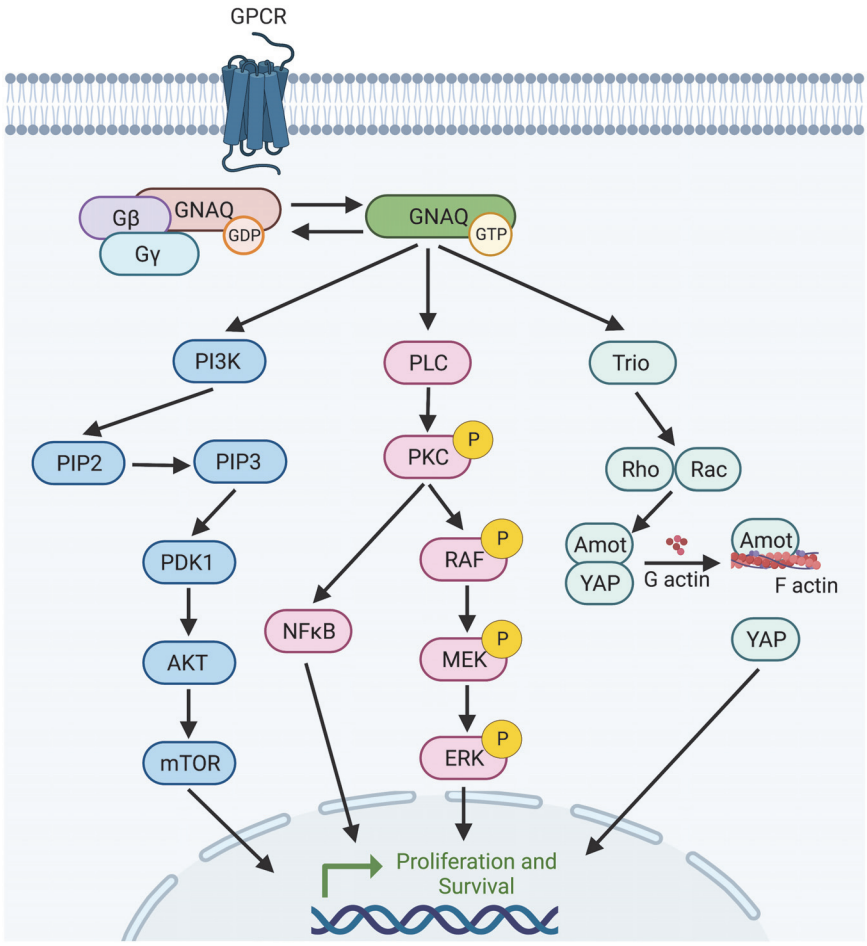

FIGURE 2
Selection of predicted downstream targets of GNAQ. GNAQ can activate PI3K leading to mTOR activation; stimulate the MAPK pathway, or activate non-canonical Hippo signaling through Rho/Rac. How GNAQ* leads to vessel instability and PWB/SWS disease progression is poorly understood. Image created using BioRender.

(Tierney and Hanke, 2009). The exact mechanisms leading to hypertrophy and nodularity are not characterized, but Yin et al. (2017) identify upregulation of PP2A, DAG, and activation of PI3K, PKCα, PDPK1, and PLCγ in the patient tissue. This aberrant signaling was mostly detected in the ECs but also had some spillover into surrounding fibroblasts and pericytes proliferating in the stromal tissue, although whether these effects are cell autonomous or due to endothelial-released factors is not known (Yin et al., 2017). However, multilineage detection of mutant GNAQ and aberrant downstream targets in PWB tissue suggest that the somatic mutation may be propagated from a progenitor cell population into several adult cell types, in addition to EC (Couto et al., 2016; Yin et al., 2017). Other researchers have predicted or detected the driving of lesion formation by mutant GNAQ (GNAQ*) through Angiopoietin 2 (ANGPT2), PI3K, and MAPK activation (Shirley et al., 2013; Nakashima et al., 2014; Huang et al., 2017; Cong et al., 2020).

Both the p.R183Q and p.Q209L GNAQ mutations are located within the predicted guanine triphosphate (GTP) binding cleft and help stabilize GNAQ affinity for the GTP-bound "on" state (**Figure 3**). Recent data suggests the p.209 position also plays a role in the switch II domain (discussed later) that helps shield the binding cleft from regulatory proteins (Higueros et al., 2017; Bichsel and Bischoff, 2019). Simultaneous GNAQ and GNA11 mutations are uncommon in patients (Daniels et al., 2012; Schneider et al., 2019). Downstream RAS pathway activation was proposed early on as the causative driver of pathogenesis because it explains how affected cells increase proliferation and inhibit apoptosis (Higueros et al., 2017). GNAQ* cells typically comprise 6–85% of the total ECs in the PWB lesion; the range in heterogeneity correlates with disease severity, with higher ratios of mutant GNAQ cells contributing to increased pathology (Couto et al., 2016; Huang et al., 2017; Martins et al., 2017; Yin et al., 2017; Jordan et al., 2020). Testing for genetic panels usually costs about US $3,000 and are often

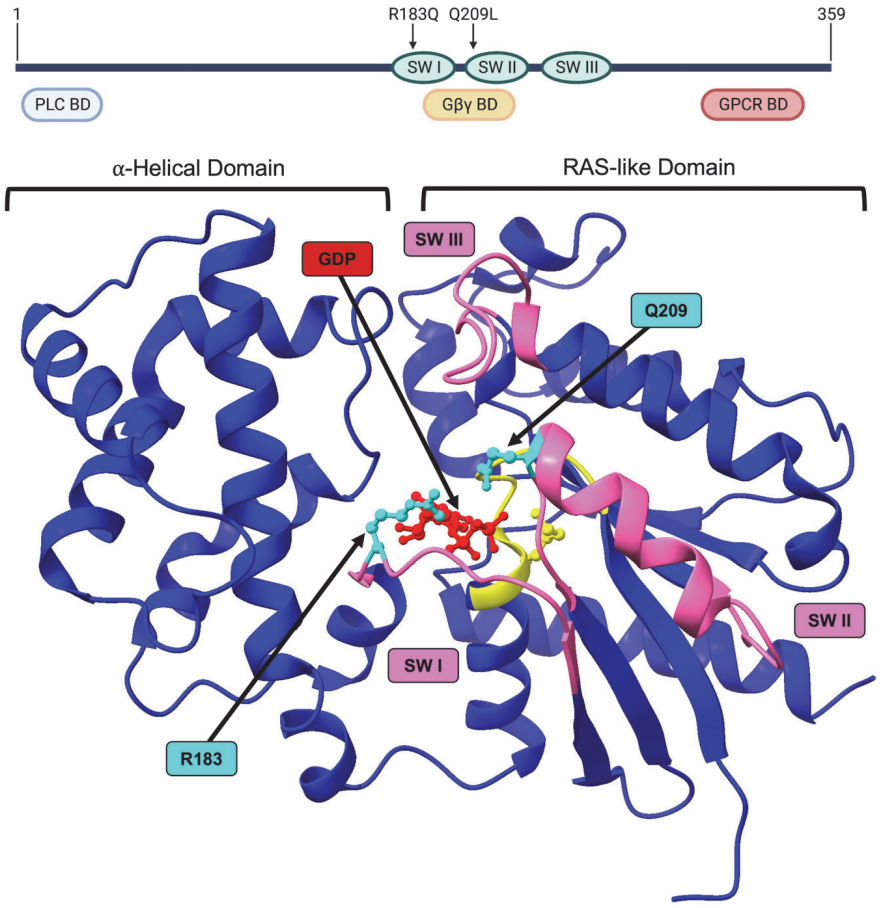

FIGURE 3
Structure of GNAQ. Protein map of GNAQ. GNAQ has 3 switch regions (SW): switch regions I and II are part of the GTP binding cleft and have a RAS-like domain for GTP hydrolysis; all three switch regions have key sites for extrinsic regulation by G protein signaling modulators. The p.R183Q and p.Q209L activating mutations are present in switch regions I and II, respectively. GNAQ has a binding domain (BD) for PLC effector function, a binding domain that interacts with the Gβγ subunit during the "off" state, and a GPCR binding domain. Image created using BioRender. Crystal structure (PDB ID: 4GNK) with GDP (red) docked in binding cleft and p.R183Q and p.Q209L mutations (cyan). P loop region with Walker A motif shown in yellow. Switch (SW) I, II, and III shown in pink. **Supplementary Video** available online. Molecular graphics performed with UCSF ChimeraX, developed by the Resource for Biocomputing, Visualization, and Informatics at the University of California, San Francisco, with support from National Institutes of Health R01-GM129325 and the Office of Cyber Infrastructure and Computational Biology, National Institute of Allergy and Infectious Diseases.

not covered by insurance (Perelman School of Medicine at the University of Pennsylvania).

Sturge-Weber syndrome

Sturge-Weber syndrome was named after William Allen Sturge and Frederick Parkes Weber (Higueros et al., 2017; Martins et al., 2017; Yin et al., 2017). PWB endothelium in what has traditionally been called the ophthalmic V1 trigeminal nerve distribution is associated with SWS, perhaps reflecting the lineage that underwent the somatic mutation in GNAQ during development (Kanada et al., 2012; Higueros et al., 2017). More recent studies have identified PWB cutaneous lesions in the triangular area from the forehead midline, outer edge of the eye, and top of the ear as the best prediction of SWS involvement (**Figure 4**; Waelchli et al., 2014; Sabeti et al., 2021). This area is called the frontal placode and typically develops its own vasculature derived from the prosencephalon and anterior mesencephalon. SWS affects approximately one in 50,000 individuals (Kanada et al., 2012; Higueros et al., 2017). About 80% of SWS patients have the p.R183Q GNAQ mutation (Shirley et al., 2013; Nakashima et al., 2014; Huang et al., 2017). SWS is characterized by cutaneous PWBs which are usually more extensive than non-syndromic PWB, ophthalmologic impairment, especially glaucoma, and malformed vessels in the thickened leptomeninges (Shirley et al., 2013). These torturous leptomeningeal vessels cause neurological deficits, macrocephaly, seizures, astrocytosis, and cortical atrophy with calcification (Shirley et al., 2013; Huang et al., 2017;

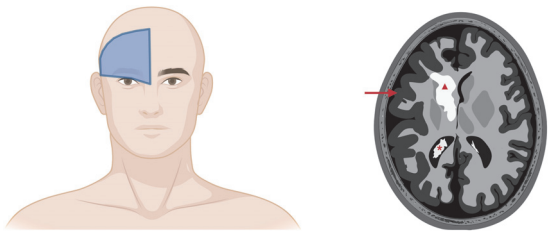

FIGURE 4
Sturge-Weber syndrome involvement of brain. **Left panel:** Cutaneous PWB in the frontal placode is the best predictor of SWS involvement of eyes and/or brain. **Right panel:** Artistic rendering of SWS complications in brain. Red triangle, cerebral calcification; red arrow, leptomeningeal thickening and cerebral atrophy; red asterisk, enlarged choroid plexus. Images created using BioRender.

Jordan et al., 2020). Dilated deep draining veins can exacerbate SWS pathology. SWS leptomeningeal vessels also have increased fibronectin and VEGF expression and EC proliferation and apoptosis (Higueros et al., 2017). Seizures occur in 75% of patients within the first year of life and 90% of SWS patients will experience seizures before 2 years of age (Higueros et al., 2017). Since the GNAQ mutations in SWS are widely prevalent in the EC compartment, many researchers speculate that the GNAQ*-EC have impaired blood–brain barrier capability and possibly aberrant interactions with surrounding tissue in the leptomeninges and cortex that cause these neurovascular dysfunctions and seizures, possibly due do hypoxia, ischemia, and gliosis (Higueros et al., 2017; Huang et al., 2017).

As noted, there are three different subclasses of SWS that are sometimes referenced in the literature and that vary from each other by the combination of tissues involved. Type I SWS involves cutaneous PWB and brain vascular malformations with or without eye involvement (usually glaucoma). Type I SWS is the most common and usually only affects one side of the brain (Sturge Weber Foundation). Type II involves facial cutaneous PWB and eye involvement but not brain. Type III characterizes SWS with brain vascular malformations without skin PWB or (rarely) eye. Type III can only be diagnosed *via* brain scanning (Sturge Weber Foundation). These categories have not been universally adopted; we and others hypothesize that the type of classification is not useful because treatment decisions are made on an individual level depending on symptoms, patient age, and disease severity (Sabeti et al., 2021).

About half of SWS patients have pathogenesis that affects the eyes (Type I and II) (Bichsel and Bischoff, 2019; Jordan et al., 2020). In this case, a patient may develop choroidal hemangioma, seen as PWB vessel overgrowth in the choroid that leads to thickening of the choroid and increased intraocular and intravenous pressures, eventually causing glaucoma (Bichsel et al., 2019; Jordan et al., 2020). Choroidal hemangioma, unlike infantile hemangioma is not responsive to propranolol treatment. Common treatment includes therapeutics to lower intraocular pressure or enucleation surgery. Only the p.R183Q GNAQ mutation has been detected in choroidal hemangioma patients, although this is probably sampling error from small datasets.

The remainder of this review will focus on GNAQ and its role in driving PWB-associated SWS. We do not intend to be exhaustive but will concentrate on the current literature regarding GNAQ signaling, the role of GNAQ in driving brain CMs, and on illuminating current exciting research on molecular mechanisms and models of disease pathology.

Diagnosis of Sturge-Weber syndrome

Extracutaneous involvement is suspected with SWS whenever patients have PWB on their forehead, even without the presentation of neurological symptoms. SWS involvement can be evaluated through a variety of imaging techniques that play a crucial role in detection, diagnosis, and follow-up of this disease.

Computed tomography

Computed tomography (CT) with or without contrast enhancement is frequently used due to its ability to detect reduced parenchymal brain volume, enlarged ventricles, or enlarged choroid plexus. CT scans can also detect calcification better than X-ray or magnetic resonance imaging (MRI) (Higueros et al., 2017).

Magnetic resonance imaging

Gadolinium enhanced MRI is the principle imaging technique used for SWS diagnosis (Higueros et al., 2017). It can effectively identify calcified areas as well as structural and functional anomalies in the leptomeninges, abnormal venous drainage, reduced and/or enlarged brain structures, and hypermyelination underneath the leptomeningeal lesion(s) (Higueros et al., 2017).

Perfusion imaging

Perfusion imaging can play a crucial role in identifying stage of disease. Perfusion imaging may be performed in several ways: in conjunction with CT or MRI; or, by using radiotracers and either single photon emission computed tomography (SPECT) or positron emission (PET) techniques. Most SWS lesions tend to be hyperperfused with blood early in childhood, but this tends to change to hypoperfusion later—leading to progressive ischemia, hypoxia, and nutrient starvation of the brain around the vascular malformation (Higueros et al., 2017). It is predicted that this switch to progressive hypoperfusion in SWS is responsible for the neurological degradation characteristic of this disease.

Electroencephalogram

Like perfusion imaging, electroencephalogram (EEG) frequently can identify progression to an increasingly abnormal SWS signature correlated with patient age. EEG readings of advanced SWS brain tissue detect epileptiform characteristics with decreased brain voltage and focal discharge in the hemisphere affected by SWS (Higueros et al., 2017).

Angiography

Angiographical imaging is not usually performed for patients with SWS unless clinically indicated. Unlike other vascular malformation diseases, SWS lesions are low-flow malformations that are unlikely to undergo thrombotic events. Angiography may be used prior to craniotomy procedures to detect bleeding risk (Higueros et al., 2017).

Sturge-Weber syndrome treatment

A recent consensus statement prepared by 12 top US expert clinicians in dermatology and SWS identified several key guidelines for the management of PWB associated with SWS (Sabeti et al., 2021).

Early diagnosis of PWB/SWS (as close to birth as possible) and intervention maximizes the success of treatment(s) (Waelchli et al., 2014; Sabeti et al., 2021). Several factors must be weighed when designing a treatment plan, including but not limited to reducing birthmark appearance, diminishing or preventing nodularity and/or soft tissue hypertrophy, minimizing the impact to patient quality of life and self-esteem, and lastly, financial considerations.

Cutaneous port-wine birthmarks treatments

Light-based therapy, especially with pulsed-dye laser (PDL), is the standard of care for PWB in the United States (Higueros et al., 2017; Sabeti et al., 2021). Experienced clinicians can safely and effectively use PDL on patients of all ages, including infants. Other wavelengths (532, 755, and 1,064 nm) have been used and are especially useful for treating PDL-resistant PWB lesions. The longer wavelengths are also better for penetrating larger or deeper vessels like those that occur in nodular or hypertrophic lesions, but these laser devices also pose an increased risk of damage to non-target adjacent tissue (Izikson et al., 2009; Sabeti et al., 2021). Laser therapies target heat absorption of hemoglobin and cause photocoagulation, with the goal to remove aberrant vasculature by selective damage and photothermolysis (Bernstein, 2009; Sabeti et al., 2021). PDL therapy has also been combined with other techniques like infrared laser pulses or bipolar radiofrequency to improve efficacy in treatment-resistant PWB (Bae et al., 2017; Sabeti et al., 2021). Pain management is an important concern with laser therapy. Topical or injected local anesthetics, skin cooling, nerve blocks, and/or general anesthesia can be used during treatment (Sabeti et al., 2021).

Pulsed-dye laser treatment response is difficult to predict, but can lighten PWB skin color by 50–70% through at least eight to ten PDL sessions, although complete clearance is rarely achieved and touch-up follow-up treatment is frequently used to maintain level of clearance (Sabeti et al., 2021). There are no consistent guidelines for intervals between treatment sessions. Patients with lighter skin tones tend to have a better PDL treatment response than those with darker skin (Higueros et al., 2017; Sabeti et al., 2021). Patients with darker skin require more skin cooling or adjustment of laser parameters to prevent scarring or blistering. PWB on the face and neck, especially the lateral sides of the face, are easier to treat than PWB on the lower body extremities (Yu et al., 2016; Sabeti et al., 2021). It is possible that patients with SWS have PWB lesions that are more likely to be treatment-resistant, although this has not been clearly established and the mechanism is unknown (Sabeti et al., 2021). As mentioned earlier, PWBs are more effectively treated in younger than older patients, especially if the affected area is still flat without signs of nodularity or hypertrophy.

There are some adjuvant treatments which have been tried with PDL, although none have achieved marked improvement over laser therapy alone and are no longer used frequently in clinical treatments (Wang et al., 2022). Combination of PDL with topical imiquimod demonstrated slightly improved effect in treating PWB over PDL alone in small scale studies through immunomodulation activity that reduces tumor necrosis factor (TNF), interferon-γ (IFN-γ), as well as decreasing pro-angiogenic production of matrix metalloproteinase 9 (MMP9) and increasing apoptosis (Sidbury et al., 2003; Lipner, 2018; Wang et al., 2022).

Rapamycin, an mTOR inhibitor, has been studied in a variety of diseases for its immunosuppressant and antiproliferative activities. Human clinical studies of topical rapamycin combined with PDL on affected areas of the face and neck showed some efficacy in limiting cutaneous vessel regrowth *via* HIF-1α and VEGF inhibition, but results were disappointing with wider clinical use (Lipner, 2018; Wang et al., 2022). Using animal models, PDL and axitinib, an inhibitor of MEK/ERK, have been shown to prevent vessel regrowth (Gao et al., 2015). Efficacy in patients has not yet been demonstrated. A small scale trial with PDL and bosentan (an endothelin receptor antagonist) showed efficacy in one of four PWB patients treated (Taquin et al., 2016).

As laser therapy works through light absorption of hemoglobin, the perfusion of hemoglobin-laden vesicles during PDL treatment has been tried and was shown to increase efficacy of PDL for dilated and deeper vessels in animal models, improving the safety of PDL by reducing the laser intensity required and thereby reducing off-target tissue effects (Rikihisa et al., 2017, 2018). In another preclinical study, PDL therapy with the α1A- and partial

α2A-adrenoreceptor agonist oxymetazoline was used for the treatment of erythematotelangiectatic rosacea and showed some efficacy for PDL combination treatment of PWB in mouse models (Kelly et al., 2020). Both of these strategies warrant further investigation.

Photodynamic therapy, unlike PDL, uses perfusion of a photosensitive dye and an excitatory source to produce reactive oxygen species (ROS) that destroy local tissue. This technique is not widely used in the US, but may be beneficial for resistant PWB, and when treating darker skin types as the melanin content of skin does not reduce photodynamic therapy efficacy (Sabeti et al., 2021).

Lastly, surgical intervention may be employed to selectively remove hypertrophic or nodular tissue.

Treatments targeted specifically for Sturge-Weber syndrome

Unfortunately, SWS-specific treatments that target neurodegeneration are not currently available. The cornerstone for treatment is anticonvulsant therapy to limit damage due to seizures. Carbamazepine and oxcarbazepine are frequently prescribed to SWS patients, sometimes even prophylactically before the first incident, to prevent epileptic events (Higueros et al., 2017). Low-dose aspirin may additionally help prevent seizures and ischemia in SWS tissue. Seizures are untreatable in about half of SWS patients; in these cases, early surgical intervention with lesionectomy, corpus callosotomy, and/or hemispherectomy may be considered (Higueros et al., 2017). Patients with these invasive brain interventions as well as patients with cognitive deficits or hyperactivity may need physiotherapy, educational therapy, and behavioral therapy. Some studies have shown oral treatment with rapamycin improves cognitive function and recovery time from stroke-like episodes (Sebold et al., 2021). Larger clinical studies are required.

Treatment for glaucoma aims to prevent degeneration of the optic nerve by decreasing intraocular pressure. Placement of a drainage device is often required and aqueous suppressants or medications to increase outflow are usually effective (Higueros et al., 2017).

Sturge-Weber syndrome patients are prone to thyroid diseases and should be routinely examined for growth hormone deficiencies and hypothyroidism (Miller et al., 2006; Bachur et al., 2015).

GNAQ and the G protein landscape

Heterotrimeric guanine nucleotide-binding proteins (G proteins) transduce a variety of important autocrine and paracrine signals from numerous receptors, such as those for hormones, neurotransmitters, and chemokines. These effect changes in such diverse cell functions as gene transcription, metabolism, cell motility, embryonic and gonadal development, and learning and memory (Neves et al., 2002). Reflecting this diversity of function, the G protein coupled receptor (GPCR) family has over 800 family members, and almost 30% of drug discovery targets influence GPCR signaling (Urtatiz and Van Raamsdonk, 2016).

The G protein complex is made up of three subunits: α, β, and γ. Upon activation of a GPCR, the Gα subunit exchanges guanine diphosphate (GDP) for GTP, dissociating Gα from the Gβγ heterodimer and allowing Gα and Gβγ to transduce downstream signals. There are currently 18 identified Gα, 5 Gβ, and 12 Gγ subunits (Syrovatkina et al., 2016). With respect to receptor and effector specificity, and sequence and functional similarities, the Gα subunit can be further divided into four families: $G\alpha_i$, $G\alpha_s$, $G\alpha_{12}$, and $G\alpha_q$ (Simon et al., 1991; Neves et al., 2002). The $G\alpha_i$ family is the biggest and most diverse group of G proteins and these are expressed in most cells, although there are a few that are specific to neurons, platelets, and rod and cone cells. The i stands for "inhibition," as a majority of these downstream responses limit activity of cAMP-dependent protein kinases (Syrovatkina et al., 2016). The $G\alpha_s$ family (s for "stimulation") only has two members; $G\alpha_s$ is expressed in most cell types while $G\alpha_{olf}$ is only expressed in olfactory sensory neurons. The $G\alpha_{12}$ family also has two members that are widely expressed. Lastly, the $G\alpha_q$ family has four members: GNAQ and its paralog $G\alpha_{11}$ are ubiquitously expressed, while $G\alpha_{14}$ and $G\alpha_{15/16}$ are expressed in soft organs (kidney, lung, and liver) and hematopoietic cells, respectively.

Gene

In humans, GNAQ is encoded by the GNAQ gene on chromosome 9 at 9q21.2 (Dong et al., 1995). There is also a pseudogene at location 2q21 as well as the paralog $G\alpha_{11}$ (GNA11) at location 19p13.31 (Dong et al., 1995). The eight-exon GNAQ mRNA transcript is 6,882 nucleotides long, coding for a 359 amino acid protein (**Figure 3**; NM_002072.5, P50148.4, CCDS6658.1). Although the GNA11 paralog is also 359 amino acids long, there are areas of dissimilarities in protein sequence. These disparities do not occur in the conserved active site amino acids, however, and the GNAQ p.R183Q or p.Q209L amino acid substitutions (c.548G > A and c.626A > T nucleotide substitutions, respectively) in SWS patients can also occur in GNA11 at the same corresponding amino acid positions in GNA11-driven SWS (Dong et al., 1995; Couto et al., 2016; Higueros et al., 2017). GNA11 mutations will not be covered in this review as they cause the same constitutive Gα constitutive activity and SWS disease pathogenesis, albeit GNA11 mutations are detected at lower patient frequency than GNAQ (Jordan et al., 2020).

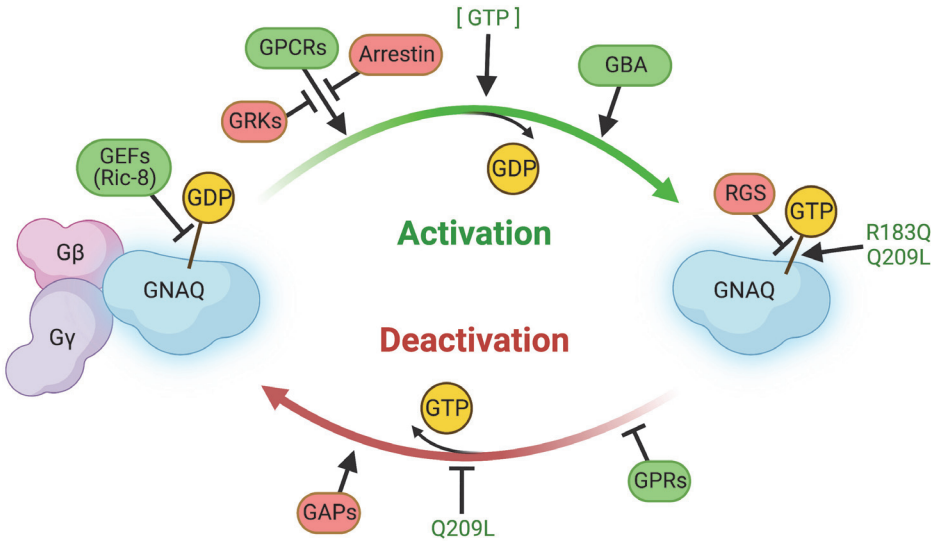

FIGURE 5
Summary of regulators of GNAQ signaling. GEFs, GPCRs, GBA proteins, and GPRs promote GNAQ-GTP "on" signaling and/or delay GTP hydrolysis. Arrestin, GRKs, RGS, and GAPS slow activation of GNAQ, stimulate GTP hydrolysis, and/or stabilize the GNAQ-Gβγ complex. The p.R183Q and p.Q209L strongly stabilize GNAQ-GTP binding and the p.Q209L mutation impairs intrinsic GNAQ GTPase activity. Image created using BioRender.

Protein

G proteins, including GNAQ, function in a GTPase cycle. GPCRs act as a kind of guanine nucleotide exchange factor (GEF) to initiate release of GDP and binding of GTP to GNAQ, causing dissociation of GNAQ from the Gβγ complex (**Figure 5**; Syrovatkina et al., 2016). GNAQ-GTP is eventually hydrolyzed back to GNAQ-GDP by its intrinsically weak GTPase activity to terminate GNAQ effector function. This process of GTP hydrolysis can be expedited by GTPase activating proteins (GAPs). Re-association of GNAQ with Gβγ terminates the signaling cascade and completes the GTPase cycle.

The amino acid sequence of the GDT/GTP binding cleft is highly conserved (Dong et al., 1995; Syrovatkina et al., 2016). The GNAQ protein has a RAS-like GTPase domain and an α-helical domain, connected by the Linker 1 and Linker 2 domains. The RAS-like GTPase and α-helical domains surround the GTP hydrolysis cleft, thereby protecting the GDP or GTP nucleotide from the surrounding solvent and serving as an inhibitory barrier for regulation by GEFs, GAPs, and the Gβγ complex (Syrovatkina et al., 2016). GDP/GTP binding and hydrolysis take place in the RAS-like domain of GNAQ through a "switch" mechanism. The domain comprises six β-sheets and five α-helices on each side, defining a nucleotide-binding fold, with several key amino acids lining the fold to specify guanine binding (Sprang, 1997; Wolf et al., 1999; Oldham and Hamm, 2006; Syrovatkina et al., 2016). The side loops around the cleft are the switch regions – Switch I and Switch II. The N-terminus of the Gα α-helix and the Switch II region associate with a propellor structure of Gβ in the Gβγ complex (Syrovatkina et al., 2016). Switch I and II together with the P loop region interact with GDP/GTP and the Mg^{2+} coordinating ion. Two of the key sequences in the cleft are the NKKD sequence in Switch II, predicted to form a bifurcated hydrogen bond between aspartate and the guanine base, while the second sequence is a Walker A motif in the P-loop region where the GTGESGKS sequence is associated with binding of the β-phosphate of GDP/GTP (Wolf et al., 1999; Bosch et al., 2012; Syrovatkina et al., 2016). The α-helical domain and switch III regions play a role in G protein regulation (discussed later).

GNAQ has a high affinity for GDP. GEFs (including GPCRs) work to weaken this affinity by causing instability in the protein switch regions. GEFs on their own have a relatively low affinity for GNAQ in either the GDP or GTP bound state. Instead, for the exchange reaction to occur, the GEF must interact with the switch regions in a way that partially displaces the Mg^{2+} ion, which destabilizes bound GDP and causes a push/pull interaction between the switch regions and GDP. The destabilized GDP is released as a stable GEF-GNAQ complex forms, leaving GNAQ available to bind GTP (GTP is usually at higher intracellular concentrations than GDP) (Syrovatkina et al., 2016). More detailed structural and mechanistic information regarding conformational state, the ways in which GEFs initiate interaction with GNAQ, as well as the way GDP is released, still need to be elucidated.

Originally, it was thought that GPCRs diffuse freely within the cell membrane and interact with G proteins though collision,

but there are data suggesting un-activated GPCRs in a pre-assembled complex with G proteins: agonist activation of the GPCR then causes a conformational change in the pre-organized complex that facilitates G protein signal transduction (Strange, 2008; Syrovatkina et al., 2016). The different kinds of GPCR and G protein interaction depend on the pair, which may explain the range of GPCR activity in different cell types and tissues. Additionally, GPCR-agonist binding alone is sometimes insufficient to cause G protein activation and may require additional interactions with other proteins. On the other hand, GPCRs may require desensitization through phosphorylation of G protein receptor kinases (GRKs) or binding of GPCR inhibitory proteins like arrestin (Venkatakrishnan et al., 2013; Syrovatkina et al., 2016). GNAQ's specific GPCR interaction type is unknown at this time, and additionally, it is possible the GPCR-ligand state is less relevant under GNAQ* constitutive activity.

G protein coupled receptor extracellular ligands are divided into three categories: agonist, inverse agonists, and antagonists. Agonists bind to GPCRs and promote G protein signal transduction while inverse agonists stabilize the inactive "off" state. Antagonists do not change the equilibrium dynamics of the GPCR's active and inactive conformations but do block binding of agonist and inverse agonist ligands.

All four $G\alpha_q$ family members are palmitoylated at the Cys^9 and Cys^{10} amino acid residues, but this post-translational modification is not well understood because it does not seem to affect association of GNAQ with Gβγ at the GPCR interface, nor downstream effector functions of GNAQ, such as activation of the phospholipase C pathway (Hepler et al., 1996).

GNAQ regulation

G proteins like GNAQ can be regulated by a variety of intracellular proteins (besides GPCRs), including Ric-8 (synembryn), G-protein regulatory (GPR)-domain containing proteins (GRPs), Gα-binding and activating (GBA) motif-containing proteins, and regulators of G-protein signaling (RGS) proteins.

Mammals have both Ric-8A and Ric-8B and both have been demonstrated to interact with GNAQ. Ric-8A is widely expressed while Ric-8B is restricted mostly to olfactory tissue. Ric-8A is a GEF that promotes GDP release and stabilizes the nucleotide-free GNAQ transition state by initiating conformational changes to Switch I and II regions, thereby exposing the GTP binding site to the solvent, leading to formation of the GNAQ-GTP complex (Tall et al., 2003; Tall and Gilman, 2004). The lack of crystal structures prevents resolution of this exact mechanism, but it is interesting that Ric-8 acts on the GNAQ-GDP monomer itself, rather than the whole GNAQ-GDP/Gβγ complex (like GPCRs), as well as in concert with other regulatory proteins like GRPs. Additionally, Ric-8 plays other roles as a chaperone during Gα folding and processing in addition to membrane translocation (Gabay et al., 2011).

G-protein regulatory-domain containing proteins contain an ∼25 amino acid long G protein regulator domain, also called a GoLoco domain, that prolongs signal transduction by sequestering Gα from the Gβγ complex and possibly assisting Ric-8A activation of the GNAQ subunit (Kimple et al., 2002).

Gα-binding and activating domain-containing proteins, like Girdin, Dapple, NUCB1/2, and GBAS-1 interact with Gα proteins to initiate Akt signaling by accelerating the exchange rate of GDP (Garcia-Marcos et al., 2009; Ghosh et al., 2011). As rheostats, these GBA proteins have a powerful ability to fine-tune the duration of signaling and have been implicated in cancer progression and metastasis (Ghosh et al., 2011). GBA-domian proteins bind to $G\alpha_i$ and $G\alpha_s$ family members, but their direct interactions with GNAQ have yet to be confirmed.

Lastly, RGS modulate the intrinsic GTPase activity of the Gα subunit by stabilizing the GTP hydrolysis transition state, thereby encouraging deactivation of Gα. Heterogeneity in the RGS domains leads to preferential selectivity between RGS proteins and Gα subunits due to sequence-specific interactions between RGS domains and the Gα Switch I, III, and N-terminal side of Switch II (Baltoumas et al., 2013). RGS1, 3, 4, 8, 16, 17, and 18 bind to GNAQ and other Gα members; RGS2 seems to be specific to GNAQ (Soundararajan et al., 2008). RGS proteins may be an attractive target for drug development for a variety of diseases, including SWS (Sjögren, 2011).

GNAQ signaling pathways

There are a variety of well-defined downstream targets of G proteins, although their role in PWB is not understood. GNAQ in particular can stimulate the phospholipase C β (PLC-β) isoforms through interactions with the GNAQ N-terminal β-1 strand, which cleaves phosphatidyl inositol 4,5-bisphosphate into inositol triphosphate (IP3) and diacylglycerol (DAG) (Hepler et al., 1996; Rhee and Bae, 1997; Baltoumas et al., 2013). IP3 opens the calcium channel IP3 receptor on the endoplasmic reticulum (ER) membrane while DAG activates protein kinase C (PKC). Additionally, GNAQ uses helix-loop-helix domains in Switch II and α-helix 3 to interact with RhoGEFs like p63RhoGEF through p63RhoGEF Dbl-homology/pleckstrin-homology (DH/PH) domains (Lutz et al., 2007; Baltoumas et al., 2013; Syrovatkina et al., 2016). Less well defined targets of GNAQ signaling include GRK2, actin, tubulin, PI3K, TPR1, Btk tyrosine kinase, phospholipase C-ε, and TRPM8 (Syrovatkina et al., 2016). The biological significances of these are not well understood and may lie in tissue-specific functions. It is unclear how EC GNAQ* affects these factors.

It is important to note there are many Gβγ interactions that are influenced by GNAQ activation, including adenylate

cyclase, PI3K, potassium and calcium channels, and possibly IP3 receptors, Raf kinases, protein kinase D, histone deacetylase 5 (HDAC5), tubulin, F-actin, vinculin, ElmoE, Rab11, mitofusinil, Radil, activator protein 1, TFE3, and TRPM1 (Syrovatkina et al., 2016).

There are no therapeutic agents used clinically to target GNAQ protein at the time of this manuscript's publication (Musi et al., 2019). Instead, many treatment strategies (discussed earlier) either manage symptoms or in the case of cutaneous lesions, aim to target pathways that limit vessel regrowth after laser treatment.

Overlap with other vascular malformations

GNAQ mutations are found in a variety of diseases, including but not limited to: p.T96S NK/T cell lymphoma and diffuse bone and soft tissue angiomatosis (Li et al., 2019; Gaeta et al., 2020); p.R183Q Klippel-Trenaunay syndrome (He et al., 2020); p.V179M and p.F335L dark skin point mutations and hyperpigmentation (Garcia et al., 2008; Van Raamsdonk et al., 2009; Jain et al., 2020); p.Q209L or silencing mutations in non-small cell lung cancers (Choi et al., 2020); p.D663fs insertion and p.R385* nonsense mutations in melanocytoma (Francis et al., 2016); p.Q209L and p.Q209P intramedullary and leptomeningeal melanomas (Fortin Ensign et al., 2020); p.S12fs*49 breast cancer (Schrader et al., 2016); and decreased GNAQ expression in brain aging and neurodegeneration (Wettschureck et al., 2005; Frederick et al., 2012; Chen et al., 2017; Arey et al., 2018; Zhai et al., 2019; Sun et al., 2020). The following diseases discussed in more detail were selected due to the possible overlap in pathogenesis or molecular interactions, with the goal of spurring synergistic research encompassing these conditions and SWS.

Brain arteriovenous malformations

Understanding the molecular etiology of PWBs may benefit from overlapping research conducted in brain arteriovenous malformations (bAVMs). bAVM form when afferent arteries abnormally communicate directly with draining veins without an intermediary capillary bed, sometimes in a tangle called a nidus. Like PWB/SWS, bAVMs can differ substantially in size, location, morphology, architecture, presentation, and clinical treatment/management between patients (Abecassis et al., 2014). The rate of detection is 1.12–1.42 per 100,000 person years. Unlike SWS, hemorrhage is the most common presenting characteristic of bAVMs, occurring in about half of new diagnoses, with larger nidus size and deep location significantly correlated with hemorrhage risk (Stefani et al., 2002; Halim et al., 2004; Abecassis et al., 2014). Seizures (30% of new diagnoses) and headaches (5–14%) are also detected. bAVMs account for a quarter of hemorrhagic stroke in adults under 50 and almost half of bAVM patients die or have significant impairments within a year of a hemorrhagic event (van Beijnum et al., 2009; Cordonnier et al., 2010).

Next-gen DNA sequencing of sporadic bAVM has identified KRAS somatic activating mutations localized to the EC compartment in about half of patients (Barbosa Do Prado et al., 2019). These KRAS mutations activate MAPK-ERK and PI3K-AKT pathways that increase phospho-ERK levels and lead to overall increases in EC angiogenesis, aberrant vascular EC cadherin localization, Notch signaling, and migration capacity; countering ERK overactivity with trametinib inhibition of MEK reversed these findings (Al-Olabi et al., 2018; Nikolaev et al., 2018). These data support the idea that MAPK-ERK activation drives bAVM formation in KRAS mutant spontaneous bAVM in a manner similar to studies that identify KRAS overactivation in PWB. Additionally, zebrafish bAVM models treated with the BRAF inhibitor vemurafenib had restored blood flow compared to their untreated controls (Al-Olabi et al., 2018).

TGFβ family signaling mutations in familial bAVMs are detected in the autosomal dominant disease hereditary hemorrhagic telangiectasia (HHT), which affects roughly 1 in 5,000 people and is characterized by AVM formation and hemorrhage in multiple organs, including the brain, lungs, liver, and/or gastrointestinal tract (Barbosa Do Prado et al., 2019). EC ENG (HHT type 1) and ALK1 (HHT type 2) mutations make up the vast majority of HHT cases, while a small number can be attributed to mutations in SMAD4. In the absence of functional Alk1 it appears that angiogenic and/or inflammatory signals subsequent to injury are required for bAVM formation, and this likely involves VEGF-stimulated angiogenesis (Chen et al., 2013). Interestingly, localized VEGF delivery in combination with ALK1 or ENG deficiency in EC, but not vascular smooth muscle cells, pericytes, or macrophages was required for bAVM formation in adult mice, suggesting that EC might be intrinsically responsible for the formation of bAVM networks (Choi and Mohr, 2005; Chen et al., 2013; Cheng et al., 2019). Others have proposed similar EC-stroma miscommunication in SWS disease pathology; although SWS dilated vessels are unlike high-risk hemorrhagic lesions seen in HHT and bAVM, similar deficiencies in mural cell recruitment and wrapping as well as the presence of pro-inflammatory immune infiltration may exacerbate vessel dilation and fibrosis, possibly through the same mechanisms (Chen et al., 2008, 2013; Couto et al., 2016).

As noted above, aberrant angiogenic control is implicated in bAVM progression. EC deficiencies in TGFβ family signaling can cause bAVM formation through several mediating factors, including loss or depletion of SMAD4, or activation of MEK/ERK (Ola et al., 2016; Kim et al., 2018). Lastly, reduced expression of integrin β8 (ITGβ8) in bAVM promotes hemorrhage in response to VEGF stimulation,

possibly through increased Notch and Sox-2 (Su et al., 2010; Yao et al., 2019). Together, these results suggest that both ITGβ8 and ALK1 are crucial for maintaining a healthy pro- versus anti-angiogenic balance. VEGF-A antagonism with bevacizumab or pazopanib can restore the angiogenic balance and prevent lesion formation (Walker et al., 2012). Further work in this area is required, especially as overlapping research in MEK/ERK activation in SWS and bAVM may synergize.

Vessel immaturity and structural defects of the bAVM vascular wall are linked to PDGF/PDGFRβ deficiency. Dilated vessels with diameters greater than typical capillaries (greater than 15 μm) are strongly correlated with decreased smooth muscle cell and pericyte coverage and increased vascular permeability and hemorrhage risk (Chen et al., 2013; Zhu et al., 2018; Winkler et al., 2019; Pan et al., 2021). At this time, it is unclear if expression causes or results from bAVM formation, but increasing pericyte recruitment in the bAVM nidus by PDGFB expression or thalidomide/lenalidomide treatment reduces future hemorrhage risk (Lindahl et al., 1997; Lebrin et al., 2010; Zhu et al., 2018). Increasing pericyte coverage in PWB lesions may help prevent progressive vessel dilation and instability.

Non-coding regulatory RNAs may also play a role in vascular malformation development and/or progression. Downregulation of nicotinamide adenine dinucleotide phosphate (NADPH) reductase and lipoprotein lipase *via* several long non-coding RNAs may be associated with patient seizures in bAVM, while dysregulated novel miRNAs have been described to affect VEGF signaling and smooth muscle cell behavior (Huang et al., 2017; Li et al., 2018; Cheng et al., 2019). Inactivating mutations in DROSHA miRNA processing machinery have also been characterized in zebrafish bAVM models and have been identified in HHT patients that lack other known AVM-causative mutations (Jiang et al., 2018). To the best of our knowledge, miRNA dysregulation or misprocessing have not been examined in PWB/SWS and warrant investigation.

Non-cutaneous melanoma

GNAQ p.Q209 mutations have been implicated in more than 90% of cases of GNAQ-driven uveal melanoma (UM), although, studies conflict regarding the downstream molecular interactions driving cancer formation and progression (Van Raamsdonk et al., 2009; Feng et al., 2019; Musi et al., 2019; Truong et al., 2020). The p.Q209P mutation is fairly common in UM and does not appear to significantly alter disease prognosis compared to p.Q209L, while the p.R183Q mutation is slightly less common and leads to less aggressive disease (Daniels et al., 2012; van Weeghel et al., 2019). The p.Q209* mutations are predicted to cause more severe effects through overactivation of the MAPK pathway (Schneider et al., 2019; Jain et al., 2020). GNAQ p.G48L mutation in UM is rare (Krebs et al., 2020).

Uveal melanoma is currently treated with surgical resection or radiation therapy at the primary tumor site, however, treatment has not improved in decades and about half of UM is diagnosed at a late stage after metastasis has already occurred (Pyrhönen, 1998; Rietschel et al., 2005; Daniels et al., 2012; Feng et al., 2019; Musi et al., 2019; van Weeghel et al., 2019). Feng et al. have demonstrated that the presence of oncogenic GNAQ mutations can cause an overactivation of FAK-mediated YAP activation, which transcriptionally activates the TEAD transcription factor family and downstream pro-growth and pro-survival genes (Feng et al., 2019; Truong et al., 2020). The tumor suppressive Hippo pathway is not able to effectively silence this cascade during constitutive GNAQ activity (Feng et al., 2019). No specific YAP inhibitors are currently in clinical use, however, Truong et al. demonstrated that combined therapy with trametinib MEK1/2 inhibition and the lysosome inhibitor chloroquine increased cytotoxicity while indirectly decreasing YAP nuclear localization and transcriptional activity (Feng et al., 2019; Truong et al., 2020). Other groups have proposed GNAQ overactivation of ERK1/2 or MEK1/2 as a driver of UM, but inhibitors of this pathway alone are typically insufficient to stop progression and the degree of MAPK activation is widely heterogeneous within tumor sites (Zuidervaart et al., 2005; Boru et al., 2019; Feng et al., 2019; Musi et al., 2019; Truong et al., 2020).

Musi et al. (2019) demonstrated a dose-dependent reduction in mutant GNAQ-driven activation of ADP-ribosylation factor 6 (ARF6) using tris dibenzylideneacetone (DBA) palladium. Moreover, ARF6 GTPase has been identified as an immediate downstream cancer driver in GNAQ-UM, where it plays a role in the localization and transactivation of β-catenin from the plasma membrane to the nucleus, as well as the activation of Rho-Rac pathway signaling (Yoo et al., 2016; Musi et al., 2019). Other groups have demonstrated that tris DBA compounds decrease MAPK, PKC, and AKT-driven cancers as a result of NMT-1 blockade, however Musi et al. (2019) did not observe suppression of these pathways nor FAK inhibition and, interestingly, saw an increase in ERK and AKT phospho-activation despite increased UM apoptosis. Gene array analysis suggests tris DBA palladium additionally interferes with tumor RNA splicing and reduces resistance to chemotherapy (Musi et al., 2019). Many of these factors driving UM may be drivers of PWB/SWS.

The presence of a nevus of Ota is one of the few predictors of risk for UM and Van Raamsdonk et al. (2009) have identified an 83 and 46% incidence of GNAQ p.Q209L mutations in blue nevi and UM, respectively,

underscoring the overlapping relationship GNAQ plays in melanocytic neoplasms and UM. On the other hand, approximately one in 400 nevi of Ota progresses to UM so other factors remain undefined. Van Raamsdonk et al. postulate that GNAQ downstream targets such as ERK- and endothelin-regulated developmental survival, as well as Wnt and metabotropic glutamate receptor (GRM1) signaling contribute to melanocytic neoplasia oncogenesis and metastasis (Van Raamsdonk et al., 2009; Jain et al., 2020). Additionally, transfection of GNAQ p.Q209L in melanocytes *in vitro* demonstrated unusual anchorage-independent growth as well as large, irregularly shaped nuclei (Van Raamsdonk et al., 2009).

Cherry angiomas

Cherry angiomas are the most common kind of vascular tumor in adults. They typically present on the trunk or upper extremities as small, round, red to purple dome-shaped papules composed of dilated, thin-walled capillaries surrounded by hyalinized stroma, somewhat similar to the dilated structure of cutaneous PWB (Liau et al., 2019). Liau et al. (2019) detected EC GNAQ mutations in cherry angioma-like lesions in about half of all patients studied and are predicted to activate the MAPK pathway to drive pathogenesis, as in PWB/SWS. It is possible that significant overlap between cherry angiomas and PWB/SWS could offer us a glimpse of how PWB/SWS lesions form *in utero* and close collaboration between researchers working in the two diseases could afford greater understanding of both.

Models of port-wine birthmark/Sturge-Weber syndrome

In vivo models

Most *in vivo* studies are typically performed using healthy animal skin models such as mice, Wistar rats, or chicken (combs or wattles) where intervention is focused on regressing normal vessels (Rikihisa et al., 2017, 2018). Alternatively, xenotransplants can be used where mutant human EC in Matrigel extracellular matrix are subcutaneously injected into mice to study vessel formation, albeit outside the normal PWB/SWS environment. Most data to date identifying mutant GNAQ and possible molecular interactions leading to pathology have been developed using genome (DNA) sequencing and histology of patient tissue samples (Shirley et al., 2013; Nakashima et al., 2014; Couto et al., 2016; Huang et al., 2017; Bichsel and Bischoff, 2019; Le Guin et al., 2019; Lee et al., 2019; Cong et al., 2020; Jordan et al., 2020). Additional *in vivo* and *in vitro* complex studies like those performed by Huang et al. are needed to advance our understanding of PWB. The authors in this study identified Angpt2 as a downstream factor increased by endothelial GNAQ p.R183Q signaling that caused vessel dilation; this feature was reversed through GNAQ inhibition using YM-254890 or shRNA knockdown of Angpt2 (Huang et al., 2022). Thorough studies that identify direct controllers of PWB vessel dysfunction are rare.

In vitro models

As noted, there is a critical need for better models of PWB and SWS due to an absence of naturally occurring GNAQ* PWB/SWS in non-human animals and an inability of engineered *in vivo* models to successfully recapitulate SWS disease biology of humans. *In vitro* models may meet this need. Unfortunately, *in vitro* monolayer studies are inadequate for studying the complex disease pathology of PWB, which involves multiple tissues and cell types and is characterized by clearly three dimensional lesions – dilated blood vessels (Sun et al., 2020; Ewald et al., 2021). Complex human disease models such as microphysiological systems (MPS) provide an exciting and untapped opportunity (Ewald et al., 2021). Frequently referred to as an organ-on-a-chip, these platforms combine relevant cell types in a three-dimensional, ECM-rich tissue bed, often with media delivered to the tissue chamber by perfusable EC-lined microvessels (Wang et al., 2016, 2017; Ewald et al., 2021; Yue et al., 2021). Phan et al. and others have demonstrated the utility of these platforms for screening novel and repurposed therapeutics (Sobrino et al., 2016; Phan et al., 2017; Liu et al., 2020; Hachey et al., 2021). In particular, MPS platforms hold promise for rare diseases like SWS, as they can successfully recapitulate many aspects of disease biology and they offer the ability to rapidly test molecular perturbations, such as gene deletion or replacement. To the best of our knowledge, no complex *in vitro* model of PWB/SWS has been published. We argue that MPS technology holds great promise for understanding the GNAQ* downstream effectors in disease progression.

In a recent manuscript posted on BioRivx, Soon et al. (2022) describe a mosaic EC $KRAS^{G12V}$ MPS of sporadic bAVM. The authors were able to detect increased vessel dilation and permeability in $KRAS^{G12V}$ EC due to breakdown in adherens junctions and increased VEGF signaling. Finally, the authors were able to reverse some of this pathology with pharmaceutical MEK inhibition but not PIK3 inhibition, supporting further

investigation in the clinic of MEK inhibition in vascular malformation studies. Complex *in vitro* studies of this nature are needed to understand PWB/SWS pathology.

Discussion

Sturge-Weber syndrome is a complicated disease in which GNAQ mutations drive progressive capillary vessel dilation and dysfunction in skin, eye, and brain tissue. The consequences for these CMs entail severe impacts to patient quality of life and include but are not limited to: glaucoma, epilepsy, cognitive deficits, and psychosocial ramifications.

As noted, in contrast to several vascular malformations, there are few good models for PWB/SWS, and as a result there are still many questions left unanswered about how PWB/SWS arises and progresses. Are the effects of GNAQ* EC autonomous or is additional dysfunction in the stroma required? How do we reconcile these disease models with the rare contribution of additional GNAQ* in non-EC cell types? What are the critical downstream effectors of GNAQ that cause disease progression, and can they be specifically targeted in affected skin, brain, and eye tissue? We desperately need better models that evaluate transcriptional changes in PWB/SWS to answer these questions and to provide platforms for therapeutic drug development.

Author contributions

WVT performed the literature review and wrote the manuscript with input from all authors. KK and CH supervised assembly of the manuscript and provided critical feedback.

Funding

WVT and CH received funding from NCATS (UG3TR002137) to study vascular malformations. WVT also received funding from NINDS/UCI Gross Hall Stem Cell Center (5T32NS82174-8). KK received support from the Sturge Weber Foundation and IQVIA.

Acknowledgments

We would like to thank the following organizations for their generous support: IQVIA, the National Center for Advancing Translational Sciences (NCATS), the National Institute for Neurological Disorders and Stroke (NINDS), the Sturge Weber Foundation (SWF), and the UCI Health Beckman Laser Institute & Medical Clinic. We would also like to thank Emily Neubert for assistance with BioRender. The Sturge Weber Foundation serves as a resource for patients, families, philanthropists, researchers, and clinicians of PWB/SWS (Sturge Weber Foundation). Additionally, the National Organization for Rare Disorders (NORD) and the Genetic and Rare Diseases (GARD) Information Center both aim to increase access to rare disease information for the general public in the hope of driving translational development (GARD; NORD).

Conflict of interest

The authors declare that the research was conducted in the absence of any commercial or financial relationships that could be construed as a potential conflict of interest.

Publisher's note

Supplementary material

The Supplementary Material for this article can be found online at: https://www.frontiersin.org/articles/10.3389/fnhum.2022.1006027/full#supplementary-material

References

Abecassis, I. J., Xu, D. S., Batjer, H. H., and Bendok, B. R. (2014). Natural history of brain arteriovenous malformations: A systematic review. *Neurosurg. Focus* 37:E7. doi: 10.3171/2014.6.FOCUS14250

Al-Olabi, L., Polubothu, S., Dowsett, K., Andrews, K. A., Stadnik, P., Joseph, A. P., et al. (2018). Mosaic RAS/MAPK variants cause sporadic vascular malformations which respond to targeted therapy. *J. Clin. Invest.* 128, 1496–1508. doi: 10.1172/JCI98589

Arey, R. N., Stein, G. M., Kaletsky, R., Kauffman, A., and Murphy, C. T. (2018). Activation of Gαq signaling enhances memory consolidation and slows cognitive decline. *Neuron* 98, 562–574.e5. doi: 10.1016/j.neuron.2018.03.039

Bachur, C. D., Comi, A. M., and Germain-Lee, E. L. (2015). Partial hypopituitarism in patients with sturge-weber syndrome. *Pediatr. Neurol.* 53, e5–e6. doi: 10.1016/j.pediatrneurol.2015.04.005

Bae, Y.-S. C., Alabdulrazzaq, H., Brauer, J. A., and Geronemus, R. G. (2017). Treatment of recalcitrant port-wine stains (PWS) using a combined pulsed dye laser (PDL) and radiofrequency (RF) energy device. *J. Am. Acad. Dermatol.* 76, 321–326. doi: 10.1016/j.jaad.2016.03.004

Baltoumas, F. A., Theodoropoulou, M. C., and Hamodrakas, S. J. (2013). Interactions of the α-subunits of heterotrimeric G-proteins with GPCRs, effectors and RGS proteins: A critical review and analysis of interacting surfaces, conformational shifts, structural diversity and electrostatic potentials. *J. Struct. Biol.* 182, 209–218. doi: 10.1016/j.jsb.2013.03.004

Barbosa Do Prado, L., Han, C., Oh, S. P., and Su, H. (2019). Recent advances in basic research for brain arteriovenous malformation. *Int. J. Mol. Sci.* 20:E5324. doi: 10.3390/ijms20215324

Bernstein, E. F. (2009). The pulsed-dye laser for treatment of cutaneous conditions. *G. Ital. Dermatol. Venereol.* 144, 557–572.

Bichsel, C., and Bischoff, J. (2019). A somatic missense mutation in GNAQ causes capillary malformation. *Curr. Opin. Hematol.* 26, 179–184. doi: 10.1097/MOH.0000000000000500

Bichsel, C. A., Goss, J., Alomari, M., Alexandrescu, S., Robb, R., Smith, L. E., et al. (2019). Association of somatic GNAQ mutation with capillary malformations in a case of choroidal hemangioma. *JAMA Ophthalmol.* 137, 91–95. doi: 10.1001/jamaophthalmol.2018.5141

Boru, G., Cebulla, C. M., Sample, K. M., Massengill, J. B., Davidorf, F. H., and Abdel-Rahman, M. H. (2019). Heterogeneity in Mitogen-Activated Protein Kinase (MAPK) pathway activation in uveal melanoma with somatic GNAQ and GNA11 mutations. *Invest. Ophthalmol. Vis. Sci.* 60, 2474–2480. doi: 10.1167/iovs.18-26452

Bosch, D. E., Willard, F. S., Ramanujam, R., Kimple, A. J., Willard, M. D., Naqvi, N. I., et al. (2012). A P-loop mutation in Gα subunits prevents transition to the active state: Implications for G-protein signaling in fungal pathogenesis. *PLoS Pathog.* 8:e1002553. doi: 10.1371/journal.ppat.1002553

Chen, W., Guo, Y., Walker, E. J., Shen, F., Jun, K., Oh, S. P., et al. (2013). Reduced mural cell coverage and impaired vessel integrity after angiogenic stimulation in the Alk1-deficient brain. *Arterioscler. Thromb. Vasc. Biol.* 33, 305–310. doi: 10.1161/ATVBAHA.112.300485

Chen, Y., Granger, A. J., Tran, T., Saulnier, J. L., Kirkwood, A., and Sabatini, B. L. (2017). Endogenous Gαq-coupled neuromodulator receptors activate protein kinase A. *Neuron* 96, 1070–1083.e5. doi: 10.1016/j.neuron.2017.10.023

Chen, Y., Zhu, W., Bollen, A. W., Lawton, M. T., Barbaro, N. M., Dowd, C. F., et al. (2008). Evidence of inflammatory cell involvement in brain arteriovenous malformations. *Neurosurgery* 62, 1340–1349; discussion 1349–1350. doi: 10.1227/01.neu.0000333306.64683.b5

Cheng, P., Ma, L., Shaligram, S., Walker, E. J., Yang, S.-T., Tang, C., et al. (2019). Effect of elevation of vascular endothelial growth factor level on exacerbation of hemorrhage in mouse brain arteriovenous malformation. *J. Neurosurg.* 132, 1566–1573. doi: 10.3171/2019.1.JNS183112

Choi, J. H., and Mohr, J. P. (2005). Brain arteriovenous malformations in adults. *Lancet Neurol.* 4, 299–308. doi: 10.1016/S1474-4422(05)70073-9

Choi, J.-Y., Lee, Y. S., Shim, D. M., and Seo, S. W. (2020). Effect of GNAQ alteration on RANKL-induced osteoclastogenesis in human non-small-cell lung cancer. *Bone Joint Res.* 9, 29–35. doi: 10.1302/2046-3758.91.BJR-2019-0085.R2

Cong, T., Liu, L., Zhang, H., Wang, L., and Jiang, X. (2020). Port-wine stains associated with large vestibular aqueduct syndrome caused by mutations in GNAQ and SLC26A4 genes: A case report. *J. Dermatol.* 47, 78–81. doi: 10.1111/1346-8138.15130

Cordonnier, C., Klijn, C. J. M., van Beijnum, J., and Al-Shahi Salman, R. (2010). Radiological investigation of spontaneous intracerebral hemorrhage: Systematic review and trinational survey. *Stroke* 41, 685–690. doi: 10.1161/STROKEAHA.109.572495

Couto, J. A., Huang, L., Vivero, M. P., Kamitaki, N., Maclellan, R. A., Mulliken, J. B., et al. (2016). Endothelial cells from capillary malformations are enriched for somatic GNAQ mutations. *Plast. Reconstr. Surg.* 137, 77e–82e. doi: 10.1097/PRS.0000000000001868

Daniels, A. B., Lee, J.-E., MacConaill, L. E., Palescandolo, E., Van Hummelen, P., Adams, S. M., et al. (2012). High throughput mass spectrometry-based mutation profiling of primary uveal melanoma. *Invest. Ophthalmol. Vis. Sci.* 53, 6991–6996. doi: 10.1167/iovs.12-10427

Dong, Q., Shenker, A., Way, J., Haddad, B. R., Lin, K., Hughes, M. R., et al. (1995). Molecular cloning of human G alpha q cDNA and chromosomal localization of the G alpha q gene (GNAQ) and a processed pseudogene. *Genomics* 30, 470–475. doi: 10.1006/geno.1995.1267

Ewald, M. L., Chen, Y.-H., Lee, A. P., and Hughes, C. C. W. (2021). The vascular niche in next generation microphysiological systems. *Lab. Chip* 21, 3244–3262. doi: 10.1039/d1lc00530h

Feng, X., Arang, N., Rigiracciolo, D. C., Lee, J. S., Yeerna, H., Wang, Z., et al. (2019). A platform of synthetic lethal gene interaction networks reveals that the GNAQ uveal melanoma oncogene controls the hippo pathway through FAK. *Cancer Cell* 35, 457–472.e5. doi: 10.1016/j.ccell.2019.01.009

Fortin Ensign, S., Bollin, K., Millis, S. Z., Hinds, B. R., Kosty, M., and Uchiyama, C. (2020). Genomic analysis reveals low tumor mutation burden which may be associated with GNAQ/11 alteration in a series of primary leptomeningeal melanomas. *Pigment Cell Melanoma Res.* 33, 458–465. doi: 10.1111/pcmr.12839

Francis, J. H., Wiesner, T., Milman, T., Won, H. H., Lin, A., Lee, V., et al. (2016). Investigation of somatic GNAQ, GNA11, BAP1 and SF3B1 mutations in ophthalmic melanocytomas. *Ocul. Oncol. Pathol.* 2, 171–177. doi: 10.1159/000442352

Frederick, A. L., Saborido, T. P., and Stanwood, G. D. (2012). Neurobehavioral phenotyping of G(αq) knockout mice reveals impairments in motor functions and spatial working memory without changes in anxiety or behavioral despair. *Front. Behav. Neurosci.* 6:29. doi: 10.3389/fnbeh.2012.00029

Gabay, M., Pinter, M. E., Wright, F. A., Chan, P., Murphy, A. J., Valenzuela, D. M., et al. (2011). Ric-8 proteins are molecular chaperones that direct nascent G protein α subunit membrane association. *Sci. Signal.* 4:ra79. doi: 10.1126/scisignal.2002223

Gaeta, R., Lessi, F., Mazzanti, C., Modena, M., Garaventa, A., Boero, S., et al. (2020). Diffuse bone and soft tissue angiomatosis with GNAQ mutation. *Pathol. Int.* 70, 452–457. doi: 10.1111/pin.12933

Gao, L., Nadora, D. M., Phan, S., Chernova, M., Sun, V., Preciado, S. M. O., et al. (2015). Topical axitinib suppresses angiogenesis pathways induced by pulsed dye laser. *Br. J. Dermatol.* 172, 669–676. doi: 10.1111/bjd.13439

Garcia, R. J., Ittah, A., Mirabal, S., Figueroa, J., Lopez, L., Glick, A. B., et al. (2008). Endothelin 3 induces skin pigmentation in a keratin-driven inducible mouse model. *J. Invest. Dermatol.* 128, 131–142. doi: 10.1038/sj.jid.5700948

Garcia-Marcos, M., Ghosh, P., and Farquhar, M. G. (2009). GIV is a nonreceptor GEF for G alpha i with a unique motif that regulates Akt signaling. *Proc. Natl. Acad. Sci. U.S.A.* 106, 3178–3183. doi: 10.1073/pnas.0900294106

Ghosh, P., Garcia-Marcos, M., and Farquhar, M. G. (2011). GIV/Girdin is a rheostat that fine-tunes growth factor signals during tumor progression. *Cell Adhes. Migr.* 5, 237–248. doi: 10.4161/cam.5.3.15909

Hachey, S. J., Movsesyan, S., Nguyen, Q. H., Burton-Sojo, G., Tankazyan, A., Wu, J., et al. (2021). An in vitro vascularized micro-tumor model of human colorectal cancer recapitulates in vivo responses to standard-of-care therapy. *Lab Chip* 21, 1333–1351. doi: 10.1039/d0lc01216e

Halim, A. X., Johnston, S. C., Singh, V., McCulloch, C. E., Bennett, J. P., Achrol, A. S., et al. (2004). Longitudinal risk of intracranial hemorrhage in patients with arteriovenous malformation of the brain within a defined population. *Stroke* 35, 1697–1702. doi: 10.1161/01.STR.0000130988.44824.29

He, R., Liao, S., Yao, X., Huang, R., Zeng, J., Zhang, J., et al. (2020). Klippel-trenaunay and sturge-weber overlap syndrome with KRAS and GNAQ mutations. *Ann. Clin. Transl. Neurol.* 7, 1258–1264. doi: 10.1002/acn3.51106

Hepler, J. R., Biddlecome, G. H., Kleuss, C., Camp, L. A., Hofmann, S. L., Ross, E. M., et al. (1996). Functional importance of the amino terminus of Gq alpha. *J. Biol. Chem.* 271, 496–504. doi: 10.1074/jbc.271.1.496

Higueros, E., Roe, E., Granell, E., and Baselga, E. (2017). Sturge-weber syndrome: A review. *Actas Dermosifiliogr.* 108, 407–417. doi: 10.1016/j.ad.2016.09.022

Huang, L., Bichsel, C., Norris, A. L., Thorpe, J., Pevsner, J., Alexandrescu, S., et al. (2022). Endothelial GNAQ p.R183Q increases ANGPT2 (Angiopoietin-2) and drives formation of enlarged blood vessels. *Arterioscler. Thromb. Vasc. Biol.* 42, e27–e43. doi: 10.1161/ATVBAHA.121.316651

Huang, L., Couto, J. A., Pinto, A., Alexandrescu, S., Madsen, J. R., Greene, A. K., et al. (2017). Somatic GNAQ mutation is enriched in brain endothelial cells in sturge-weber syndrome. *Pediatr. Neurol.* 67, 59–63. doi: 10.1016/j.pediatrneurol.2016.10.010

Izikson, L., Nelson, J. S., and Anderson, R. R. (2009). Treatment of hypertrophic and resistant port wine stains with a 755 nm laser: A case series of 20 patients. *Lasers Surg. Med.* 41, 427–432. doi: 10.1002/lsm.20793

Jain, F., Longakit, A., Huang, J. L.-Y., and Van Raamsdonk, C. D. (2020). Endothelin signaling promotes melanoma tumorigenesis driven by constitutively active GNAQ. *Pigment Cell Melanoma Res.* 33, 834–849. doi: 10.1111/pcmr.12900

Jiang, X., Wooderchak-Donahue, W. L., McDonald, J., Ghatpande, P., Baalbaki, M., Sandoval, M., et al. (2018). Inactivating mutations in Drosha mediate vascular abnormalities similar to hereditary hemorrhagic telangiectasia. *Sci. Signal.* 11:eaan6831. doi: 10.1126/scisignal.aan6831

Jordan, M., Carmignac, V., Sorlin, A., Kuentz, P., Albuisson, J., Borradori, L., et al. (2020). Reverse phenotyping in patients with skin capillary malformations and mosaic GNAQ or GNA11 mutations defines a clinical spectrum with genotype-phenotype correlation. *J. Invest. Dermatol.* 140, 1106–1110.e2. doi: 10.1016/j.jid.2019.08.455

Kanada, K. N., Merin, M. R., Munden, A., and Friedlander, S. F. (2012). A prospective study of cutaneous findings in newborns in the United States: Correlation with race, ethnicity, and gestational status using updated classification and nomenclature. *J. Pediatr.* 161, 240–245. doi: 10.1016/j.jpeds.2012.02.052

Kelly, A., Pai, A., Lertsakdadet, B., Choi, B., and Kelly, K. M. (2020). Microvascular effects of pulsed dye laser in combination with oxymetazoline. *Lasers Surg. Med.* 52, 17–22. doi: 10.1002/lsm.23186

Kim, T., Kwon, O.-K., Bang, J. S., Lee, H., Kim, J. E., Kang, H.-S., et al. (2018). Epidemiology of ruptured brain arteriovenous malformation: A National Cohort Study in Korea. *J. Neurosurg.* [Epub ahead of print]. doi: 10.3171/2018.1.JNS172766

Kimple, R. J., Kimple, M. E., Betts, L., Sondek, J., and Siderovski, D. P. (2002). Structural determinants for GoLoco-induced inhibition of nucleotide release by Galpha subunits. *Nature* 416, 878–881. doi: 10.1038/416878a

Krebs, F. S., Gérard, C., Wicky, A., Aedo-Lopez, V., Missiaglia, E., Bisig, B., et al. (2020). Trametinib induces the stabilization of a dual *GNAQ* p.Gly48Leu- and *FGFR4* p.Cys172Gly-mutated uveal melanoma. The role of molecular modelling in personalized oncology. *Int. J. Mol. Sci.* 21:8021. doi: 10.3390/ijms21218021

Le Guin, C. H. D., Metz, K. A., Kreis, S. H., Bechrakis, N. E., Bornfeld, N., Zeschnigk, M., et al. (2019). GNAQ Q209R mutations are highly specific for circumscribed choroidal hemangioma. *Cancers* 11:1031. doi: 10.3390/cancers11071031

Lebrin, F., Srun, S., Raymond, K., Martin, S., van den Brink, S., Freitas, C., et al. (2010). Thalidomide stimulates vessel maturation and reduces epistaxis in individuals with hereditary hemorrhagic telangiectasia. *Nat. Med.* 16, 420–428. doi: 10.1038/nm.2131

Lee, J. W., Chung, H. Y., Cerrati, E. W., Teresa, M. O., and Waner, M. (2015). The natural history of soft tissue hypertrophy, bony hypertrophy, and nodule formation in patients with untreated head and neck capillary malformations. *Dermatol. Surg.* 41, 1241–1245. doi: 10.1097/DSS.0000000000000525

Lee, K.-T., Park, J. E., Eom, Y., Lim, H. S., Ki, C.-S., and Lim, S. Y. (2019). Phenotypic association of presence of a somatic GNAQ mutation with port-wine stain distribution in capillary malformation. *Head Neck* 41, 4143–4150. doi: 10.1002/hed.25962

Li, Z., Ma, L., Wu, C., Ma, J., and Chen, X. (2018). Pediatric brain arteriovenous malformation unfavorable hemorrhage risk: Extrapolation to a morphologic model. *Chin. Neurosurg. J.* 4:15. doi: 10.1186/s41016-018-0123-x

Li, Z., Zhang, X., Xue, W., Zhang, Y., Li, C., Song, Y., et al. (2019). Recurrent GNAQ mutation encoding T96S in natural killer/T cell lymphoma. *Nat. Commun.* 10:4209. doi: 10.1038/s41467-019-12032-9

Liau, J.-Y., Lee, J.-C., Tsai, J.-H., Chen, C.-C., Chung, Y.-C., and Wang, Y.-H. (2019). High frequency of GNA14, GNAQ, and GNA11 mutations in cherry hemangioma: A histopathological and molecular study of 85 cases indicating GNA14 as the most commonly mutated gene in vascular neoplasms. *Mod. Pathol.* 32, 1657–1665. doi: 10.1038/s41379-019-0284-y

Lindahl, P., Johansson, B. R., Levéen, P., and Betsholtz, C. (1997). Pericyte loss and microaneurysm formation in PDGF-B-deficient mice. *Science* 277, 242–245. doi: 10.1126/science.277.5323.242

Lipner, S. R. (2018). Topical adjuncts to pulsed dye laser for treatment of port wine stains: Review of the literature. *Dermatol. Surg.* 44, 796–802. doi: 10.1097/DSS.0000000000001507

Liu, Y., Sakolish, C., Chen, Z., Phan, D. T. T., Bender, R. H. F., Hughes, C. C. W., et al. (2020). Human in vitro vascularized micro-organ and micro-tumor models are reproducible organ-on-a-chip platforms for studies of anticancer drugs. *Toxicology* 445:152601. doi: 10.1016/j.tox.2020.152601

Lutz, S., Shankaranarayanan, A., Coco, C., Ridilla, M., Nance, M. R., Vettel, C., et al. (2007). Structure of Galphaq-p63RhoGEF-RhoA complex reveals a pathway for the activation of RhoA by GPCRs. *Science* 318, 1923–1927. doi: 10.1126/science.1147554

Martins, L., Giovani, P. A., Rebouças, P. D., Brasil, D. M., Haiter Neto, F., Coletta, R. D., et al. (2017). Computational analysis for GNAQ mutations: New insights on the molecular etiology of Sturge-Weber syndrome. *J. Mol. Graph. Model.* 76, 429–440. doi: 10.1016/j.jmgm.2017.07.011

Miller, R. S., Ball, K. L., Comi, A. M., and Germain-Lee, E. L. (2006). Growth hormone deficiency in Sturge-Weber syndrome. *Arch. Dis. Child.* 91, 340–341. doi: 10.1136/adc.2005.082578

Musi, E., Schwartz, G. K., Yoo, J. H., Odelberg, S. J., Li, D. Y., Bonner, M. Y., et al. (2019). Tris DBA palladium is an orally available inhibitor of GNAQ mutant uveal melanoma in vivo. *Oncotarget* 10, 4424–4436. doi: 10.18632/oncotarget.27040

Nakashima, M., Miyajima, M., Sugano, H., Iimura, Y., Kato, M., Tsurusaki, Y., et al. (2014). The somatic GNAQ mutation c.548G>A (p.R183Q) is consistently found in Sturge-Weber syndrome. *J. Hum. Genet.* 59, 691–693. doi: 10.1038/jhg.2014.95

Neves, S. R., Ram, P. T., and Iyengar, R. (2002). G protein pathways. *Science* 296, 1636–1639. doi: 10.1126/science.1071550

Nikolaev, S. I., Vetiska, S., Bonilla, X., Boudreau, E., Jauhiainen, S., Rezai Jahromi, B., et al. (2018). Somatic activating KRAS mutations in arteriovenous malformations of the brain. *N. Engl. J. Med.* 378, 250–261. doi: 10.1056/NEJMoa1709449

NORD *NORD Natl. Organ. Rare Disord*. Available Online at: https://rarediseases.org/ [accessed June 16, 2022].

Ola, R., Dubrac, A., Han, J., Zhang, F., Fang, J. S., Larrivée, B., et al. (2016). PI3 kinase inhibition improves vascular malformations in mouse models of hereditary haemorrhagic telangiectasia. *Nat. Commun.* 7:13650. doi: 10.1038/ncomms13650

Oldham, W. M., and Hamm, H. E. (2006). Structural basis of function in heterotrimeric G proteins. *Q. Rev. Biophys.* 39, 117–166. doi: 10.1017/S0033583506004306

Pan, P., Shaligram, S. S., Do Prado, L. B., He, L., and Su, H. (2021). The role of mural cells in hemorrhage of brain arteriovenous malformation. *Brain Hemorrhages* 2, 49–56. doi: 10.1016/j.hest.2020.10.005

Phan, D. T. T., Wang, X., Craver, B. M., Sobrino, A., Zhao, D., Chen, J. C., et al. (2017). A vascularized and perfused organ-on-a-chip platform for large-scale drug screening applications. *Lab Chip* 17, 511–520. doi: 10.1039/c6lc01422d

Pyrhönen, S. (1998). The treatment of metastatic uveal melanoma. *Eur. J. Cancer Oxf. Engl.* 34(Suppl. 3), S27–S30. doi: 10.1016/s0959-8049(97)10161-7

Rhee, S. G., and Bae, Y. S. (1997). Regulation of phosphoinositide-specific phospholipase C isozymes. *J. Biol. Chem.* 272, 15045–15048. doi: 10.1074/jbc.272.24.15045

Rietschel, P., Panageas, K. S., Hanlon, C., Patel, A., Abramson, D. H., and Chapman, P. B. (2005). Variates of survival in metastatic uveal melanoma. *J. Clin. Oncol.* 23, 8076–8080. doi: 10.1200/JCO.2005.02.6534

Rikihisa, N., Tominaga, M., Watanabe, S., Mitsukawa, N., Saito, Y., and Sakai, H. (2018). Intravenous injection of artificial red cells and subsequent dye laser irradiation causes deep vessel impairment in an animal model of port-wine stain. *Lasers Med. Sci.* 33, 1287–1293. doi: 10.1007/s10103-018-2480-2

Rikihisa, N., Watanabe, S., Satoh, K., Saito, Y., and Sakai, H. (2017). Photosensitizer effects of artificial red cells on dye laser irradiation in an animal model assuming port-wine stain treatment. *Plast. Reconstr. Surg.* 139, 707e–716e. doi: 10.1097/PRS.0000000000003082

Sabeti, S., Ball, K. L., Burkhart, C., Eichenfield, L., Fernandez Faith, E., Frieden, I. J., et al. (2021). Consensus statement for the management and treatment of port-wine birthmarks in sturge-weber syndrome. *JAMA Dermatol.* 157, 98–104. doi: 10.1001/jamadermatol.2020.4226

Schneider, B., Riedel, K., Zhivov, A., Huehns, M., Zettl, H., Guthoff, R. F., et al. (2019). Frequent and yet unreported GNAQ and GNA11 mutations are found in uveal melanomas. *Pathol. Oncol. Res.* 25, 1319–1325. doi: 10.1007/s12253-017-0371-7

Schrader, K. A., Cheng, D. T., Joseph, V., Prasad, M., Walsh, M., Zehir, A., et al. (2016). Germline variants in targeted tumor sequencing using matched normal DNA. *JAMA Oncol.* 2, 104–111. doi: 10.1001/jamaoncol.2015.5208

Sebold, A. J., Day, A. M., Ewen, J., Adamek, J., Byars, A., Cohen, B., et al. (2021). Sirolimus treatment in sturge-weber syndrome. *Pediatr. Neurol.* 115, 29–40. doi: 10.1016/j.pediatrneurol.2020.10.013

Shirley, M. D., Tang, H., Gallione, C. J., Baugher, J. D., Frelin, L. P., Cohen, B., et al. (2013). Sturge-Weber syndrome and port-wine stains caused by somatic mutation in GNAQ. *N. Engl. J. Med.* 368, 1971–1979. doi: 10.1056/NEJMoa1213507

Sidbury, R., Neuschler, N., Neuschler, E., Sun, P., Wang, X., Miller, R., et al. (2003). Topically applied imiquimod inhibits vascular tumor growth in vivo. *J. Invest. Dermatol.* 121, 1205–1209. doi: 10.1046/j.1523-1747.2003.12521.x

Simon, M. I., Strathmann, M. P., and Gautam, N. (1991). Diversity of G proteins in signal transduction. *Science* 252, 802–808. doi: 10.1126/science.1902986

Sjögren, B. (2011). Regulator of G protein signaling proteins as drug targets: Current state and future possibilities. *Adv. Pharmacol. San Diego Calif.* 62, 315–347. doi: 10.1016/B978-0-12-385952-5.00002-6

Sobrino, A., Phan, D. T. T., Datta, R., Wang, X., Hachey, S. J., Romero-López, M., et al. (2016). 3D microtumors in vitro supported by perfused vascular networks. *Sci. Rep.* 6:31589. doi: 10.1038/srep31589

Soon, K., Li, M., Wu, R., Turner, W. D., Wythe, J. D., Fish, J. E., et al. (2022). Development and characterization of a human model of arteriovenous malformation (AVM)-on-a-chip. *bioRxiv [Preprint]* doi: 10.1101/2022.01.20.477166

Soundararajan, M., Willard, F. S., Kimple, A. J., Turnbull, A. P., Ball, L. J., Schoch, G. A., et al. (2008). Structural diversity in the RGS domain and its interaction with heterotrimeric G protein alpha-subunits. *Proc. Natl. Acad. Sci. U.S.A.* 105, 6457–6462. doi: 10.1073/pnas.0801508105

Sprang, S. R. (1997). G protein mechanisms: Insights from structural analysis. *Annu. Rev. Biochem.* 66, 639–678. doi: 10.1146/annurev.biochem.66.1.639

Stefani, M. A., Porter, P. J., terBrugge, K. G., Montanera, W., Willinsky, R. A., and Wallace, M. C. (2002). Large and deep brain arteriovenous malformations are associated with risk of future hemorrhage. *Stroke* 33, 1220–1224. doi: 10.1161/01.str.0000013738.53113.33

Strange, P. G. (2008). Signaling mechanisms of GPCR ligands. *Curr. Opin. Drug Discov. Devel.* 11, 196–202.

Sturge Weber Foundation *Sturge weber found*. Available Online at: https://sturge-weber.org/ [accessed June 21, 2022].

Su, H., Kim, H., Pawlikowska, L., Kitamura, H., Shen, F., Cambier, S., et al. (2010). Reduced expression of integrin alphavbeta8 is associated with brain arteriovenous malformation pathogenesis. *Am. J. Pathol.* 176, 1018–1027. doi: 10.2353/ajpath.2010.090453

Sun, X., Li, G.-P., Huang, P., Wei, L.-G., Guo, J.-Z., Ao, L.-J., et al. (2020). Gnaq protects PC12 cells from oxidative damage by activation of Nrf2 and inhibition of NF-kB. *Neuromol. Med.* 22, 401–410. doi: 10.1007/s12017-020-08598-z

Syrovatkina, V., Alegre, K. O., Dey, R., and Huang, X.-Y. (2016). Regulation, signaling, and physiological functions of G-proteins. *J. Mol. Biol.* 428, 3850–3868. doi: 10.1016/j.jmb.2016.08.002

Tall, G. G., and Gilman, A. G. (2004). Purification and functional analysis of Ric-8A: A guanine nucleotide exchange factor for G-protein alpha subunits. *Methods Enzymol.* 390, 377–388. doi: 10.1016/S0076-6879(04)90023-7

Tall, G. G., Krumins, A. M., and Gilman, A. G. (2003). Mammalian Ric-8A (synembryn) is a heterotrimeric Galpha protein guanine nucleotide exchange factor. *J. Biol. Chem.* 278, 8356–8362. doi: 10.1074/jbc.M211862200

Taquin, H., Lacour, J.-P., Le Duff, F., Chiaverini, C., and Passeron, T. (2016). Treatment of resistant port-wine stains with bosentan and pulsed dye laser: A pilot prospective study. *J. Eur. Acad. Dermatol. Venereol.* 30, 1432–1434. doi: 10.1111/jdv.13275

Tierney, E. P., and Hanke, C. W. (2009). Treatment of nodules associated with port wine stains with CO2 laser: Case series and review of the literature. *J. Drugs Dermatol.* 8, 157–161.

Truong, A., Yoo, J. H., Scherzer, M. T., Sanchez, J. M. S., Dale, K. J., Kinsey, C. G., et al. (2020). Chloroquine sensitizes GNAQ/11-mutated melanoma to MEK1/2 inhibition. *Clin. Cancer Res.* 26, 6374–6386. doi: 10.1158/1078-0432.CCR-20-1675

Urtatiz, O., and Van Raamsdonk, C. D. (2016). Gnaq and Gna11 in the endothelin signaling pathway and melanoma. *Front. Genet.* 7:59. doi: 10.3389/fgene.2016.00059

van Beijnum, J., Lovelock, C. E., Cordonnier, C., Rothwell, P. M., Klijn, C. J. M., Al-Shahi Salman, R., et al. (2009). Outcome after spontaneous and arteriovenous malformation-related intracerebral haemorrhage: Population-based studies. *Brain J. Neurol.* 132, 537–543. doi: 10.1093/brain/awn318

Van Raamsdonk, C. D., Bezrookove, V., Green, G., Bauer, J., Gaugler, L., O'Brien, J. M., et al. (2009). Frequent somatic mutations of GNAQ in uveal melanoma and blue naevi. *Nature* 457, 599–602. doi: 10.1038/nature07586

van Weeghel, C., Wierenga, A. P. A., Versluis, M., van Hall, T., van der Velden, P. A., Kroes, W. G. M., et al. (2019). Do GNAQ and GNA11 differentially affect inflammation and HLA expression in uveal melanoma? *Cancers* 11:1127. doi: 10.3390/cancers11081127

Venkatakrishnan, A. J., Deupi, X., Lebon, G., Tate, C. G., Schertler, G. F., and Babu, M. M. (2013). Molecular signatures of G-protein-coupled receptors. *Nature* 494, 185–194. doi: 10.1038/nature11896

Waelchli, R., Aylett, S. E., Robinson, K., Chong, W. K., Martinez, A. E., and Kinsler, V. A. (2014). New vascular classification of port-wine stains: Improving prediction of Sturge-Weber risk. *Br. J. Dermatol.* 171, 861–867. doi: 10.1111/bjd.13203

Walker, E. J., Su, H., Shen, F., Degos, V., Amend, G., Jun, K., et al. (2012). Bevacizumab attenuates VEGF-induced angiogenesis and vascular malformations in the adult mouse brain. *Stroke* 43, 1925–1930. doi: 10.1161/STROKEAHA.111.647982

Wang, B., Mei, X., Wang, Y., Hu, X., and Li, F. (2022). Adjuncts to pulsed dye laser for treatment of port wine stains: A literature review. *J. Cosmet. Laser Ther.* 23, 209–217. doi: 10.1080/14764172.2022.2052901

Wang, X., Phan, D. T. T., George, S. C., Hughes, C. C. W., and Lee, A. P. (2017). 3D anastomosed microvascular network model with living capillary networks and endothelial cell-lined microfluidic channels. *Methods Mol. Biol.* 1612, 325–344. doi: 10.1007/978-1-4939-7021-6_24

Wang, X., Phan, D. T. T., Sobrino, A., George, S. C., Hughes, C. C. W., and Lee, A. P. (2016). Engineering anastomosis between living capillary networks and endothelial cell-lined microfluidic channels. *Lab Chip* 16, 282–290. doi: 10.1039/c5lc01050k

Wettschureck, N., Moers, A., Wallenwein, B., Parlow, A. F., Maser-Gluth, C., and Offermanns, S. (2005). Loss of Gq/11 family G proteins in the nervous system causes pituitary somatotroph hypoplasia and dwarfism in mice. *Mol. Cell. Biol.* 25, 1942–1948. doi: 10.1128/MCB.25.5.1942-1948.2005

Winkler, E. A., Lu, A. Y., Raygor, K. P., Linzey, J. R., Jonzzon, S., Lien, B. V., et al. (2019). Defective vascular signaling & prospective therapeutic targets in brain arteriovenous malformations. *Neurochem. Int.* 126, 126–138. doi: 10.1016/j.neuint.2019.03.002

Wolf, Y. I., Brenner, S. E., Bash, P. A., and Koonin, E. V. (1999). Distribution of protein folds in the three superkingdoms of life. *Genome Res.* 9, 17–26.

Yao, R., Alkhawtani, A. Y. F., Chen, R., Luan, J., and Xu, M. (2019). Rapid and efficient in vivo angiogenesis directed by electro-assisted bioprinting of alginate/collagen microspheres with human umbilical vein endothelial cell coating layer. *Int. J. Bioprint.* 5:194. doi: 10.18063/ijb.v5i2.1.194

Yin, R., Gao, L., Tan, W., Guo, W., Zhao, T., Nelson, J. S., et al. (2017). Activation of PKCα and PI3K kinases in hypertrophic and nodular port wine stain lesions. *Am. J. Dermatopathol.* 39, 747–752. doi: 10.1097/DAD.0000000000000785

Yoo, J. H., Shi, D. S., Grossmann, A. H., Sorensen, L. K., Tong, Z., Mleynek, T. M., et al. (2016). ARF6 is an actionable node that orchestrates oncogenic GNAQ signaling in uveal melanoma. *Cancer Cell* 29, 889–904. doi: 10.1016/j.ccell.2016.04.015

Yu, W., Ma, G., Qiu, Y., Chen, H., Jin, Y., Yang, X., et al. (2016). Why do port-wine stains (PWS) on the lateral face respond better to pulsed dye laser (PDL) than those located on the central face? *J. Am. Acad. Dermatol.* 74, 527–535. doi: 10.1016/j.jaad.2015.08.026

Yue, T., Zhao, D., Phan, D. T. T., Wang, X., Park, J. J., Biviji, Z., et al. (2021). A modular microfluidic system based on a multilayered configuration to generate large-scale perfusable microvascular networks. *Microsyst. Nanoeng.* 7:4. doi: 10.1038/s41378-020-00229-8

Zhai, M., Zhao, Z., Yang, M., Liang, Y., Liang, H., Xie, Y., et al. (2019). The effect of GNAQ methylation on GnRH secretion in sheep hypothalamic neurons. *J. Cell. Biochem.* 120, 19396–19405. doi: 10.1002/jcb.29021

Zhu, W., Chen, W., Zou, D., Wang, L., Bao, C., Zhan, L., et al. (2018). Thalidomide reduces hemorrhage of brain arteriovenous malformations in a mouse model. *Stroke* 49, 1232–1240. doi: 10.1161/STROKEAHA.117.020356

Zuidervaart, W., van Nieuwpoort, F., Stark, M., Dijkman, R., Packer, L., Borgstein, A.-M., et al. (2005). Activation of the MAPK pathway is a common event in uveal melanomas although it rarely occurs through mutation of BRAF or RAS. *Br. J. Cancer* 92, 2032–2038. doi: 10.1038/sj.bjc.6602598

frontiers | Frontiers in Human Neuroscience

TYPE Review
PUBLISHED 24 November 2022
DOI 10.3389/fnhum.2022.1006115

OPEN ACCESS

EDITED BY
Richard Daneman,
University of California, San Diego,
United States

REVIEWED BY
Sabine Bailly,
INSERM, France
Hua Su,
University of California, San Francisco,
United States
Helen Mary Arthur,
Newcastle University, United Kingdom

*CORRESPONDENCE
Bruno Larrivée
bruno.larrivee@umontreal.ca
Alexandre Dubrac
alexandre.dubrac@umontreal.ca

SPECIALTY SECTION
This article was submitted to
Brain Health and Clinical
Neuroscience,
a section of the journal
Frontiers in Human Neuroscience

RECEIVED 29 July 2022
ACCEPTED 27 October 2022
PUBLISHED 24 November 2022

CITATION
Drapé E, Anquetil T, Larrivée B and
Dubrac A (2022) Brain arteriovenous
malformation in hereditary
hemorrhagic telangiectasia: Recent
advances in cellular and molecular
mechanisms.
Front. Hum. Neurosci. 16:1006115.
doi: 10.3389/fnhum.2022.1006115

Brain arteriovenous malformation in hereditary hemorrhagic telangiectasia: Recent advances in cellular and molecular mechanisms

Elise Drapé[1,2], Typhaine Anquetil[1,3], Bruno Larrivée[4,5]* and Alexandre Dubrac[1,3,4]*

[1]Centre de Recherche, CHU St. Justine, Montréal, QC, Canada, [2]Département de Pharmacologie et de Physiologie, Université de Montréal, Montréal, QC, Canada, [3]Département de Pathologie et Biologie Cellulaire, Université de Montréal, Montréal, QC, Canada, [4]Département d'Ophtalmologie, Université de Montréal, Montréal, QC, Canada, [5]Centre de Recherche, Hôpital Maisonneuve-Rosemont, Montréal, QC, Canada

Hereditary hemorrhagic telangiectasia (HHT) is a genetic disorder characterized by vessel dilatation, such as telangiectasia in skin and mucosa and arteriovenous malformations (AVM) in internal organs such as the gastrointestinal tract, lungs, and brain. AVMs are fragile and tortuous vascular anomalies that directly connect arteries and veins, bypassing healthy capillaries. Mutations in transforming growth factor β (TGFβ) signaling pathway components, such as *ENG* (ENDOGLIN), *ACVRL1* (ALK1), and *SMAD4* (SMAD4) genes, account for most of HHT cases. 10–20% of HHT patients develop brain AVMs (bAVMs), which can lead to vessel wall rupture and intracranial hemorrhages. Though the main mutations are known, mechanisms leading to AVM formation are unclear, partially due to lack of animal models. Recent mouse models allowed significant advances in our understanding of AVMs. Endothelial-specific deletion of either *Acvrl1*, *Eng* or *Smad4* is sufficient to induce AVMs, identifying endothelial cells (ECs) as primary targets of BMP signaling to promote vascular integrity. Loss of ALK1/ENG/SMAD4 signaling is associated with NOTCH signaling defects and abnormal arteriovenous EC differentiation. Moreover, cumulative evidence suggests that AVMs originate from venous ECs with defective flow-migration coupling and excessive proliferation. Mutant ECs show an increase of PI3K/AKT signaling and inhibitors of this signaling pathway rescue AVMs in HHT mouse models, revealing new therapeutic avenues. In this review, we will summarize recent advances and current knowledge of mechanisms controlling the pathogenesis of bAVMs, and discuss unresolved questions.

KEYWORDS

HHT, AVM, BMP, ALK1, ENG, SMAD4, endothelial cells

Introduction

Hereditary hemorrhagic telangiectasia (HHT), or Rendu-Osler disease, is an autosomal-dominant inherited syndrome with a prevalence of around 1:5,000–8,000 people (Bideau et al., 1989; Kjeldsen et al., 1999), characterized by vascular anomalies. The major lesions found are telangiectasia, widened small vessels located near the surface of the skin or mucous membranes such as lips, tongue, nasal, buccal, and gastrointestinal mucosa. These lesions are fragile and prone to bleeding mostly in the nasal mucosa and gastrointestinal tract (Shovlin, 2010). Most HHT patients also develop pulmonary, hepatic, spinal or brain arteriovenous malformations (AVMs), which are abnormal connections between arteries and veins. While 33% of patients develop pulmonary AVMs, 10–20% will develop brain AVMs (bAVMs) (Haitjema et al., 1995). Although bAVMs are less frequent, their consequences can be detrimental for the patient. Indeed, in addition to intracranial hemorrhages, bAVMs can lead to blood-brain-barrier (BBB) defects, promoting neuronal dysfunction and seizure such as epilepsy (Mohr et al., 2013; Rohn et al., 2014). However, bAVM pathogenesis is not well understood.

It is now well known that ALK1 signaling, one of the canonical pathways of the TGFβ superfamily, plays a critical role in vascular morphogenesis (Roman and Hinck, 2017). BMP9 and BMP10 are cytokines produced by the liver and the heart, respectively (**Figure 1**; Neuhaus et al., 1999; Bidart et al., 2012). BMP9 expression has also been reported in the lung and the brain septum, although at a significantly lower level than in the liver (López-Coviella et al., 2000; Bidart et al., 2012). Cardiac BMP10 expression is associated with the development of the trabeculated myocardium during embryonic development and then becomes mainly restricted to the right atria in post-natal life (Neuhaus et al., 1999; Somi et al., 2004). These cytokines can have an autocrine and paracrine action but can also enter blood circulation to act on endothelial cells (David et al., 2008; Chen H. et al., 2013). Indeed, BMP9/10 bind with high affinity to the TGFβ receptor 1 ALK1, a serine/threonine kinase receptor, and its coreceptor, ENDOGLIN (**Figure 1**), which is expressed predominantly on ECs (David et al., 2006; Alt et al., 2012; Townson et al., 2012). BMP9/10 ligands bind to ALK1 which will heterodimerize with BMP receptor II (BMPRII) to transduce downstream signaling. The ENDOGLIN receptor interacts with the receptor complex to promote the phosphorylation of the transcription factors SMAD1/5/8 (Chen and Massagué, 1999; Oh et al., 2000), leading to their association with the common regulator SMAD4 (Nakao et al., 1997). Then, the SMAD complex translocates and accumulates into the nucleus (**Figure 1**) in order to regulate the expression of specific target genes such as DNA-binding protein inhibitor 1 (*ID1*) and *ID3* (Valdimarsdottir et al., 2002). For example, the BMP9/ALK1 signaling pathway regulates angiogenesis by modulating the expression of genes involved in vascular quiescence, cell junction, response to shear stress, and the recruitment of mural cells.

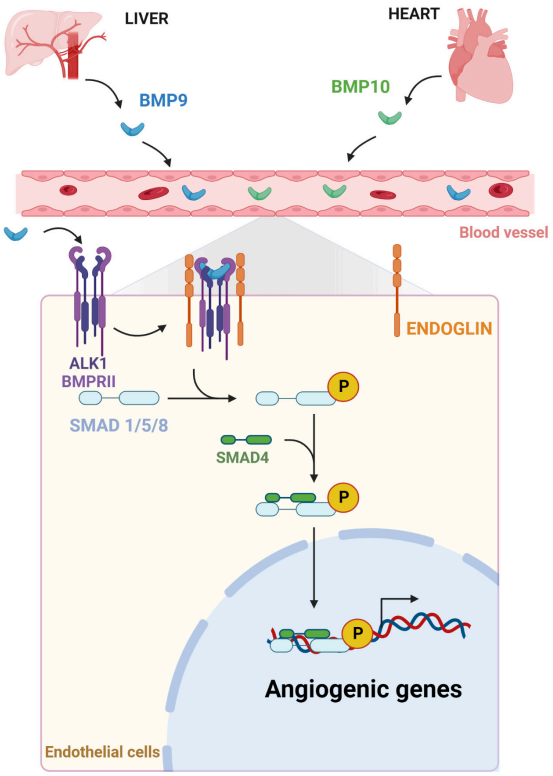

FIGURE 1
Endothelial BMP/ALK1 signaling pathway. Soluble BMP9 and BMP10, secreted, respectively, by the liver and the heart in the bloodstream, bind their receptor ALK1, a SER/THR kinase, and its coreceptors BMPRII and ENDOGLIN at the surface of ECs. The activation of the BMP receptor complex will trigger the downstream SMAD signaling. Phosphorylated SMAD1/5/8 will recruit SMAD4. This SMAD complex accumulates in nucleus to regulate transcription of target genes, including genes involved in angiogenic processes.

HHT patients can be subdivided into five groups. Mutations in the *ENG* gene (encoding for ENDOGLIN) are responsible for HHT1 (McAllister et al., 1994), while mutation of *ACVRL1* (encoding for ALK1) leads to HHT2 (Johnson et al., 1996). HHT1 and HHT2 represent around 90% of HHT cases (Prigoda et al., 2006). Moreover, mutations of *SMAD4* represent 2% of a

Abbreviations: ACVRL1, Activin A receptor like type 1; AVF, Arteriovenous fistulas; AVM, Arteriovenous malformations; bAVM, Brain AVM; BBB, Blood-brain-barrier; BMP, Bone Morphogenetic Protein; CK2, Casein Kinase 2; CNS, Central nervous system; CVM, Capillary vascular malformation; EC, Endothelial cell; ENG, Endoglin; HHT, Hereditary hemorrhagic telangiectasia; JP-HHT, Juvenile polyposis-HHT; LSS, Laminar Shear Stress; NVU, Neurovascular unit; PC, Pericyte; PDGF, Platelet-derived growth factor B; PDGFR, Platelet-derived growth factor B receptor; PNVP, Perineural vascular plexus; SMC, Smooth muscle cells; TGFβ, Transforming growth factor β; VEGF, Vascular endothelial growth factor; VEGFR, Vascular endothelial growth factor receptor.

type of HHT called juvenile polyposis (JP)-HHT (Howe et al., 1998; Gallione et al., 2004). Finally, loci on chromosomes 5 and 7, unlinked to *ENG*, *ACVRL*1, or *SMAD4* mutations, have been associated with subsets of HHT patients and have been referred to as HHT3 and HHT4, respectively (Cole et al., 2005; Bayrak-Toydemir et al., 2006), while HHT features (HHT5) have also been observed in individuals with heterozygous mutations of growth differentiation factor 2 (GDF2), which encodes BMP9 (Wooderchak-Donahue et al., 2013). It should be noted that the vascular phenotype varies depending on the mutated HHT genes but also on the individual. Indeed, mutations in the same gene can trigger different vascular anomalies from one patient to another, suggesting context-dependent pathogenicity of vascular malformations (Kjeldsen et al., 2005; Bayrak-Toydemir et al., 2006).

This review will focus on HHT bAVMs and summarize recent advances in organotypic pathogenicity, animal models, cellular and molecular mechanisms, and therapeutics.

Cerebral arteriovenous malformation anatomy

Brain vasculature

The blood supply of the human brain relies on only two pairs of large arteries: the internal carotids, which supply the blood to the cerebrum, and the vertebral arteries, which join distally to form the basilar artery, and finally vascularize the cerebellum and the brain stem. Proximally, the basilar artery and the internal carotid arteries join to form a ring at the brain's base known as the circle of Willis.

The circle of Willis gives rise to three pairs of main arteries: the anterior, middle, and posterior cerebral arteries, which divide progressively into smaller arteries and pial arterioles within the brain's subarachnoid space meninges. Then, penetrating arterioles dive into the cortex and divide into precapillary arterioles and capillaries, the most predominant brain vessels. Similarly, the pial venular network from the brain surface is connected to ascending venules diving into the parenchyma, followed by postcapillary venules, which branch to capillaries.

Even if human brain vascularization is well described, its development is based on studies done in animal models, such as rodents. Comprehensive studies on the mouse brain showed that vascularization starts at embryonic day (E) 7.5–8.5 by vasculogenesis at the ventral region of the neural tube, followed by the invasion of capillary sprouts into the neuroepithelium at E9.5 (Hogan et al., 2004). Branching and arborization of capillary sprouts from the pial surface subsequently lead to the formation of the perineural vascular plexus (PNVP) at the brain's surface (Tata et al., 2015; Biswas et al., 2020). Then, the first sprouts of the PNVP invade the ventrolateral forebrain following an angiogenic gradient of Vascular Endothelial Growth Factor (VEGF) induced by the hypoxic tissue at postnatal day (P) 9.5 (Bautch and James, 2009; Tata et al., 2015; Peguera et al., 2021). The vascularization will then continue to invade the tissue in a ventrolateral to dorsomedial fashion by angiogenesis, the growth of pre-existing blood vessels. The cerebral vascular network is still expanding and remodeling for a few weeks after birth (Biswas et al., 2020). While canonical pro-angiogenic signaling pathways, such as VEGF, WNT, and TGFß, are essential, mechanisms controlling this postnatal angiogenesis wave remain unclear (Paredes et al., 2018). Neo-angiogenic sprouts and EC proliferation are observed until P14. Then, from P14 to P25, a progressive decrease in the angiogenic rate will favor the stabilization of the vasculature (Biswas et al., 2020; Coelho-Santos and Shih, 2020). Moreover, the capillary density varies depending on the brain region. Indeed, the angiogenesis rate is far higher in gray matter, enriched in neuronal cell bodies, than in white matter to supply the energy needed (Coelho-Santos and Shih, 2020).

The ECs lining vessels have developed a unique and highly selective BBB to maintain brain homeostasis and neural function (Daneman and Prat, 2015). This organotypic feature of the CNS capillaries depends on the interaction and communication between the neurovascular unit (NVU) cells, which includes ECs, pericytes (PCs), astrocyte endfeet as well as neurons (Siegenthaler et al., 2013; Kaplan et al., 2020). In the mouse, brain angiogenesis begins at E9.5-E11.5, and the initiation of BBB starts soon after (Biswas et al., 2020). ECs acquire both paracellular and transcellular barriers to prevent the movement of small molecules between ECs (Daneman and Prat, 2015; Biswas et al., 2020). The endothelial BBB is characterized by abundant tight junctions (paracellular barrier) and a low rate of endocytosis (transcellular barrier) to control passive exchanges and caveolae-dependent receptor-mediated transcytosis. Therefore, the BBB allows a high control of the nutrient exchange, low permeability, and immune privileges (Siegenthaler et al., 2013; Daneman and Prat, 2015; Haddad-Tóvolli et al., 2017).

Brain AVMs anatomy

A healthy blood vascular network has capillary plexuses between arteries, a high flow region, and veins, a low flow region. Capillaries are essential for the delivery of oxygen and nutrients. Therefore, neurovascular coupling, the blood flow regulation by neurons, is essential for neuronal function (Kaplan et al., 2020). The main characteristic of AVM is a direct connection between veins and arteries, bypassing the capillary bed. The loss of capillaries in bAVMs leads to cerebral hemodynamic changes with the increased blood flow in the arteries and veins. Thus, bAVMs are considered high-flow vascular malformations. bAVMs are also characterized by one or several feeding arteries

and one draining vein. Moreover, bAVMs are associated with ECs proliferation and mural cell coverage defects.

There are different types of bAVMs defined by specific features (Matsubara et al., 2000): arteriovenous fistulas (AVF), nidal AVMs, and capillary vascular malformations (CVM). AVFs correspond to direct fistula connections between one artery and one vein, whereas nidal AVMs and CVMs are characterized by the presence of a nidus, defined as tangles of abnormal blood vessels. Nidal AVMs have a nidus between 1 and 3 cm with multiple feeding arteries and veins, whereas the nidus of CVM is less than 1 cm and has one feeding artery and vein (Matsubara et al., 2000; Griauzde et al., 2020). Patients with AVF and nidal AVM have more chance of rupture risk and may present symptoms such as seizure, hemorrhage, and headache, whereas most patients with CVM are asymptomatic (Matsubara et al., 2000; Brinjikji et al., 2017). The different types of bAVMs can also be discerned by the age of the patients. Indeed, AVFs are observed in young children, whereas nidus AVMs and CVMs develop later in life (Matsubara et al., 2000; Krings et al., 2005).

Even if the different AVMs have different characteristics, no differences in the localization in the brain have been reported (Krings et al., 2005). AVMs are located mostly in superficial regions of the cerebral cortex, with a majority in the supratentorial region compared to the infratentorial region. However, very few AVMs can be found in deeper areas such as the basal ganglia or brain stem (Matsubara et al., 2000; Saleh et al., 2013; Komiyama et al., 2015; Krings et al., 2015).

Consequences and symptoms of brain AVMs

Most bAVMs are asymptomatic, and the diagnosis is often made by brain imaging after hospitalization or examination for another medical reason. However, some patients may develop symptoms such as headaches, seizures, and hemorrhages (Brown et al., 1996). In addition, it seems that there is a correlation between the hemodynamic changes, the patients' age, and the AVM's cerebral location (Gross and Du, 2013; Abecassis et al., 2014). The exact causes of seizures are not yet well understood. However, frontal or temporal lobe locations of AVMs are associated with a higher risk of seizure compared to a deep location (Hoh et al., 2002). In addition, it also appears that hemodynamic changes may influence the occurrence of seizures (Fierstra et al., 2011).

The risks of hemorrhage may be increased by the position of the AVM in the brain, with a deep location having a higher risk of rupture (Yamada et al., 2007). However, the bAVMs found in HHT patients predominantly have a cortical area and therefore have a relatively low risk of rupture (around 2% per year) (Willemse et al., 2000). Moreover, it has also been documented that the size of the AVM and its association with aneurysms may also influence the risk of hemorrhage (Gross and Du, 2013). The high blood pressure generated by bAVM may also increase the risk of rupture (Langer et al., 1998). Hemorrhage after bAVM rupture leads to mortality or morbidity development (Fleetwood and Steinberg, 2002). Indeed, it has been shown that patients with hemorrhagic bAVMs have a higher risk of subsequent epileptic seizure (Josephson et al., 2011).

However, mechanisms that lead to the development of those symptoms are not yet well understood, mainly because only a few patients develop cerebral symptoms, the distribution of these symptoms are heterogeneous among patients, and the lack of experimental models.

Animal models of hereditary hemorrhagic telangiectasia

Mouse models

It is crucial to develop animal models that recapitulate HHT pathophysiology to improve our knowledge of AVMs' pathogenesis and reveal new therapeutic avenues. Several studies have used new sophisticated models to decipher AVM mechanisms in the last two decades, as summarized below (Tual-Chalot et al., 2015).

Three transgenic mouse models with global knockout for *Eng* were first developed in order to recapitulate HHT1 (Bourdeau et al., 1999; Li et al., 1999; Arthur et al., 2000). These mice show marked defects in yolk sac angiogenesis and cardiac development, leading to lethality at E10.5. Similarly, global knockout mice for *Acvrl1* have been developed to study HHT2 (Oh et al., 2000; Urness et al., 2000; Srinivasan et al., 2003). These mice also die around E10.5 with pronounced angiogenic defects. Indeed, mutant embryos exhibit hyperdilated vessels and the formation of arteriovenous shunts. The embryonic lethality of these mutant mice highlights the importance of the BMP/ALK1/ENG signaling pathway in vascular development and morphogenesis but makes it challenging to study the mechanisms underlying these angiogenic defects. Thus, the following studies were carried out on heterozygous mice. In addition, to be viable, these models are closer to HHT physiopathology, as HHT patients also carry heterozygous mutations (Srinivasan et al., 2003; Torsney et al., 2003). Moreover, heterozygous mutant mice display some features found in patients, such as mucocutaneous vascular lesions in internal organs, such as lungs, liver, spleen, and intestines. However, these mice develop very few cerebral AVMs at a lower frequency than that found in patients.

The creation of inducible and tissue-specific mutant mice was crucial for the investigation of the role of key genes in developmental and pathological processes. Reporter mice have shown that ALK1 and ENG are mainly expressed in ECs of blood vessels (Jonker and Arthur, 2002; Seki et al., 2003). In line with these findings, the endothelial-specific *Acvrl1* deletion

is sufficient to trigger blood vessels dilation, hemorrhages and AVMs in the brain, lungs and intestine (Park et al., 2009). However, endothelial mutant mice showed improved survival until postnatal day 5 compared to global KO which induces embryonic lethality. New inducible and endothelial-specific models allowed studying AVMs in postnatal mice. Interestingly, an early postnatal endothelial-specific deletion of *Eng* or *Acvrl1* is sufficient to induce an HHT-like phenotype, including AVM (**Table 1**; Allinson et al., 2007; Park et al., 2008, 2009; Mahmoud et al., 2010). However, the deletion of *Eng* in perivascular smooth muscle cells does not promote arteriovenous shunt formation, in line with its expression profile (Garrido-Martin et al., 2014). Altogether, these findings revealed the essential role of ECs in the pathogenesis of HHT. These models also confirmed the hypothesis that a second hit is necessary to induce AVM in HHTs, also known as the three events hypothesis (Tual-Chalot et al., 2015). This refers to the fact that 3 stimuli are necessary for AVM formation: gene loss, protein loss, and then an angiogenic stimulus. While an early endothelial deletion of *Eng* and *Acvrl1* promotes AVMs formation in the angiogenic context of developing tissues, the deletion in adults is not sufficient unless there is an angiogenic or inflammatory stimulus. Indeed, local injection of VEGF or LPS following an endothelial *Acvrl1* or *Eng* deletion induces several vascular anomalies including bAVMs in adult mice (Walker et al., 2011; Choi et al., 2012, 2014; Han et al., 2014). In addition, AVMs also develop in the skin of adult *Acvrl1* mutant mice when angiogenesis is induced with a wound, proving the necessity of an angiogenic hit for AVM formation (Park et al., 2009).

In patients, heterozygous mutations in *Smad4* lead to JP-HHT, but the mechanisms are still poorly understood. Similar to *Acvrl1* and *Eng* knockout mice, a global loss of *Smad4* results in lethality at the E10.5 (Lan et al., 2007). Constitutive endothelial *Smad4* deletion decreases blood vessel integrity and leads to cerebral bleeding, specifically during embryonic development (Li et al., 2011). In addition, postnatal loss of *Smad4* induces the formation of AVMs in the retina, brain, and gastrointestinal tract, phenocopying vascular phenotypes observed in endothelial *Acvrl1* and *Eng* mutant mice (**Table 1**; Ola et al., 2018).

Mutations in the GDF2 gene are responsible for less than 1% of HHTs (Wooderchak-Donahue et al., 2013; Hernandez et al., 2015). In mice, injection of antibodies blocking both BMP9 and BMP10 has been shown to phenocopy endothelial *Eng*, *Acvrl1*, and *Smad4* mutant mice to some degree, with AVM formation in the retina and the gastrointestinal tract, suggesting that it could be a model of HHT (**Table 1**; Baeyens et al., 2016; Ola et al., 2016; Ruiz et al., 2016, 2020). Moreover, while deletion of either *Gdf2* or *Bmp10* does not promote vessel dilatation and AVM formation (Ricard et al., 2012), postnatal double *Gdf2* and *Bmp10* deletion induces vascular anomalies, including AVMs in the gastrointestinal tract (Bouvard et al., 2021).

Recently, new genetic tools have been developed to delete genes in specific EC subtypes, such as capillaries, veins, arteries, and tip cells, to study the onset and progression of AVMs. Therefore, it has been shown that deletion of *Eng* (Singh et al., 2020), *Smad4* (Lee et al., 2021), and *Acvrl1* (Park H. et al., 2021) in venous ECs is sufficient to induce AVMs, unlike deletion in other EC subpopulations (**Table 1**). The underlying mechanisms will be discussed in later sections.

Despite the development of new mouse models, the study of bAVMs remains complicated due to their 3D structure and unpredicted location in the brain. Therefore, many studies have been performed on the retina which has a vascular network growing in 2D that can be imaged in wholemount. Moreover, retina and brain blood vessels share numerous features including the NVU and Blood Retina Barrier (BRB). The retina is a part of the central nervous system and is a well-established model for studying angiogenic processes such as endothelial sprouting, arterio-venous specification, and vascular remodeling (Adams and Alitalo, 2007; Fonseca et al., 2020). In mice, the vascularization of the retina starts at birth, and blood vessels grow from the optic nerve to the periphery until P7 to form a superficial vascular plexus. Then, blood vessels dive into the neuroretina to form the deep vascular plexus until P12, followed by the formation of the intermediate plexus until P15, and the vascular network is completed and fully mature at P21 (Gariano and Gardner, 2005). Compared to the brain, the superficial retinal plexus is a stereotypic vascular network that can be imaged by wholemount, allowing the study of complex vascular structures such as AVMs. Therefore, we and others have shown that endothelial deletion of *Eng*, *Acvrl1*, or *Smad4* induces AVMs in mouse retinas, which has greatly improved our understanding of the mechanisms involved in the pathogenesis (Mahmoud et al., 2010; Tual-Chalot et al., 2014; Baeyens et al., 2016; Ola et al., 2016, 2018; Crist et al., 2018).

All this work shows that endothelial deletion of *Eng*, *Acvrl1* and *Smad4* are appropriate models to study pathology. In the retina, in addition to the formation of AVMs, mutants show an increase in EC sprouting, proliferation, and vessel dilatation. Mural cells are also affected with a decrease in pericyte coverage on the one hand and arterialization of the veins on the other with the recruitment of vascular smooth muscle cells (vSMC). However, despite some degree of similarity in the vascular phenotype, these mutant mice also present distinct phenotypes. For example, 60% of *Acvrl1* mutants develop AVMs in the retina (Tual-Chalot et al., 2014), whereas this percentage is around 70 and 82% in *Eng* and *Smad4* mutants, respectively (Mahmoud et al., 2010; Crist et al., 2018). Moreover, both *Eng* and *Smad4* mutants exhibit a delay in vessel outgrowth but not *Acvrl1* mutants. *Acvrl1* mutants show a hyperbranching more pronounced than *Eng* and *Smad4* mutants, which is associated with a strong increase

TABLE 1 Summary of the major HHT mouse models.

Target genes	Deletion site	CRE-line	Brain/Retina phenotype	Other phenotype	References
Eng	All cell type	–	–	Homozygous deletion: Lethality at E.10 - E.10.5/Altered angiogenesis in the yolk sac/Defects in cardiac development	Bourdeau et al., 1999; Li et al., 1999; Arthur et al., 2000; Torsney et al., 2003
				Heterozygous deletion: Viable/Telangiectasia in the nose, mouth and ears/Hemorrhages/Subcutaneous AVMs	
Acvrl1	All cell type	–	–	Homozygous deletion: Lethality at E.10 - E.10.5/Angiogenesis defect/Vessel hyperdilatation/Arterio-venous shunt	Oh et al., 2000 Urness et al., 2000; Srinivasan et al., 2003
				Heterozygous deletion: Viable/Cutaneous, mucocutaneous and internal organ vascular defects (Vessel dilatation)	
Eng	Endothelial cell	*Cdh5-CRE^{ERT2}*	Postnatal deletion: Dense capillary plexus increase ECs proliferation and AVMs formation in the retina.	Adult deletion: Angiogenesis defect in subdermal matrigel assay with vessel dilatation	Mahmoud et al., 2010
Eng	Endothelial cell	*Scl-CRE^{ERT2}*	–	Adult deletion: AVMs formation after skin injury	Garrido-Martin et al., 2014
Eng	Venous and capillary endothelial cell	*Apj-CRE^{ERT2}*	Postnatal deletion: AVMs formation in retina	–	Singh et al., 2020
Acvrl1	Endothelial cell	*Scl-CRE^{ERT2}*	–	Adult deletion: AVMs formation after skin injury, in gastrointestinal tract and hemorrhages in caecum	Garrido-Martin et al., 2014
Acvrl1	Endothelial cell	*Cdh5-CRE^{ERT2}*	Postnatal deletion: Hyperbranching, ECs proliferation and AVMs formation	Postnatal deletion: Lung hemorrhages	Tual-Chalot et al., 2014
				Adult deletion: Ceacal hemorrhages	
Acvrl1	Endothelial cell	*Pdgfb-CRE^{ERT2}*	Adult deletion: bAVMs formation after VEGF stimulation	–	Chen W. et al., 2014
Acvrl1	Venous and capillary endothelial cell	*Mfsd2a-CRE^{ERT2}*	Postnatal deletion: brain and retinal AVMs	Postnatal deletion: Gastrointestinal AVMs	Park H. et al., 2021
Acvrl1	Arterial endothelial cell	*Bmx-CRE^{ERT2}*	Post-natal deletion: no AVMs in brain or retina	–	Park H. et al., 2021
Acvrl1	Tip cell	*Esm1-CRE^{ERT2}*	Post-natal deletion: Vascular malformation in retina and brain but no AVM	Post-natal deletion: AVMs in intestinal villi and mesenteries	Park H. et al., 2021
Smad4	Brain endothelial cell	*SP-A-CRE*	Embryonic deletion: brain hemorrhages, BBB breakdown and ECs proliferation	–	Li et al., 2011
Smad4	Endothelial cell	*Cdh5-CRE^{ERT2}*	Postnatal deletion: bAVMs and retinal AVMs associated with ECs proliferation and change in arterio-venous identity	Postnatal deletion: Gastrointestinal AVMs	Ola et al., 2018
Smad4	Venous endothelial cell	*Gm5127-CRE^{ERT2}*	Postnatal deletion: AVMs formation in retina with ECs proliferation	–	Lee et al., 2021
Bmp9/10	Blood circulation (Blocking Ab)	–	Postnatal deletion: Hypervascularization and AVMs formation in the retina	–	Ruiz et al., 2016; Baeyens et al., 2016; Ola et al., 2016
Eng	Smooth muscle cell	*Myh11-CRE^{ERT2}*	Adult deletion: No AVM formation	Adult deletion: No AVM formation	Garrido-Martin et al., 2014
Acvrl1	Smooth muscle cell	*Myh11-CRE^{ERT2}*	Adult deletion: No AVM formation	Adult deletion: No AVM formation	Garrido-Martin et al., 2014
Acvrl1	Smooth muscle cell	*Tagln-CRE*	Embryonic deletion: AVM formation in the brain and microhemorrhages	–	Han et al., 2021

in the number of tip cells. However, it should be noted that the dose of tamoxifen used and the age of the mice at time of injection could also influence these differences. Further investigation is required to accurately compare vascular phenotypes of those models.

Overall, these new transgenic mouse models showed that the BMP/ALK1/ENG/SMAD4 signaling pathway is essential for both developmental and adult vascular morphogenesis. Indeed, in addition to AVMs, the postnatal endothelial deletion of *Eng*, *Acvrl1*, and *Smad4* are lethal, and survival varies depending on the gene and age.

Zebrafish models

Zebrafish also represent an important model for studying bAVMs. First, because of the high degree of homology between zebrafish and vertebrates regarding vasculature and angiogenic mechanisms (Schuermann et al., 2014). Secondly, thanks to the transparency of the embryos it is easy to follow the vasculature and the development of vascular malformation using fluorescence imaging. Finally, the facility to perform genetic mutations makes the zebrafish an essential model for studying vascular development and disease. *acvrl1* mutation in zebrafish induces cranial vessel defects and enlargement, ultimately leading to the formation of AVMs with direct connections between the basilar and basal communicating arteries with the primordial midbrain and hindbrain veins (Roman et al., 2002; Corti et al., 2011). Moreover, *bmp10* mutants phenocopy *acvrl1* mutants, with vessel enlargement, increase of ECs number and formation of direct connection between arteries and the midbrain and hindbrain veins (Laux et al., 2013). Indeed, *bmp10* mutants exhibit blood vessel abnormalities in liver, heart dysmorphology, vascular defects correlating with increased cardiac output and embryonic lethal cranial AVMs indistinguishable from *acvrl1* mutants (Capasso et al., 2020), highlighting that in zebrafish, *bmp10* encodes the only required Alk1 ligand in the juvenile-to-adult period. By contrast, *bmp9* mutants survive to adulthood and do not develop cranial AVMs (Capasso et al., 2020), although they do display transient remodeling defects of the caudal venous plexus (Wooderchak-Donahue et al., 2013). Recently, Sugden et al. (2017) have shown that zebrafish mutated for *eng* at the embryonic stage survive, whereas they develop AVM-like vascular defects. The authors also showed that loss of *eng* in adults leads to dilation of cerebral vessels, and that only induction of an angiogenic hit through fin amputation lead to bAVM formation (Sugden et al., 2017). Finally, the contribution of Smad signaling in AVM formation was also highlighted in zebrafish by a study showing that *Smad9* morphants develop cranial AVMs with morphologic similarities to human bAVMs (Walcott et al., 2018).

Hereditary hemorrhagic telangiectasia and BMP/ALK1 signaling pathway

AVMs develop in high blood flow regions and are often associated with vascular proliferation. The ECs lining blood vessels are exposed to blood flow which induces mechanical forces. The generated laminar shear stress (LSS), within the physiological range, triggers a number of flow responses in EC, including PI3K/AKT signaling pathway activation, alignment in the direction of flow (Tzima et al., 2003; Coon et al., 2015), migration against the blood flow (Parmar et al., 2006; Ouarné et al., 2021), inhibition of proliferation (Akimoto et al., 2000), and PCs recruitment (Van Gieson et al., 2003). Therefore, LSS is essential for blood vessel integrity, vascular remodeling, and morphogenesis. Recent studies have demonstrated an essential role for the BMP/ALK1/ENG signaling pathway in the LSS-induced PI3K/AKT activation and vascular quiescence (Laux et al., 2013; Ola et al., 2016, 2018; Jin et al., 2017). Indeed, PI3K/AKT signaling pathway is an important regulator of EC proliferation (Graupera and Potente, 2013), and it can be inhibited to promote vascular quiescence. Therefore, the understanding of the BMP/ALK1/ENG-LSS crosstalk could allow the identification of new therapeutic strategies.

Cellular and molecular regulation of hereditary hemorrhagic telangiectasia arteriovenous malformations

HHT1: *ENG* mutation

Angiogenic ECs express high levels of *Eng* in development and disease, whereas its expression is attenuated in adult quiescent endothelium (Miller et al., 1999; Jonker and Arthur, 2002; Torsney et al., 2002). Moreover, *Eng* depletion inhibits TGFβ-induced proliferation arrest *in vitro* and *in vivo*, resulting in hyperproliferation and migration defects (Park et al., 2013).

In endothelial *Eng* mutant mice mimicking HHT1, 70% of retinas develop multiple AVMs and bleeding. These retinas also exhibit several other vascular anomalies, such as increased vascular branching, sprouting, vessel diameter, and endothelial proliferation (Mahmoud et al., 2010). Loss of *Eng* induces arterial and venous identity defects, and it can also be noted that AVMs are positive for venous markers such as EPHRIN B4 (*EphB4*) and APELIN receptor (*AplnR*). Blood flow was shown to promote the association of ALK1 and ENG at the EC membrane, thereby enhancing BMP signaling and vascular quiescence (Baeyens et al., 2016). A recent study showed that *Eng* mutant ECs fail to migrate against the flow and exhibit an increase in VEGF-induced PI3K/AKT activation (Jin et al., 2017). Inhibition of VEGFR2 or PI3K/AKT signaling decreased the number of AVMs in *Eng* mutant retinas. In addition, the

authors also showed that *Eng* mutant ECs tend to proliferate mainly in arteries. One study in which *Eng* was specifically deleted only in capillaries and veins but not in arteries (Singh et al., 2020) showed that these mice still have AVMs in the retinas, suggesting that the loss of *Eng* in arteries is not involved in the development of AVMs. Similar observations have been made in zebrafish, where *eng* mutations lead to the formation of AVMs with an increase in vessel diameter (Sugden et al., 2017) caused by defects in flow response and cell polarization leading to vessel enlargement. The role of *Eng* in the flow response and the pathogenesis of AVMs, therefore, appears to be a conserved process. Altogether, these studies demonstrate that *Eng* is essential for EC specification, migration against the flow, and shear stress-induced quiescence to prevent AVMs formation.

HHT2: *ACVRL1* mutation

In the HHT2 mouse model, the endothelial *Acvrl1* deletion induces an increase in vascular density, endothelial sprouting as well as the formation of AVMs in the retina (Park et al., 2009; Larrivée et al., 2012; Ola et al., 2016). Similar to HHT1 models, endothelial *Acvrl1* deletion decreases PC recruitment, arterial marker expression such as JAGGED1, and AVMs are positive for the venous marker EPHRIN B4. Interestingly, retinal shunts develop near the optic nerve in high flow regions, while hyperbranching and hypersprouting develop mainly at the migration front, a low flow region (Bernabeu et al., 2014; Baeyens et al., 2016). These data suggest that, like the HHT1 models, LSS is important in the development of HHT2's AVMs. Moreover, several studies in zebrafish have shown that *acvrl1* expression is induced by blood flow (Corti et al., 2011; Laux et al., 2013). *acvrl1* deletion also decreased the expression of genes involved in the flow-response, such as *Edn1* and *Cxcr4*. However, the expression of *Klf2*, a transcription factor essential for the endothelial flow-response (Parmar et al., 2006), is not altered. Although endothelial *Acvrl1* inhibition promotes arterial enlargement associated with an increase in the number of ECs, a recent study showed AVMs formation requires mutant capillary and venous and not arterial ECs (Park H. et al., 2021). While arterial-specific *Acvrl1* deletion did not induce obvious vascular phenotypes and lethality, deletion in venous ECs results in retinal AVMs and is lethal 5–6 days after gene deletion. Moreover, *Acvrl1* inhibition in endothelial tip cells, cells leading vascular sprouts and arteries formation (Xu et al., 2014; Pitulescu et al., 2017), failed to induce retinal AVMs (Park H. et al., 2021). However, these mutant mice develop capillary malformations in the retina, intestinal villi, and brain, and they die 10–11 days after tamoxifen injection, suggesting that they might develop AVMs in other tissues. Therefore, Park H. et al. (2021) proposed that HHT2's AVMs originate from defective venous ECs. Indeed, mutant ECs present a polarization defect and migrate randomly instead of being directed against the blood flow. This phenomenon has also been observed in the zebrafish model (Rochon et al., 2016).

Skin biopsies of HHT2 patients showed an increase in the PI3K/AKT pathway suggesting an involvement of this pathway in AVM formation (Alsina-Sanchís et al., 2018). *In vitro*, BMP9 stimulation blocks VEGF-induced EC proliferation, and this effect is lost with the *ACVRL1* knockdown. Moreover, inhibition of *ACVRL1* increased VEGF-induced VEGFR2 activation and AKT phosphorylation (Ola et al., 2016; Alsina-Sanchís et al., 2018). While VEGFR2 is the main VEGF receptor that mediates VEGF-induced EC proliferation and angiogenesis, VEGFR1 cannot transduce VEGF signaling and acts as a decoy receptor. Therefore, VEGFR1 traps VEGF ligand, and VEGFR1 inhibition increases VEGF bioavailability and signaling. Interestingly, patients and mouse models of HHT2 show decreased VEGFR1 expression. Thalgott et al. (2018) have recently shown that blocking VEGFR1 induces retinal AVMs in a VEGFR2-dependent manner. In addition, VEGFR2 inhibition, using DC101 blocking antibody, can also rescue the formation of AVMs, as well as hypersprouting and hyperbranching, in *Acvrl1* mutant retinas highlighting that exacerbated VEGF signaling is associated with AVM formation in *Acvrl1* mutant models (Ola et al., 2016).

Pharmacological or genetic inhibition of the PI3K/AKT signaling pathway also rescues EC proliferation and AVMs in *Acvrl1* mutant mice (Ola et al., 2016; Alsina-Sanchís et al., 2018), demonstrating the contribution of this signaling pathway in the development of AVMs. PTEN is a phosphatase that negatively regulates the PI3K/AKT pathway by modulating the phosphatidylinositol 3,4,5-trisphosphate (PIP3) conversion into phosphatidylinositol 4,5-bisphosphate (PIP2) (Graupera and Potente, 2013). *In vitro* studies have shown that BMP9/ALK1 signaling increase PTEN activity in ECs, thereby decreasing PI3K/AKT signaling (Ola et al., 2016; Alsina-Sanchís et al., 2018). However, while the loss of endothelial PTEN in ECs increases EC proliferation and induces retinal vascular hyperplasia, it does not induce AVM formation (Serra et al., 2015).

LSS-induced EC polarity and migration are regulated by integrin binding to extracellular matrix proteins and signaling to CDC42 (cell division control protein 42 homolog) (Etienne-Manneville and Hall, 2001; Tzima et al., 2003). Integrins are transmembrane receptors that allow the adhesion of ECs to the extracellular matrix, which is an important process for angiogenesis (Serini et al., 2008). Some integrins interact with VEGFR2 at the EC membrane regulating its activity and the activation of the PI3K/AKT and YAP/TAZ signaling pathways. A recent study showed that *Acvrl1* deletion increased the expression of integrin β1, α5, and αv in AVMs (Park H. et al., 2021). They also found an increase in the integrins-VEGFR2 interaction and the YAP/TAZ signaling pathway activation. In addition, pharmacological inhibition of integrins or YAP/TAZ signaling prevents the formation of AVMs as well as the endothelial polarization defects in *Acvrl1* mutant mice.

All these studies demonstrate that BMP9/ALK1 signaling is essential to control LSS-induced EC quiescence and polarity *via* the VEGFR2-integrins complex and the activation of downstream signaling pathways, such as PI3K/AKT and YAP/TAZ.

JP-HHT: *SMAD4* mutation

In the mouse model of JP-HHT, postnatal endothelial *Smad4* deletion induces retinal AVMs and hypersprouting, as observed in the *Acvrl1* and *Eng* mutant mice (Crist et al., 2018; Ola et al., 2018). However, the authors found a vascular outgrowth defect that was also found in the HHT1 models but not in the HHT2 model (Crist et al., 2018). Similar to *Acvrl1* and *Eng* deletion, AVMs developed near the optic nerve where blood flow is high, and *Smad4* AVMs originate from defective venous ECs (Lee et al., 2021). In line with its upstream effectors, *Smad4* deletion also increased EC proliferation and PI3K/AKT signaling and inhibited EC migration against the flow, suggesting a similar mechanism in SMAD4 AVMs. Indeed, the inhibition of the BMP9/ALK1/SMAD4 signaling pathway promotes excessive AKT signaling, which inhibits the transcription factor Forkhead box protein O1 (FOXO1) and increases the expression of the proto-oncogene c-MYC (Ola et al., 2018). Ola et al. (2018) proposed that SMAD4 activation regulates Casein Kinase 2 (CK2) expression, which is responsible for PTEN phosphorylation and inhibition. Moreover, CK2 inhibition prevents PI3K/AKT overactivation and the formation of AVMs in *Smad4* mutant mice. These data suggest that the BMP9/ALK1/SMAD4 signaling pathway is essential in venous EC to prevent abnormal PI3K/AKT signaling, proliferation, and LSS-induced migration defect.

In line with these observations, knockdown of receptor-regulated SMADs (R-SMADs) SMAD1 and SMAD5 has also been shown to result in the formation of AVMs. Benn and colleagues reported that endothelial-specific simultaneous deletion of *Smad1* and *Smad5* resulted in the formation of retinal AVMs in areas with high blood flow, while reduced vessel regression and increased loop formation were observed in areas of lower blood flow (Benn et al., 2020). The formation of vascular shunts was also observed in yolk sacs of endothelial-specific *Smad1/5* knockout embryos at E9.25, which occurred in part as a consequence of decreased *Cx37* expression, leading to vessel enlargement and the formation of shunts in vessel segments of higher flow (Peacock et al., 2020). Altogether, these studies further highlight the crucial role of SMAD signaling in preventing AVM development.

Constitutive *Smad4* deletion in brain ECs increased EC proliferation, leading to cerebral hemorrhages (Li et al., 2011). In addition, the authors observed a decrease in NOTCH expression, suggesting a connection between the NOTCH and ALK1/SMAD4 pathways in the maintenance of brain vascular integrity. Interestingly, mutant mouse embryos for NOTCH effectors, such as delta-like-4 (*Dll4)* and Recombination Signal Binding Protein For Immunoglobulin Kappa J Region (*Rbpj*), exhibit bAVMs (Krebs et al., 2004). The involvement of this pathway in bAVM formation is discussed in a later section.

HHT5-BMP9/10

BMP9 and BMP10 signaling have redundant functions in mice during postnatal life, and both ligands have to be inhibited to phenocopy *Acvrl1* and *Eng* mutant mice. Indeed, the injection of BMP9 and BMP10 blocking antibodies in neonatal pups induces retinal AVMs near the optic nerve, as well as hypersprouting and hyperplasia (Baeyens et al., 2016; Ruiz et al., 2016). Moreover, BMP9 inhibition is sufficient to increase PI3K/AKT signaling and proliferation of EC under-flow *in vitro*. Similar to other HHT models, inhibition of the PI3K/AKT or VEGFR2 pathway prevents and rescues EC proliferation and AVMs formation induced by BMP9 and BMP10 blockade (Baeyens et al., 2016; Ola et al., 2016).

Interestingly, sirolimus, an inhibitor of AKT downstream effector mammalian target of rapamycin (mTOR) pathway, can rescue SMAD1/5/8 signaling and AVMs by activating ALK2 in BMP9/10 immunodepleted mice (Ruiz et al., 2020).

Despite the specificities of distinct HHT types, the different mouse models suggest that there is one common mechanism that controls AVM formation. The loss of the BMP/ALK1/SMAD4 signaling pathway in venous ECs leads to an abnormal response to blood flow, including the increase of PI3K/AKT signaling activation and EC proliferation and inhibition of LSS-induced EC polarity and migration against the flow. Then, mutant ECs accumulate in abnormal capillaries, which get enlarged, experience higher blood flow, and acquire venous markers. Whereas arterial ECs might be dispensable, the decrease of NOTCH signaling and arterial marker expression are associated with AVMs. Ultimately, the loss of capillary bed and distinct EC phenotypes forms fragile AVMs (**Figure 2**). Further studies are required to investigate whether this mechanism is conserved in other tissues and humans.

NOTCH signaling and brain AVMs

The NOTCH pathway is a highly conserved cell signaling system involved in cell fate decisions during several developmental processes, including cardiovascular development and neurogenesis. Mammalian cells possess four specific transmembrane NOTCH receptors, NOTCH1, NOTCH2, NOTCH3, and NOTCH4 (Gordon et al., 2008). NOTCH ligands are also transmembrane proteins that are members of the Delta-like and Jagged families in mammals: delta-like-1 (DLL1), DLL3, and DLL4, JAGGED-1, and JAGGED-2 (D'Souza et al., 2008). Upon activation by their specific ligands, NOTCH receptors undergo proteolytic processing, releasing the NOTCH intracellular domain (NICD), which translocates to the nucleus, where it can form a complex

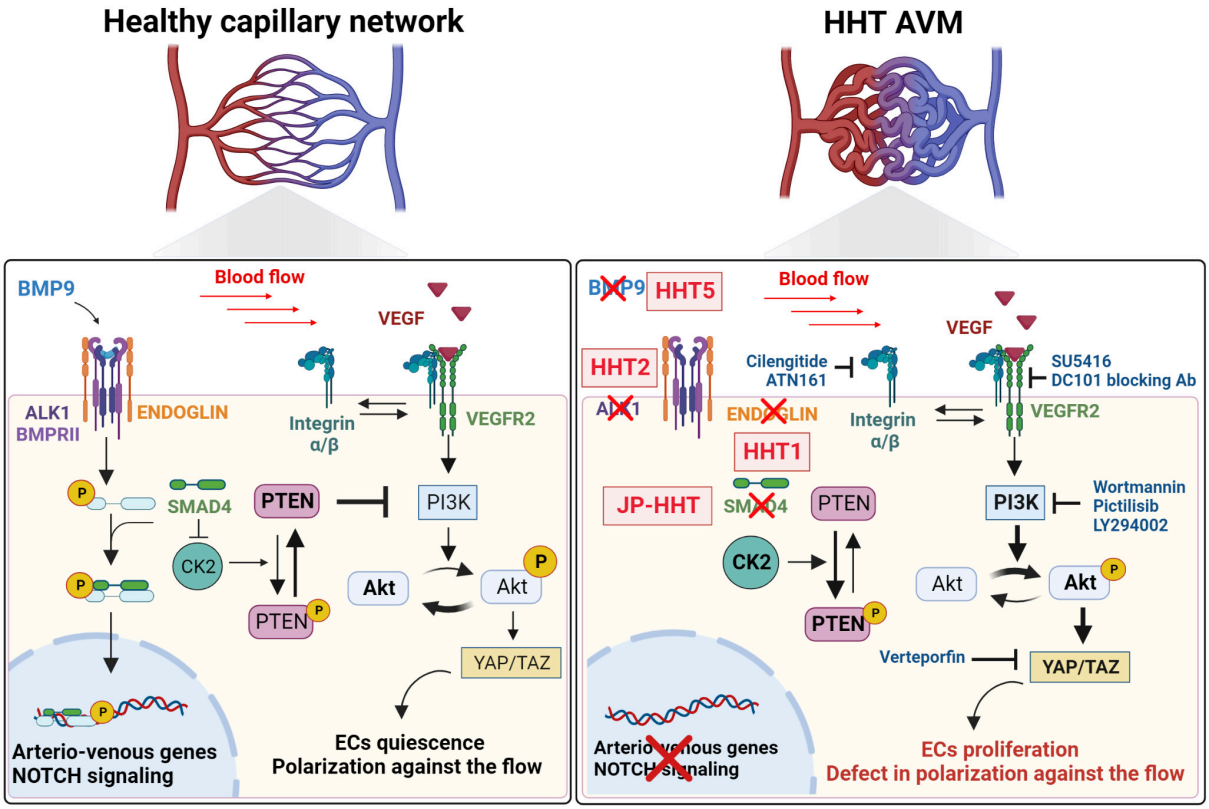

FIGURE 2
Signaling pathways known to be involved in the pathogenesis of AVMs. In healthy capillary networks, blood flow potentiates BMP/ALK1 signaling pathway in ECs to regulate the expression of genes involved in arterio-venous specification and NOTCH signaling pathway. BMP/ALK1/SMAD4 pathway will inhibit blood flow- and VEGFR2-induced PI3K/AKT signaling. Indeed SMAD4 inhibits the expression of CK2, which allows the phosphorylation, and inhibition of PTEN, a negative regulator of the PI3K/AKT signaling, which will promote ECs quiescence and polarization against the flow. HHT1, HHT2, JP-HHT, and HHT5 are induced by *ENG*, *ACVRL1* (ALK1), *SMAD4,* and *GDF2* (BMP9) heterozygous mutations, respectively. CK2 inhibition is removed and its expression increases leading to an enhanced phosphorylation of PTEN which will not be able to inhibit PI3K/AKT signaling induced by blood flow and VEGFR2. Increased AKT phosphorylation leads to higher YAP/TAZ expression and activity, hyperproliferation of ECs and migration defects against the flow.

with the DNA-binding protein RBP-J to initiate transcription of its downstream targets, such as members of the Hairy and enhancer-of-split (HES), and Hairy and enhancer-of-split-related (HEY, HESR, HRT, or CHF) gene families (Castel et al., 2013). NOTCH signaling plays a critical role during vascular morphogenesis, as demonstrated by several studies in which deletion of genes coding for NOTCH receptors, ligands, or downstream effectors results in severe angiogenic defects (Swiatek et al., 1994; Hamada et al., 1999; Xue et al., 1999; Krebs et al., 2000; Domenga et al., 2004; Duarte et al., 2004). Specifically loss of NOTCH signaling has been associated with impaired tip/stalk EC specification in several *in vitro* and animal models (Noguera-Troise et al., 2006; Hellström et al., 2007; Leslie et al., 2007; Suchting et al., 2007). In addition to its roles in sprouting angiogenesis, NOTCH signaling has also been implicated in the specification of artery/vein EC. Indeed, studies have shown that NOTCH signaling induces the expression of several arterial markers and can suppress the expression of venous markers in developing blood vessels (Lawson et al., 2001; Iso et al., 2006; Trindade et al., 2008). As such, both gain-of-function and loss-of-function in NOTCH have resulted in abnormal arterial and venous specification (Lawson et al., 2001; Duarte et al., 2004; Trindade et al., 2008).

The abnormal arteriovenous specification has in several cases been associated with the development of arteriovenous shunts, suggesting a role for NOTCH signaling in the pathophysiology of AVMs. Interestingly, elevated NOTCH signaling has been found in human patients with idiopathic AVMs (ZhuGe et al., 2009, 2013; Yao et al., 2013; Li et al., 2014). Moreover, AVMs have been found in both Notch gain- and loss-of-function animal models, indicating that NOTCH signaling must be tightly regulated in ECs to regulate proper vascular morphogenesis. In mice, the expression of a constitutively active NOTCH4 results in AVMs in the liver, uterus, skin, and brain (Murphy et al., 2008, 2014). Similarly, EC-specific, constitutively active NOTCH1 also results in AVM formation

during embryonic development, suggesting that increased activity of either Notch receptor is sufficient to cause brain AVMs (Krebs et al., 2010). DLL4 overexpression models have also been shown to be prone to AVM formation (Trindade et al., 2008). Conversely, decreased NOTCH signaling has also been associated with the development of AVM lesions. In zebrafish embryos, reduction of NOTCH signaling results in the formation of AVMs (Lawson et al., 2001), while in mouse embryos, both *Dll4* ± and *Rbpj* null embryos exhibit the presence of AVMs (Krebs et al., 2004). Endothelial-specific deletion of *Rbpj* from birth also results in abnormal AV shunting and tortuous vessels in the brain, intestine, and heart of P14 mice (Nielsen et al., 2014).

Several studies have documented the crosstalk between endothelial BMP/ALK1/SMAD and NOTCH signaling pathways during vascular development (Larrivée et al., 2012; Moya et al., 2012; Ricard et al., 2012). Functionally, it was observed that BMP9 stimulation could counteract the effects of NOTCH inhibition using *in vitro* angiogenesis assays as well as mouse models of vascular development (Larrivée et al., 2012). It was also demonstrated that NOTCH target genes are decreased in *Eng*-deficient cells, but that ALK1 overexpression could rescue their expression confirming the regulatory effects of ALK1 on NOTCH signaling (Hwan Kim et al., 2020). Interestingly, activated SMADs can co-immunoprecipitate with NICD to potentiate HEY1 expression, suggesting a direct interaction between components of these signaling pathways (Itoh et al., 2004). Finally, similarly to flow-dependent activation of ALK1 (Baeyens et al., 2016), LSS at an arterial magnitude also activates NOTCH signaling to control arterial specification and ECs quiescence (Fang et al., 2017). These insights suggest that mechanical forces may also contribute to the crosstalk between ALK1 and NOTCH signaling. Taken together, these studies demonstrate that ALK1/BMP/SMAD signaling is an important modulator of NOTCH signaling in ECs.

In contrast to several models of idiopathic AVMs, which display increased NOTCH signaling, AVMs in HHT models tend to display decreased NOTCH signaling. In *Acvrl1* knockout mouse models, the development of AVMs has been associated with reduced *Notch1* and *Jag1* expression (Tual-Chalot et al., 2014). Other components of BMP signaling, which directly affect ALK1 signaling and lead to AVM formation, have also been shown to have decreased Notch signaling. For example, deletion of *Mgp*, which can act as a regulatory protein for BMPs, causes AVM formation in multiple organs partly by modulating *Acvrl1* expression. *Mgp* depletion in ECs upregulated *Acvrl1* expression and, in turn, increased NOTCH signaling in an ALK1-dependent manner (Yao et al., 2011, 2013). On the other hand, other studies did not report alterations in NOTCH signaling following impairment of ALK1 or ENG signaling. In zebrafish, Rochon et al. (2015) showed that AVMs in *acvrl1* mutants arose independently of perturbations in NOTCH signaling, suggesting that it may not be critical for AVM formation in this context. Therefore, the role of NOTCH signaling in HHT pathophysiology still remains unclear, and further evaluations of NOTCH signaling components and downstream targets in AVMs from HHT patients will be needed to offer additional insights into its role in the pathogenesis of these lesions.

Sporadic brain AVMs and RAS signaling

bAVMs found in HHT patients are a familial form with well identified mutations. However, most cases of bAVMs are sporadic, involving somatic mutations mainly associated with RAS signaling, and mechanisms are not well understood.

The MAPK/ERK signaling pathway is also involved in controlling EC proliferation and arteriovenous specification during development. Growth factor receptors, such as EGFR2 or VEGFR2, activate proto-oncogene Rat sarcoma virus proteins (RAS; HRAS, KRAS, and NRAS in humans), which triggers the downstream MAPK/ERK chain, including Rapidly Accelerated Fibrosarcoma (RAF) and Mitogen-activated protein kinase kinase (MEK). Finally, the activated ERK will translocate into the nucleus to regulate the expression of genes involved in cell proliferation (Karar and Maity, 2011; Tan et al., 2013; Simons et al., 2016).

Somatic mutations in the MAPK pathway lead to AVMs formation, such as activating mutations of KRAS, BRAF, or MAPK1/2. Moreover, loss-of-function mutations of RASA1, a negative regulator of RAS signaling, are associated with capillary-malformation arteriovenous malformation (CM-AVM1) and bAVMs in humans (Eerola et al., 2003; Revencu et al., 2008). These AVMs are all characterized by increased ERK phosphorylation and cell proliferation (Eerola et al., 2003; Boon et al., 2005; Couto et al., 2017; Hong et al., 2019).

In mice, overexpression of KRAS in brain ECs specifically leads to the formation of bAVMs, confirming the importance of ECs in the pathogenesis of AVMs (Fish et al., 2020; Park H. et al., 2021). Furthermore, overexpression of KRAS in zebrafish embryos leads to AVMs and increased activity of proteins involved in angiogenesis, such as DLL4 (Al-Olabi et al., 2018; Fish et al., 2020). Interestingly, overexpression of KRAS in mouse cerebral ECs results in overexpression of VEGFR2 expression (Park E. S. et al., 2021). Surprisingly, while *Rasa1* loss of function mice exhibit vascular and lymphatic defects, they did not feature bAVMs (Henkemeyer et al., 1995; Lapinski et al., 2012, 2017; Lubeck et al., 2014; Chen et al., 2019). MEK inhibition decreases the number of shunts induced by KRAS overexpression in brain ECs. Interestingly, inhibition of the PI3K/AKT pathway has no effect (Fish et al., 2020). Therefore, while EC proliferation is a common feature with HHT AVM, mechanisms might differ regarding EC polarity and migration against the flow.

Perivascular cells contribution to brain AVMs

The various HHT models developed in recent years have demonstrated the importance of the endothelial BMP/ALK1 pathway in the pathogenesis of AVMs. However, PCs are also essential for vascular integrity and morphogenesis (Armulik et al., 2011). To control capillary coverage by PCs, ECs express soluble Platelet-derived growth factor B (PDGFB), which activates the PDGF receptor (PDGFR) at the PC membrane. PDGFB deletion induces PC loss and micro aneurysms (Lindahl et al., 1997; Hellström et al., 2001; Lindblom et al., 2003). While AVMs are associated with decreased PC coverage in mice and humans (Chen W. et al., 2013; Winkler et al., 2018), the PC contribution to HHT AVMs remains unclear.

It has been shown that following *Acvrl1* deletion, there was a decrease in the expression of PDGFRB, but not PDGFB, which could explain the defect in PC recruitment (Chen W. et al., 2013). Thalidomide had already been shown to inhibit angiogenesis. The injection of thalidomide, a drug that reduced the severity and frequency of epistaxis in HHT patients, into mice depleted for *Eng* prevented AVMs-induced bleeding and excessive angiogenesis. Interestingly, it also restores PC coverage by increasing PDGFRB levels (Lebrin et al., 2010; Zhu et al., 2018).

These data suggest that PCs may be involved in the onset or progression of AVMs. Recently, it was shown that a PC-specific deletion of *Rbpj* was sufficient to induce the formation of retinal AVMs. Interestingly, the deletion of *Rbpj* in SMC leads to the formation of AVMs in the retina (Nadeem et al., 2020). It was also reported that *Notch1* ±; *Notch3*-/- mice developed AVMs in the retina (Kofler et al., 2015). Notch3 deficiency in this model compromised PC function, which in turn exacerbated EC activation caused by Notch1 haploinsufficiency.

vSMCs are cells found in arteries and veins, and this coverage is also reduced in bAVMs. However, their involvement in the formation of AVMs is controversial. Indeed, in 2014 a study compared the effect of *Acvrl1* and *Eng* deletion in ECs and SMCs using *Scl*-CreER and *Myh11*-CreER driver mice (**Table 1**). The authors showed that only endothelial deletion allowed AVMs formation in a model of injury-induced skin AVMs (Garrido-Martin et al., 2014). However, a recent study showed that deletion of *Acvrl1* in SMCs using *Tagln*-Cre mice induced the formation of bAVMs associated with a better survival of the mice that allows the monitoring of bAVMs formation over time, and to have a pathological model more representative of the patients. However, *Tagln*-CRE can be expressed by some ECs which could be sufficient to induce AVMs. It is therefore possible that *Acvrl1* mosaic deletion in ECs would be the primary cause of these bAVMs over time rather than the deletion in SMCs (Han et al., 2021). Further studies are needed to understand the exact role of SMCs and PCs in developing bAVMs.

Therapeutic perspectives

Currently, treatment options for bAVMs are limited and only based on surgeries: surgical resection, endovascular embolization, and/or stereotactic radiosurgery. Knowing the risk of intracranial hemorrhage (ICH) (which varies from 0.9 to 34.3%), the treatment of unruptured bAVMs has become controversial, as untreated patients' fate may be less morbid than those treated with invasive therapies. Thus, the demand for pharmacologic treatment options is high (Chen W. et al., 2014; Shaligram et al., 2019).

Because of the enhanced angiogenesis associated with bAVMs formation, the most common pharmacologic target is VEGF. The anti-VEGF drug bevacizumab is currently undergoing phase III clinical trial for HHT (NCT 03227263) after showing promising effects on other HHT symptoms such as epistaxis and gastrointestinal bleedings in phase II clinical trials and case reports (Oosting et al., 2009), without showing adverse effects. Altogether, these results suggest that anti-VEGF therapies could represent good alternatives or complements to surgical procedures (Chen W. et al., 2014; Epperla and Hocking, 2015; Snodgrass et al., 2021).

Elucidation of the signaling events associated with HHT has confirmed the contribution of inadequate BMP9/ALK1/SMAD signaling in the formation of bAVMs, and as such, some research was done using tacrolimus, an anti-inflammatory FDA-approved drug, to evaluate whether it could potentiate the activity of the impaired BMP9/ALK1/SMAD pathway present in HHT patients resulting from haploinsufficiency. Indeed, a preclinical study demonstrated that tacrolimus could reduce the development of retinal AVMs in BMP9/10 immunodepleted mice, and it is currently undergoing a clinical trial to evaluate its ability to reduce epistaxis (NCT 03152019) (Robert et al., 2020; Snodgrass et al., 2021).

A better understanding of the signaling pathways inducing bAVMs opens up opportunities for pharmacological treatments using other drugs such as tyrosine kinase inhibitors. Some case reports already showed an improvement of epistaxis and telangiectasia in mostly HHT1 and two patients with different tyrosine kinase inhibitors (Robert et al., 2020; Snodgrass et al., 2021) targeting the VEGFR2 and the ANGPT2 receptor TIE2, which are overactivated in HHT. Thus, two clinical trials are beginning to test the impact of pazopanib, a selective multi-targeted receptor tyrosine kinase inhibitor, on epistaxis and telangiectasia (NCT03850964/NCT03850964). However, preclinical studies in mouse models showed no improvement in wound-induced skin AVMs, leaving little hope for a potential rescue of bAVMs (Robert et al., 2020; Snodgrass et al., 2021).

Other potential treatments are based on inhibiting the PI3K/AKT/mTOR pathway, which is highly activated

downstream of ANGPT2 and VEGF signaling. The most common mTOR inhibitor is sirolimus (rapamycin), which was shown to prevent bleeding and anemia in preclinical mouse models of HHT by controlling VEGFR2 and mTOR overactivation (Robert et al., 2020). One case report and a clinical study suggested that sirolimus could control and rescue HHT-induced bleedings and vascular malformations (Skaro et al., 2006; Dupuis-Girod et al., 2010). Apart from sirolimus, using PI3K inhibitors that are already FDA-approved for chemotherapy could also represent an excellent potential therapeutic avenue.

Altogether, although preclinical and clinical tests on pharmacological treatments are ongoing, the probability of reversing the bAVMs is still weak. Despite advances in research to identify the mechanisms, surgical treatments are still the best option to treat bAVMs. Thus, improving surgical conditions and tools currently remains the optimal avenue to improve the survival of HHT patients (Chen W. et al., 2014; Shaligram et al., 2019; Robert et al., 2020).

Conclusion

Identifying the molecular mechanisms associated with bAVM formation is an essential step toward elucidating the mechanisms of these malformations. Several additional questions, however, remain to be addressed. Are there modifying genes that may explain the clinical variability of bAVMs? How does inadequate ALK1/ENG signaling affect the response of ECs to mechanical stress, and how does this contribute to bAVM formation? Is PI3K/AKT signaling increased in HHT bAVMs, and could it be targeted to improve the malformations? What is the contribution of NOTCH signaling in the formation of bAVMs in HHT patients? In addition to these questions, one significant challenge remains to characterize and understand the common mechanisms underlying idiopathic bAVMs and those observed in HHT patients. The recent identification of several signaling pathways involved in bAVMs formation, as well as the analysis of several experimental animal models, have provided several clues to this goal and could pave the way for developing novel therapies.

Author contributions

ED, TA, BL, and AD wrote the manuscript, collected literature information, and edited the manuscript. All authors reviewed and commented on the manuscript.

Funding

This work was supported by the Canadian Institutes of Health Research (project grant PJT-165871 and PJT-183658) and the Vision Health Research Network (project grant RRSV_PP1920) to AD, from Fonds de Recherche en Ophtalmologie de l'Université de Montréal (FROUM) to ED and TA, and from the Canadian Institutes of Health Research (project grant FRN-148525) and Fonds de Recherche du Québec - Santé (FRQS) AMD Research Program (Funding reference #269835) to BL. AD and BL were FRQS Research Scholars.

Acknowledgments

We apologize to colleagues whose work could not be cited in this review due to space limitations. All figures were created with BioRender.com.

Conflict of interest

The authors declare that the research was conducted in the absence of any commercial or financial relationships that could be construed as a potential conflict of interest.

Publisher's note

All claims expressed in this article are solely those of the authors and do not necessarily represent those of their affiliated organizations, or those of the publisher, the editors and the reviewers. Any product that may be evaluated in this article, or claim that may be made by its manufacturer, is not guaranteed or endorsed by the publisher.

References

Abecassis, I. J., Xu, D. S., Batjer, H. H., and Bendok, B. R. (2014). Natural history of brain arteriovenous malformations: A systematic review. *Neurosurg. Focus* 37:E7. doi: 10.3171/2014.6.FOCUS14250

Adams, R. H., and Alitalo, K. (2007). Molecular regulation of angiogenesis and lymphangiogenesis. *Nat. Rev. Mol. Cell Biol.* 8, 464–478. doi: 10.1038/nrm2183

Akimoto, S., Mitsumata, M., Sasaguri, T., and Yoshida, Y. (2000). Laminar shear stress inhibits vascular endothelial cell proliferation by inducing cyclin-dependent kinase inhibitor p21Sdi1/Cip1/Waf1. *Circ. Res.* 86, 185–90. doi: 10.1161/01.RES.86.2.185

Allinson, K. R., Carvalho, R. L., van den Brink, S., Mummery, C. L., and Arthur, H. M. (2007). Generation of a floxed allele of the mouse endoglin gene. *Genesis* 45, 391–95. doi: 10.1002/dvg.20284

Al-Olabi, L., Polubothu, S., Dowsett, K., Andrews, K. A., Stadnik, P., Joseph, A. P., et al. (2018). Mosaic RAS/MAPK variants cause sporadic vascular

malformations which respond to targeted therapy. *J. Clin. Investig.* 128, 1496–1508. doi: 10.1172/JCI98589

Alsina-Sanchís, E., García-Ibáñez, Y., Figueiredo, A. M., Riera-Domingo, C., Figueras, A., Matias-Guiu, X., et al. (2018). ALK1 loss results in vascular hyperplasia in mice and humans through PI3K activation. *Arterioscler. Thromb. Vasc. Biol.* 38, 1216–29. doi: 10.1161/ATVBAHA.118.310760

Alt, A., Miguel-Romero, L., Donderis, J., Aristorena, M., Blanco, F. J., and Round, A. (2012). Structural and functional insights into endoglin ligand recognition and binding. *PLoS One* 7:12. doi: 10.1371/journal.pone.0029948

Armulik, A., Genové, G., and Betsholtz, C. (2011). Pericytes: Developmental, physiological, and pathological perspectives, problems, and promises. *Dev. Cell* 21, 193–215. doi: 10.1016/j.devcel.2011.07.001

Arthur, H. M., Ure, J., Smith, A. J., Renforth, G., Wilson, D. I., Torsney, E., et al. (2000). Endoglin, an ancillary TGFβ receptor, Is required for extraembryonic angiogenesis and plays a key role in heart development. *Dev. Biol.* 217, 42–53. doi: 10.1006/dbio.1999.9534

Baeyens, N., Larrivée, B., Ola, R., Hayward-Piatkowskyi, B., Dubrac, A., Huang, B., et al. (2016). Defective fluid shear stress mechanotransduction mediates hereditary hemorrhagic telangiectasia. *J. Cell Biol.* 214, 807–16. doi: 10.1083/jcb.201603106

Bautch, V. L., and James, J. M. (2009). Neurovascular development. *Cell Adhes. Migr.* 3, 199–204. doi: 10.4161/cam.3.2.8397

Bayrak-Toydemir, P., McDonald, J., Markewitz, B., Lewin, S., Miller, F., Chou, L. S., et al. (2006). Genotype-phenotype correlation in hereditary hemorrhagic telangiectasia: Mutations and manifestations. *Am. J. Med. Genet. Part A* 140, 463–70. doi: 10.1002/ajmg.a.31101

Benn, A., Alonso, F., Mangelschots, J., Génot, E., Lox, M., and Zwijsen, A. (2020). BMP-SMAD1/5 Signaling regulates retinal vascular development. *Biomolecules* 10:488. doi: 10.3390/biom10030488

Bernabeu, M. O., Jones, M. L., Nielsen, J. H., Krüger, T., Nash, R. W., Groen, D., et al. (2014). Computer simulations reveal complex distribution of haemodynamic forces in a mouse retina model of angiogenesis. *J. R. Soc. Interface* 11:20140543. doi: 10.1098/rsif.2014.0543

Bidart, M., Ricard, N., Levet, S., Samson, M., Mallet, C., David, L., et al. (2012). BMP9 Is produced by hepatocytes and circulates mainly in an active mature form complexed to its prodomain. *Cell. Mol. Life Sci.* 69, 313–24. doi: 10.1007/s00018-011-0751-1

Bideau, A., Plauchu, H., Brunet, G., and Robert, J. (1989). Epidemiological investigation of rendu-osler disease in France: Its geographical distribution and prevalence. *Popul. Engl. Sel.* 44, 3–22.

Biswas, S., Cottarelli, A., and Agalliu, D. (2020). Neuronal and glial regulation of CNS angiogenesis and barriergenesis. *Development* 147:dev182279. doi: 10.1242/dev.182279

Boon, L. M., Mulliken, J. B., and Vikkula, M. (2005). RASA1: Variable phenotype with capillary and arteriovenous malformations. *Curr. Opin. Genet. Dev. Genet. Dis.* 15, 265–69. doi: 10.1016/j.gde.2005.03.004

Bourdeau, A., Dumont, D. J., and Letarte, M. (1999). A murine model of hereditary hemorrhagic telangiectasia. *J. Clin. Investig.* 104, 1343–51.

Bouvard, C., Tu, L., Rossi, M., Desroches-Castan, A., Berrebeh, N., Helfer, E., et al. (2021). Different cardiovascular and pulmonary phenotypes for single- and double-knock-out mice deficient in BMP9 and BMP10. *Cardiovasc. Res.* 118, 1805–20. doi: 10.1093/cvr/cvab187

Brinjikji, W., Iyer, V. N., Lanzino, G., Thielen, K. R., and Wood, C. P. (2017). Natural history of brain capillary vascular malformations in hereditary hemorrhagic telangiectasia patients. *J. Neurointerv. Surg.* 9, 26–28. doi: 10.1136/neurintsurg-2015-012252

Brown, R. D., Wiebers, D. O., Torner, J. C., and O'Fallon, W. M. (1996). Frequency of intracranial hemorrhage as a presenting symptom and subtype analysis: A population-based study of intracranial vascular malformations in Olmsted County, Minnesota. *J. Neurosurg.* 85, 29–32. doi: 10.3171/jns.1996.85.1.0029

Capasso, T. L., Li, B., Volek, H. J., Khalid, W., Rochon, E. R., Anbalagan, A., et al. (2020). BMP10-mediated ALK1 signaling is continuously required for vascular development and maintenance. *Angiogenesis* 23, 203–20. doi: 10.1007/s10456-019-09701-0

Castel, D., Mourikis, P., Bartels, S. J., Brinkman, A. B., Tajbakhsh, S., and Stunnenberg, H. G. (2013). Dynamic binding of RBPJ is determined by notch signaling status. *Genes Dev.* 27, 1059–71. doi: 10.1101/gad.211912.112

Chen, D., Teng, J. M., North, P. E., Lapinski, P. E., and King, P. D. (2019). RASA1-Dependent cellular export of collagen IV controls blood and lymphatic vascular development. *J. Clin. Investig.* 129, 3545–61. doi: 10.1172/JCI124917

Chen, H., Brady Ridgway, J., Sai, T., Lai, J., Warming, S., Chen, H., et al. (2013). Context-dependent signaling defines roles of BMP9 and BMP10 in embryonic and postnatal development. *Proc. Natl. Acad. Sci. U.S.A.* 110, 11887–92. doi: 10.1073/pnas.1306074110

Chen, W., Choi, E. J., McDougall, C. M., and Su, H. (2014). Brain arteriovenous malformation modeling, pathogenesis, and novel therapeutic targets. *Transl. Stroke Res.* 5, 316–29. doi: 10.1007/s12975-014-0343-0

Chen, W., Guo, Y., Walker, E. J., Shen, F., Jun, K., Oh, S. P., et al. (2013). Reduced mural cell coverage and impaired vessel integrity after angiogenic stimulation in the Alk1-deficient brain. *Arterioscler. Thromb. Vasc. Biol* 33, 305–10. doi: 10.1161/ATVBAHA.112.300485

Chen, Y. G., and Massagué, J. (1999). Smad1 recognition and activation by the ALK1 group of transforming growth factor-β family receptors. *J. Biol. Chem.* 274, 3672–77. doi: 10.1074/jbc.274.6.3672

Choi, E. J., Chen, W., Jun, K., Arthur, H. M., Young, W. L., and Su, H. (2014). Novel brain arteriovenous malformation mouse models for type 1 hereditary hemorrhagic telangiectasia. *PLoS One* 9:e88511. doi: 10.1371/journal.pone.0088511

Choi, E. J., Walker, E. J., Shen, F., Oh, S. P., Arthur, H. M., and Young, W. L. (2012). Minimal homozygous endothelial deletion of eng with VEGF stimulation is sufficient to cause cerebrovascular dysplasia in the adult mouse. *Cerebrovasc. Dis.* 33, 540–47. doi: 10.1159/000337762

Coelho-Santos, V., and Shih, A. Y. (2020). Postnatal development of cerebrovascular structure and the neurogliovascular unit. *Wiley Interdiscip. Rev. Dev. Biol.* 9:e363. doi: 10.1002/wdev.363

Cole, S. G., Begbie, M. E., Wallace, G. M. F., and Shovlin, C. L. (2005). A new locus for Hereditary haemorrhagic telangiectasia (HHT3) maps to chromosome 5. *J. Med. Genet.* 42, 577–82. doi: 10.1136/jmg.2004.028712

Coon, B. G., Baeyens, N., Han, J., Budatha, M., Ross, T. D., Fang, J. S., et al. (2015). Intramembrane binding of VE-cadherin to VEGFR2 and VEGFR3 assembles the endothelial mechanosensory complex. *J. Cell Biol.* 208, 975–86. doi: 10.1083/jcb.201408103

Corti, P., Young, S., Chen, C. Y., Patrick, M. J., Rochon, E. R., and Pekkan, K. (2011). Interaction between Alk1 and blood flow in the development of arteriovenous malformations. *Development* 138, 1573–82. doi: 10.1242/dev.060467

Couto, J. A., Huang, A. Y., Konczyk, D. J., Goss, J. A., Fishman, S. J., and Mulliken, J. B. (2017). Somatic MAP2K1 mutations are associated with extracranial arteriovenous malformation. *Am. J. Hum. Genet.* 100, 546–54. doi: 10.1016/j.ajhg.2017.01.018

Crist, A. M., Lee, A. R., Patel, N. R., Westhoff, D. E., and Meadows, S. M. (2018). Vascular deficiency of Smad4 causes arteriovenous malformations: A mouse model of hereditary hemorrhagic telangiectasia. *Angiogenesis* 21, 363–80. doi: 10.1007/s10456-018-9602-0

Daneman, R., and Prat, A. (2015). The blood–brain barrier. *Cold Spring Harb. Perspect. Biol.* 7:a020412. doi: 10.1101/cshperspect.a020412

David, L., Mallet, C., Keramidas, M., Lamandé, N., Gasc, J. M., and Dupuis-Girod, S. (2008). Bone morphogenetic protein-9 is a circulating vascular quiescence factor. *Circ. Res.* 102, 914–22. doi: 10.1161/CIRCRESAHA.107.165530

David, L., Mallet, C., Mazerbourg, S., Feige, J. J., and Bailly, S. (2006). Identification of BMP9 and BMP10 as functional activators of the orphan activin receptor-like kinase 1 (ALK1) in endothelial cells. *Blood* 109, 1953–61. doi: 10.1182/blood-2006-07-034124

Domenga, V., Fardoux, P., Lacombe, P., Monet, M., Maciazek, J., Krebs, L. T., et al. (2004). Notch3 Is required for arterial identity and maturation of vascular smooth muscle cells. *Genes Dev.* 18, 2730–35. doi: 10.1101/gad.308904

D'Souza, B., Miyamoto, A., and Weinmaster, G. (2008). The many facets of Notch ligands. *Oncogene* 27, 5148–67. doi: 10.1038/onc.2008.229

Duarte, A., Hirashima, M., Benedito, R., Trindade, A., Diniz, P., and Bekman, E. (2004). Dosage-sensitive requirement for mouse Dll4 in artery development. *Genes Dev.* 18, 2474–78. doi: 10.1101/gad.1239004

Dupuis-Girod, S., Chesnais, A. L., Ginon, I., Dumortier, J., Saurin, J. C., and Finet, G. (2010). Long-term outcome of patients with hereditary hemorrhagic telangiectasia and severe hepatic involvement after orthotopic liver transplantation: A single-center study. *Liver Transplant.* 16, 340–47. doi: 10.1002/lt.21990

Eerola, I., Boon, L. M., Mulliken, J. B., Burrows, P. E., Dompmartin, A., Watanabe, S., et al. (2003). Capillary malformation–arteriovenous malformation, a new clinical and genetic disorder caused by RASA1 mutations. *Am. J. Hum. Genet.* 73, 1240–49. doi: 10.1086/379793

Epperla, N., and Hocking, W. (2015). Blessing for the bleeder: Bevacizumab in hereditary hemorrhagic telangiectasia. *Clin. Med. Res.* 13, 32–35. doi: 10.3121/cmr.2013.1205

Etienne-Manneville, S., and Hall, A. (2001). Integrin-mediated activation of Cdc42 controls cell polarity in migrating astrocytes through PKCζ. *Cell* 106, 489–98. doi: 10.1016/S0092-8674(01)00471-8

Fang, J. S., Coon, B. G., Gillis, N., Chen, Z., Qiu, J., Chittenden, T. W., et al. (2017). Shear-induced notch-Cx37-P27 axis arrests endothelial cell cycle to enable arterial specification. *Nat. Commun.* 8:2149. doi: 10.1038/s41467-017-01742-7

Fierstra, J., Conklin, J., Krings, T., Slessarev, M., Han, J. S., Fisher, J. A., et al. (2011). Impaired Peri-Nidal Cerebrovascular Reserve in Seizure Patients with Brain Arteriovenous Malformations. *Brain* 134, 100–109. doi: 10.1093/brain/awq286

Fish, J. E., Flores Suarez, C. P., Boudreau, E., Herman, A. M., Gutierrez, M. C., Gustafson, D., et al. (2020). Somatic gain of KRAS function in the endothelium is sufficient to cause vascular malformations that require MEK but not PI3K signaling. *Circ. Res.* 127, 727–43. doi: 10.1161/CIRCRESAHA.119.316500

Fleetwood, I. G., and Steinberg, G. K. (2002). Arteriovenous malformations. *Lancet* 359, 863–73. doi: 10.1016/S0140-6736(02)07946-1

Fonseca, C. G., Barbacena, P., and Franco, C. A. (2020). Endothelial cells on the move: Dynamics in vascular morphogenesis and disease. *Vasc. Biol.* 2:H29–43. doi: 10.1530/VB-20-0007

Gallione, C. J., Repetto, G. M., Legius, E., Rustgi, A. K., Schelley, S. L., and Tejpar, S. (2004). A combined syndrome of juvenile polyposis and hereditary haemorrhagic telangiectasia associated with mutations in MADH4 (SMAD4). *Lancet* 363, 852–59. doi: 10.1016/S0140-6736(04)15732-2

Gariano, R. F., and Gardner, T. W. (2005). Retinal angiogenesis in development and disease. *Nature* 438, 960–66. doi: 10.1038/nature04482

Garrido-Martin, E. M., Nguyen, H. L., Cunningham, T. A., Choe, S. W., Jiang, Z., and Arthur, H. M. (2014). Common and distinctive pathogenetic features of arteriovenous malformations in hereditary hemorrhagic telangiectasia 1 and hereditary hemorrhagic telangiectasia 2 animal models—brief report. *Arterioscler. Thromb. Vasc. Biol.* 34, 2232–36. doi: 10.1161/ATVBAHA.114.303984

Gordon, W. R., Arnett, K. L., and Blacklow, S. C. (2008). The molecular logic of notch signaling – a structural and biochemical perspective. *J. Cell Sci.* 121, 3109–19. doi: 10.1242/jcs.035683

Graupera, M., and Potente, M. (2013). Regulation of angiogenesis by PI3K signaling networks. *Exp. Cell Res.* 319, 1348–55. doi: 10.1016/j.yexcr.2013.02.021

Griauzde, J., Wilseck, Z. M., Chaudhary, N., Pandey, A. S., Vercler, C. J., Kasten, S. J., et al. (2020). Endovascular treatment of arteriovenous malformations of the head and neck: Focus on the yakes classification and outcomes. *J. Vasc. Int. Radiol.* 31, 1810–16. doi: 10.1016/j.jvir.2020.01.036

Gross, B. A., and Du, R. (2013). Natural history of cerebral arteriovenous malformations: A meta-analysis: Clinical article. *J. Neurosurg.* 118, 437–43. doi: 10.3171/2012.10.JNS121280

Haddad-Tóvolli, R., Dragano, N. R. V., Ramalho, A. F. S., and Velloso, L. A. (2017). Development and function of the blood-brain barrier in the context of metabolic control. *Front. Neurosci.* 11:224. doi: 10.3389/fnins.2017.00224

Haitjema, T., Disch, F., Overtoom, T. T., Westermann, C. J., and Lammers, J. W. (1995). Screening family members of patients with hereditary hemorrhagic telangiectasia. *Am. J. Med.* 99, 519–24. doi: 10.1016/S0002-9343(99)80229-0

Hamada, Y., Kadokawa, Y., Okabe, M., Ikawa, M., Coleman, J. R., and Tsujimoto, Y. (1999). Mutation in ankyrin repeats of the mouse notch2 gene induces early embryonic lethality. *Development* 126, 3415–24. doi: 10.1242/dev.126.15.3415

Han, C., Choe, S.-W., Kim, Y. H., Acharya, A. P., Keselowsky, B. G., Sorg, B. S., et al. (2014). VEGF neutralization can prevent and normalize arteriovenous malformations in an animal model for hereditary hemorrhagic telangiectasia 2. *Angiogenesis* 17, 823–30. doi: 10.1007/s10456-014-9436-3

Han, C., Lang, M. J., Nguyen, C. L., Melendez, E. L., Mehta, S., Turner, G. H., et al. (2021). Novel experimental model of brain arteriovenous malformations using conditional Alk1 gene deletion in transgenic mice. *J. Neurosurg.* 137, 163–74. doi: 10.3171/2021.6.JNS21717

Hellström, M., Gerhardt, H., Kalén, M., Li, X., Eriksson, U., Wolburg, H., et al. (2001). Lack of pericytes leads to endothelial hyperplasia and abnormal vascular morphogenesis. *J. Cell Biol.* 153, 543–54. doi: 10.1083/jcb.153.3.543

Hellström, M., Phng, L.-K., Hofmann, J. J., Wallgard, E., Coultas, L., Lindblom, P., et al. (2007). Dll4 signalling through notch1 regulates formation of tip cells during angiogenesis. *Nature* 445, 776–80. doi: 10.1038/nature05571

Henkemeyer, M., Rossi, D. J., Holmyard, D. P., Puri, M. C., Mbamalu, G., Harpal, K., et al. (1995). Vascular system defects and neuronal apoptosis in mice lacking ras GTPase-activating protein. *Nature* 377, 695–701. doi: 10.1038/377695a0

Hernandez, F., Huether, R., Carter, L., Johnston, T., Thompson, J., Gossage, J. R., et al. (2015). Mutations in RASA1 and GDF2 identified in patients with clinical features of hereditary hemorrhagic telangiectasia. *Hum. Genome Var.* 2:15040. doi: 10.1038/hgv.2015.40

Hogan, K. A., Ambler, C. A., Chapman, D. L., and Bautch, V. L. (2004). The neural tube patterns vessels developmentally using the VEGF signaling pathway. *Development* 131, 1503–13. doi: 10.1242/dev.01039

Hoh, B. L., Chapman, P. H., Loeffler, J. S., Carter, B. S., and Ogilvy, C. S. (2002). Results of multimodality treatment for 141 patients with brain arteriovenous malformations and seizures: Factors associated with seizure incidence and seizure outcomes. *Neurosurgery* 51, 303–11.

Hong, T., Yan, Y., Li, J., Radovanovic, I., Ma, X., Shao, Y. W., et al. (2019). High prevalence of KRAS/BRAF somatic mutations in brain and spinal cord arteriovenous malformations. *Brain* 142, 23–34. doi: 10.1093/brain/awy307

Howe, J. R., Roth, S., Ringold, J. C., Summers, R. W., Järvinen, H. J., Sistonen, P. I., et al. (1998). Mutations in the SMAD4/DPC4 gene in juvenile polyposis. *Science* 280, 1086–88. doi: 10.1126/science.280.5366.1086

Hwan Kim, Y., Vu, P. N., Choe, S. W., Jeon, C. J., Arthur, H. M., Vary, C. P. H., et al. (2020). Overexpression of activin receptor-like kinase 1 in endothelial cells suppresses development of arteriovenous malformations in mouse models of hereditary hemorrhagic telangiectasia. *Circ. Res.* 127, 1122–37. doi: 10.1161/CIRCRESAHA.119.316267

Iso, T., Maeno, T., Oike, Y., Yamazaki, M., Doi, H., Arai, M., et al. (2006). Dll4-selective notch signaling induces EphrinB2 gene expression in endothelial cells. *Biochem. Biophys. Res. Commun.* 341, 708–14. doi: 10.1016/j.bbrc.2006.01.020

Itoh, F., Itoh, S., Goumans, M.-J., Valdimarsdottir, G., Iso, T., Dotto, G. P., et al. (2004). Synergy and antagonism between Notch and BMP receptor signaling pathways in endothelial cells. *EMBO J.* 23, 541–51. doi: 10.1038/sj.emboj.7600065

Jin, Y., Muhl, L., Burmakin, M., Wang, Y., Duchez, A. C., Betsholtz, C., et al. (2017). Endoglin prevents vascular malformation by regulating flow-induced cell migration and specification through VEGFR2 signalling. *Nat. Cell Biol.* 19, 639–52. doi: 10.1038/ncb3534

Johnson, D. W., Berg, J. N., Baldwin, M. A., Gallione, C. J., Marondel, I., Yoon, S.-J., et al. (1996). Mutations in the activin receptor–like kinase 1 gene in hereditary haemorrhagic telangiectasia type 2. *Nat. Genet.* 13, 189–95. doi: 10.1038/ng0696-189

Jonker, L., and Arthur, H. M. (2002). Endoglin expression in early development is associated with vasculogenesis and angiogenesis. *Mech. Dev.* 110, 193–96. doi: 10.1016/S0925-4773(01)00562-7

Josephson, C. B., Leach, J.-P., Duncan, R., Roberts, R. C., Counsell, C. E., and Al-Shahi Salman, R. (2011). Seizure risk from cavernous or arteriovenous malformations. *Neurology* 76, 1548–54. doi: 10.1212/WNL.0b013e3182190f37

Kaplan, L., Chow, B. W., and Gu, C. (2020). Neuronal regulation of the blood–brain barrier and neurovascular coupling. *Nat. Rev. Neurosci.* 21, 416–32. doi: 10.1038/s41583-020-0322-2

Karar, J., and Maity, A. (2011). PI3K/AKT/mTOR pathway in angiogenesis. *Front. Mol. Neurosci.* 4:51. doi: 10.3389/fnmol.2011.00051

Kjeldsen, A. D., Møller, T. R., Brusgaard, K., Vase, P., and Andersen, P. E. (2005). Clinical symptoms according to genotype amongst patients with hereditary haemorrhagic telangiectasia. *J. Intern. Med.* 258, 349–55. doi: 10.1111/j.1365-2796.2005.01555.x

Kjeldsen, A. D., Vase, P., and Green, A. (1999). Hereditary haemorrhagic telangiectasia: A population-based study of prevalence and mortality in danish patients. *J. Intern. Med.* 245, 31–39. doi: 10.1046/j.1365-2796.1999.00398.x

Kofler, N. M., Cuervo, H., Uh, M. K., Murtomäki, A., and Kitajewski, J. (2015). Combined deficiency of Notch1 and Notch3 causes pericyte dysfunction, models CADASIL, and results in arteriovenous malformations. *Sci. Rep.* 5:16449. doi: 10.1038/srep16449

Komiyama, M., Terada, A., Ishiguro, T., Watanabe, Y., Nakajima, H., and Yamada, O. (2015). Neuroradiological manifestations of hereditary hemorrhagic telangiectasia in 139 Japanese patients. *Neurol. Med. Chir.* 55, 479–86. doi: 10.2176/nmc.oa.2015-0040

Krebs, L. T., Shutter, J. R., Tanigaki, K., Honjo, T., Stark, K. L., and Gridley, T. (2004). Haploinsufficient lethality and formation of arteriovenous malformations in notch pathway mutants. *Genes Dev.* 18, 2469–73. doi: 10.1101/gad.1239204

Krebs, L. T., Starling, C., Chervonsky, A. V., and Gridley, T. (2010). Notch1 activation in mice causes arteriovenous malformations phenocopied by ephrinB2 and EphB4 mutants. *Genesis* 48, 146–50. doi: 10.1002/dvg.20599

Krebs, L. T., Xue, Y., Norton, C. R., Shutter, J. R., Maguire, M., Sundberg, J. P., et al. (2000). Notch signaling is essential for vascular morphogenesis in mice. *Genes Dev.* 14, 1343–52. doi: 10.1101/gad.14.11.1343

Krings, T., Kim, H., Power, S., Nelson, J., Faughnan, M. E., and Young, W. L. (2015). Neurovascular manifestations in hereditary hemorrhagic telangiectasia:

Imaging features and genotype-phenotype correlations. *Am. J. Neuroradiol.* 36, 863–70. doi: 10.3174/ajnr.A4210

Krings, T., Ozanne, A., Chng, S. M., Alvarez, H., Rodesch, G., and Lasjaunias, P. L. (2005). Neurovascular phenotypes in hereditary haemorrhagic telangiectasia patients according to age. *Neuroradiology* 47, 711–20. doi: 10.1007/s00234-005-1390-8

Lan, Y., Liu, B., Yao, H., Li, F., Weng, T., Yang, G., et al. (2007). Essential role of endothelial Smad4 in vascular remodeling and integrity. *Mol. Cell. Biol.* 27, 7683–92. doi: 10.1128/MCB.00577-07

Langer, D. J., Lasner, T. M., Hurst, R. W., Flamm, E. S., Zager, E. L., and King, J. T. (1998). Hypertension, small size, and deep venous drainage are associated with risk of hemorrhagic presentation of cerebral arteriovenous malformations. *Neurosurgery* 42, 481–86. doi: 10.1097/00006123-199803000-00008

Lapinski, P. E., Kwon, S., Lubeck, B. A., Wilkinson, J. E., Srinivasan, R. S., Sevick-Muraca, E., et al. (2012). RASA1 maintains the lymphatic vasculature in a quiescent functional state in mice. *J. Clin. Investig.* 122, 733–47. doi: 10.1172/JCI46116

Lapinski, P. E., Lubeck, B. A., Chen, D., Doosti, A., Zawieja, S. D., and Davis, M. J. (2017). RASA1 regulates the function of lymphatic vessel valves in mice. *J. Clin. Investig.* 127, 2569–85. doi: 10.1172/JCI89607

Larrivée, B., Prahst, C., Gordon, E., del Toro, R., Mathivet, T., Duarte, A., et al. (2012). ALK1 signaling inhibits angiogenesis by cooperating with the notch pathway. *Dev. Cell* 22, 489–500. doi: 10.1016/j.devcel.2012.02.005

Laux, D. W., Young, S., Donovan, J. P., Mansfield, C. J., Upton, P. D., and Roman, B. L. (2013). Circulating Bmp10 Acts through endothelial Alk1 to mediate flow-dependent arterial quiescence. *Development* 140, 3403–12. doi: 10.1242/dev.095307

Lawson, N. D., Scheer, N., Pham, V. N., Kim, C. H., Chitnis, A. B., and Campos-Ortega, J. A. (2001). Notch signaling is required for arterial-venous differentiation during embryonic vascular development. *Development* 128, 3675–83. doi: 10.1242/dev.128.19.3675

Lebrin, F., Srun, S., Raymond, K., Martin, S., van den Brink, S., Freitas, C., et al. (2010). Thalidomide stimulates vessel maturation and reduces epistaxis in individuals with hereditary hemorrhagic telangiectasia. *Nat. Med.* 16, 420–28. doi: 10.1038/nm.2131

Lee, H.-W., Xu, Y., He, L., Choi, W., Gonzalez, D., Jin, S.-W., et al. (2021). Role of venous endothelial cells in developmental and pathologic angiogenesis. *Circulation* 144, 1308–22. doi: 10.1161/CIRCULATIONAHA.121.054071

Leslie, J. D., Ariza-McNaughton, L., Bermange, A. L., McAdow, R., Johnson, S. L., and Lewis, J. (2007). Endothelial signalling by the notch ligand delta-like 4 restricts angiogenesis. *Development* 134, 839–44. doi: 10.1242/dev.003244

Li, D. Y., Sorensen, L. K., Brooke, B. S., Urness, L. D., Davis, E. C., Taylor, D. G., et al. (1999). Defective angiogenesis in mice lacking endoglin. *Science* 284, 1534–37. doi: 10.1126/science.284.5419.1534

Li, F., Lan, Y., Wang, Y., Wang, J., Yang, G., Meng, F., et al. (2011). Endothelial Smad4 maintains cerebrovascular integrity by activating N-cadherin through cooperation with notch. *Dev. Cell* 20, 291–302. doi: 10.1016/j.devcel.2011.01.011

Li, S., Wang, R., Wang, Y., Li, H., Zheng, J., Duan, R., et al. (2014). Receptors of the notch signaling pathway are associated with hemorrhage of brain arteriovenous malformations. *Mol. Med. Rep.* 9, 2233–38. doi: 10.3892/mmr.2014.2061

Lindahl, P., Johansson, B. R., Levéen, P., and Betsholtz, C. (1997). Pericyte loss and microaneurysm formation in PDGF-B-deficient mice. *Science* 277, 242–45. doi: 10.1126/science.277.5323.242

Lindblom, P., Gerhardt, H., Liebner, S., Abramsson, A., Enge, M., Hellstrom, M., et al. (2003). Endothelial PDGF-B retention is required for proper investment of pericytes in the microvessel wall. *Genes Dev.* 17, 1835–40. doi: 10.1101/gad.266803

López-Coviella, I., Berse, B., Krauss, R., Thies, R. S., and Blusztajn, J. K. (2000). Induction and maintenance of the neuronal cholinergic phenotype in the central nervous system by BMP-9. *Science* 289, 313–16. doi: 10.1126/science.289.5477.313

Lubeck, B. A., Lapinski, P. E., Bauler, T. J., Oliver, J. A., Hughes, E. D., Saunders, T. L., et al. (2014). Blood vascular abnormalities in Rasa1R780Q knockin mice: Implications for the pathogenesis of capillary malformation–arteriovenous malformation. *Am. J. Pathol.* 184, 3163–69. doi: 10.1016/j.ajpath.2014.08.018

Mahmoud, M., Allinson, K. R., Zhai, Z., Oakenfull, R., Ghandi, P., Adams, R. H., et al. (2010). Pathogenesis of arteriovenous malformations in the absence of endoglin. *Circ. Res.* 106, 1425–33. doi: 10.1161/CIRCRESAHA.109.211037

Matsubara, S., Mandzia, J. L., ter Brugge, K., Willinsky, R. A., and Faughnan, M. E. (2000). Angiographic and clinical characteristics of patients with cerebral arteriovenous malformations associated with hereditary hemorrhagic telangiectasia. *AJNR* 21, 1016–20.

McAllister, K. A., Grogg, K. M., Johnson, D. W., Gallione, C. J., Baldwin, M. A., Jackson, C. E., et al. (1994). Endoglin, a TGF-β binding protein of endothelial cells, is the gene for hereditary haemorrhagic telangiectasia type 1. *Nat. Genet.* 8, 345–51. doi: 10.1038/ng1294-345

Miller, D. W., Graulich, W., Karges, B., Stahl, S., Ernst, M., Ramaswamy, A., et al. (1999). Elevated expression of endoglin, a component of the TGF-β-receptor complex, correlates with proliferation of tumor endothelial cells. *Int. J. Cancer* 81, 568–72.

Mohr, J. P., Kejda-Scharler, J., and Spellman, J. P. - (2013). Diagnosis and treatment of arteriovenous malformations. *Curr. Neurol. Neurosci. Rep.* 13:324. doi: 10.1007/s11910-012-0324-1

Moya, I. M., Umans, L., Maas, E., Pereira, P. N. G., Beets, K., Francis, A., et al. (2012). Stalk cell phenotype depends on integration of notch and Smad1/5 signaling cascades. *Dev. Cell* 22, 501–14. doi: 10.1016/j.devcel.2012.01.007

Murphy, P. A., Kim, T. N., Huang, L., Nielsen, C. M., Lawton, M. T., Adams, R. H., et al. (2014). Constitutively active Notch4 receptor elicits brain arteriovenous malformations through enlargement of capillary-like vessels. *Proc. Natl. Acad. Sci. U.S.A.* 111, 18007–12. doi: 10.1073/pnas.1415316111

Murphy, P. A., Lam, M. T. Y., Wu, X., Kim, T. N., Vartanian, S. M., Bollen, A. W., et al. (2008). Endothelial Notch4 signaling induces hallmarks of brain arteriovenous malformations in mice. *Proc. Natl. Acad. Sci. U.S.A.* 105, 10901–6. doi: 10.1073/pnas.0802743105

Nadeem, T., Bogue, W., Bigit, B., and Cuervo, H. (2020). Deficiency of notch signaling in pericytes results in arteriovenous malformations. *JCI Insight* 5:e125940. doi: 10.1172/jci.insight.125940

Nakao, A., Imamura, T., Souchelnytskyi, S., Kawabata, M., Ishisaki, A., Oeda, E., et al. (1997). TGF-beta receptor-mediated signalling through Smad2, Smad3 and Smad4. *EMBO J.* 16, 5353–62. doi: 10.1093/emboj/16.17.5353

Neuhaus, H., Rosen, V., and Thies, R. S. (1999). Heart specific expression of mouse BMP-10 a novel member of the TGF-beta superfamily. *Mech. Dev.* 80, 181–84. doi: 10.1016/s0925-4773(98)00221-4

Nielsen, C. M., Cuervo, H., Ding, V. W., Kong, Y., Huang, E. J., and Wang, R. A. (2014). Deletion of Rbpj from postnatal endothelium leads to abnormal arteriovenous shunting in mice. *Development* 141, 3782–92. doi: 10.1242/dev.108951

Noguera-Troise, I., Daly, C., Papadopoulos, N. J., Coetzee, S., Boland, P., Gale, N. W., et al. (2006). Blockade of Dll4 inhibits tumour growth by promoting non-productive angiogenesis. *Nature* 444, 1032–37. doi: 10.1038/nature05355

Oh, S. P., Seki, T., Goss, K. A., Imamura, T., Yi, Y., Donahoe, P. K., et al. (2000). Activin receptor-like kinase 1 modulates transforming growth factor-beta 1 signaling in the regulation of angiogenesis. *Proc. Natl. Acad. Sci. U.S.A.* 97, 2626–31. doi: 10.1073/pnas.97.6.2626

Ola, R., Dubrac, A., Han, J., Zhang, F., Fang, J. S., Larrivée, B., et al. (2016). PI3 kinase inhibition improves vascular malformations in mouse models of hereditary haemorrhagic telangiectasia. *Nat. Commun.* 7:13650. doi: 10.1038/ncomms13650

Ola, R., Künzel, S. H., Zhang, F., Genet, G., Chakraborty, R., Pibouin-Fragner, L., et al. (2018). SMAD4 prevents flow induced arteriovenous malformations by inhibiting casein kinase 2. *Circulation* 138, 2379–94. doi: 10.1161/CIRCULATIONAHA.118.033842

Oosting, S., Nagengast, W., and de Vries, E. (2009). More on bevacizumab in hereditary hemorrhagic telangiectasia. *N. Engl. J. Med.* 361:931. doi: 10.1056/NEJMc091271

Ouarné, M., Pena, A., and Franco, C. A. (2021). From remodeling to quiescence: The transformation of the vascular network. *Cells Dev. Quan. Cell Dev. Biol.* 168:203735. doi: 10.1016/j.cdev.2021.203735

Paredes, I., Himmels, P., and Ruiz de Almodóvar, C. (2018). Neurovascular communication during CNS development. *Dev. Cell* 45, 10–32. doi: 10.1016/j.devcel.2018.01.023

Park, E. S., Kim, S., Huang, S., Yoo, J. Y., Körbelin, J., Lee, T. J., et al. (2021). Selective endothelial hyperactivation of oncogenic KRAS induces brain arteriovenous malformations in mice. *Ann. Neurol.* 89, 926–41. doi: 10.1002/ana.26059

Park, H., Furtado, J., Poulet, M., Chung, M., Yun, S., Lee, S., et al. (2021). Defective flow-migration coupling causes arteriovenous malformations in hereditary hemorrhagic telangiectasia. *Circulation* 144, 805–22. doi: 10.1161/CIRCULATIONAHA.120.053047

Park, S., DiMaio, T. A., Liu, W., Wang, S., Sorenson, C. M., and Sheibani, N. (2013). Endoglin regulates the activation and quiescence of endothelium by participating in canonical and non-canonical TGF-β signaling pathways. *J. Cell Sci.* 126, 1392–1405. doi: 10.1242/jcs.117275

Park, S., Ok, M., Wankhede, Y. J., Lee, E.-J., Choi, N., Fliess, S.-W., et al. (2009). Real-time imaging of de novo arteriovenous malformation in a mouse

model of hereditary hemorrhagic telangiectasia. *J. Clin. Investig.* 119, 3487–96. doi: 10.1172/JCI39482

Park, S. O., Lee, Y. J., Seki, T., Hong, K. H., Fliess, N., Jiang, Z., et al. (2008). ALK5- and TGFBR2-independent role of ALK1 in the pathogenesis of hereditary hemorrhagic telangiectasia type 2. *Blood* 111, 633–42. doi: 10.1182/blood-2007-08-107359

Parmar, K. M., Larman, H. B., Dai, G., Zhang, Y., Wang, E. T., Moorthy, S. N., et al. (2006). Integration of flow-dependent endothelial phenotypes by kruppel-like factor 2. *J. Clin. Investig.* 116, 49–58. doi: 10.1172/JCI24787

Peacock, H. M., Tabibian, A., Criem, N., Caolo, V., Hamard, L., Deryckere, A., et al. (2020). Impaired SMAD1/5 mechanotransduction and Cx37 (Connexin37) expression enable pathological vessel enlargement and shunting. *Arterioscler. Thromb. Vasc. Biol.* 40:e87–104. doi: 10.1161/ATVBAHA.119.313122

Peguera, B., Segarra, M., and Acker-Palmer, A. (2021). Neurovascular crosstalk coordinates the central nervous system development. *Curr. Opin. Neurobiol. Mol. Neurosci.* 69, 202–13. doi: 10.1016/j.conb.2021.04.005

Pitulescu, M. E., Schmidt, I., Giaimo, B. D., Antoine, T., Berkenfeld, F., Ferrante, F., et al. (2017). Dll4 and notch signalling couples sprouting angiogenesis and artery formation. *Nat. Cell Biol.* 19, 915–27. doi: 10.1038/ncb3555

Prigoda, N. L., Savas, S., Abdalla, S. A., Piovesan, B., Rushlow, D., Vandezande, K., et al. (2006). Hereditary haemorrhagic telangiectasia: Mutation detection, test sensitivity and novel mutations. *J. Med. Genet.* 43, 722–28. doi: 10.1136/jmg.2006.042606

Revencu, N., Boon, L. M., Mulliken, J. B., Enjolras, O., Cordisco, M. R., Burrows, P. E., et al. (2008). Parkes weber syndrome, vein of galen aneurysmal malformation, and other fast-flow vascular anomalies are caused by RASA1 mutations. *Hum. Mutat.* 29, 959–65. doi: 10.1002/humu.20746

Ricard, N., Ciais, D., Levet, S., Subileau, M., Mallet, C., Zimmers, T. A., et al. (2012). BMP9 and BMP10 are critical for postnatal retinal vascular remodeling. *Blood* 119, 6162–71. doi: 10.1182/blood-2012-01-407593

Robert, F., D-Castan, A., Bailly, S., Girod, S. D. -, and Feige, J.-J. (2020). Future treatments for hereditary hemorrhagic telangiectasia. *Orphanet J. Rare Dis.* 15:4. doi: 10.1186/s13023-019-1281-4

Rochon, E. R., Menon, P. G., and Roman, B. L. (2016). Alk1 controls arterial endothelial cell migration in lumenized vessels. *Development* 143, 2593–2602. doi: 10.1242/dev.135392

Rochon, E. R., Wright, D. S., Schubert, M. M., and Roman, B. L. (2015). Context-specific interactions between notch and ALK1 cannot explain ALK1-associated arteriovenous malformations. *Cardiovasc. Res.* 107, 143–52. doi: 10.1093/cvr/cvv148

Rohn, B., Haenggi, D., Etminan, N., Kunz, M., Turowski, B., and Steiger, H.-J. (2014). Epilepsy, headache, and quality of life after resection of cerebral arteriovenous malformations. *J. Neurol. Surg. Part A* 75, 282–88. doi: 10.1055/s-0033-1358611

Roman, B. L., and Hinck, A. P. (2017). ALK1 signaling in development and disease: New paradigms. *Cell. Mol. Life Sci.* 74, 4539–60. doi: 10.1007/s00018-017-2636-4

Roman, B. L., Pham, V. N., Lawson, N. D., Kulik, M., Childs, S., Lekven, A. C., et al. (2002). Disruption of acvrl1 increases endothelial cell number in zebrafish cranial vessels. *Development* 129, 3009–19. doi: 10.1242/dev.129.12.3009

Ruiz, S., Zhao, H., Chandakkar, P., Chatterjee, P. K., Papoin, J., Blanc, L., et al. (2016). A mouse model of hereditary hemorrhagic telangiectasia generated by transmammary-delivered immunoblocking of BMP9 and BMP10. *Sci. Rep.* 5:37366. doi: 10.1038/srep37366

Ruiz, S., Zhao, H., Chandakkar, P., Papoin, J., Choi, H., Kitabayashi, A. N. -, et al. (2020). Correcting Smad1/5/8, MTOR, and VEGFR2 treats pathology in hereditary hemorrhagic telangiectasia models. *J. Clin. Investig.* 130, 942–57. doi: 10.1172/JCI127425

Saleh, M., Carter, M. T., Latino, G. A., Dirks, P., and Ratjen, F. (2013). Brain arteriovenous malformations in patients with hereditary hemorrhagic telangiectasia: Clinical presentation and anatomical distribution. *Pediatr. Neurol.* 49, 445–50. doi: 10.1016/j.pediatrneurol.2013.07.021

Schuermann, A., Helker, C. S. M., and Herzog, W. (2014). Angiogenesis in zebrafish. *Semin. Cell Dev. Biol.* 31, 106–14. doi: 10.1016/j.semcdb.2014.04.037

Seki, T., Yun, J., and Oh, S. P. (2003). Arterial endothelium-specific activin receptor-like kinase 1 expression suggests its role in arterialization and vascular remodeling. *Circ. Res.* 93, 682–89. doi: 10.1161/01.RES.0000095246.40391.3B

Serini, G., Napione, L., Arese, M., and Bussolino, F. (2008). Besides adhesion: New perspectives of integrin functions in angiogenesis. *Cardiovasc. Res.* 78, 213–22. doi: 10.1093/cvr/cvn045

Serra, H., Chivite, I., A-Urarte, A., Soler, A., Sutherland, J. D., A-Aristorena, A., et al. (2015). PTEN mediates notch-dependent stalk cell arrest in angiogenesis. *Nat. Commun.* 6:7935. doi: 10.1038/ncomms8935

Shaligram, S. S., Winkler, E., Cooke, D., and Su, H. (2019). Risk factors for hemorrhage of brain arteriovenous malformation. *CNS Neurosci. Ther.* 25, 1085–95. doi: 10.1111/cns.13200

Shovlin, C. L. (2010). Hereditary haemorrhagic telangiectasia: Pathophysiology, diagnosis and treatment. *Blood Rev.* 24, 203–19. doi: 10.1016/j.blre.2010.07.001

Siegenthaler, J. A., Sohet, F., and Daneman, R. (2013). 'Sealing off the CNS': Cellular and molecular regulation of blood–brain barriergenesis. *Curr. Opin. Neurobiol.* 23, 1057–64. doi: 10.1016/j.conb.2013.06.006

Simons, M., Gordon, E., and Welsh, L. C. (2016). Mechanisms and regulation of endothelial VEGF receptor signalling. *Nat. Rev. Mol. Cell Biol.* 17, 611–25. doi: 10.1038/nrm.2016.87

Singh, E., Redgrave, R. E., Phillips, H. M., and Arthur, H. M. (2020). Arterial endoglin does not protect against arteriovenous malformations. *Angiogenesis* 23, 559–66. doi: 10.1007/s10456-020-09731-z

Skaro, A. I., Marotta, P. J., and McAlister, V. C. (2006). Regression of cutaneous and gastrointestinal telangiectasia with sirolimus and aspirin in a patient with hereditary hemorrhagic telangiectasia. *Ann. Intern. Med.* 144, 226–27. doi: 10.7326/0003-4819-144-3-200602070-00030

Snodgrass, R. O., Chico, T. J. A., and Arthur, H. M. (2021). Hereditary haemorrhagic telangiectasia, an inherited vascular disorder in need of improved evidence-based pharmaceutical interventions. *Genes* 12:174.

Somi, S., Buffing, A. A. M., Moorman, A. F. M., and Van Den Hoff, M. J. B. (2004). Expression of bone morphogenetic protein-10 MRNA during chicken heart development. *Anat. Rec. Part A Discov. Mol. Cell. Evol. Biol.* 279, 579–82. doi: 10.1002/ar.a.20052

Srinivasan, S., Hanes, M. A., Dickens, T., Porteous, M. E. M., Oh, S. P., Hale, L. P., et al. (2003). A mouse model for hereditary hemorrhagic telangiectasia (HHT) type 2. *Hum. Mol. Genet.* 12, 473–82. doi: 10.1093/hmg/ddg050

Suchting, S., Freitas, C., Noble, F. L., Benedito, R., Bréant, C., Duarte, A., et al. (2007). The notch ligand delta-like 4 negatively regulates endothelial tip cell formation and vessel branching. *Proc. Natl. Acad. Sci. U.S.A.* 104, 3225–30. doi: 10.1073/pnas.0611177104

Sugden, W. W., Meissner, R., Wilmsen, T. A. -, Tsaryk, R., Leonard, E. V., Bussmann, J., et al. (2017). Endoglin controls blood vessel diameter through endothelial cell shape changes in response to haemodynamic cues. *Nat. Cell Biol.* 19, 653–65. doi: 10.1038/ncb3528

Swiatek, P. J., Lindsell, C. E., del Amo, F. F., Weinmaster, G., and Gridley, T. (1994). Notch1 Is essential for postimplantation development in mice. *Genes Dev.* 8, 707–19. doi: 10.1101/gad.8.6.707

Tan, W. H., Popel, A. S., and Gabhann, F. M. (2013). Computational model of VEGFR2 pathway to ERK activation and modulation through receptor trafficking. *Cell. Signal.* 25, 2496–510. doi: 10.1016/j.cellsig.2013.08.015

Tata, M., Ruhrberg, C., and Fantin, A. (2015). Vascularisation of the central nervous system. *Mech. Dev.* 138, 26–36. doi: 10.1016/j.mod.2015.07.001

Thalgott, J. H., D-Santos-Luis, D., Hosman, A. E., Martin, S., Lamandé, N., Bracquart, D., et al. (2018). Decreased expression of vascular endothelial growth factor receptor 1 contributes to the pathogenesis of hereditary hemorrhagic telangiectasia type 2. *Circulation* 138, 2698–2712. doi: 10.1161/CIRCULATIONAHA.117.033062

Torsney, E., Charlton, R., Diamond, A. G., Burn, J., Soames, J. V., and Arthur, H. M. (2003). Mouse model for hereditary hemorrhagic telangiectasia has a generalized vascular abnormality. *Circulation* 107, 1653–57. doi: 10.1161/01.CIR.0000058170.92267.00

Torsney, E., Parums, R. C. D., Collis, M., and Arthur, H. M. (2002). Inducible expression of human endoglin during inflammation and wound healing *in vivo*. *Inflamm. Res.* 51, 464–70. doi: 10.1007/PL00012413

Townson, S. A., M-Hackert, E., Greppi, C., Lowden, P., Sako, D., Liu, J., et al. (2012). Specificity and structure of a high affinity activin receptor-like kinase 1 (ALK1) signaling complex. *J. Biol. Chem.* 287, 27313–25. doi: 10.1074/jbc.M112.377960

Trindade, A., Kumar, S. R., Scehnet, J. S., Lopes-da-Costa, L., Becker, J., Jiang, W., et al. (2008). Overexpression of delta-like 4 induces arterialization and attenuates vessel formation in developing mouse embryos. *Blood* 112, 1720–29. doi: 10.1182/blood-2007-09-112748

Tual-Chalot, S., Mahmoud, M., Allinson, K. R., Redgrave, R. E., Zhai, Z., Oh, S. P., et al. (2014). Endothelial depletion of acvrl1 in mice leads to arteriovenous malformations associated with reduced endoglin expression. *PLoS One* 9:e98646. doi: 10.1371/journal.pone.0098646.

Tual-Chalot, S., Oh, P., and Arthur, H. (2015). Mouse models of hereditary haemorrhagic telangiectasia: Recent advances and future challenges. *Front. Genet.* 6:25. doi: 10.3389/fgene.2015.00025

Tzima, E., Kiosses, W. B., del Pozo, M. A., and Schwartz, M. A. (2003). Localized Cdc42 activation, detected using a novel assay, mediates microtubule organizing center positioning in endothelial cells in response to fluid shear stress. *J. Biol. Chem.* 278, 31020–3. doi: 10.1074/jbc.M301179200

Urness, L. D., Sorensen, L. K., and Li, D. Y. (2000). Arteriovenous malformations in mice lacking activin receptor-like kinase-1. *Nat. Genet.* 26, 328–31. doi: 10.1038/81634

Valdimarsdottir, G., M-J, Goumans, Rosendahl, A., Brugman, M., Itoh, S., Lebrin, F., et al. (2002). Stimulation of Id1 expression by bone morphogenetic protein is sufficient and necessary for bone morphogenetic protein-induced activation of endothelial cells. *Circulation* 106, 2263–70. doi: 10.1161/01.cir.0000033830.36431.46

Van Gieson, E. J., Murfee, W. L., Skalak, T. C., and Price, R. J. (2003). Enhanced smooth muscle cell coverage of microvessels exposed to increased hemodynamic stresses *in vivo*. *Circ. Res.* 92, 929–36. doi: 10.1161/01.RES.0000068377.01063.79

Walcott, B. P., Winkler, E. A., Zhou, S., Birk, H., Guo, D., Koch, M. J., et al. (2018). Identification of a rare BMP pathway mutation in a non-syndromic human brain arteriovenous malformation via exome sequencing. *Hum. Genome Var.* 5:18001. doi: 10.1038/hgv.2018.1

Walker, E. J., Su, H., Shen, F., Choi, E.-J., Oh, S. P., Chen, G., et al. (2011). Arteriovenous malformation in the adult mouse brain resembling the human disease. *Ann. Neurol.* 69, 954–62. doi: 10.1002/ana.22348

Willemse, R. B., Mager, J. J., Westermann, C. J., Overtoom, T. T., Mauser, H., and Wolbers, J. G. (2000). Bleeding risk of cerebrovascular malformations in hereditary hemorrhagic telangiectasia. *J. Neurosurg.* 92, 779–84. doi: 10.3171/jns.2000.92.5.0779

Winkler, E. A., Birk, H., Burkhardt, J.-K., Chen, X., Yue, J. K., Guo, D., et al. (2018). Reductions in brain pericytes are associated with arteriovenous malformation vascular instability. *J. Neurosurg.* 129, 1464–74.

Wooderchak-Donahue, W. L., McDonald, J., O'Fallon, B., Upton, P. D., Li, W., Roman, B. L., et al. (2013). BMP9 mutations cause a vascular-anomaly syndrome with phenotypic overlap with hereditary hemorrhagic telangiectasia. *Am. J. Hum. Genet.* 93, 530–37. doi: 10.1016/j.ajhg.2013.07.004

Xu, C., Hasan, S. S., Schmidt, I., Rocha, S. F., Pitulescu, M. E., Bussmann, J., et al. (2014). Arteries are formed by vein-derived endothelial tip cells. *Nat. Commun.* 5:5758. doi: 10.1038/ncomms6758

Xue, Y., Gao, X., Lindsell, C. E., Norton, C. R., Chang, B., Hicks, C., et al. (1999). Embryonic lethality and vascular defects in mice lacking the notch ligand jagged1. *Hum. Mol. Genet.* 8, 723–30. doi: 10.1093/hmg/8.5.723

Yamada, S., Takagi, Y., Nozaki, K., Kikuta, K.-I., and Hashimoto, N. (2007). Risk factors for subsequent hemorrhage in patients with cerebral arteriovenous malformations. *J. Neurosurg.* 107, 965–72. doi: 10.3171/JNS-07/11/0965

Yao, Y., Jumabay, M., Wang, A., and Boström, K. I. (2011). Matrix Gla protein deficiency causes arteriovenous malformations in mice. *J. Clin. Investig.* 121, 2993–3004. doi: 10.1172/JCI57567

Yao, Y., Yao, J., Radparvar, M., Blazquez-Medela, A. M., Guihard, P. J., Jumabay, M., et al. (2013). Reducing Jagged 1 and 2 levels prevents cerebral arteriovenous malformations in matrix Gla protein deficiency. *Proc. Natl. Acad. Sci. U.S.A.* 110, 19071–76. doi: 10.1073/pnas.1310905110

Zhu, W., Chen, W., Zou, D., Wang, L., Bao, C., Zhan, L., et al. (2018). Thalidomide reduces hemorrhage of brain arteriovenous malformations in a mouse model. *Stroke* 49, 1232–40. doi: 10.1161/STROKEAHA.117.020356

ZhuGe, Q., Wu, Z., Huang, L., Zhao, B., Zhong, M., Zheng, W., et al. (2013). Notch4 is activated in endothelial and smooth muscle cells in human brain arteriovenous malformations. *J. Cell. Mol. Med.* 17, 1458–64. doi: 10.1111/jcmm.12115

ZhuGe, Q., Zhong, M., Zheng, W., Yang, G.-Y., Mao, X., Xie, L., et al. (2009). Notch-1 signalling is activated in brain arteriovenous malformations in humans. *Brain* 132, 3231–41. doi: 10.1093/brain/awp246

frontiers | Frontiers in Human Neuroscience

TYPE Review
PUBLISHED 15 December 2022
DOI 10.3389/fnhum.2022.982190

OPEN ACCESS

EDITED BY
Richard Daneman,
University of California, San Diego,
United States

REVIEWED BY
Nalin Gupta,
University of California, San Francisco,
United States
Manish N. Shah,
University of Texas Health Science
Center at Houston, United States

*CORRESPONDENCE
Timothy H. Ung
Timothy.Ung@CUAnschutz.edu

SPECIALTY SECTION
This article was submitted to
Brain Health and Clinical
Neuroscience,
a section of the journal
Frontiers in Human Neuroscience

RECEIVED 30 June 2022
ACCEPTED 23 November 2022
PUBLISHED 15 December 2022

CITATION
Ung TH, Belanger K, Hashmi A,
Sekar V, Meola A and Chang SD (2022)
Microenvironment changes in
arteriovenous malformations after
stereotactic radiation.
Front. Hum. Neurosci. 16:982190.
doi: 10.3389/fnhum.2022.982190

Microenvironment changes in arteriovenous malformations after stereotactic radiation

Timothy H. Ung[1,2]*, Katherine Belanger[2], Ayesha Hashmi[1], Vashisht Sekar[1], Antonio Meola[1] and Steven D. Chang[1]

[1]Department of Neurosurgery, Stanford University, Palo Alto, CA, United States, [2]Department of Neurosurgery, University of Colorado School of Medicine, Aurora, CO, United States

Cerebral arteriovenous malformations are dysplastic vascular tangles with aberrant vascular dynamics and can result significant morbidity and mortality. A myriad of challenges are encountered when treating these lesions and are largely based on nidal size, location, and prior hemorrhage. Currently, stereotactic radiosurgery is an accepted form of treatment for small to medium sized lesions and is especially useful in the treatment of lesions in non-surgically assessable eloquent areas of the brain. Despite overall high rates of nidal obliteration, there is relatively limited understand on the mechanisms that drive the inflammatory and obliterative pathways observed after treatment with stereotactic radiosurgery. This review provides an overview of arteriovenous malformations with respect to stereotactic radiosurgery and the current understanding of the mechanisms that lead to nidal obliteration.

KEYWORDS

arteriovenous malformation, microenvironment changes in AVM, radiation for AVM, stereotactic radiosurgery for AVM, changes after radiation in AVMs

Introduction

Arteriovenous malformations of the brain are dysplastic tangles of low-resistance channels between arteries and veins. These are vascular lesions characterized by a web of abnormal vessels that directly shunt high flow blood from the feeding arteries to draining veins. They undergo dynamic changes in growth, vascular remodeling, and regression, which makes these vascular lesions difficult to characterize and can result in intracranial hemorrhage. Ruptured of AVMs can carry significant morbidity and patients are at risk for future hemorrhages. Unruptured AVMs are controversial as the morbidity and mortality of treatment may exceed that of the AVM's natural history. Increased use of non-invasive cranial imaging has also increased the prevalence of incidentally discovered lesions and studies have been aimed at investigating the natural history of AVMs in a more comprehensive nature. Patient presentation differs from patient to patient and is dependent on the size, location, and venous drainage.

Management of ruptured and unruptured AVMs necessitates a multidisciplinary team and treatment strategies include observation, microsurgical resection, endovascular embolization, and stereotactic radiosurgery. The goal of treatment is complete obliteration of the AVM with preservation of neurologic function. SRS has become increasingly important in the management of AVMs and can offer favorable outcomes in AVMs located in eloquent and deep brain areas. Understanding the mechanisms that drive nidal obliteration and microvascular changes is critical and further understanding will continue to advance treatment strategies. In this review, we aim to provide a brief overview of the AVMs with a focus on SRS and a comprehensive review of the current understood mechanisms that drive the microvascular changes observed after radiation treatment. To fully understand the mechanisms that drive microenvironment and biological changes after radiosurgery, we will first review the current evidence for treatment of AVMs with radiosurgery followed by a review of AVM biology and AVM microenvironment and biological changes after radiosurgery.

Epidemiology

AVMs occur at an incidence of 0.69–1.42 per 100 000 as described by a collection of population-based studies from the literature (Steiner et al., 1972; Jessurun et al., 1993; Brown et al., 1996; Hofmeister et al., 2000; Choi and Mohr, 2005; Laakso and Hernesniemi, 2012; Nagy et al., 2012; Mohr et al., 2014; Cohen-Inbar et al., 2016; Osbun et al., 2017). Historically, incidence was primarily based on patients with symptomatic presentation, but increased use of non-invasive cranial imaging has led to a paralleled increase in the overall prevalence of AVMs in modern population-based studies. The risk of hemorrhage for untreated unruptured AVMs is 1–5% per year as reported by natural-history studies and an increased risk of rupture is observed in patients with a history of prior AVM rupture. This risk of re-hemorrhage in ruptured AVM patients is greatest within the first year of the patient's initial AVM hemorrhage (Jessurun et al., 1993; Brown et al., 1996; Zhu et al., 1997). In all, 5–25% of all AVM hemorrhages are fatal and the susceptibility for rupture is related to the vascular architecture, intrinsic flow dynamics, venous drainage characteristics, nidus location, and relative size (Mast et al., 1997; Hernesniemi et al., 2008; da Costa et al., 2009; Kim et al., 2014). In addition to hemorrhage, seizure is a common presenting symptom and is more common in patients with cortically based lesions, especially within the temporal lobe. Up to one third of patients with AVMs can present with seizures and post hemorrhagic development of seizures can occur in up to one-half of all patients (Josephson et al., 2011, 2012; Garcin et al., 2012). Other focal neurologic symptoms can be present in patients and is largely dependent on lesion location, size, and vascular flow.

Radiosurgery for AVMs

Initial radiosurgery for AVMs was marked by successful obliteration of the lesion and demonstrated overall safety (Steiner et al., 1972; Colombo et al., 1987; Betti et al., 1989). SRS technologies have advanced remarkably, and minimally invasive SRS has become a standard management option for AVMs. It is particularly useful for lesions located in deep or eloquent regions with high surgical risks. AVM obliteration with LINAC-based radiosurgery is safe and effective and achieved complete AVM obliteration in about 60–80% of cases with an approximate obliteration time of 3–5 years depending on various factors (Paul et al., 2014; Pollock et al., 2016; Ding et al., 2017a; Starke et al., 2017). The most prominent predictors of AVM success included AVM size, volume, radiation dose, number of draining veins, and patient age (Ding et al., 2016). Stereotactic radiosurgery has been found to be particularly effective for small to medium-sized AVMs with diameter of <30 mm and is especially effective for small lesions in eloquent areas of the brain (Ding et al., 2017b; Chan et al., 2019; Karlsson et al., 2019; Peciu-Florianu et al., 2020). For larger AVMs with a volume >10 cm^3, a staged fractionated approach may be used (Franzin et al., 2016). Additional treatment options for larger and more complex lesions employ a combination of stereotactic radiosurgery with endovascular embolization and open cranial resection.

Given the diversity of AVMs, scoring systems have been developed aimed at predicting outcomes after SRS. Two important scoring systems include the modified Radiosurgery-Based AVM score (RBAS) and the Virgina Radiosurgery AVM Scale (VRAS). The RBAS includes nidus volume, location, and patients age and is used to calculate AVM obliteration without a new neurologic deficit (Pollock and Flickinger, 2002; Raffa et al., 2009). Alternatively, the VRAS score is composed of the nidal volume, location, and includes prior hemorrhage and outcomes are defined as lesional obliteration without post radiation hemorrhage or permanent radiation-induced complications (RIC) (Starke et al., 2013) (Table 1).

Delayed RIC including neural degeneration can occur after SRS and represented by peri-nidal edema. Depending on the location, patients can be asymptomatic or present with neurologic sequalae that include headache, seizures, and focal weakness (Pollock et al., 2017; Hasegawa et al., 2018; Ilyas et al., 2018). In a recent meta-analysis, the overall rates of radiographic, symptomatic, and permanent RIC were found to be 35.5, 9.2, and 3.8%. Pediatric patients were found to have decreased rates with radiographic RIC in 32.8%, symptomatic RIC in 7.0%, and permanent RIC in 3.2% of patients (Ilyas et al., 2018). Therefore, radiosurgical marginal dose and obliteration rates observed a sigmoid shaped dose-response relationship

TABLE 1 Both the Modified radiosurgery-based AVM score and Virgina radiosurgery AVM scale are accepted scoring systems used with radiosurgical treatment of AVMs.

SRS AVM Scores

Modified radiosurgery-based AVM score	[0.1 × nidus volume (cm^3)] + [0.02 × patient age (years)] + [0.5 × nidus location score] Deep locations = 1 • Basal ganglia • Brainstem • Thalamus Other locations = 0 • Frontal • Temporal • Parietal • Occipital • Intraventricular • Corpus callosum • Cerebellar	AVM obliteration without new neurologic deficit Score total ≤1.00 = 62% >1.00 – 2.00 = 53% <2.00 = 32 %
Virginia radiosurgery AVM scale	AVM volume <2 cm^3 = 0 points 2–4 cm^3 = 1 point >4 cm^3 = 2 points AVM location Non-eloquent = 0 points Eloquent = 1 point Eloquent = Sensorimotor, language and visual cortex, hypothalamus, internal capsule, brainstem, cerebellar peduncles, and deep cerebellar nuclei History of hemorrhage No = 0 points Yes = 1 point	Favorable outcome with AVM obliteration with no post-radiation hemorrhage or symptomatic RIC Score total 0 points = 83% 1 point = 79% 2 points = 70% 3 points = 48% 4 points – 39%

with a balance between obliteration and adverse radiation effects (Flickinger et al., 1996, 2002). Additional nidal treatment effects of SRS include cyst formation and can be found in ∼1–3% of patients at an average of 6.5–7.3 years after treatment (Shuto et al., 2012, 2015). Risk factors that influence cyst formation include higher doses, larger lesions, and lobar locations. Development of cyst are secondary to rupture of delicate telangiectatic nidal vessels after radiation (Chen et al., 2020). Until complete obliteration, the risk of re-bleeding and hemorrhage is unreliable predicted and varies based on lesional size, vascular flow dynamics, and location. Despite this risk, stereotactic radiosurgery remains an essential treatment tool for patients with AVMs.

AVM biology and development

Brain AVMs are thought to be idiopathic congenital lesions in a developing embryo which present with complications later in life. The pathogenesis and biological development of brain AVMs remains poorly understood, but recent evidence suggests that aberrant angiogenesis may be embroiled in the expansion, development, and rupture of AVMs (Berman et al., 2000; Leblanc et al., 2009; Chen et al., 2014; Rangel-Castilla et al., 2014). Vasculogenesis precedes embryologic cortical folding and studies have found no difference in the cortical folding patterns in normal vs. AVM brains (Shah et al., 2016). Digressive expression of angiogenic factors in central nervous system is a main contributor to vascular malformations including brain AVMs (Mouchtouris et al., 2015). In the surgical specimens derived from brain AVM patients, increased expression of vascular endothelial growth factor (VEGF) in the endothelial cells of AVM nidus vessels has been demonstrated (Hashimoto et al., 2000; Murukesh et al., 2010; Cheng et al., 2019). VEGF expression has potential to up regulated dynamic changes in angiogenesis and expression by nidal tissue can influence AVM formation and resistance to hypoxic factors (Murukesh et al., 2010). Given this, upstream

transcription factor signaling networks can influence VEGF and factors such as AKL-1 and can lead to promotion of angiogenesis (Schimmel et al., 2021). Increased soluble endoglin on conjunction with VEGF-A has also been shown to induce dysplastic vessel formation and can influence microglial inflammatory pro-angiogenic endothelial cell dysfunction (Park et al., 2022).

Additionally, arteriovenous specification and vascular stability are regulated by transforming growth factor-β (TGF-β) and its receptors. There are mutations in genes encoding TGF-β signaling molecules which are involved in hereditary hemorrhagic telangiectasia and are also often presented with cranial AVMs. Irregular signaling of TGF-β can cause downstream activation of pro-angiogenic pathways and has been shown to promote cerebrovascular branching and drive angiogenesis (Ferrari et al., 2009; Choi et al., 2012; Cunha et al., 2017; Siqueira et al., 2018; Zhang and Yang, 2020). Additional studies have demonstrated high prevalence of somatic KRAS mutations within blood and tissue derived samples with potentiated mitogen-activating protein kinase pathways (MAPK) and extracellular signal-regulated kinase (ERK) activity. This increased expression of transcription factor mediated changes increases angiogenesis and promotes cellular migration (Cheng and Nussinov, 2018; Nikolaev et al., 2018; Gao et al., 2022). Over expression of such factors as angiopoietin-2 (Ang-2) have been found to regulate angiogenesis and vascular stability (Crist et al., 2019). There is also an elevation in expression of basic fibroblast growth factor b-FGF, interleukin-1β, endoglin, and G protein coupled receptors (Kilic et al., 2000; Lawton et al., 2015).

Dynamic remodeling and nidal growth are known characteristics of AVMs and is influenced by inflammatory specific factors. Genetic inflammatory polymorphisms associated to AVM hemorrhage include interleukin-1β, APOE, and IL-6 (Lawton et al., 2015). Abnormalities in the extracellular matrix of AVMs leads to destabilization of the nidus. Observed changes in metalloproteinases and induced proteolytic degradation can promote structural destabilization and vascular remodeling (Rangel-Castilla et al., 2014).

The altered cellular and structural biology of AVMs deviates from the normal angiogenic principles of cerebral vascular development and regulation of vascular stability. The observed polymorphisms described above promote angiogenesis, influence dynamic remodeling, and destabilize nidal vasculature. Ultimately, this leads to a patient specific lesional characteristics with varying vascular architecture and hemorrhage risk. Radiosurgery for AVMs has proven to be a viable and effect treatment option for AVMs however, changes in the biologic micro-environment are poorly understood.

Micro-environment changes in AVM after radiosurgery

General changes in AVM vasculature

The exact mechanism and micro-environmental changes in AVMs in response to radiation has yet to be fully elucidated, though many studies have used *ex-vivo* tissue models, animal models and human histopathology to try and determine the response to radiation (Liu et al., 2012; Simonian et al., 2018; Xu et al., 2018). It is understood that radiation results in cellular damage, particularly to the vasculature endothelium, which demonstrates some of the earliest ultrastructural changes after radiation and are considered the most radiosensitive cells of the vessel wall. Their damage is hypothesized to play a pivotal role in vessel occlusion in AVMs after radiosurgery (Schneider et al., 1997; O'Connor and Mayberg, 2000; Tu et al., 2006; Karunanyaka et al., 2008; Liu et al., 2012; Szeifert et al., 2013). Following separation of the endothelium from underlying vessel wall there is leaking of proteinaceous material into the intimal space (Schneider et al., 1997; Tu et al., 2006, 2009). This is accompanied by proliferation of the subendothelium, smooth muscle cells and spindle cells (Schneider et al., 1997; Sammons et al., 2011; Kashba et al., 2015; Ilyas et al., 2018; Xu et al., 2018; Lee et al., 2019a). These spindle cells have immunohistochemical, ultrastructural and experimental characteristics resembling myofibroblasts, and have contractile capacity through α-smooth-muscle actin production and contribute to vessel occlusion (Sammons et al., 2011; Szeifert et al., 2013; Shoemaker et al., 2020). Smooth muscle cell proliferation occurs with the tunica media of the artery in a circumferential fashion contributing to concentric or eccentric narrowing of the vessel lumen (Schneider et al., 1997; Tu et al., 2006, Figure 1). These smooth muscle cells are found to have Weibel-Palade bodies suggesting a role in protein storage and secretion, such as VEGF, in response to von Willebrand Factor expression post-radiation (Tu et al., 2006). These cell types work synergistically to start the inflammatory and pro-thrombotic process following radiosurgery.

Following initial cellular degeneration and proliferation, there is extracellular matrix expansion in the intimal layer with deposition of dense fibrillar collagen and hyaline change (Schneider et al., 1997). Fibroblasts and fibrocytes are central to deposition of collagen and clot formation. They produce collagen bundles to replace the myofibroblasts. These changes are slow to occur and several years post-radiosurgery there is evidence of transformation of the initial proteinaceous clots into fibrin thrombi. This is thought to be mediated by growth factors, cytokines, chemokines, and extracellular matrix proteins secreted by fibroblasts and myofibroblasts

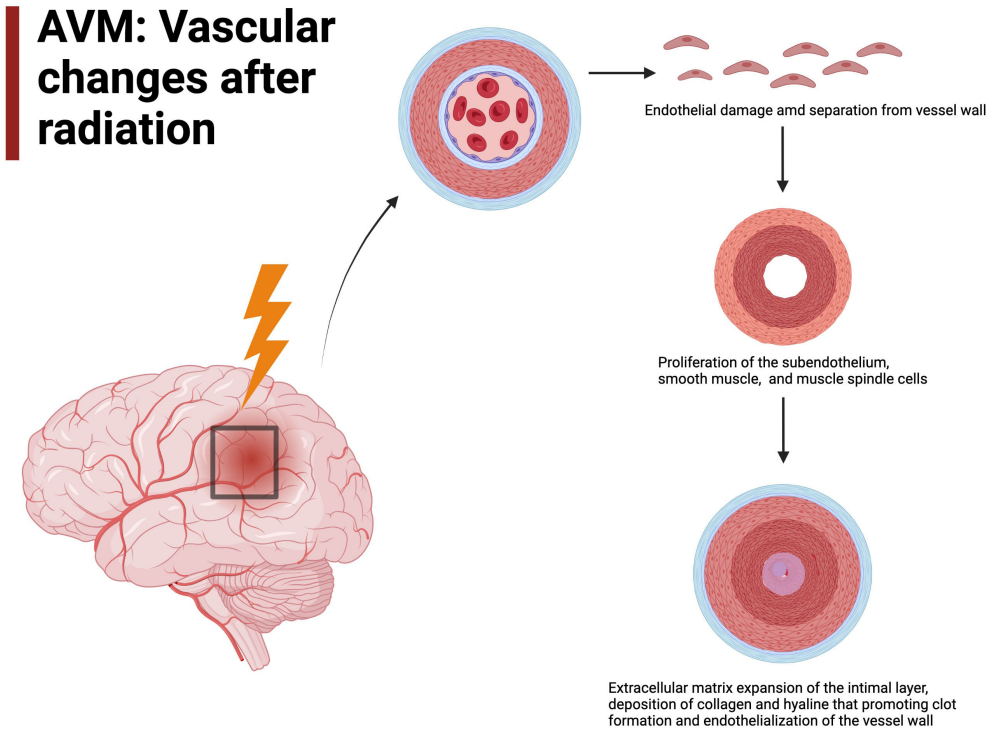

FIGURE 1
AVM vascular changes after radiation include endothelial damage will lead to endothelialization of the vessel wall.

(Schneider et al., 1997; Tu et al., 2006, 2009). Overtime there is progressive hyalinization of collagen fibers and fibrin thrombi to form scar tissue (Tu et al., 2006; Szeifert et al., 2013). In pathological specimens completely obliterated vessels demonstrate degenerated hyaline scar tissue while incompletely obliterated vessels still have fibrin thrombi indicating this is one of the last steps in the occlusive process in response to radiosurgery (Tu et al., 2006; Szeifert et al., 2013).

Overall, progressive luminal narrowing, medial and intimal thickening, hyalinization and fibrosis occurs leading to intraluminal thrombosis and reduced vessel density due to progressive vascular stenosis (Lo, 1993; Schneider et al., 1997; Tu et al., 2006, 2009; Karunanyaka et al., 2008; Liu et al., 2012; Kashba et al., 2015; Ilyas et al., 2018; Lee et al., 2019a; Xu et al., 2018). Importantly these changes in response to radiation appear to occur in a concentric or eccentric fashion involving all or nearly all of the vessel wall circumference (Schneider et al., 1997). This helps with flow dynamics and vessel wall stress in high flow AVMs. Most data demonstrates the majority of radiation changes occurring no later than 2–3 years after radiosurgery with several studies finding that after 3 years there were no further changes in AVMs in response to radiosurgery. Other studies demonstrate minor changes that continue to occur up to 4–5 years after radiosurgery. Undoubtably, the initial period after radiosurgery is the most critical to obtain AVM occlusion (Chang et al., 1997; Tu et al., 2006, 2013).

Endothelial structural and molecular changes

In AVMs the endothelium plays a critical role in the pathogenesis of the AVM as well as in its response to radiosurgery. Thus, most research on AVM radiation response has focused on the endothelium and demonstrated a central role in AVM obliteration and vascular remodeling (O'Connor and Mayberg, 2000; Karunanyaka et al., 2008; Xu et al., 2018). There are baseline molecular differences in endothelial cells compared to normal cerebral vasculature, such as increased expression of VEGF, bFGF, TGF-α/β, angiopoietin-2 and NO synthase. These molecular changes suggest a pro-angiogenic process occurring in AVMs compared to normal vasculature. It is unclear if this pro-angiogenic state is part of the primary pathogenesis of AVMs or is secondary to increased shear stress and high flow of the AVM resulting in a pro-angiogenic state (Karunanyaka et al., 2008; Storer et al., 2008; Xu et al., 2018; Lee et al., 2019b). Regardless, evidence demonstrates that AVMs have upregulation of pro-angiogenic molecules which contribute to

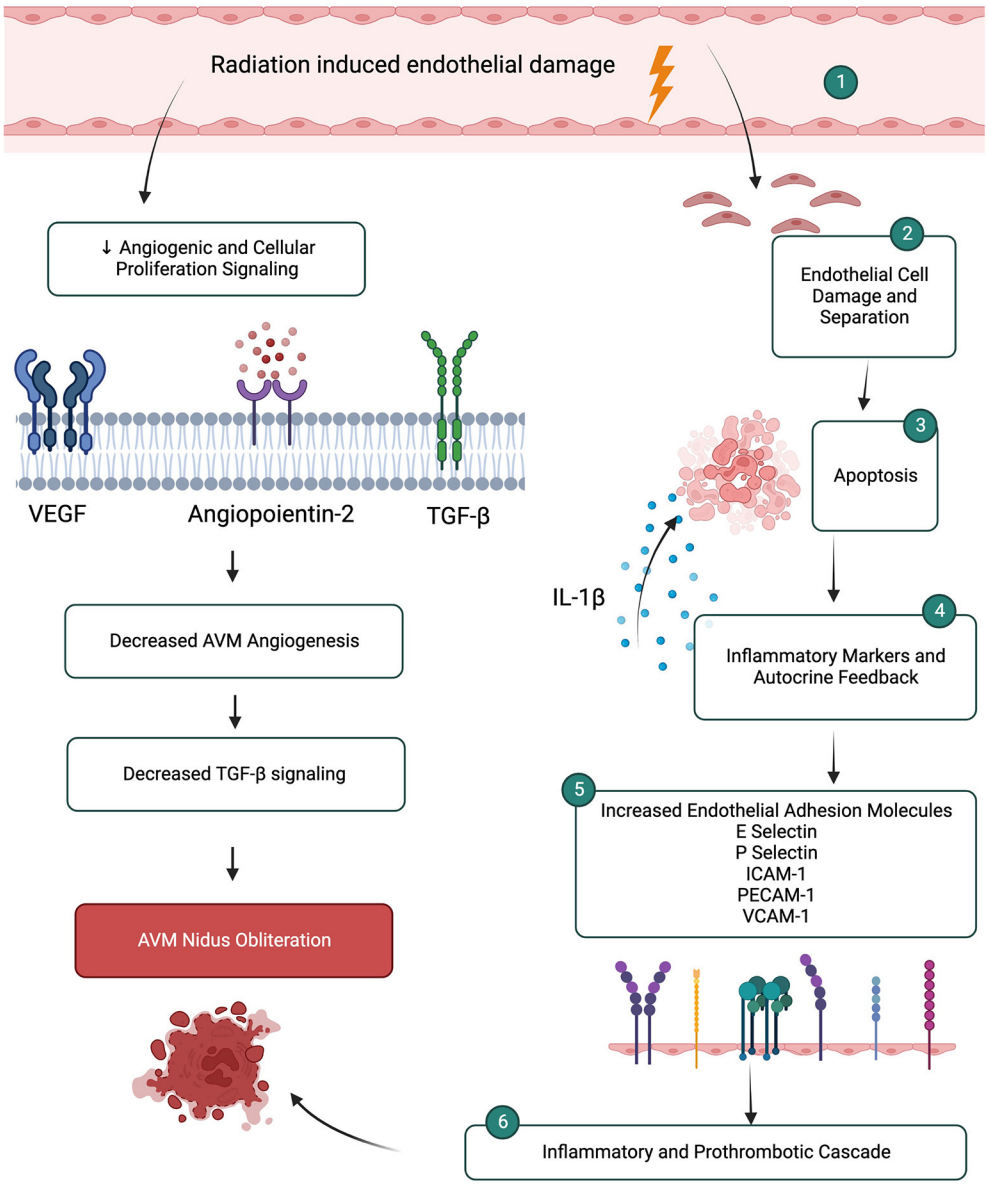

FIGURE 2
Microenvironment changes after radiation induced endothelial damage leads to inflammatory and prothrombotic cascades promoting AVM nidus obliteration. Simultaneous mechanisms lead to decreased angiogenic and proliferation pathways.

AVM maintenance. In response to radiation there are several changes to angiogenic molecules that occur. Several studies demonstrate a decrease in angiogenic factors, such as VEGF, TGF-β, and angiopoientin-2, after radiosurgery (Xu et al., 2018; Lee et al., 2019b). These changes were as early as 3 months after radiosurgery with angiopoientin-2 having the greatest reduction immediately after radiosurgery, and well before visible alterations on CT or MRI scans in patients (Xu et al., 2018). Yet, other studies have demonstrated an increase in pro-angiogenic factors after radiation as an initial survival response (Sammons et al., 2011). The exact role of angiogenic factors in AVM occlusion after radiosurgery is not fully elucidated.

There are several other pro-inflammatory and pro-thrombotic molecular changes that occur in the endothelium in response to radiosurgery. After radiosurgery, endothelial cells are damaged, separate and become disrupted and denuded (Sammons et al., 2011). While undergoing apoptosis endothelial cells release IL-1β which acts as an autocrine positive feedback on apoptotic mechanisms and as a paracrine signal to induce expression of endothelial adhesion molecules

and pro-inflammatory cytokines on surrounding endothelial cells (Tu et al., 2013). This importantly starts an inflammatory and pro-thrombotic cascade necessary for AVM obliteration (Karunanyaka et al., 2008). This molecular change starts as early as 4 h after radiation exposure and results in transcriptional upregulation of adhesion molecules E-selectin, P-selectin, ICAM-1, PECAM-1, and VCAM-1 (Karunanyaka et al., 2008; Storer et al., 2008; Sammons et al., 2011; Liu et al., 2012; Tu et al., 2013). While several *in vivo* and *in vitro* studies demonstrate early upregulation of E-selectin within hours of radiosurgery, other studies demonstrate an initial downregulation followed by increased expression (Storer et al., 2008; Liu et al., 2012). The differences in studies may be related to tissue origin of the study, radiation dose, tissue cellular make-up since there is a strong relationship reliance on the subendothelial milieu for E-selectin regulation (Liu et al., 2012). E-selectin and ICAM-1 are upregulated in response to reactive oxygen intermediates generated by radiation that activate NFκB causing increased transcription (Tu et al., 2013). Both, in addition to VCAM-1, are expressed on endothelial cells and facilitate inflammatory cell rolling, adhesion and migration (Tu et al., 2013). P-selectin in stored in Weibel-Palade bodies and mediates leukocyte rolling during inflammation as well as participates in coagulation by binding to tissue factor to accelerate the formation of fibrin during thrombogenesis (Karunanyaka et al., 2008; Tu et al., 2013) (Figure 2).

Pro-thrombogenic molecules are also upregulated in response to radiosurgery in addition to the cell adhesion molecules. Following radiosurgery, the disruption of the endothelial layer results in exposure of the subendothelium which exposes tissue factor, collagen, the basement membrane, von Willebrand Factor, microfibrils and fibronectin which create a procoagulant state (Storer et al., 2007). Importantly, there is exposure of phosphatidylserine, which provides a negatively charged lipid surface for the assembly of coagulation complexes and is necessary for coagulation initiation (Storer et al., 2007, 2010). Phosphatidylserine acts as a co-factor of tissue factor, an important factor in the induction of thrombosis. There is conflicting evidence about the upregulation of tissue factor in response to radiosurgery (Storer et al., 2007, 2010; Liu et al., 2012). Several studies demonstrate an upregulation of tissue factor after radiation that is in a time-dependent manner, yet other studies do not demonstrate a difference in tissue factor expression after radiation (Storer et al., 2007, 2010; Liu et al., 2012). Contrasting evidence also exists for upregulation of von Willebrand Factor and down regulation of thrombomodulin, an anti-coagulation molecule (Storer et al., 2007; Liu et al., 2012). Ultimately, the exact process of intravascular thrombosis after radiosurgery is not well understood but likely involves platelet adhesion followed by thrombus formation due to alteration of pro-thrombotic factors in response to radiosurgery (Karunanyaka et al., 2008).

Current limitations and future considerations

Ultimately the exact mechanisms of how radiosurgery changes the micro-environment of AVMs and causes obliteration is not understood. Several studies demonstrate that the effects of radiation appear to be a function of vessel size with potentially different responses to radiation dependent on vessel size (Schneider et al., 1997; Storer et al., 2007). Studies also use different experimental AVM models. Human histopathologic studies predominantly look at irradiated AVMs that need to be microsurgically removed secondary to neurologic impairment, and thus are often not AVMs that have been fully responsive to radiosurgery or have been pathologic specimens taken at autopsy many years after radiation exposure. Thus, initial changes after radiation to AVMs in humans is hard to elucidate. Studies use animal models or *ex-vivo* tissue cultures as alternative models for AVM radiation response. Differences in animal physiology, tissue of origin and how tissue culture are prepared can result in different outcomes. As well, it is not difficult to understand how differences in radiation dosing can result in conflicting data in the body of literature (Schneider et al., 1997). Thus, further research needs to be done to fully determine how AVMs respond to radiosurgery at the micro-environmental level.

Author contributions

TU, KB, AM, and VS were involved in drafting and revision of the original manuscript. TU, KB, AM, and SC were involved in the original conception. TU designed the figure and table. TU, KB, AH, and VS drafted sections of the manuscript. All authors contributed to manuscript revision, read, and approved the submitted version.

Conflict of interest

The authors declare that the research was conducted in the absence of any commercial or financial relationships that could be construed as a potential conflict of interest.

Publisher's note

References

Berman, M. F., Sciacca, R. R., Pile-Spellman, J., Stapf, C., Connolly, E. S., Mohr, J. P., et al. (2000). The epidemiology of brain arteriovenous malformations. *Neurosurgery* 47, 389–396. doi: 10.1097/00006123-200008000-00023

Betti, O. O., Munari, C., and Rosler, R. (1989). Stereotactic radiosurgery with the linear accelerator: treatment of arteriovenous malformations. *Neurosurgery* 24, 311–321. doi: 10.1227/00006123-198903000-00001

Brown, R. D., Wiebers, D.O., Torner, J.C., and O'Fallon, W.M. (1996). Incidence and prevalence of intracranial vascular malformations in Olmsted County, Minnesota, 1965 to 1992. *Neurology* 46, 949–952. doi: 10.1212/WNL.46.4.949

Chan, M. D., Soltys, S. G., Halasz, L. M., Laack, N. N., Minniti, G., Kirkpatrick, J. P., et al. (2019). Management of unruptured AVMs: the pendulum swings. *Int. J. Radiat. Oncol. Biol. Phys.* 105, 687–689. doi: 10.1016/j.ijrobp.2019.08.026

Chang, S. D., Shuster, D. L., Steinberg, G. K., Levy, R. P., and Frankel, K. (1997). Stereotactic radiosurgery of arteriovenous malformations: pathologic changes in resected tissue. *Clin. Neuropathol.* 16, 111–116.

Chen, C. J., Ding, D., Derdeyn, C. P., Lanzino, G., Friedlander, R. M., Southerland, A. M., et al. (2020). Brain arteriovenous malformations: a review of natural history, pathobiology, and interventions. *Neurology* 95, 917–927. doi: 10.1212/WNL.0000000000010968

Chen, W., Choi, E. J., McDougall, C. M., and Su, H. (2014). Brain arteriovenous malformation modeling, pathogenesis, and novel therapeutic targets. *Transl. Stroke Res.* 5, 316–329. doi: 10.1007/s12975-014-0343-0

Cheng, F., and Nussinov, R. (2018). KRAS activating signaling triggers arteriovenous malformations. *Trends Biochem. Sci.* 43, 481–483. doi: 10.1016/j.tibs.2018.04.007

Cheng, P., Ma, L., Shaligram, S., Walker, E. J., Yang, S. T., Tang, C., et al. (2019). Effect of elevation of vascular endothelial growth factor level on exacerbation of hemorrhage in mouse brain arteriovenous malformation. *J. Neurosurg.* 132, 1566–1573. doi: 10.3171/2019.1.JNS183112

Choi, E. J., Walker, E. J., Shen, F., Oh, S. P., Arthur, H. M., Young, W. L., et al. (2012). Minimal homozygous endothelial deletion of Eng with VEGF stimulation is sufficient to cause cerebrovascular dysplasia in the adult mouse. *Cerebrovasc. Dis.* 33, 540–547. doi: 10.1159/000337762

Choi, J. H., and Mohr, J. P. (2005). Brain arteriovenous malformations in adults. *Lancet Neurol.* 4, 299–308. doi: 10.1016/S1474-4422(05)70073-9

Cohen-Inbar, O., Ding, D., Chen, C. J., and Sheehan, J. P. (2016). Stereotactic radiosurgery for deep intracranial arteriovenous malformations, part 1: brainstem arteriovenous malformations. *J. Clin. Neurosci.* 24, 30–36. doi: 10.1016/j.jocn.2015.11.007

Colombo, F., Benedetti, A., Casentini, L., Zanusso, M., and Pozza, F. (1987). Linear accelerator radiosurgery of arteriovenous malformations. *Appl. Neurophysiol.* 50, 257–261. doi: 10.1159/000100721

Crist, A. M., Zhou, X., Garai, J., Lee, A. R., Thoele, J., Ullmer, C., et al. (2019). Angiopoietin-2 inhibition rescues arteriovenous malformation in a Smad4 hereditary hemorrhagic telangiectasia mouse model. *Circulation* 139, 2049–2063. doi: 10.1161/CIRCULATIONAHA.118.036952

Cunha, S. I., Magnusson, P. U., Dejana, E., and Lampugnani, M. G. (2017). Deregulated TGF-beta/BMP signaling in vascular malformations. *Circ. Res.* 121, 981–999. doi: 10.1161/CIRCRESAHA.117.309930

da Costa, L., Wallace, M. C., Ter Brugge, K. G., O'Kelly, C., Willinsky, R. A., and Tymianski, M. (2009). The natural history and predictive features of hemorrhage from brain arteriovenous malformations. *Stroke* 40, 100–105. doi: 10.1161/STROKEAHA.108.524678

Ding, D., Starke, R. M., Kano, H., Lee, J. Y. K., Mathieu, D., Pierce, J., et al. (2017a). Radiosurgery for unruptured brain arteriovenous malformations: an international multicenter retrospective cohort study. *Neurosurgery* 80, 888–898. doi: 10.1093/neuros/nyx181

Ding, D., Starke, R. M., Kano, H., Mathieu, D., Huang, P., Kondziolka, D., et al. (2016). Radiosurgery for cerebral arteriovenous malformations in a randomized trial of unruptured brain arteriovenous malformations (ARUBA)-eligible patients: a multicenter study. *Stroke* 47, 342–349. doi: 10.1161/STROKEAHA.115.011400

Ding, D., Starke, R. M., Kano, H., Mathieu, D., Huang, P. P., Kondziolka, D., et al. (2017b). Stereotactic radiosurgery for ARUBA (a randomized trial of unruptured brain arteriovenous malformations)-eligible spetzler-martin grade i and ii arteriovenous malformations: a multicenter study. *World Neurosurg.* 102, 507–517. doi: 10.1016/j.wneu.2017.03.061

Ferrari, G., Cook, B. D., Terushkin, V., Pintucci, G., and Mignatti, P. (2009). Transforming growth factor-beta 1 (TGF-beta1) induces angiogenesis through vascular endothelial growth factor (VEGF)-mediated apoptosis. *J. Cell Physiol.* 219, 449–458. doi: 10.1002/jcp.21706

Flickinger, J. C., Kondziolka, D., Maitz, A. H., and Lunsford, L. D. (2002). An analysis of the dose-response for arteriovenous malformation radiosurgery and other factors affecting obliteration. *Radiother. Oncol.* 63, 347–354. doi: 10.1016/S0167-8140(02)00103-2

Flickinger, J. C., Pollock, B. E., Kondziolka, D., and Lunsford, L. D. (1996). A dose-response analysis of arteriovenous malformation obliteration after radiosurgery. *Int. J. Radiat. Oncol. Biol. Phys.* 36, 873–879. doi: 10.1016/S0360-3016(96)00316-1

Franzin, A., Panni, P., Spatola, G., Del Vecchio, A., Gallotti, A. L., Gigliotti, C. R., et al. (2016). Results of volume-staged fractionated Gamma Knife radiosurgery for large complex arteriovenous malformations: obliteration rates and clinical outcomes of an evolving treatment paradigm. *J. Neurosurg.* 125, 104–113. doi: 10.3171/2016.7.GKS161549

Gao, S., Nelson, J., Weinsheimer, S., Winkler, E. A., Rutledge, C., Abla, A. A., et al. (2022). Somatic mosaicism in the MAPK pathway in sporadic brain arteriovenous malformation and association with phenotype. *J. Neurosurg.* 136, 148–155. doi: 10.3171/2020.11.JNS202031

Garcin, B., Houdart, E., Porcher, R., Manchon, E., Saint-Maurice, J. P., Bresson, D., et al. (2012). Epileptic seizures at initial presentation in patients with brain arteriovenous malformation. *Neurology* 78, 626–631. doi: 10.1212/WNL.0b013e3182494d40

Hasegawa, H., Hanakita, S., Shin, M., Sugiyama, T., Kawashima, M., Takahashi, W., et al. (2018). A comprehensive study of symptomatic late radiation-induced complications after radiosurgery for brain arteriovenous malformation: incidence, risk factors, and clinical outcomes. *World Neurosurg.* 116, e556–e565. doi: 10.1016/j.wneu.2018.05.038

Hashimoto, T., Emala, C. W., Joshi, S., Mesa-Tejada, R., Quick, C. M., Feng, L., et al. (2000). Abnormal pattern of Tie-2 and vascular endothelial growth factor receptor expression in human cerebral arteriovenous malformations. *Neurosurgery* 47, 910–918. doi: 10.1097/00006123-200010000-00022

Hernesniemi, J. A., Dashti, R., Juvela, S., Vaart, K., Niemela, M., Laakso, A., et al. (2008). Natural history of brain arteriovenous malformations: a long-term follow-up study of risk of hemorrhage in 238 patients. *Neurosurgery* 63, 823–829. doi: 10.1227/01.NEU.0000330401.82582.5E

Hofmeister, C., Stapf, C., Hartmann, A., Sciacca, R. R., and Mansmann, U. terBrugge, K., et al. (2000). Demographic, morphological, and clinical characteristics of 1289 patients with brain arteriovenous malformation. *Stroke* 31, 1307–1310. doi: 10.1161/01.STR.31.6.1307

Ilyas, A., Chen, C. J., Ding, D., Buell, T. J., Raper, D. M. S., Lee, C. C., et al. (2018). Radiation-induced changes after stereotactic radiosurgery for brain arteriovenous malformations: a systematic review and meta-analysis. *Neurosurgery* 83, 365–376. doi: 10.1093/neuros/nyx502

Jessurun, G. A. J., Kamphuis, D. J., van der Zande, F. H. R., and Nossent, J. C. (1993). Cerebral arteriovenous malformations in the Netherlands Antilles. *Clin. Neurol. Neurosurgery* 95, 193–198. doi: 10.1016/0303-8467(93)90123-X

Josephson, C. B., Bhattacharya, J. J., Counsell, C. E., Papanastassiou, V., Ritchie, V., Roberts, R., et al. (2012). Seizure risk with AVM treatment or conservative management: prospective, population-based study. *Neurology* 79, 500–507. doi: 10.1212/WNL.0b013e3182635696

Josephson, C. B., Leach, J. P., Duncan, R., Roberts, R. C., Counsell, C. E., Al-Shahi Salman, R., et al. (2011). Seizure risk from cavernous or arteriovenous malformations: prospective population-based study. *Neurology* 76, 1548–1554. doi: 10.1212/WNL.0b013e3182190f37

Karlsson, B., Jokura, H., Yang, H. C., Yamamoto, M., Martinez, R., Kawagishi, J., et al. (2019). The NASSAU (New ASSessment of cerebral Arteriovenous Malformations yet Unruptured) analysis: are the results from the ARUBA trial also applicable to unruptured arteriovenous malformations deemed suitable for gamma knife surgery? *Neurosurgery* 85, E118–E124. doi: 10.1093/neuros/nyy391

Karunanyaka, A., Tu, J., Watling, A., Storer, K. P., Windsor, A., Stoodley, M. A., et al. (2008). Endothelial molecular changes in a rodent model of arteriovenous malformation. *J Neurosurg* 109, 1165–1172. doi: 10.3171/JNS.2008.109.12.1165

Kashba, S. R., Patel, N. J., Grace, M., Lee, V. S., Raoufi-Rad, N., Raj, J. V., et al. (2015). Angiographic, hemodynamic, and histological changes in an animal model of brain arteriovenous malformations treated with Gamma Knife radiosurgery. *J. Neurosurg.* 123, 954–960. doi: 10.3171/2014.10.JNS1435

Kilic, T., Pamir, M. N., Kullu, S., Eren, F., Ozek, M. M., Black, P. M., et al. (2000). Expression of structural proteins and angiogenic factors in cerebrovascular anomalies. *Neurosurgery* 46, 1179–1191. doi: 10.1097/00006123-200005000-00032

Kim, H., Al-Shahi Salman, R., McCulloch, C. E., Stapf, C., Young, W. L., Coinvestigators, M., et al. (2014). Untreated brain arteriovenous malformation: patient-level meta-analysis of hemorrhage predictors. *Neurology* 83, 590–597. doi: 10.1212/WNL.0000000000000688

Laakso, A., and Hernesniemi, J. (2012). Arteriovenous malformations: epidemiology and clinical presentation. *Neurosurg. Clin. N Am.* 23, 1–6. doi: 10.1016/j.nec.2011.09.012

Lawton, M. T., Rutledge, W. C., Kim, H., Stapf, C., Whitehead, K. J., Li, D. Y., et al. (2015). Brain arteriovenous malformations. *Nat. Rev. Dis. Primers* 1, 15008. doi: 10.1038/nrdp.2015.8

Leblanc, G. G., Golanov, E., Awad, I. A., Young, W. L., and Biology of Vascular Malformations of the Brain NWC. (2009). Biology of vascular malformations of the brain. *Stroke* 40, e694–702. doi: 10.1161/STROKEAHA.109.563692

Lee, C. C., Yang, H. C., Lin, C. J., Chen, C. J., Wu, H. M., Shiau, C. Y., et al. (2019a). Intervening nidal brain parenchyma and risk of radiation-induced changes after radiosurgery for brain arteriovenous malformation: a study using an unsupervised machine learning algorithm. *World Neurosurgery* 125, E132–E138. doi: 10.1016/j.wneu.2018.12.220

Lee, J. G., Park, S. H., Park, K. S., Kang, D. H., Hwang, J. H., Hwang, S. K., et al. (2019b). Do serum vascular endothelial growth factor and endostatin reflect radiological radiation-induced changes after stereotactic radiosurgery for cerebral arteriovenous malformations? *World Neurosurg.* 126, e612–e618. doi: 10.1016/j.wneu.2019.02.101

Liu, S., Sammons, V., Fairhall, J., Reddy, R., Tu, J., Duong, T. T., et al. (2012). Molecular responses of brain endothelial cells to radiation in a mouse model. *J. Clin. Neurosci.* 19, 1154–1158. doi: 10.1016/j.jocn.2011.12.004

Lo, E. H. (1993). A theoretical analysis of hemodynamic and biomechanical alterations in intracranial AVMs after radiosurgery. *Int. J. Radiat. Oncol. Biol. Phys.* 27, 353–361. doi: 10.1016/0360-3016(93)90247-S

Mast, H., Young, W. L., Koennecke, H-. C., Sciacca, R. R., Osipov, A., Pile-Spellman, J., et al. (1997). Risk of spontaneous haemorrhage after diagnosis of cerebral arteriovenous malformation. *Lancet* 350, 1065–1068. doi: 10.1016/S0140-6736(97)05390-7

Mohr, J. P., Parides, M. K., Stapf, C., Moquete, E., Moy, C. S., Overbey, J. R., et al. (2014). Medical management with or without interventional therapy for unruptured brain arteriovenous malformations (ARUBA): a multicentre, non-blinded, randomised trial. *Lancet* 383, 614–621. doi: 10.1016/S0140-6736(13)62302-8

Mouchtouris, N., Jabbour, P. M., Starke, R. M., Hasan, D. M., Zanaty, M., Theofanis, T., et al. (2015). Biology of cerebral arteriovenous malformations with a focus on inflammation. *J. Cereb. Blood Flow Metab.* 35, 167–175. doi: 10.1038/jcbfm.2014.179

Murukesh, N., Dive, C., and Jayson, G. C. (2010). Biomarkers of angiogenesis and their role in the development of VEGF inhibitors. *Br. J. Cancer.* 102, 8–18. doi: 10.1038/sj.bjc.6605483

Nagy, G., Major, O., Rowe, J. G., Radatz, M. W., Hodgson, T. J., Coley, S. C., et al. (2012). Stereotactic radiosurgery for arteriovenous malformations located in deep critical regions. *Neurosurgery* 70, 1458–1469. doi: 10.1227/NEU.0b013e318246a4d0

Nikolaev, S. I., Vetiska, S., Bonilla, X., Boudreau, E., Jauhiainen, S., Rezai Jahromi, B., et al. (2018). Somatic activating KRAS mutations in arteriovenous malformations of the brain. *N Engl. J. Med.* 378, 250–261. doi: 10.1056/NEJMoa1709449

O'Connor, M. M., and Mayberg, M. R. (2000). Effects of radiation on cerebral vasculature: a review. *Neurosurgery* 46, 138–149. doi: 10.1093/neurosurgery/46.1.138

Osbun, J. W., Reynolds, M. R., and Barrow, D. L. (2017). Arteriovenous malformations: epidemiology, clinical presentation, and diagnostic evaluation. *Handb. Clin. Neurol.* 143, 25–29. doi: 10.1016/B978-0-444-63640-9.00003-5

Park, E. S., Kim, S., Yao, D. C., Savarraj, J. P. J., Choi, H. A., Chen, P. R., et al. (2022). Soluble endoglin stimulates inflammatory and angiogenic responses in microglia that are associated with endothelial dysfunction. *Int. J. Mol. Sci.* 23:1225. doi: 10.3390/ijms23031225

Paul, L., Casasco, A., Kusak, M. E., Martinez, N., Rey, G., Martinez, R., et al. (2014). Results for a series of 697 arteriovenous malformations treated by gamma knife: influence of angiographic features on the obliteration rate. *Neurosurgery* 75, 568–583. doi: 10.1227/NEU.0000000000000506

Peciu-Florianu, I., Leroy, H. A., Drumez, E., Dumot, C., Aboukais, R., Touzet, G., et al. (2020). Radiosurgery for unruptured brain arteriovenous malformations in the pre-ARUBA era: long-term obliteration rate, risk of hemorrhage and functional outcomes. *Sci. Rep.* 10, 21427. doi: 10.1038/s41598-020-78547-0

Pollock, B. E., and Flickinger, J. C. (2002). A proposed radiosurgery-based grading system for arteriovenous malformations. *J. Neurosurg.* 96, 79–85. doi: 10.3171/jns.2002.96.1.0079

Pollock, B. E., Link, M. J., Branda, M. E., and Storlie, C. B. (2017). Incidence and management of late adverse radiation effects after arteriovenous malformation radiosurgery. *Neurosurgery* 81, 928–934. doi: 10.1093/neuros/nyx010

Pollock, B. E., Link, M. J., Stafford, S. L., Garces, Y. I., and Foote, R. L. (2016). Stereotactic radiosurgery for arteriovenous malformations: the effect of treatment period on patient outcomes. *Neurosurgery* 78, 499–509. doi: 10.1227/NEU.0000000000001085

Raffa, S. J., Chi, Y. Y., Bova, F. J., and Friedman, W. A. (2009). Validation of the radiosurgery-based arteriovenous malformation score in a large linear accelerator radiosurgery experience. *J. Neurosurg.* 111, 832–839. doi: 10.3171/2009.4.JNS081532

Rangel-Castilla, L., Russin, J. J., Martinez-Del-Campo, E., Soriano-Baron, H., Spetzler, R. F., Nakaji, P., et al. (2014). Molecular and cellular biology of cerebral arteriovenous malformations: a review of current concepts and future trends in treatment. *Neurosurg. Focus* 37, E1. doi: 10.3171/2014.7.FOCUS14214

Sammons, V., Davidson, A., Tu, J., and Stoodley, M. A. (2011). Endothelial cells in the context of brain arteriovenous malformations. *J. Clin. Neurosci.* 18, 165–170. doi: 10.1016/j.jocn.2010.04.045

Schimmel, K., Ali, M. K., Tan, S. Y., Teng, J., Do, H. M., Steinberg, G. K., et al. (2021). Arteriovenous malformations-current understanding of the pathogenesis with implications for treatment. *Int. J. Mol. Sci.* 22, 9037. doi: 10.3390/ijms22169037

Schneider, B. F., Eberhard, D. A., and Steiner, L. E. (1997). Histopathology of arteriovenous malformations after gamma knife radiosurgery. *J. Neurosurg.* 87, 352–357. doi: 10.3171/jns.1997.87.3.0352

Shah, M. N., Smith, S. E., Dierker, D. L., Herbert, J. P., Coalson, T. S., Bruck, B. S., et al. (2016). The relationship of cortical folding and brain arteriovenous malformations. *Neurovasc. Imag.* 2, 1–10. doi: 10.1186/s40809-016-0024-3

Shoemaker, L. D., McCormick, A. K., Allen, B. M., and Chang, S. D. (2020). Evidence for endothelial-to-mesenchymal transition in human brain arteriovenous malformations. *Clin. Transl. Med.* 10, e99. doi: 10.1002/ctm2.99

Shuto, T., Ohtake, M., and Matsunaga, S. (2012). Proposed mechanism for cyst formation and enlargement following gamma knife surgery for arteriovenous malformations. *J. Neurosurg.* 117, 135–143. doi: 10.3171/2012.6.GKS12318

Shuto, T., Yagishita, S., and Matsunaga, S. (2015). Pathological characteristics of cyst formation following gamma knife surgery for arteriovenous malformation. *Acta Neurochir.* 157, 293–298. doi: 10.1007/s00701-014-2298-z

Simonian, M., Shirasaki, D., Lee, V. S., Bervini, D., Grace, M., Loo, R. R. O., et al. (2018). Proteomics identification of radiation-induced changes of membrane proteins in the rat model of arteriovenous malformation in pursuit of targets for brain AVM molecular therapy. *Clin. Proteom.* 15, 1–8. doi: 10.1186/s12014-018-9217-x

Siqueira, M., Francis, D., Gisbert, D., Gomes, F. C. A., and Stipursky, J. (2018). Radial glia cells control angiogenesis in the developing cerebral cortex through TGF-beta1 signaling. *Mol. Neurobiol.* 55, 3660–3675. doi: 10.1007/s12035-017-0557-8

Starke, R. M., Kano, H., Ding, D., Lee, J. Y., Mathieu, D., Whitesell, J., et al. (2017). Stereotactic radiosurgery for cerebral arteriovenous malformations: evaluation of long-term outcomes in a multicenter cohort. *J. Neurosurg.* 126, 36–44. doi: 10.3171/2015.9.JNS151311

Starke, R. M., Yen, C. P., Ding, D., and Sheehan, J. P. (2013). A practical grading scale for predicting outcome after radiosurgery for arteriovenous malformations: analysis of 1012 treated patients. *J. Neurosurg.* 119, 981–987. doi: 10.3171/2013.5.JNS1311

Steiner, L., Leksell, L., Greitz, T., Forster, D. M., and Backlund, E. O. (1972). Stereotaxic radiosurgery for cerebral arteriovenous malformations. Report of a case. *Acta Chir. Scand.* 138, 459–464.

Storer, K. P., Tu, J., Karunanayaka, A., Morgan, M. K., and Stoodley, M. A. (2007). Thrombotic molecule expression in cerebral vascular malformations. *J. Clin. Neurosci.* 14, 975–980. doi: 10.1016/j.jocn.2006.12.005

Storer, K. P., Tu, J., Karunanayaka, A., Morgan, M. K., and Stoodley, M. A. (2008). Inflammatory molecule expression in cerebral arteriovenous malformations. *J. Clin. Neurosci.* 15, 179–184. doi: 10.1016/j.jocn.2006.10.013

Storer, K. P., Tu, J., Stoodley, M. A., and Smee, R. I. (2010). Expression of endothelial adhesion molecules after radiosurgery in an animal model of arteriovenous malformation. *Neurosurgery* 67, 976–983. doi: 10.1227/NEU.0b013e3181ee36bc

Szeifert, G. T., Levivier, M., Lorenzoni, J., Nyary, I., Major, O., Kemeny, A. A., et al. (2013). Morphological observations in brain arteriovenous malformations after gamma knife radiosurgery. *Prog. Neurol. Surg.* 27, 119–129. doi: 10.1159/000341772

Tu, J., Hu, Z., and Chen, Z. (2013). Endothelial gene expression and molecular changes in response to radiosurgery in *in vitro* and *in vivo* models of cerebral arteriovenous malformations. *Biomed. Res. Int.* 2013, 408253. doi: 10.1155/2013/408253

Tu, J., Stoodley, M. A., Morgan, M. K., and Storer, K. P. (2006). Responses of arteriovenous malformations to radiosurgery: ultrastructural changes. *Neurosurgery* 58, 749–758. doi: 10.1227/01.NEU.0000192360.87083.90

Tu, J., Stoodley, M. A., Morgan, M. K., Storer, K. P. and Smee, R. (2009). Different responses of cavernous malformations and arteriovenous malformations to radiosurgery. *J. Clin. Neurosci.* 16, 945–949. doi: 10.1016/j.jocn.2008.09.017

Xu, M., Liu, X., Mei, G., Zhang, J., Wang, W., Xu, H., et al. (2018). Radiosurgery reduces plasma levels of angiogenic factors in brain arteriovenous malformation patients. *Brain Res. Bull.* 140, 220–225. doi: 10.1016/j.brainresbull.2018.05.007

Zhang, Y., and Yang, X. (2020). The roles of TGF-beta signaling in cerebrovascular diseases. *Front. Cell Dev. Biol.* 8, 567682. doi: 10.3389/fcell.2020.567682

Zhu, X. L., Chan, M. S., and Poon, W. S. (1997). Spontaneous intracranial hemorrhage: which patients need diagnostic cerebral angiography? A prospective study of 206 cases and review of the literature. *Stroke* 28, 1406–1409. doi: 10.1161/01.STR.28.7.1406

frontiers | Frontiers in Neurology

TYPE Review
PUBLISHED 10 February 2023
DOI 10.3389/fneur.2023.1099328

OPEN ACCESS

EDITED BY
Lorelei Shoemaker,
Stanford University, United States

REVIEWED BY
Mirna Lechpammer,
Foundation Medicine Inc., United States
Ethan Winkler,
University of California, San Francisco,
United States

*CORRESPONDENCE
Ivan Radovanovic
✉ ivan.radovanovic@uhn.ca

SPECIALTY SECTION
This article was submitted to Stroke, a section of the journal Frontiers in Neurology

RECEIVED 15 November 2022
ACCEPTED 25 January 2023
PUBLISHED 10 February 2023

CITATION
Mansur A and Radovanovic I (2023) Vascular malformations: An overview of their molecular pathways, detection of mutational profiles and subsequent targets for drug therapy. *Front. Neurol.* 14:1099328. doi: 10.3389/fneur.2023.1099328

Vascular malformations: An overview of their molecular pathways, detection of mutational profiles and subsequent targets for drug therapy

Ann Mansur[1,2] and Ivan Radovanovic[1,3,4]*

[1]Division of Neurosurgery, Department of Surgery, Faculty of Medicine, University of Toronto, Toronto, ON, Canada, [2]Department of Laboratory Medicine and Pathobiology, School of Graduate Studies, University of Toronto, Toronto, ON, Canada, [3]Division of Neurosurgery, Department of Surgery, Toronto Western Hospital, University Health Network, Toronto, ON, Canada, [4]Krembil Brain Institute, University Health Network, Toronto, ON, Canada

Vascular malformations are anomalies in vascular development that portend a significant risk of hemorrhage, morbidity and mortality. Conventional treatments with surgery, radiosurgery and/or endovascular approaches are often insufficient for cure, thereby presenting an ongoing challenge for physicians and their patients. In the last two decades, we have learned that each type of vascular malformation harbors inherited germline and somatic mutations in two well-known cellular pathways that are also implicated in cancer biology: the PI3K/AKT/mTOR and RAS/RAF/MEK pathways. This knowledge has led to recent efforts in: (1) identifying reliable mechanisms to detect a patient's mutational burden in a minimally-invasive manner, and then (2) understand how cancer drugs that target these mutations can be repurposed for vascular malformation care. The idea of precision medicine for vascular pathologies is growing in potential and will be critical in expanding the clinician's therapeutic armamentarium.

KEYWORDS

vascular malformation (VMs), targeted therapy, precision medicine, liquid biopsy, signaling pathway

Introduction

Vascular malformations (VMs) are inborn errors of vascular development that result in abnormally formed vessels. They are classified into slow- and fast-flow malformations based on the absence or presence of an arterial component, respectively. They include venous, lymphatic, arterial, capillary and mixed malformations, alongside those associated with other anomalies (1). While majority of VMs are present at birth, they can sometimes form *de novo* in post-natal development. Of those present at birth, 5% are caused by inherited loss-of-function (LOF) germline mutations with a somatic second hit, while the remaining 95% are sporadic in nature, meaning that they occur due to gain-of-function (GOF) mutations occurring after conception in clusters of non-gametal cells (2). These mutations occur in one of two major cellular signaling pathways: the PI3KCA-AKT-mTOR and the RAS-RAF-MEK-ERK pathways, which govern angiogenesis, cell growth and proliferation, motility and apoptosis (Figure 1). Both pathways are implicated in various cancers and through their assessment in these populations, targeted therapeutics were developed that address various aspects of these intricate cascades. These systemic agents are being introduced in the management of vascular malformations, albeit at a largely experimental level. This review summarizes the literature to date on the molecular pathophysiology of VMs and novel methods to detect their mutational burden, alongside an update on their potential targeted therapies.

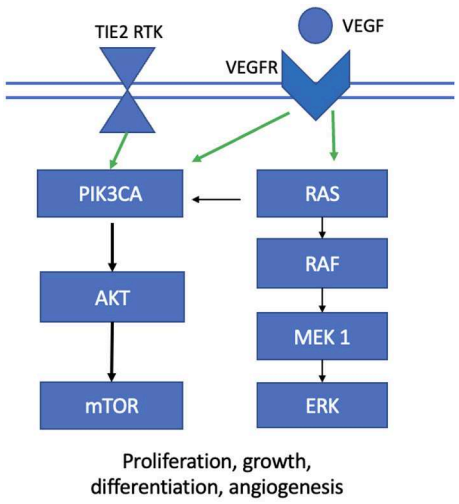

FIGURE 1
Two major cellular signaling pathways implicated in the development of vascular malformations. TIE2 RTK, *TEK* gene receptor tyrosine kinase; VEGF, vascular endothelial growth factor; VEGFR, vascular endothelial growth factor receptor.

Slow-flow malformations

Slow-flow malformations include venous malformations (VeMs), lymphatic malformations (LMs), and mixed vascular malformations, alongside overgrowth syndromes. These malformations are characterized by overactivation of phosphoinositide 3-kinase (PI3K) through mutations in the PI3K/AKT/mTOR signaling pathway (3–5). In the normal state, ligand binding results in phosphorylation of phosphatidylinositol-4,5-bisphosphate to phosphatidylinositol-3,4,5-triphosphate through PI3K, which then recruits the downstream target AKT (6). Phosphate and tensin homolog (PTEN) normally inhibits P13K, thereby downregulating this signal cascade (Figure 1).

VeMs are soft and compressible blue lesions that typically occur in the skin or mucosal membranes. Most are sporadic and are caused by somatic GOF mutations in the *TEK* gene, which encodes the endothelial receptor tyrosine kinase TIE2 (7). When angiopoietin 1 (ANPT1) binds TIE2 in endothelial cells, it then activates the canonical PI3K-AKT-mTOR pathway leading to endothelial cell proliferation (2, 8). Somatic *TIE2* mutations occur in unifocal and multifocal VMs and blue rubber bled nevus syndrome (7–9). Those with inherited cutaneomucosal VeMs have autosomal dominant *TIE2* mutations and together with a somatic second hit mutation in *TEK*, these patients then demonstrate their multifocal lesion phenotype (10).

A smaller subset of VeMs (20%) harbor somatic mutations in the *PIK3CA* gene, which encodes the alpha subunit of the downstream effector PI3K (11, 12). In endothelial cells, the alpha subunit is activated by the VEGF and TIE receptors to eventually phosphorylate AKT, especially its AKT1 isoform (13, 14) (Figure 2). Similar to *TIE2* mutations, a GOF mutation in *PIK3CA* thereby leads to overactivation of AKT (15). These mutations are also commonly found in *PIK3CA*-related overgrowth syndromes (PROS) such as Klippel-Trenaunay syndrome (KTS), megalencephaly-capillary malformation syndrome (MCAP), and congenital lipomatous overgrowth with vascular anomalies, epidermal nevi and scoliosis syndrome (CLOVES) (16, 17) (Figure 2). These syndromic forms of LM have more wide-spread *PIK3CA* mutations in non-hot spot loci (18). Proteus syndrome, another overgrowth syndrome, harbors somatic mutations in the downstream effector *AKT* (19).

LMs (microcystic and macrocystic) and complex lymphatic anomalies (CLAs) are localized or multifocal lesions of the lymphatic vasculature, respectively (17). CLAs include Gorham-Stout Disease (GSD), generalized lymphatic anomalies, central conducting lymphatic anomalies (CCLA), and kaposiform lymphangiomatosis (KLA) (20). In normal lymphatic vascular development, differentiation is initiated by the *PROX1* gene and maintained by VEGF signaling (21). Postnatally, vessel morphology is matured by angiopoietin-2 (ANGPT2) via the TIE2 receptor that is involved in PI3K-AKT-mTOR signaling; valves are developed under the regulation of the EPHB4 receptor tyrosine kinase, which recruits RASA1 to normally inhibit the RAS-MAPK-ERK signaling pathway (18) (Figure 2). Hence, lymphatic development relies on transduction of both the PI3K-AKT-mTOR (for sprouting and maturation) and RAS-MAPK-ERK (for growth and proliferation) pathways. Like VeMs, the majority of cystic LMs harbor the same types of *PIK3CA* hot-spot mutations which cause increased PI3K activity as well as increased phosphorylation of downstream AKT (15, 22). More rarely, some patients with CLA have mutations in the RAS-MAPK/ERK pathway including *KRAS, NRAS* and *EPHB4* (23–26). In addition to these two cellular pathways, the LM growth is supported by paracrine secretion of VEGF, likely mediated by immune cells (27).

If left untreated, slow-flow malformations harbor significant morbidity, commonly presenting with lesions, coagulopathy, thrombosis, pain/migraine, and location-specific functional limitations that worsen through puberty. Lesions of the central nervous system (CNS) include: (1) developmental venous anomalies that are benign but can present with thrombosis leading to hemorrhage or infarction with an incidence of 0.22–0.68% per year, and even higher if associated with cerebral cavernous malformations; (2) sinus peri-cranii which can result in headaches, tinnitus or issues with cosmesis that cause impairments in quality of life, and (3) cavernous malformations that occur with an incidence of 0.1–0.8% and present with seizures in up to 50% of patients, hemorrhage in 25% and focal neurological deficits in 5–10% of patients (9, 17, 28). Generally, CNS lesions can have significant morbidity if a patient is plagued with intractable seizures, headaches, tinnitus, cranial nerve dysfunction, and even heart failure in newborns. Some slow-flow malformations are life-threatening due to extension into vital tissues such as the airway, due to cardiac failure, or due to severe impairments in coagulopathy and uncontrolled bleeding; mortality rates for slow-flow malformations if left untreated range from 0.1 to 20%, with VeMs and deep seated cerebral cavernous malformations, respectively (28).

Standard treatments of these slow-flow malformations include: (1) supportive management with compression, analgesia and correction of coagulopathy; (2) medical management of seizures and heart failure; (3) surgical resection; (4) sclerotherapy and/or laser therapy for symptom relief and cosmesis; and (5) endovascular treatment for specific slow-flow malformations such as accessory sinus pericrania. Laser ablation is typically used for superficial dermal or mucosal lesions, and surgery is often limited to focal lesions in easily accessible locations to ensure a complete resection,

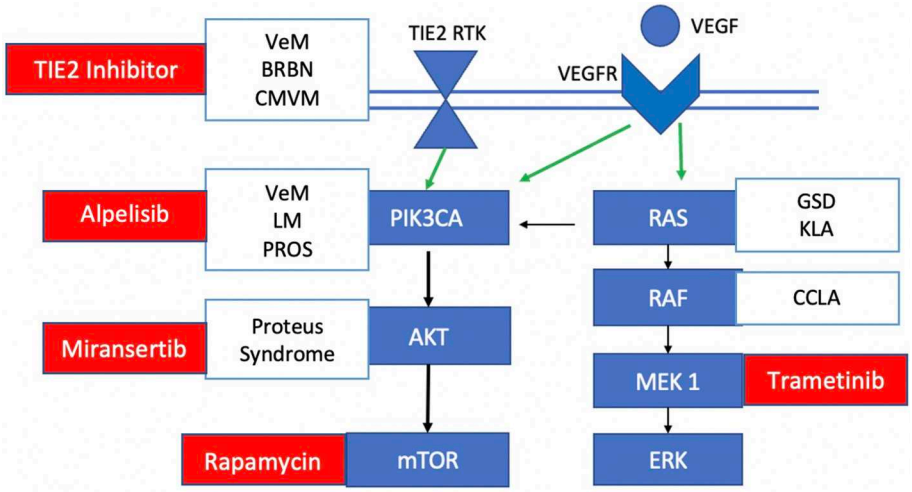

FIGURE 2
Mutations and targeted therapies for slow-flow malformations. TIE2 RTK, *TEK* gene receptor tyrosine kinase; VEGF, vascular endothelial growth factor; VEGFR, vascular endothelial growth factor receptor. Somatic TIE2 mutations are observed in unifocal and multifocal venous malformations (VeMs), blue rubber bled nevus syndrome (BRBN) and cutaneomucosal venous malformations. Somatic PIK3CA mutations are seen in venous malformations, lymphatic malformations and PROS. Some central lymphatic anomalies such as Gorham Stout Disease (GSD) and kaposiform lymphangiomatosis (KLA) harbor RAS mutations while patients with central conducting lymphatic anomalies (CCLA) have ARAF mutations. Currently investigated targeted therapies for each component of the pathway in slow-flow malformations are shown in red.

which if cured can significantly reduce the morbidity and mortality rate. Sclerotherapy with either doxycycline, bleomycin or 3% sodium tetradecyl sulfate is frequently used but often repeated treatments are needed, yet insufficient for cure; sclerotherapy is complicated by skin necrosis, pain, blistering and peripheral neuropathy in up to 10% of patients, and less commonly by venous thromboembolism/pulmonary embolism, pulmonary fibrosis and cardiopulmonary failure (28, 29). Treatment of patients with CLAs and syndromic VeMs is particularly challenging given the extensive tissue involvement and deep location of vascular lesions; an approach with systemic agents would be useful in targeting the molecular biology of the disease, and particularly ideal for these complex syndromes. To date, there are several systemic agents being investigated for slow-flow malformations that target different parts of the PI3K-AKT-mTOR and RAS-MAPK-ERK signaling pathways (Figure 2).

PI3K-AKT-mTOR pathway inhibitors

MTOR inhibitor

Rapamycin (also known as sirolimus) a is a commonly used drug in clinical practice for its immunosuppressive and antiangiogenic properties. It works by disrupting mTORC1, thereby preventing it from phosphorylating downstream proteins S6Rp and 4E-BP1, which are critical for cellular differentiation, proliferation and motility (30). Its relevance to VMs was only recently discovered. In a mouse model of VMs with injected $TIE2^{L914F}$-mutated endothelial cells, mice that were injected with rapamycin-pretreated cells had smaller and more poorly developed vasculature than those who did not get the rapamycin-pretreated or TIE2 inhibitor-pretreated cells (31). Established VMs in both the mice and murine models treated with rapamycin had delayed growth and reduced VM volume compared to vehicle and TIE2 inhibitor-treated groups (31).

Rapamycin was assessed in a variety of retrospective studies for both pediatric and adult patients with severe slow-flow malformations including syndromic VMs and CLAs (32–35). The starting dose was 2mg daily for adults and 0.8 mg/m^2 twice daily for children, with target trough levels of 10–15ng/mL. At this dose, rapamycin was well tolerated with mostly minor yet frequent adverse events necessitating conservative management. Twelve patients had grades 1–2 mucositis, four had opportunistic infections, one had a headache and one had hypertension; four of these patients required a dose reduction and only one patient discontinued the treatment due to severe mucositis. On laboratory testing, 10 patients had hyperlipidemia, four had elevated liver enzymes and one patient had lymphopenia. Patient symptoms, including pain, hemodynamic instability, and functional status improved in over 80% of patients within 3 months; no patient had complete cure with rapamycin treatment.

A pilot prospective trial on rapamycin in six adult patients with palliative slow-flow VMs showed clinical efficacy with significant reduction in pain, over 50% improvement in quality of life, decreased D-dimer levels, and improved signs of coagulopathy, all of which occurred in the first 3 months (31). Magnetic resonance imaging follow-up scans showed an average of 20% reduction in the size of the lesions and in some, complete disappearance of the lesion (31). The follow up phase IIB study included 19 patients with severe slow-flow VMs who all benefited from an improvement in quality of life within the first 3 months of daily rapamycin treatment (36).

The clinical efficacy of Rapamycin in patients with PROS is less evident (37, 38). One study on 39 patients with PROS trialed low-dose rapamycin (2–6 ng/mL) and found that while there was an observable effect on lesion overgrowth, it did not translate into functional improvements and quality of life (38). It is unclear if this is due to the lower dose target.

Finally, the VASE trial is the largest Phase III multicentre trial currently underway to evaluate the efficacy of rapamycin in pediatric

and adult patients with slow-flow VMs refractory to standard treatment (EudraCT2015-001703-32; https://www.clinicaltrials.gov; NCT02638389). Rapamycin is administered over a two-year period before being stopped; patients can resume the treatment if symptoms resurge. While they aim to enroll 250 patients, the preliminary analysis on the first 101 patients with at least six months follow up showed that 87% had improvements in their pain and functional outcome. Thirty-six patients were able to stop the medication after 2 years, of which half needed to restart the medication due to eventual symptom resurgence. Queisser et al. recently reviewed the data on rapamycin's clinical efficacy in severe slow-flow VMs; in combining the data from the Phase II and VASE Phase III trials ($N = 122$), they report an 85% toxicity rate, mostly constituting mild adverse events that were managed conservatively (9). The most common side effects included fatigue, nausea, headache and cutaneous rash. In 18% of patients, a dose reduction or temporary arrest was sufficient in alleviating these mild adverse events whereas a definitive arrest was needed in 10% of patients. For patients undergoing surgical resection after therapy with sirolimus, the preliminary experience in patients with VMs is that it should perhaps be maintained during surgical management in order to facilitate wound healing through decreased lymphatic leakage, which is contrary to the experience in oncological population (39). More surgical studies are needed to validate the drug's effect on wound healing in this particular population.

While tolerance of rapamycin is good with mild-to-moderate and manageable side effects, optimizing dose requirements is clearly still important in ameliorating the drug's safety profile. In studying rapamycin's pharmacokinetics, strategies in altering dose targets and routes of administration have recently been explored, in addition to adding prophylactic agents to target the more common side effects. In one approach, Harbers et al. retrospectively analyzed the effect of a lower drug target level in 12 patients with therapy-resistant low-flow VMs; they found that in doing so, they achieved similar clinically efficacy with reduced adverse events using low rapamycin target levels of 4–10 ng/ml (40). A lower drug target for rapamycin in a study on PROS patients, however, did not reach its intended safety effect (38). It's unclear if this is related to rapamycin's effect in PROS patients specifically or it is a mere reflection of patient heterogeneity. A body-surface area dosing approach often unnecessarily exposes tissues outside of the lesion target to the drug; instead, we know that in the pediatric population, the cytochrome P450 metabolic activity evolves through development and with this knowledge, an age-appropriate and pharmacokinetic based rapamycin dosing regimen was proposed (41, 42).

A topical route might also help to alleviate some of these toxicities; topical sirolimus at 1% concentration was recently assessed in a systemic review on 23 patients with cutaneous vascular anomaly manifestations and found to be effective in improving cutaneous lesion appearance in 86% of patients and improving lymphatic blebbing in 90% of patients over an average length of treatment of 10.2 months (43). There were no severe adverse events although one patient electively stopped treatment due to pruritis (43). A multicentre randomized controlled trial is planned to assess topical sirolimus for patients with lingual microcystic LMs, where other treatment options are quite limited (www.clinicaltrials.gov; NCT04128722).

Lastly, prophylactic agents for common or severe reactions were used in some studies, including the use of mouth washes and topical agents for stomatitis or antibiotics for opportunistic pneumonia in the solid organ transplant population; however, there is currently insufficient evidence to support guidelines for prophylactic measures for patients with VMs and these practices remain at the physician's discretion.

PI3K inhibitor

Alpelisib (BTL719) is an oral specific allosteric inhibitor of PI3K by the company Novartis that selectively inhibits the p110alpha subunit (44). It acts by inhibiting the phosphorylation of downstream target AKT. Alpelisib was initially studied in patients with *PIK3CA*-altered oncological diagnoses, including Phase I trials in advanced solid tumors (45–47) and more recently, an ongoing Phase III trial on alpelisib with fulvestrant for patients with hormone receptor-positive advanced breast cancer (SOLAR-1 trial) (48). Evidence from the oncology literature demonstrated significant improvements in progression-free survival when combined with other chemotherapeutic agents with mostly mild side-effects including hyperglycemia, gastrointestinal symptoms, cutaneous irritations, fatigue and mucositis (48). Severe reactions including diabetic ketoacidosis, diarrhea, hypertension, hypersensitivity reactions, osteonecrosis of the jaw, and severe cutaneous adverse events have all been reported, and occur in up to 35% of patients in the SOLAR-1 trial (48).

Alpelisib was then tested in a preclinical study on PROS/CLOVES mutant mice with established lesions. They found that like rapamycin, alpelisib improved vascular morphology and reduced lesion size but was superior to rapamycin in restoring organ dysfunction (49). Isolated case reports in infants with severe PROS demonstrated similar clinical improvements and reductions in lesion volume with no adverse events (50). A larger clinical prospective study on 19 patients with PROS trialed alpelisib at 250 mg daily for adults and 50 mg daily for children; they found that the drug was well tolerated with grade one hyperglycemia in two patients and mucositis in three patients. Importantly, all patients experienced significant clinical improvement in their symptoms alongside reduction of lesion volume by 30% within 6 months of daily use (49). Six of these patients had trialed rapamycin without success, which corroborates the role of rapamycin in treating actively growing lesions (38) while alpelisib can reverse existing lesions in this population.

Alpelisib's clinical efficacy in the PROS population was later supported by the findings of the EPIK-PP1 (NCT04285723) study, which is a retrospective chart review on patients with PROS above the age of 2 with severe or life-threatening disease. These patients had confirmed mutation in the *PIK3CA* gene and took at least one dose of alpelisib (adult 250 mg/d; pediatric: 50 mg/d) for >24 weeks before March 2020 (4). Their primary outcome was radiological response with at least 20% reduction in sum of the target lesion volume in up to three lesions confirmed on repeat imaging. Secondary objectives included safety and clinical efficacy with change in patient symptomatology. Of the 57 patients (39 pediatric, 18 adult) included in this study, 32 patients had complete follow up data for primary endpoint analysis. Twelve patients (37.5%) (95% CI: 21.1–56.3%) were radiological responders by Week 24 and 60% of these patients had sustained response for at least 1 year. Improvements in symptomatology were reported in 90.9% of patients for pain, 78.9% for VM appearance, 76.2% for fatigue, 69.0% for limb asymmetry, and 55.2% for disseminated intravascular coagulation. Treatment-related adverse events were mild and occurred in 38.6% of patients,

of which the most common were hyperglycemia, stomatitis and self-limiting mouth ulcers. Based on such robust evidence of its safety and efficacy in this population, Alpelisib (Vijoice R) (51) was just recently approved by the American Federal Drug Administration under a Managed Access Program for patients with severe PROS requiring systemic treatment (Novartis: Vijoice; www.clinicaltrials.gov; NCT NCT04085653). A phase 2 upfront 16-week randomized control trial on the pharmacokinetics, safety and efficacy of alpelisib for pediatric and adult PROS patients is underway with the anticipated study completion date being in December 2029 (www.clinicaltrials.gov, NCT NCT04589650).

There have only been preclinical studies and small case series on oral and topical alpelisib for other isolated VMs, demonstrating restored vascular morphology, reduced lesion size, improved fibronectin levels and improvements in symptoms such as pain and inflammatory flares (11, 12, 52, 53). In one study, these effects were similar to mTOR inhibition (12), whereas in the other it was significantly better than rapamycin (11). It's clinical application to patients with other slow-flow malformations remains unclear at this time and requires further large prospective trials to confirm its safety and efficacy in distinct VM populations (54).

AKT inhibitor

Miransertib (ARQ 092) is an oral selective AKT inhibitor with higher specificity for the AKT1 isoform; it works by inhibiting the membrane-bound active form of ACT and preventing the conversion of its inactive form to its active state (55). It was initially investigated in oncological models (55, 56) before being assessed in preclinical models of *PIK3CA*-mutant endothelial cells, demonstrating regression of existing proliferating VM lesions (5). Its clinical efficacy has most recently been explored only in a handful of case reports and series of patients with PROS/CLOVES (5, 57, 58). In 6 patients with PROS, miransertib had greater antiproliferative activity as measured by fibroblasts compared to mTOR inhibitors (57). In a preclinical study on human derived endothelial cells from *PIK3CA* and *TEK/TIE2* driven VMs, miransertib impacted the viability of the endothelial cells at even low concentrations and helped to restore the wild-type endothelial cell phenotype (5). In a case report on a 16-year-old female patient with CLOVES that progressed on rapamycin, miransertib at 30 mg daily dose resulted in 15% reduction in fatty overgrowth volume over 28 months and improvements in respiratory function with mild hyperlipidemia as a side effect; however, treatment was discontinued due to lack of sustained response and poor patient adherence after 28 months (58). There is currently an ongoing phase I/II trial on Miransertib for patients with PIK3CA-related overgrowth diseases and Proteus syndrome (MOSAIC-study: www.clinicaltrials.gov; unique identifier NCT03094832).

RAS-MAPK-ERK pathway inhibitors

MEK inhibitor

Trametinib is an allosteric MEK1/MEK2 inhibitor from the company Novartis that is Health Canada and Food and Drug Administration approved for certain *KRAS* pathway-driven cancers, including metastatic melanoma and non-small cell lung cancer. It however was recently applied to both a transgenic zedbrafish model of CCLA and a single patient with advanced CCLA with *ARAF* mutation (59). They found that MEK inhibition restored the endothelial cell monolayer and adherens junctions and rescued duct morphology without changes in cell proliferation in the preclinical model. In the 12-year-old patient with CCLA, they observed an improvement in pulmonary function with reduced lymphatic fluid retention and oxygen requirements in the first 3–6 months of treatment that was sustained after 1 year (59). Similarly, in both a transgenic mouse model of GSD and patient harboring *KRAS* G12V somatic mutation, Trametinib regressed the lymphatic valves, improved chylothorax and restored lymphatic flow (60). Finally, in another patient with KLA and *NRAS* mutation, trametinib was well tolerated and resulted in improved clinical symptoms (61) (Figure 2).

Overall, there is good evidence for the clinical efficacy of oral rapamycin for patients with severe VeMs, LMs and mixed VMs (32, 36, 37, 40, 62), and promising future in the application of direct PIK3CA and AKT inhibitors for patients with PROS. MEK inhibitors may play a role for RAS-RAF-ERK pathway driven lymphatic anomalies and possibly complimentary to PI3K-mTOR pathway targeted therapies as a combinatorial approach for inhibiting angiogenesis and proliferation in these patients. Further work is needed on determining pharmacokinetically-driven drug regimens for each agent in specific VM subpopulations, and then trialing a combinatorial approach to better address tolerance and resistance in chronic therapy.

High-flow malformations

Our initial insight into the molecular biology of high-flow VMs was based on an assessment of germline inherited mutations in familial vascular syndromes. These mutations are inherited in an autosomal dominant fashion with a LOF mutation followed by a second somatic hit. To date, the most well-known familial AVM disorders include hereditary hemorrhagic telangiectasia (HHT) and capillary malformation- arteriovenous malformation syndrome (CM-AVM) (Figure 3).

HHT (Osler-Weber-Rendu syndrome) manifests as multiple cutaneous telangiectasias, recurrent epistaxis or gastrointestinal bleeding, and AVMs in various internal organs, including the lungs, liver and central nervous system. In HHT, there are five loci implicated in the development of this disease, most of which involve the bone morphogenetic protein (BMP) signaling pathway and are upregulated alongside VEGF signaling. Both HHT1 and HHT2 are caused by heterozygous LOF mutations in *endoglin* (*ENG*) and *activin receptor-like kinase 1* (*ALK1*), respectively. HHT syndrome (also known as juvenile polyposis) is linked with LOF mutations in genes that encode SMAD (mothers against decapentaplegic homolog). Other loci were found implicated on chromosome 5q31.3-32 (HHT3) and 7p14 (HHT4). *ALK1* and *ENG* are expressed on endothelial cells. *ENG* induces the BMP/ALK1 signaling cascade by receptor phosphorylation and activation of various SMAD transcription factors that typically suppress endothelial cell migration and proliferation (Figure 3). Hence, LOF mutation in these genes disinhibits these activities, causing enhanced aberrant vessel formation. Similarly, experiments with knockout or blockade of ALK1 and BMP9/10 ligand demonstrate inhibition of PTEN and an associated increased activation of AKT.

Systemic therapies for HHT have largely focused on inhibiting VEGF directly or indirectly. Bevacizumab (Avastin) is a widely

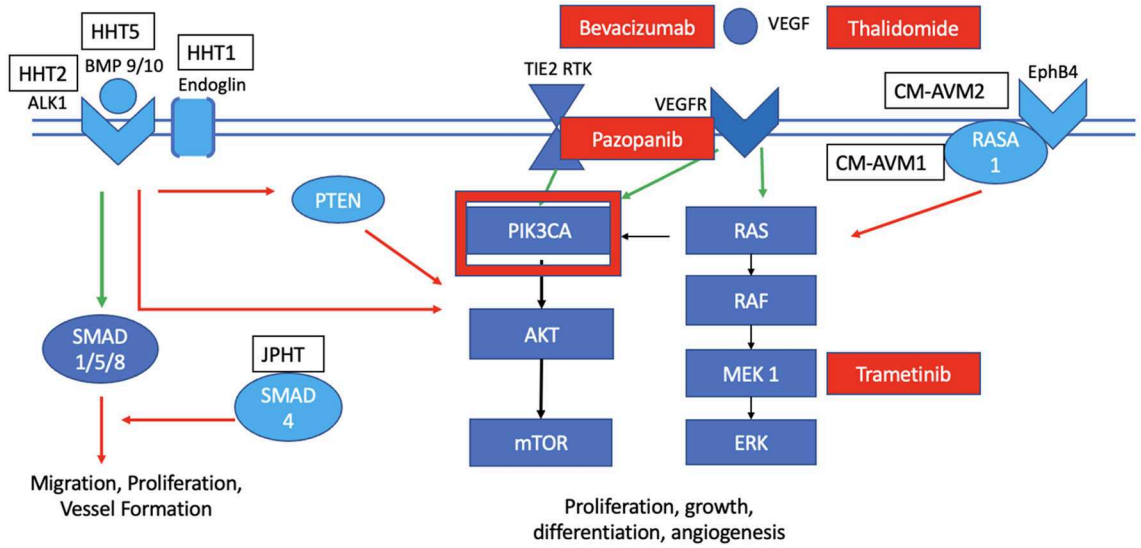

FIGURE 3
Mutations and targeted therapies for slow-flow malformations. HHT1 is known to have multiple affected loci in the BMP signaling pathway that generally act to inhibit the PIK3CA pathway in the wild-type state. CM-AVM 1 is characterized by a LOF mutation in RASA1, while CM-AVM2 has the mutation in the EphB4; both activate the KRAS pathway in the wild-type state. Targeted therapies for HHT include bevacizumab, pazopanib and thalidomide. There is a potential to also explore PI3KCA with Alpelsib for HHT. Targeted therapies for CM-AVM include Trametinib, while those for sporadic AVMs include bevacizumab, thalidomide, and Trametinib.

used recombinant monoclonal antibody that inhibits VEGF and was studied in several clinical trials in patients with HHT (39, 63, 64). They observed improvements in liver lesions, telangiectasis and bleeding (especially refractory gastrointestinal bleeding) (64) with no serious adverse events. Intramucosal injections were superior to intravenous or intranasal administrations in this population (39, 64). There is now a randomized phase III clinical trial underway studying the safety and efficacy of bevacizumab for patients with HHT (NCT 03227263). Recently, indirect inhibitors of VEGF signaling such as pazopanib (inhibits various tyrosine kinase receptors such as VEGFR2) (65) and thalidomides were experimented in a small number of patients with HHT with some early success in reducing bleeding (64, 66). There are now ongoing trials planned in North America to study the clinical utility of these anti-angiogenic drugs for severe cases of HHT (NCT03850730, NCT03850964). Finally, common downstream effectors such as PI3K may be future candidates for targeted drug trials since they showed promise in reducing the levels of the BMP9/10 antibodies in the mouse model (67, 68) (Figure 3).

Patients with CM-AVM have multifocal maroon-colored lesions and sometimes high flow lesions including AVMs. CM-AVM1 is caused primarily by *RASA1* mutations. *RASA1* encodes the RAS p21 protein activator 1 (p120RasGAP) that when recruited, it inhibits the RAS/MAPK/ERK signaling pathway; hence, LOF mutations in *RASA1* cause abnormal activation of this pathway with increased cellular proliferation, growth, differentiation and motility. CM-AVM2 is caused by LOF mutations in the transmembrane receptor *EPHB4* that is expressed on venous cells, which interacts with p120RasGAP to inhibit the RAS/MAPK/ERK signaling pathway. Once again, mutated *EPHB4* then leads to constitutive activation of this pathway (69). Given the upregulation of the RAS/MAPK/ERK pathway in these diseases, MEK inhibition can perhaps play a role in targeting this aberrant pathology (Figure 3). A case report was published just this year on the successful management of a 16-year-old female patient with CM-AVM and cardiac compromise (70). Further studies are needed to elucidate the role of pathway-targeted treatments such as Trametinib in the care of CM-AVM patients.

Most patients with fast-flow lesions have sporadic AVMs that are not caused by these inherited LOF mutations. Without any intervention, the hemorrhage rate for AVMs is around 2% and higher (around 4–10%) if there is a previous rupture or an angiographic weak point (71). These lesions are typically treated with surgery, radiosurgery, embolization or a combination of these approaches with a risk of intervention being variable depending on the anatomy and location of the lesion; however, many lesions are either too complex to achieve a cure with the most aggressive of these approaches or they are located in areas that are difficult to access. Hence, systemic therapies can play an important role in this debilitating disease. Early studies on targeted therapies for AVMs focused on decreasing the angiogenic upstream stimulus or the resultant inflammation that weakens the vessel wall (Figure 3). In an open label pilot study on the safety of tetracycline derivatives in 12 adult patients with inoperable AVMs and 14 patients with giant cerebral aneurysms, Frenzel et al. found that a third of these patients had dose-limiting intolerance (72). Bevacizumab was also trialed in this population to reduce the angiogenic activity but while there was a reduction in serum VEGF levels with no serious drug toxicity, this did not translate into clinical improvements in the two patients with AVMs (73). The most promising systemic agent targeting upstream actors in the angiogenic signaling pathway for AVM care is thalidomide. This drug was initially used as a sedative for pregnant women decades ago and was stopped for its teratogenic side effects. In this pursuit, we also learned that it has antiangiogenic properties by inhibiting cytokines such as VEGF, affecting cell migration and adhesion, and modulating the

inflammatory response through inhibition of tumor-necrosis factor alpha and nitric oxide (74). Given its anti-angiogenic and anti-inflammatory potential, it was tested in patients with age-related macular degeneration, HHT and explored in an AVM mouse model (39). Boon et al. have since highlighted a prospective observational case series of 18 adult patients with severe extracranial AVMs and functional impairment who were treated with thalidomide (66). They found that all patients experienced a reduction in pain and improvement in both bleeding and ulceration. Two patients (11.1%) had concomitant reduction in vascularity on follow-up angiography. Of the 12 patients who stopped thalidomide treatment due to clinical improvement, 8 remained stable and 4 had lesion recurrence within the first year. The first 5 patients were administered the drug at initial dose of 50 mg per day which was escalated to 200 mg daily within the first 2 weeks. At this dose regimen, 80% of these patients had grade 3 complications including asthenia, erythroderma and cerebral infarct (the latter was unclear if caused by thalidomide). The remaining patients were trialed on the lower dose regimen of 50 mg daily with no significant effect on the drug's efficacy but an observable reduction in the rate of toxicity (66). Further prospective trials on thalidomide in patients with severe AVMs are needed to determine its safety and efficacy in clinical practice.

These studies all predate a seminal discovery in 2017 that the overwhelming majority of sporadic brain AVMs harbor activating *KRAS* mutations in nidal endothelial cells (75) (Figure 3) and sporadic extracranial AVMs have mutations in *MAP2K1* (76). *In vitro* and immunohistochemistry experiments demonstrated that mutant KRAS expression increased downstream ERK phosphorylation, increased expression of angiogenic signaling, and enhanced the cell's migratory behavior. With deeper genomic sequencing depths, *KRAS* mutant prevalence increases to almost 90% of brain and spine AVMs and is sufficient to induce AVMs in preclinical models (77, 78). Mosaic variants in components of the *KRAS* pathway (*KRAS, NRAS, BRAF* and *MAP2K1*) were discovered as activating drivers in the development of extracranial AVMs as well (79). Their aberrant features were reversed through *in vitro* and preclinical *in vivo* experiments with MEK inhibition. Hence, there is a growing body of knowledge that *KRAS* mutations drive sporadic AVM development (80); this pathway then serves as a logical target for therapeutic drug discovery with MEK inhibition.

To date, isolated case reports illustrated the application of Trametinib to pediatric patients with severe extra-cranial AVMs with good tolerance and excellent clinical response. Two patients with chest wall AVMs experienced significant reduction in the volume, redness and deformity of their lesion, alongside a reduction in the overall cardiac output and blood supply to the AVM (81, 82). One of these patients with Cobb syndrome had intermittent drug holidays and observed resurgences of symptoms during these off-periods, which is similar to what is seen in the rapamycin experience in low-flow VMs (83). Importantly, this patient also had a spinal intramedullary component to the AVM that was the first example of a CNS-lesion responding well to MEK inhibition; he had a reduction in shunting over 12 days of daily Trametinib and no serious adverse events (83). The most common side effects of Trametinib include cutaneous rash, gastrointestinal symptoms, fatigue and hair loss/thinning, albeit being mostly mild-to-moderate in severity.

Given the preliminary success of Trametinib for severe AVMs, a new phase II European trial, TRAMAV, has just started to recruit adult patients with severe extracranial AVMs to study the safety and efficacy of Trametinib in this population (EudraCT: 2019-003573-26). Our group is also embarking on a prospective study assessing the safety and efficacy of MEK inhibition for patients in Toronto with palliative extra-cranial and intra-cranial AVMs under compassionate use. Further preclinical work and clinical trials are needed to determine which molecular activities specifically drive AVM pathogenesis and alter its natural history, and then ensure the targeted therapy works on addressing those features in particular with a good tolerance profile. Combining pathway-specific therapeutics (such as MEK inhibitors) with more upstream anti-angiogenic drugs (such as thalidomide) might confer a more synergistic clinical effect while also: (1) reducing drug resistance, and (2) enabling a lower minimal therapeutic dose to mitigate unwanted side effects. These drugs can then act to either bridge a palliative patient to conventional treatments, support conventional treatments such as reducing flow alongside radiosurgery, or potentially facilitating cure in small niduses or residual shunts/recurrences after conventional treatments.

Minimally invasive techniques in detecting mutational burden

Our understanding of the molecular biology driving VM development has significantly evolved from the first discovery of a somatic mutation causing a venous malformation around a decade ago. With the growing evidence of the various mutational variants in both major cellular signaling pathways and the potential for various systemic therapeutics in VM care, the need for an accurate molecular diagnosis becomes crucial. The early experience with repurposing cancer drugs for VMs involved an exploration of mutational burden using invasive biopsy methods, which was naturally applied to peripheral lesions. Nevertheless, a cutaneous biopsy still holds a risk of bleeding and issues with wound healing; access to deeper lesions and those in the central nervous system pose significant additional safety challenges. To address these concerns, investigators from Italy attempted to recapitulate the mutational burden in a plasma draw, in the form of a modified "liquid biopsy" (84). Liquid biopsies are commonly used in oncology patients where there is a high amount of shedding circulating tumor DNA that can be detected from a peripheral draw and used either for molecular staging or confirmation of response to treatment (85). In AVMs, the amount of cell-free DNA is significantly lower than in tumors, which means that the amount of cell-free DNA in a peripheral draw would be well below the level of detection. Instead, they captured blood from 5 patients that was intimate with the lesion at the time of angiography, alongside paired blood from a peripheral venous draw (negative control). Using next-generation sequencing, they were able to detect known mutations in the isolated cell-free DNA specifically the efferent vein DNA with (1) an allele frequency at an order of magnitude above the limit of detection, and (2) with no serious adverse events from the procedure (84). A subsequent report from Seattle also highlighted the safety and utility of a liquid biopsy technique on plasma derived from 8 peripheral AVMs, 3 VeMs, and cystic fluid samples from 7 LMs; they were able to detect the driving mutation in 25, 33, and 100% of those samples, respectively (86). In one patient with MCAP, a cerebrospinal fluid sample was obtained for cancer staging and

a similar method of extracting cell-free DNA from CSF instead of plasma was conducted. *PIK3CA* mutant variants were detected with allele frequency of 3.08%, which is slightly higher than what was reported in the lesional plasma literature, but naturally lower than a cutaneous biopsy (87). Lastly, a slightly more invasive approach was proposed by the group at University of San Francisco termed "endoluminal biopsy" whereby a coil is placed intimate to the wall of the vessel lumen just prior to a planned endovascular treatment session. In doing so, the coil gets coated with genomic mutant cells and upon retrieval, DNA can be isolated for genomic sequencing. They were able to successfully and safely employ this technique to detect mutations including *KRAS* in four patients with brain AVMs (88). These novel minimally-invasive methods in detecting mutational burden in VMs are certainly in their infancy and require further validation so that they can be used safely and in a way that is reliable and accessible, even from very small amounts of DNA.

Conclusions

A decade's worth of expanding knowledge on the molecular biology of VMs has paved the way for repurposing cancer therapeutics to VM care, with significant promise in the most complex of cases. The ability to detect a patient's unique mutational profile and then safely apply an appropriate cocktail of targeted treatments will be the future of VM precision medicine; further large prospective trials and preclinical work are needed to facilitate our understanding of these complex diseases and expand their treatment potential.

Author contributions

AM and IR both contributed to the conception of the review, manuscript preparation, and final review. AM conducted literature review and data synthesis. Both authors contributed to the article and approved the submitted version.

Conflict of interest

The authors declare that the research was conducted in the absence of any commercial or financial relationships that could be construed as a potential conflict of interest.

Publisher's note

References

1. Kunimoto K, Yamamoto Y, Jinnin M, ISSVA. Classification of vascular anomalies and molecular biology. *Int J Mol Sci.* (2022) 23:2358. doi: 10.3390/ijms23042358

2. Queisser A, Boon LM, Vikkula M. Etiology and genetics of congenital vascular lesions. *Otolaryngol Clin North Am.* (2018) 51:41–53. doi: 10.1016/j.otc.2017.09.006

3. Castillo SD, Tzouanacou E, Zaw-Thin M, Berenjeno IM, Parker VER, Chivit I, et al. Somatic activating mutations in *PIk3CA* cause sporadic venous malformations in mice and humans. *Sci Transl Med.* (2016) 8:332ra43. doi: 10.1126/scitranslmed.aad9982

4. Canaud G, Lopez Gutierrez JC, Irvine A, Ankrah N, Papadimitriou A, Ridolfi A, Adams DM. EPIK-P1: Retrospective chart review of patients with *PIK3CA*-related overgrowth spectrum who have received Alpelisib as part of a compassionate use programme. *Ann Oncol.* (2021) 32:S1297. doi: 10.1016/j.annonc.2021.08.2097

5. Kobialka P, Sabata H, Vilalta O, Gouveia L, Angulo-Urarte A, Muixi L, et al. The onset of *PI3K*-related vascular malformations occurs during angiogenesis and is prevented by the AKT inhibitor miransertib. *EMBO Mol Med.* (2022) 14:e15619. doi: 10.15252/emmm.202115619

6. Pang C, Lim CS, Vrookes J, Tsui J, Hamilton G. Emerging importance of molecular pathogenesis of vascular malformations in clinical practice and classifications. *Vasc Med.* (2020) 25:364–77. doi: 10.1177/1358863X20918941

7. Limaye N, Wouters V, Uebelhoer M, Tuominen M, Wirkkala R, Mulliken JB, et al. Somatic mutations in angiopoietin receptor gene *TEK* cause solitary and multiple sporadic venous malformations. *Nat Genet.* (2009) 41:118–24. doi: 10.1038/ng.272

8. Seront E, Van Damme A, Boon LM, Vikkula M. Rapamycin and treatment of venous malformations. *Curr Opin Hematol.* (2019) 26:185–92. doi: 10.1097/MOH.0000000000000498

9. Queisser A, Seront E, Boon LM, Vikkula M. Genetic basis and therapies for vascular anomalies. *Circ Res.* (2021) 129:155–73. doi: 10.1161/CIRCRESAHA.121.318145

10. Boon LM, Vikkula M. Multiple cutaneous and mucosal venous malformations. In: Pagon RA, Adam MP, Ardinger HH, Wallace SE, Amemiya A, Bean LJH, Bird TD, Ledbetter N, Mefford HC, Smith RJH, et al. (eds). *GeneReviews(R)*. Seattle (WA) (1993).

11. Limaye N, Kangas J, Mendola A, Godfraind C, Schlogel MJ, Helaers R, et al. Somatic activating PIK3CA mutations cause venous malformation. *Am J Hum Genet.* (2015) 87:914–92. doi: 10.1016/j.ajhg.2015.11.011

12. Castel P, Carmona FJ, Grego-Bessa J, Berger MF, Viale A, et al. Somatic PIK3CA mutations as a driver of sporadic malformations. *Sci Transl Med.* (2016) 8:332–42. doi: 10.1126/scitranslmed.aaf1164

13. Chen J, Somanath PR, Razorenova O, Chen WS, Hay N, Bornstein P, et al. *Akt1* regulates pathological angiogenesis, vascular maturation and permeability *in vivo*. *Nat Med.* (2005) 11:1188–96. doi: 10.1038/nm1307

14. Graupera M. & Potente M. Regulation of angiogenesis by P13K signaling networks. *Exp Cell Res.* (2013) 319:1348–55. doi: 10.1016/j.yexcr.2013.02.021

15. Burke JE, Perisic O, Masson GR, Vadas O, Williams RL. Oncogenic mutations mimic and enhance dynamic events in the natural activation of phosphoinositide 3-kinase p110a (PIK3CA). *Proc Natl Acad Sci USA*. (2012) 109:15259–64. doi: 10.1073/pnas.1205508109

16. Kurek KC, Luks VL, Ayturk UM, Alomari AI, Fishman SJ, Spencer SA, et al. Somatic mosaic activating mutations in *PIK3CA* cause CLOVES syndrome. *Am J Hum Genet.* (2012) 90:1108–15. doi: 10.1016/j.ajhg.2012.05.006

17. Wassef M, Blei FA, Adams D, Alomari A, Baselga E, et al. Vascular Anomalies Classification: Recommendations From the International Society for the Study of Vascular Anomalies. *Pediatrics.* (2015) 136:e203–14. doi: 10.1542/peds.2014-3673

18. Makinen T, Boon LM, Vikkula M, Alitalo K. Lymphatic malformations: genetics, mechanisms and therapeutic strategies. *Circ Res.* (2021) 129:136–54. doi: 10.1161/CIRCRESAHA.121.318142

19. Lindhurst MJ, Sapp JC, Teer JK, Johnston JJ, Fin EM, et al. A mosaic activating mutation in *AKT1* associated with the Proteus syndrome. *N Eng J Med.* (2011) 365:611–9. doi: 10.1056/NEJMoa1104017

20. Oliver G, Kipnis J, Randolph GJ, Harvey NL. The lymphatic vasculature in the 21st century: novel functional roles in homeostasis and disease. *Cell.* (2020) 182:270–96. doi: 10.1016/j.cell.2020.06.039

21. Petrova TV, Mäkinen T, Mäkelä TP, Saarela J, Virtanen I, Ferrell RE, et al. Lymphatic endothelial reprogramming of vascular endothelial cells by the Prox-1 homeobox transcription factor. *EMBO J.* (2002) 21:4593–9. doi: 10.1093/emboj/cdf470

22. Osborn AJ, Dickie P, Neilson DE, Glaser K, Lynch KA, Gupta A, et al. Activating *PIK3CA* alleles and lymphangiogenic phenotype of lymphatic endothelial cells isolated from lymphatic malformations. *Human Mol Genet.* (2015) 24:926–38. doi: 10.1093/hmg/ddu505

23. Li D, Wenger TL, Seiler C. March ME, Gutierrez-Uzquiza A, et al. Pathogenic variant in EPHB4 results in central conducting lymphatic anomaly. *Hum Mol Genet.* (2018) 27:3233–45. doi: 10.1093/hmg/ddy218

24. Manevitz-Mendelson E, Leichner GS, Barel O, Davidi-Avrahami I, et al. Somatic NRAS mutation in patient with generalized lymphatic anomaly. *Angiogenesis.* (2018) 21:287–98. doi: 10.1007/s10456-018-9595-8

25. Barclay SF, Inman KW, Luks VL, McINtyre JB, Al-Ibraheemi A, et al. A somatic activating *NRAS* variant associated with kaposiform lymphangiomatosis. *Genet Med.* (2019) 21:1517–24. doi: 10.1038/s41436-018-0390-0

26. Nozawa A, Ozeki M, Niihori T, Suzui N, Miyazaki T, Aoki Y, et al. somatic activating *KRAS* variant identified in an affected lesion of a patient with Gorham-Stout disease. *J Hum Genet.* (2020) 65:995–1001. doi: 10.1038/s10038-020-0794-y

27. Martinez-Corral I, Zhang Y, Petkova M, Ortsater H, Sjoberg S, et al. Blockade of VEGF-C signaling inhibits lymphatic malformations driven by oncogenic *PIK3CA* mutation. *Nat Commun.* (2020) 11:2869. doi: 10.1038/s41467-020-16496-y

28. Sabayan B, Lineback C. Viswanathan, Leslie-Mazwi TM, Shaibani A. Central nervous system vascular malformations: a clinical review. *Ann Clin Transl Neurol.* (2021) 8:504–22. doi: 10.1002/acn3.51277

29. McCafferty I. Management of low-flow vascular malformations: clinical presentation, classification, patient selection, imaging and treatment. *Cardiovasc Intervent Radiol.* (2015) 38:1082–104. doi: 10.1007/s00270-015-1085-4

30. Li J, Kim SG, Blenis J. Rapamycin: one drug, many effects. *Cell Metab.* (2014) 19:373–9. doi: 10.1016/j.cmet.2014.01.001

31. Boscolo E, Limaye N, Huang L, Kang KT, Soblet J, Uebelhoer M, et al. Rapamycin improves TIE2-mutated venous malformation in murine model and human subjects. *J Clin Invest.* (2015) 125:3491–504. doi: 10.1172/JCI76004

32. Hammill AM, Wentzel M, Gupta A, Nelson S, Lucky A, Elluru R, et al. Sirolimus for the treatment of complicated vascular anomalies in children. *Pediatr Blood Cancer.* (2011) 57:1018–24. doi: 10.1002/pbc.23124

33. Lackner H, Karastaneva A, Schwinger W, Benesch M, Sovinz P, Seidel M, et al. Sirolimus for the treatment of children with various complicated vascular anomalies. *Eur J Pediatr.* (2015) 174:1579–84. doi: 10.1007/s00431-015-2572-y

34. Nadal M, Giraudeau B, Tavernier E, Jonville-Bera AP, Lorette G, Maruani A. Efficacy and safety of mammalian target of rapamycin inhibitors in vascular anomalies: a systematic review. *Acta Derm Venereol.* (2016) 96:448–52. doi: 10.2340/00015555-2300

35. Triana P, Dore M, Cerezo VN, Cervantes M, Sánchez AV, Ferrero MM, et al. Sirolimus in the treatment of vascular anomalies. *Eur J Pediatr Surg.* (2017) 27:86–90. doi: 10.1055/s-0036-1593383

36. Hammer J, Seront E, Duez S, Dupont S, Van Damme A, Schmitz S, et al. Sirolimus is efficacious in treatment for extensive and/or complex slow-flow vascular malformations: a monocentric prospective phase II study. *Orphanet J Rare Dis.* (2018) 13:191. doi: 10.1186/s13023-018-0934-z

37. Adams DM, Trenor CC. 3rd, Hammill AM, Vinks AA, Patel MN, Chaudry G, Wentzel MS, Mobberley-Schuman PS, Campbell LM, Brookbank C, et al. Efficacy and safety of sirolimus in the treatment of complicated vascular anomalies. *Pediatrics.* (2016) 137:e20153257. doi: 10.1542/peds.2015-3257

38. Parker VER, Keppler-Noreuil KM, Faivre L, Luu M, Oden NL, De Silva L, et al. PROMISE Working Group. Safety and efficacy of low-dose sirolimus in the PIK3CA-related overgrowth spectrum. *Genet Med.* (2019) 21:1189–98. doi: 10.1038/s41436-018-0297-9

39. Van Damme A, Seront E, Dekeuleneer V, Boon LM, Vikkula M. New and emerging targeted therapies for vascular malformations. *Am J Clin Dermatol.* (2020) 21:657–68. doi: 10.1007/s40257-020-00528-w

40. Harbers VEM, Rongen GAPJM, van der Vleuten CJM, Verhoeven BH, de Laat PCJ, van der Horst CMAM, et al. Patients with congenital low-flow vascular malformation treated with low dose sirolimus. *Adv Therap.* (2021) 38:3465–82. doi: 10.1007/s12325-021-01758-y

41. Mizuno T, Fakuda T, Emoto C, Mobberley-Schuman PS, Hammill AM, Adams DM, et al. Developmental pharmacokinetics of sirolimus: implications for precision dosing in neonates and infants with complicated vascular anomalies. *Pediatr Blood Cancer.* (2017) 64:e26470. doi: 10.1002/pbc.26470

42. Mizuno T, Emoto C, Fakuda T, Hammill AM, Adams DM, Vinks AA. Model-based precision dosing of sirolimus in pediatric patients with vascular anomalies. *Eur J Pharm Sci.* (2017) 109S:S124–31131. doi: 10.1016/j.ejps.2017.05.037

43. Badia P, Ricci K, Gurria JP, Dasgupta R, Patel M, Hammill A. Topical sirolimus for the treatment of cutaneous manifestations of vascular anomalies: a case series. *Pediatr Blood Cancer.* (2020) 67:e28088. doi: 10.1002/pbc.28088

44. Fritsch C, Huang A, Chatenay-Rivauday C, Schnell C, Reddy A, Liu M, et al. Characterization of the novel and specific PI3Kα inhibitor NVP-BYL719 and development of the patient stratification strategy for clinical trials. *Mol Cancer Ther.* (2014) 13:1117–29. doi: 10.1158/1535-7163.MCT-13-0865

45. Ando Y, Iwasa S, Takahashi S, Saka H, Kakizume T, Natsume K, et al. Phase I study in alpelisib (BYLO719), an alpha specific PI3K inhibitor, in Japanase patients with advanced solid tumors. *Cancer Sci.* (2019) 110:1021–31. doi: 10.1111/cas.13923

46. Juric D, Janku F, Rodón J, Burris HA, Mayer IA, Schuler M, et al. Alpelisib Plus Fulvestrant in PIK3CA-Altered and PIK3CA-wild-type estrogen receptor-positive advanced breast cancer: a phase 1b clinical trial. *JAMA Oncol.* (2019) 5:e184475. doi: 10.1001/jamaoncol.2018.4475

47. Juric D, Rodon J, Tabernero J, Janku F, Burris HA, Schellens JHM, et al. Phosphatidylinositol 3-Kinase α-Selective Inhibition With Alpelisib (BYL719) in PIK3CA-Altered Solid Tumors: Results From the First-in-Human Study. *J Clin Oncol.* (2018) 36:1291–9. doi: 10.1200/JCO.2017.72.7107

48. Andre F, Ciruelos E, Rubovsky G, Campone M, Loibl S, Rugo HS, et al. Alpelisib for PIK3CA-mutated, hormone receptor-positive advanced breast cancer. *N Engl J Med.* (2019) 380:1929–40. doi: 10.1056/NEJMoa1813904

49. Venot Q, Blanc T, Rabia SH, Berteloot L, Ladraa S, Duong JP, et al. Targeted therapy in patients with PIK3CA-related overgrowth syndrome. *Nature.* (2018) 588:540–6. doi: 10.1038/s41586-018-0217-9

50. Morin G, Degrugillier-Chopinet C, Vincent M, Fraissenon A, Aubert H, Chapelle C, et al. Treatment of two infants with PIK3CA-related overgrowth spectrum by alpelisib. *J Exp Med.* (2022) 219:e20212148. doi: 10.1084/jem.20212148

51. Novartis Pharmaceuticals Corporation. *Vijoice: Prescribing Information*. East Hanover, New Jersey, USA: Novartis Pharmaceuticals Corporation (2022).

52. Delestre F, Venot Q, Bayard C, Fraissenon A, Ladraa S, Hoguin C, et al. Alpelisib administration reduced lymphatic malformations in a mouse model and in patients. *Sci Transl Med*. (2021) 13:eabg0809. doi: 10.1126/scitranslmed.abg0809

53. Shaheen MF, Tse JY, Sokol ES, Masterson M, Bansal P, Rabinowitz I, et al. Genomic landscape of lymphatic malformations: a case series and response to PI3Ka inhibitor alpelisib in an N-of-1 clinical trial. *Elife.* (2022) 11:e74510. doi: 10.7554/eLife.74510

54. Madsen RR, Semple RK. PIK3CA-related overgrowth: silver bullets from the cancer arsenal? *Trends Mol Med.* (2022) 28:255–7. doi: 10.1016/j.molmed.2022.02.009

55. Yu Y, Savage RE, Eathiraj S, Meade J, Wick MJ, Hall T, et al. Targeting AKT1-E17K and the PI3K/AKT pathway with an allosteric AKT inhibitor, ARQ 092. *PLoS ONE.* (2015) 10:e0140479. doi: 10.1371/journal.pone.0140479

56. Yu Y, Hall T, Eathiraj S, Wick MJ, Schwartz B, Abbadessa G. *In-vitro* and *in-vivo* combined effect of ARQ 092, an AKT inhibitor, with ARQ 087, a FGFR inhibitor. *Anticancer Drugs.* (2017) 28:503–13. doi: 10.1097/CAD.0000000000000486

57. Ranieri C, Di Tommaso S, Loconte DC, Grossi V, Sanese P, Bagnulo R, et al. *In vitro* efficacy of ARq092, an allosteric AKT inhibitor, on primary fibroblast cells derived from patients with PIK3CA-related overgrowth spectrum (PROS). *Neurogenetics.* (2018) 19:77–91. doi: 10.1007/s10048-018-0540-1

58. Forde K, Resta N, Ranieri C, Rea D, Kubassova O, Hinton M, et al. Clinical experience with the AKT1 inhibi- tor miransertib in two children with PIK3CA-related overgrowth syndrome. *Orphanet J Rare Dis.* (2021) 16:109. doi: 10.1186/s13023-021-01745-0

59. Li D, March ME, Gutierrez-Uzquiza A, Kao C, Seiler C, Pinto E, et al. ARAF recurrent mutation causes central conducting lymphatic anomaly treatable with a MEK inhibitor. *Nat Med.* (2019) 25:1116–22. doi: 10.1038/s41591-019-0479-2

60. Homayun-Sepehr N, McCarter AL, Helaers R, Galant C, Boon LM, Brouillard P, et al. KRAS-driven model of Gorham-Stout disease effectively treated with trametinib. *JCI Insight.* (2021) 6:e149831. doi: 10.1172/jci.insight.149831

61. Foster JB Li D, March ME, Sheppard SE, Adams DM, Hakonarson H, Dori Y. Kaposiform lymphangiomatosis effectively treated with MEK inhibition. *EMBO Mol Med.* (2020) 12:e12324. doi: 10.15252/emmm.202012324

62. Tian R, Liang Y, Zhang W, Wang J, Shan Y, Gao H, Xie C, Li J, Xu M, Gu S. Effectiveness of sirolimus in the treatment of complex lymphatic malformations: single center report of 56 cases. *J Pediatr Surg.* (2020) 55:2454–8. doi: 10.1016/j.jpedsurg.2019.12.021

63. Halderman AA, Ryan MW, Clark C, Sindwani R, Reh DD, Poetker DM, et al. Medical treatment of epistaxis in hereditary hemorrhagic telangiectasia: an evidence-based review. *Int Forum Allergy Rhinol.* (2018) 8:713–28. doi: 10.1002/alr.22094

64. Robert F, Desroches-Castan A, Bailly S, Dupuis-Girod S, Feige JJ. Future treatments of hereditary hemorrhagic telangiectasia. *Orphanet J rare Dis.* (2020) 15:4. doi: 10.1186/s13023-019-1281-4

65. Faughnan ME, Gossage JR, Chaknala MM, Oh SP, Kasturi R, Hughes CCW, et al. Pazopanib may reduced bleeding in hereditary hemorrhagic telangiectasia. *Angiogenesis.* (2019) 22:145–55. doi: 10.1007/s10456-018-9646-1

66. Boon LM, Dekeuleneer V, Coulie J, Marot L, Bataille AC, Hammer F, et al. Case report study of thalidomide therapy in 18 patients with severe arteriovenous malformations. *Nat Cardiovasc Res.* (2022) 1:562–7. doi: 10.1038/s44161-022-00080-2

67. Ola R, Dubrac A, Han J, Zhang F, Fang JS, Larrivee B, et al. PI3 kinase inhibition improves vascular malformations in mouse models of hereditary haemorrhagic telangiectasia. *Nat Commun.* (2016) 7:13650. doi: 10.1038/ncomms13650

68. Alsina-Sanchis E, Garcia-Ibanez Y. FigueiredoAM, Riera-Domingo C, Figueras A, Matias-Guiu X, et al. Alk1 loss results in vascular hyperplasia in mice and humans through Pi3K activation. *Arterioscler Thromb Vasc Biol.* (2018) 38:216–29. doi: 10.1161/ATVBAHA.118.310760

69. Bayrak-Toydemir P, Stevenson DA. Capillary malformation-arteriovenous malformation syndrome. In: Adam MP, Everman DB, Mirzaa GM, et al., editors. *GeneReviews®*. Seattle (WA): University of Washington, Seattle, 1993-2022. Available from: https://www.ncbi.nlm.nih.gov/books/NBK52764/

70. Nicholson CL, Flanagan S, Murati M, Boull C, McGough E, Ameduri R, et al. Successful management of an arteriovenous malformation with trametinib in a patient with capillary-malformation arteriovenous malformation syndrome and cardiac compromise. *Pediatr Dermatol.* (2022) 39:316–9. doi: 10.1111/pde.14912

71. Mansur A, Kostynskyy A, Krings T, Agid R, Radovanovic I, Pereira VM. The safety profile and angioarchitectural changes after acute targeted embolization of ruptured arteriovenous malformations. *J Neurosurg.* (2021) 7:1–10. doi: 10.3171/2020.9.JNS201558

72. Frenzel T, Lee CZ, Kim H, Quinnine NJ, Hashimoto T, Lawton MT, et al. Feasibility of minocycline and doxycycline use as potential vasculostatic therapy for brain vascular malformations: pilot study of adverse events and tolerance. *Cerebrovasc Dis.* (2008) 25:157–63. doi: 10.1159/000113733

73. Muster R, Ko N, Smith W, Su H, Dickey MA, Nelson J, et al. Proof-of-concept single-arm trial of bevacizumab therapy for brain arteriovenous malformations. *BMJ Neurol Open*. (2021) 3:e000114. doi: 10.1136/bmjno-2020-000114

74. D'Amato RJ, Loughnan MS, Flynn E, Folkman J. Thalidomide is an inhibitor of angiogenesis. *Proc Natl Acad Sci USA*. (1994) 91:4082–5. doi: 10.1073/pnas.91.9.4082

75. Nikolaev SI, Vetiska S, Bonilla X, Boudreau E, Jauhiainen S, Jahromi BR, et al. Somatic activating KRAS mutations in arteriovenous malformations of the brain. *N Engl J Med*. (2018) 378:250–61. doi: 10.1056/NEJMoa1709449

76. Couto JA, Huang AY, Konczyk DJ, Goss JA, Fishman SJ, Mulliken JB, et al. Somatic MAP21 mutations are associated with extracranial arteriovenous malformation. *Am J Hum Genet*. (2017) 100:546–54. doi: 10.1016/j.ajhg.2017.01.018

77. Hong T, Yan Y, Li J, Radovanovic I, Ma X, Shao YW, et al. High prevalence of KRAS/BRAF somatic mutations in brain and spinal cord arteriovenous malformations. *Brain J Neurol*. (2019) 142:23–34. doi: 10.1093/brain/awy307

78. Fish JE, Flores Suarez CP, Boudreau E, et al. Somatic Gain of KRAS Function in the Endothelium Is Sufficient to Cause Vascular Malformations That Require MEK but Not PI3K Signaling. *Circ Res*. (2020) 127:727–43. doi: 10.1161/CIRCRESAHA.119.316500

79. Al-Olabi L, Polubothu S, Dowsett K, Andrews KA, Stadnik P, Joseph AP, et al. Mosaic RAS/MAPK variants cause sporadic vascular malformations which respond to targeted therapy. *J Clin Invest*. (2018) 128:1496–508. doi: 10.1172/JCI98589

80. Pan P, Weinsheimer S, Cooke D, Winkler E, Abla A, Kim H, et al. Review of treatment and therapeutic targets in brain arteriovenous malformation. *J Cereb Blood Flow Metab*. (2021) 41:3141–56. doi: 10.1177/0271678X211026771

81. Lekwuttikarn R, Lim YH, Admani S, Choate KA, Teng JMC. Genotype-guided medical treatment of an arteriovenous malformation in a child. *JAMA Dermatol*. (2019) 155:256–7. doi: 10.1001/jamadermatol.2018.4653

82. Edwards EA, Phelps AS, Cooke D, Frieden IJ, Zapala MA, Fullerton HJ, et al. Monitoring Arteriovenous Malformation Response to Genotype-Targeted Therapy. *Pediatrics*. (2020) 146:e20193206. doi: 10.1542/peds.2019-3206

83. Cooke DL, Frieden IJ, Shimano KA. Angiographic evidence of response to trametinib therapy for a spinal cord arteriovenous malformation. *J Vasc Anom*. (2021) 2:e018. doi: 10.1097/JOVA.0000000000000018

84. Palmieri M, Curro A, Tommasi A, Di Sarno L, Doddato G, Baldassarri M, et al. Cell-free DNA next-generation sequencing liquid biopsy as a new revolutionary approach for arteriovenous malformation. *J Vasc Sci*. (2020) 1:176–80. doi: 10.1016/j.jvssci.2020.08.002

85. Cescon DW, Bratman SV, Chan SM, Siu LL. Circulating tumor DNA and liquid biopsy in oncology. *Nat Cancer*. (2020) 1:276–90. doi: 10.1038/s43018-020-0043-5

86. Zenner K, Jensen DM, Cook TT, Dmyterko V, Bly RA, Ganti S, et al. Cell-free DNA as a diagnostic analyte for molecular diagnosis of vascular malformations. *Genet Med*. (2021) 23:123–30. doi: 10.1038/s41436-020-00943-8

87. Chen WL, Pao E, Owens J, Glass I, Pritchard C, Shirts BH, et al. The utility of cerebrospinal fluid-derived cell-free DNA in molecular diagnostics for the PIK3CA-related megalencephaly-capillary malformation (MCAP): a case report. *Cold Spring Harb Mol Case Stud*. (2022) 8:a006188. doi: 10.1016/j.gim.2022.01.134

88. Winkler EA, Wu D, Gil E, McCoy D, Narsinh K, Sun Z, et al. Endoluminal biopsy for molecular profiling of human brain vascular malformations. *Neurology*. (2022) 98:e1637–47. doi: 10.1212/WNL.0000000000200109

Frontiers in
Human Neuroscience

Bridges neuroscience and psychology to understand the human brain

The second most-cited journal in the field of psychology, that bridges research in psychology and neuroscience to advance our understanding of the human brain in both healthy and diseased states.

Discover the latest Research Topics

See more →

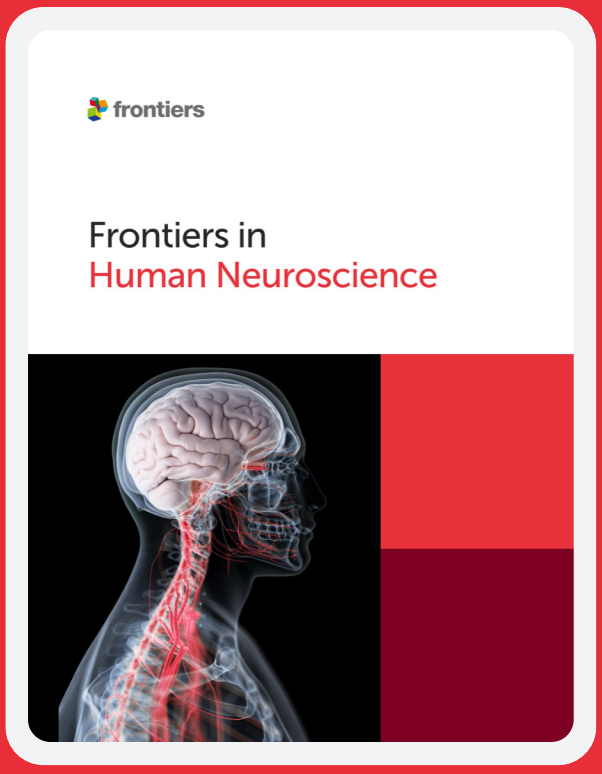

Frontiers

Avenue du Tribunal-Fédéral 34
1005 Lausanne, Switzerland
frontiersin.org

Contact us

+41 (0)21 510 17 00
frontiersin.org/about/contact